SELECTIVE DISSOLVED AIR FLOTATION OF FINE MINERAL PARTICLES

A thesis submitted for the degree of

* Doctor of Philosophy of the University of London

and the

Diploma of Imperial College

by

JAIME ANTONIO SOLARI SAAVEDRA

Department of Mineral Resources Engineering
Royal School of Mines
Imperial College
London SW7

May 1980

To Chela and Enrique,
my parents.

ABSTRACT

The limitations of the froth flotation process in the separation of fine particles have been discussed with particular reference to the influence of particle and bubble sizes on the bubble-particle attachment mechanism.

The fundamentals of the dissolved air flotation (DAF) process have been reviewed and its application to the selective recovery of fine mineral particles has been investigated using cassiterite/quartz suspensions. The dissolved air flotation of fine quartz and cassiterite particles has been studied in the presence of cationic (dodecylamine) and anionic (sodium dodecyl sulphate, sodium sulphosuccinamate) surfactants in a batch DAF system that produced bubbles of 50 μm average diameter.

Evidence is presented that show that the fundamental mechanism of bubble-particle attachment in dissolved air flotation is the adhesion of bubbles to hydrophobic particles upon collisions. Hydrophilic particles were not floated by the DAF process irrespective of their degree of aggregation. Flotation through bubbles forming from supersaturated solution on the solid phase was studied and estimated to be of little significance as a bubble-particle attachment mechanism in DAF.

The dissolved air flotation of both oxide minerals correlated well with the adsorption behaviour of surfactants at the oxide mineral/solution interface as determined by adsorption, electrokinetic and suspension stability measurements. Mineral recovery by DAF was maximized when the particles were hydrophobic and the suspension exhibited a degree of destabilization. Long-chain surfactants were found to accomplish this twofold objective.

Results are presented that show that the adsorption of dodecylamine

on quartz and of the anionic surfactants on cassiterite and stannic oxide is primarily the result of electrostatic attraction for the surface followed by hydrophobic chain-chain associations at high adsorption densities and surfactant concentrations.

Separation tests showed that fine cassiterite particles could be selectively recovered from quartz suspensions by the dissolved air flotation process. The factors influencing cassiterite recovery and the selectivity of the separations were the surface chemical characteristics of both minerals in the presence of the collector and parameters associated with the operation of the dissolved air flotation system.

ACKNOWLEDGEMENTS

I wish to express my sincere thanks to my supervisor, Dr. R.J. Gochin, for his guidance, encouragement and unfailing support over the past three years.

I should also like to extend my gratitude to Dr. H.L. Shergold and Dr. J.A. Kitchener for many useful suggestions and discussions throughout the course of this project.

I am also grateful to my colleagues and members of the Department of Mineral Resources Engineering for their invaluable comments, assistance and friendship.

The support of the World University Service (U.K.) in the form of a grant that enabled me to carry out this work is gratefully acknowledged. I am also indebted to Professor M.G. Fleming and Dr. H.L. Shergold for the provision of financial assistance during part of this project.

Finally, I should like to thank all who helped me in the preparation of this work, Particularly, Janis, who managed to decipher my handwriting and carefully typed this thesis, and Enrique, Claudio and Barry for their invaluable help with photography. Special thanks to Maite for her inexhaustible support and patience.

CONTENTS

LIST OF FIGURES

LIST OF TABLES

Chapter 1. INTRODUCTION

1. INTRODUCTION

1.1. The recovery of fine mineral particles by flotation.

Flotation is a process used for the separation or recovery of solids in suspension by means of their attachment to gas bubbles. In mineral processing, where flotation has been applied for over sixty years, the air bubbles attach selectively to the valuable mineral particles forming bubble-particle aggregates that concentrate into a froth from which the mineral product is recovered; because of the existence of this mineralized froth layer, the mineral flotation process is known as froth flotation (1).

Most minerals have strong affinity for water (hydrophilicity), and therefore the process of attachment of an air bubble involves the displacement of a water film from the mineral surface (2). This displacement process is not spontaneous unless the forces acting between the mineral surface and the water molecules are considerably weakened (3). In froth flotation, the selective attachment of air bubbles to determined mineral particles is accomplished by modifying the hydrophilic surface properties of those minerals. This modification is brought about by reagents ('collectors') which adsorb at the particular mineral/water interface with the effect of diminishing the mineral surface/water interaction, therefore rendering the surface more amenable to the displacement of the wetting film by an air bubble.

For bubble-particle attachment to occur, thermodynamic and kinetic conditions have to be fulfilled. The thermodynamic condition for the equilibrium attachment of a gas bubble to a flat solid surface upon the replacement of the solid/liquid interface is given by the Young-Dupré equation (4):

$$\Delta G = \gamma_{LG}(\cos\theta - 1) \qquad (1.1)$$

where ΔG = free energy change accompanying the replacement of a unit area of solid/liquid interface by a solid/gas interface

θ = gas bubble/solid surface contact angle (measured through the liquid)

γ_{LG} = surface tension of the liquid/gas interface

Thus, equation 1.1 shows that only for $\theta > 0$ (hydrophobic surface) the attachment of an air bubble to a mineral surface is thermodynamically feasible. It may be shown (5) that equation 1.1 is equivalent to the difference between the work of adhesion of the liquid to the solid (W_{ad}) and the work of cohesion of the liquid (W_{co}); as $W_{co} = 2\gamma_{LG}$, flotation would only be possible if $W_{ad} < 2\gamma_{LG}$ ($\simeq$144 mJ/m^2 for water). Hence the energetics of the flotation process may be calculated for hydrophobic solids from the relationship:

$$W_{ad} = \gamma_{LG}(1 + \cos\theta) \qquad (1.2)$$

where W_{ad} = work required to separate liquid water from a solid/water interface, leaving behind an adsorbed layer in equilibrium with saturated water vapour

For hydrophilic solids ($\theta = 0^o$), other methods have been proposed to determine the solid/water energy of interaction (5).

It has been proposed by some authors (6)(7) that the flotation process involves the adsorption of collector not only at the solid/liquid interface but also at the solid/gas interface. Thus, assuming that the interfacial tension change produced upon collector adsorption at each interface is given by the Gibbs equation, then for dilute collector concentrations

$$d\gamma_{ij} = -RT \sum_x \Gamma_x^{ij} \, d\ln C_x \qquad (1.3)$$

where $d\gamma_{ij}$ = tension change of the interface ij

Γ_x^{ij} = surface excess of component x at the interface ij

C_x = concentration of component x in the bulk solution

and assuming that the contact angle of an air bubble on the solid is described by the Young's equation

$$\gamma_{SG} = \gamma_{SL} + \gamma_{LG}\cos\theta \qquad (1.4)$$

it is possible to show that for $\theta < 90^o$ $\quad \Gamma_x^{SG} > \Gamma_x^{SL} \qquad (1.5)$

The kinetic factors intervening in the flotation process arise from the requirements of the mechanism of particle capture, namely,

i) a collision between bubble and particle

ii) the thinning and rupture of the liquid film separating bubble and particle during the collision period, and

iii) the rapid expansion of the contact meniscus over the particle so that subsequent detachment due to collisions or otherwise may be resisted.

The bubble-particle collision stage is basically a hydrodynamic phenomenon. It is highly dependent on particle and bubble sizes and on particle inertia as will be shown later (section 1.3). Derjaguin and Dukhin (8) have proposed the existence of another mechanism, the diffusiophoretic effect', influencing particle capture. They postulated that as the result of unequal distribution of ions on the bubble surface, an electrical field arises which exerts its influence on particles entering the boundary diffusion layer of the bubble. The sign and magnitude of the diffusiophoretic force will be most important for very small particles (less than 10 μm). Even though experimental evidence (9) corroborates the existence of this phenomenon, its influence in flotation systems is not yet clear (10).

A bubble-particle collision will lead to a stable attachment only

if the contact time between particle and bubble is longer than the time required to thin and rupture the liquid film separating them (11). The induction time has been defined as the time necessary for the thinning of the liquid film to such a thickness that rupture can take place (12). Measurements of induction times (13)(14) indicate that they are of the order of a few milliseconds for moderately hydrophobic surfaces. The thinning and rupture of liquid films in flotation has been studied thermodynamically by several authors (15)(16)(17). The forces acting in thin films arise from double layer, molecular interaction and surface hydration effects (18); the combined action of these forces gives rise to the 'disjoining pressure' of the thin film (19). The disjoining pressure (P) is a function of the film thickness (h); if P(h) is negative then the thin film will rupture and the air bubble will establish contact with the solid surface.

The probability of flotation has been described in terms of the probability of occurrence of separate consecutive events (20)(21). Thus, it has been proposed that the probability of flotation, P, can be expressed as:

$$P = P_c \cdot P_a \cdot P_s \qquad (1.6)$$

where P_c = probability of collision of a bubble and a particle

P_a = probability of attachment of the particle to the bubble after collision

P_s = probability of formation of a stable particle-bubble aggregate.

P_c and P_a are directly related with hydrodynamic collision and liquid film thinning phenomena respectively. P_s is related to the tenacity of attachment of the particle to the bubble which is a function of the contact angle, the particle and bubble sizes, and the particle

density (22)(23).

1.2. Problems in froth flotation

With the development of froth flotation as the major process for the concentration of metallic sulphide ores, its application to the separation of other minerals has increased considerably. Hence, flotation has been used for the processing of oxide minerals, silicates, phosphates, clays and other non-metallic minerals (24).

The spread of selective froth flotation has posed many problems from a surface chemistry point of view given the increased complexity of the separation operations and the need for new collectors to work under conditions entirely different to those found in sulphide mineral flotation. Thus, for example, oxide minerals are difficult to float selectively due to their similar nature and high resistance to chemical action when compared to sulphides.

The recovery of oxide minerals by flotation is important because: a) for some ores, flotation is the only economic way of recovering those minerals, b) for some oxide minerals, flotation is the only technical way of recovering particles below certain particle size (25), and c) for some metals, oxide minerals constitute the largest source of resources. Hence, research into the flotation of oxide minerals has received increased attention, especially in the development of new collectors specific to certain oxide minerals. Recently, several new collectors have been reported: chelating agents for cassiterite (26), lead oxide (26) and zinc oxide minerals (27); a non-ionic collector for cassiterite (28); and various other collectors for cassiterite (29) (183), hematite and iron ores (30), and other oxide minerals (29).

Another major problem in froth flotation practice is the lower

recovery obtained for very large or very fine particles. While in practice the large particles can be re-ground, many valuable fine mineral particles are lost into the flotation tailings. The critical particle size below which recovery falls depends on the mineral and the flotation system but data compiled from the literature suggest that it is of the order of 10 μm (31). This drop of flotation recovery with particle size has been widely associated with the slower rate of flotation of fine particles although other factors may also be acting (31)(32)(33). The floatability of fine particles will be discussed in more detail in the next section. Fine particles or 'slimes' may also affect the overall flotation system through several processes; the formation of slime coatings on the valuable mineral, their increased solubility and dissolution rates, their entrainment in the concentrate, their high reagent consumption and through their influence on processes subsequent to flotation (31)(32)(33).

The economic losses stemming from slime formation may be very considerable in the processing of minerals of a brittle nature. For example, cassiterite contained in lode ores is very finely disseminated or associated with other minerals. It requires, therefore, a fine grinding stage that is the source of a major slimes problem. Ottley (25) reports that in the processing of a tin lode ore combining gravity concentration and flotation 20.7% of the total tin losses are lost as slimes and flotation tailings (10.8% of total Sn losses). At Wheal Jane, Cornwall, 47% of the tin losses are in the -7 μm fraction, for an overall tin recovery of below 70% (34). Cassiterite flotation performance is seldom over 60% Sn recovery.

Several processes have been used for the treatment of fine mineral particles (32). The recovery of fine particles by systems involving

the addition of oils has received increased attention (35). Amongst the methods that have been claimed to improve the flotation of fine particles are (31): addition of neutral oils, addition of hydrophobic carrier mineral, separate flotation of the slimes, aggregation of the slimes, vacuum flotation, reduction of bubble size. While most of these methods have been subjected to experimental testing, the effect of reducing bubble size has received little attention in the literature.

1.3. The floatability of fine particles.

Particle size effects in flotation has been investigated experimentally from flotation rate and particle capture measurements. Experimental studies of the effect of particle size on the flotation rate have given contradictory results, although they generally indicate a drop of flotation rate with decreasing particle size.

Gaudin et al (36) found that the rate of flotation for galena particles was independent of particle diameter (d_p) up to 4 μm, and between 4 and 20 μm was proportional to particle size. Morris (37) found from batch experiments that the flotation rate was proportional to the logarithm of d_p. Bushell (38) reported that the flotation rate of quartz with dodecylammonium acetate was independent of particle size, whereas de Bruyn and Modi (39) reported for the same system that flotation rate was proportional to d_p for values of d_p less than 37 μm, and it was independent of particle diameter for coarser particle sizes. Tomlinson and Fleming (20) conducted experiments in a modified Hallimond tube under 'free' flotation conditions (sparsely coated bubbles) and found that the flotation rate varied proportionally to the square of particle diameter for apatite, galena and hematite whereas for quartz it was directly proportional to d_p.

More recently, studies have been conducted by Flint and Howarth (40), Reay and Ratcliff (41)(42), Collins and Jameson (43)(44) and by Anfruns and Kitchener (45) on the mechanism of particle capture by bubbles in flotation; the influence of particle and bubble size on the flotation rate has been extrapolated from those studies (33).

A model, originally proposed by Sutherland (46) (see equation 1.6), assumes that the capture of a particle by a bubble can be split into a hydrodynamic collision stage followed by an attachment stage where forces other than hydrodynamic come into play. The collection efficiency (E_c) of a bubble is then defined as the product of a collision and attachment efficiencies:

$$E_c = E_1 \cdot E_2 \qquad (1.7)$$

where E_1 ≡ collision efficiency: the fraction of particles that collide with the bubble

E_2 ≡ attachment efficiency: the fraction of particles that attach to the bubble after colliding with it.

This model considers a spherical bubble of diameter d_b rising vertically at constant velocity and a spherical particle of diameter d_p in the path of the bubble whose inertia can be ignored. Depending on the bubble size a flow pattern around the front of the bubble may be assumed, and the fraction of particles in the path of the bubble that will collide with it can be calculated from the streamlines of the flow pattern. Reay and Ratcliff (41) assumed a flow pattern given by the Stokes solution for creeping flow around a solid sphere and predicted for $d_p < 100$ μm:

$$E_1 \propto (d_p/d_b)^2 \qquad (1.8)$$

in agreement with Flint and Howarth (40). However, experimental studies on collection efficiencies of particles of diameter between 3 and 30 μm

indicated that $E_c \alpha d_p^{1.5}$, at odds with equation 1.8 since the model assumes that E_2 is independent of bubble and particle sizes. This discrepancy has been attributed to the distortions of the velocity field produced at short bubble-particle distances (47)(48). When this hydrodynamic effect is taken into account in the model the collision efficiency tends to be proportional to $d_p^{1.5}$.

Anfruns and Kitchener (45) measured the collection efficiencies of methylated quartz and glass beads (12 - 40 μm) by single bubbles of conventional flotation size (0.5 - 1.0 mm). They found that the collection efficiency of the spherical glass beads was only 20% of the theoretically calculated efficiencies whereas for the angular quartz particles they agreed very closely. The capture of spherical particles was enhanced by the addition of a simple electrolyte (1 M KCl) and suppressed by the addition of an anionic surfactant (10^{-3} M sodium dodecylsulphate) known to adsorb strongly at the air/liquid interface. As this amount only caused a 25% reduction in the collection efficiency of the quartz particles, these tests showed the importance of particle shape and the action of double-layer repulsion forces on the mechanism of particle capture in flotation. These workers also showed that the collection efficiency was proportional to the square of particle diameter ($E_c \alpha d_p^2$) in agreement with equation 1.8 and the flow pattern assumed ($R_e = 40$). Collection efficiencies increased with decreasing bubble size as $E_c \alpha d_b^{-1.69}$.

Jameson et al (33) correlated theoretical values predicted by the capture model with experimental data and showed that the flotation rate 'constant' (K) is strongly dependent on particle and bubble size as follows:

for $4 \leq d_p \leq 30$ μm with $d_b \leq 100$ μm

$$K \alpha \frac{E_c}{d_b} \alpha \frac{d_p^{1.5}}{d_b^3} \qquad (1.9)$$

and for $12 \leq d_p \leq 40$ μm

with $0.6 \leq d_b \leq 1.0$ mm $\quad K \propto \frac{E_c}{d_b} \propto \frac{d_p^2}{d_b^{2.69}}$ (1.10)

which indicate that for a given air flow rate, the flotation rate of fine particles could be increased by reducing the size of the bubbles.

Rulev, Derjaguin and Dukhin (49) predicted $K \propto d_p^2/d_b^3$ for the kinetics of flotation of small particles by monodispersed bubbles rising in Stokes flow and fulfilling the condition $d_b >> d_p$. They had previously shown (50) that the flotation efficiency for spherical particles and bubbles under Stokessian conditions was proportional to $(d_p/d_b)^2$ in agreement with equation 1.8. Samygin et al (54) measured various parameters related to the floatability of particles in the range 40 - 160 μm for bubble sizes between 1.12 and 3.12 mm. They concluded that for a given number of bubbles flotation recovery is higher for large bubbles, but for a given volume of air a decrease in bubble size leads to an increase in flotation performance through increases in the total value of the collision cross section and in the probability of attachment.

The flotation rate constant has also been found to depend on electrical interactions between particles and bubbles. It has been shown experimentally (44) that the flotation rate of polystyrene latex particles by microbubbles depends on the electrophoretic mobility of both particles and bubbles. Derjaguin and Dukhin (8) have postulated the existence of an electrophoretic force acting in the diffusion layer of the bubble which might be determinant in particle-bubble attachment for very small particles and conditions of mobility of the bubble surface. Blake and Kitchener (55) showed experimentally that surface forces exert

a positive disjoining pressure that poses a considerable potential barrier to particle-bubble attachment even when the solid is strongly hydrophobic.

The discrepancies found between measured collection efficiencies with respect to the theoretical model (42)(45)(56) may be associated with the action of repulsive surface forces between bubble and particle (absent from the theoretical model), and with the assumption that the efficiency of attachment is independent of particle and bubble size. Klassen and Moukrosov (57) quoted experimental results of Bodganov which showed that the probability of attachment was independent of particle size up to 10 μm but for smaller particles the probability of attachment had a twofold increase. Derjaguin et al (51) postulated that the attachment efficiency was a function of h_c/d_p (h_c: the critical thickness of the interfacial film at which it is ruptured) and therefore dependent on particle size. Rulev (58) calculated the efficiency of particle capture by a bubble summarizing the theoretical work on the subject by Derjaguin, Dukhin and Rulev (48 - 53). These workers have developed a model of particle capture that takes into account long and short range hydrodynamic interactions between bubble and particle as well as the effect of surface forces. Analytical solutions of the relevant equations are complicated and experimental testing on some aspects of the theory is now being carried out (56). From Rulev's calculations it is possible to see that when the electrostatic component of the disjoining pressure can be neglected (high concentration of electrolyte), the efficiency of attachment (E_2) is weakly dependent on the particle and bubble sizes.

Klassen and Moukrosov (59) pointed out that the probability of flotation would be highest for fine particles in the case of bubbles

forming from supersaturated solutions where the need of a bubble-particle hydrodynamic collision would be avoided. They based this statement on the assumption that the probability of formation of bubbles from supersaturated solution is maximum for small particles; as they also postulated that the probability of attachment is highest for fine particles then the overall flotation process would be very favourable for small particles by using this method of bubble generation.

Summarizing, as a first approximation the recovery drop in flotation for fine particles may be explained through a decrease of the collection efficiency of bubbles with decreasing particle size. A decrease in the collection efficiency of bubbles brings about a corresponding decrease in the flotation rate approximately proportional to the square of the particle diameter. The theory predicts that the flotation rate is increased if bubble size is diminished (at constant air flow rate). Methods of improving the flotation recovery of fine particles by increasing their flotation time lead generally to a decrease in selectivity (31). Models of particle capture that take into account both hydrodynamic and surface forces are still in development and lack experimental proof; it has been shown, however, that double-layer repulsion forces can lead to a substantial decrease in the flotation rate. Generation of bubbles in such a way as to avoid the hydrodynamic collision needed to establish bubble-particle attachment has been postulated to favour fine particle size flotation.

1.4. Bubble generation in flotation systems.

Flotation systems can be classified according to the method employed to generate the dispersed gaseous phase required to levitate the particles. Gas bubbles can be generated by mechanical means (a), from gas-super-

saturated solutions (processes b), c) and d)) and by electrolysis. These processes are described below.

a) Dispersed air flotation. Bubbles are generated mechanically by the action of an impeller or by passing air through porous media. Froth flotation is the typical case of dispersed air flotation. Bubbles generated in froth flotation machines are usually of the order of 1 mm (24).

b) Dissolved air flotation. Water is saturated with air at pressures greater than atmospheric; upon supersaturation of the system by reducing the pressure, the excess dissolved air is released as very small bubbles. This process is widely used in solid/liquid separation operations. Bubble diameters generated from the precipitation of dissolved air are between 40 and 100 μm.

c) Vacuum flotation. Bubbles are generated from the supersaturation of the liquid upon the application of a vacuum. The diameter of bubbles so generated depends on the degree of supersaturation applied and on the liquid surface tension, typical values vary between 0.1 - 1.0 mm (60). Although this flotation process is not being applied at the present on a large scale, there have been reports of vacuum flotation of minerals at the laboratory scale (section 2.6.1).

d) Microflotation. Air supersaturation is induced by dissolving air into a stream as it flows down a deep shaft (10 m) and then by making it rise to atmospheric level. As the stream rises the excess dissolved air comes out of solution as bubbles. This flotation process is successfully used for wastewater treatment. No values of the bubble sizes produced by the microflotation process are given in the literature (61).

e) Electroflotation. Bubbles are generated by the electrolysis of

the water in the pulp or effluent. This process has been applied successfully in the treatment of effluents and attempts have been made to apply it to the processing of minerals (62). Bubble sizes generated by electroflotation are the smallest of all flotation systems with mean bubble diameters of around 30 μm, depending on current density.

1.5. Dissolved air flotation.

Dissolved air flotation (DAF) is a process whose fine mineral particle flotation remains to be assessed. It offers the advantages, in principle, of generating very small bubbles and the attractive possibility of bubble formation from supersaturated solution on the mineral particles. The energy requirements, while being greater than mechanical methods, are less than for electroflotation.

Dissolved air flotation is being successfully employed in a broad range of industries as a solid/liquid separation process. Current industrial applications include water clarification (63), activated sludge thickening (64), effluent treatment in the food processing and paper mill industries (65), oil refinery and emulsified oil wastewater recovery (65).

The DAF process is based upon Henry's law which states that the solubility of a gas in a liquid is directly proportional to the partial pressure of the gas above the liquid (66). Henry's law, therefore, would determine the theoretical amount of air available for flotation when saturating water with air at a pressure P_o and then lowering the pressure to atmospheric pressure P_a.

$$\Delta x = H(P_o - P_a) \qquad (1.11)$$

where Δx = mole fraction of dissolved air available for flotation

H = Henry's law constant

The main characteristic of the process is that bubble formation relies upon the air-supersaturation of water. In practice, air is dissolved in water under pressure and the air-saturated water is injected through a pressure reducing device at atmospheric pressure, into a tank or a stream containing the suspended phase. Upon water supersaturation the excess air is released under the form of very fine bubbles, usually in the 50 μm range which attach themselves to the components of the suspended phase forming stable aggregates that rise out of suspension.

There exist three DAF systems according to the type of pressurization of the system (Figure 1.1). They are: full influent pressurization, where the whole waste stream is pressurized; partial influent pressurization, when only a section of the influent is pressurized to provide the microbubbles; and, recycle effluent pressurization, where a portion of the clarified DAF effluent is recycled, pressurized and mixed with the wastewater feed to provide the microbubbles.

The mechanisms by which the microbubbles produced by DAF are believed to attach to the suspended phase are (67):

i) The adhesion of air bubbles to the suspended phase as a result of collisions or air precipitation on the suspended phase.

ii) The trapping of rising air bubbles in a structure formed by aggregated particles (flocs).

iii) The absorption of an air bubble into a floc structure as it is formed.

It is worth noting that, as stated, mechanisms ii) and iii) are non-selective whereas mechanism i) requires the existence of a contact angle between bubble and particle. In addition, the possibility of attachment through preferential air precipitation, e.g. bubble formation

(a) Full influent pressurization system

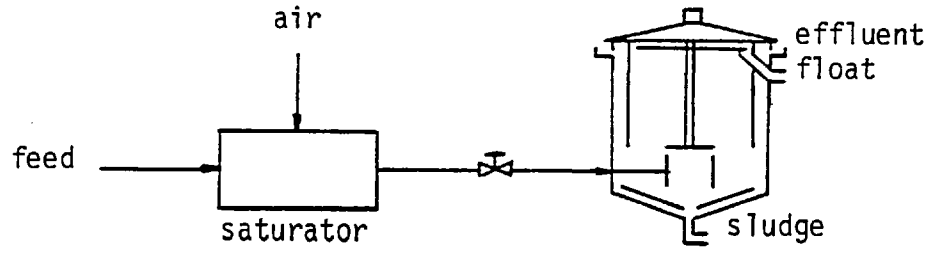

(b) Partial influent pressurization system

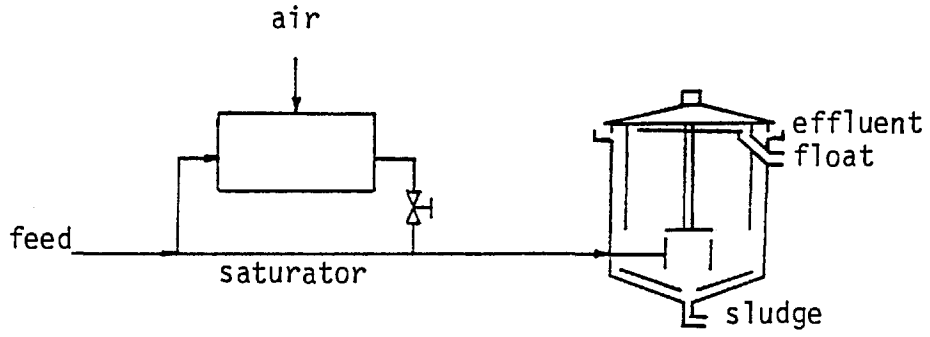

(c) Recycle effluent pressurization system

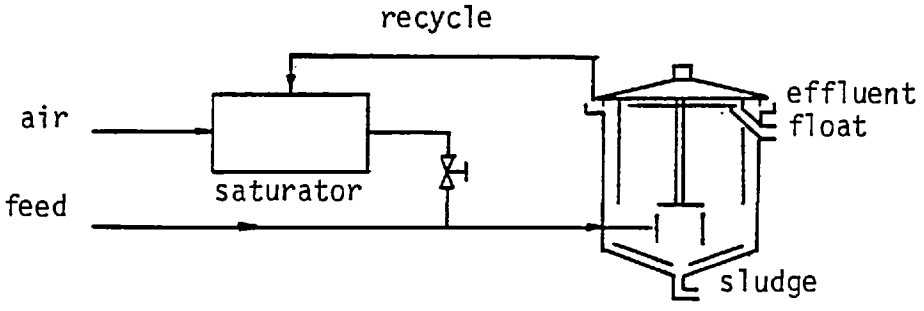

Figure 1.1. Classification of dissolved air flotation systems according to type of pressurization

only on hydrophobic surfaces, would make the process especially suitable for the flotation of fine particles. There are no reports in the literature, however, confirming the existence and relative importance of any of these mechanisms in the bubble-particle attachment mechanism in DAF.

The fact that DAF is used to treat effluents and wastewaters with a wide range of surface characteristics without the aid of 'collectors' gives the process, at first sight, a non-selective character which would make it inapplicable to mineral processing operations where selectivity is essential. On the other hand, DAF has shown an ability to recover very fine and even colloidal particles through the successful application of flocculation or coagulation techniques (the need of flocculation would obviously impose another restriction to the application of DAF in mineral processing operations).

Dissolved air flotation is an established process in its practical application (section 2.5). Much less is known about fundamental stages of the process such as bubble formation and bubble-particle attachment mechanisms. The current state of knowledge about these mechanisms will be reviewed in Chapter 2.

1.6. Aim of the project

As outlined in this introduction, the DAF process has two characteristics that might improve the floatability of fine particles: production of small bubbles and bubble-particle attachment through bubble formation directly onto the mineral particles. This latter possibility has not yet been subjected to experimental investigation.

The aim of this project was to study the feasibility of using the dissolved air flotation system to selectively separate minerals,

especially in the fine particle size range where conventional, dispersed-air, flotation becomes ineffective.

To successfully carry out this work it seemed essential to investigate the conditions under which bubble-particle attachment will occur in DAF, to decide whether those conditions would allow for selective flotation, and then to carry out mineral separations under those optimum conditions. Quartz was chosen for studies on the mechanism of attachment in DAF since a great deal is already known about its surface chemistry and flotation properties. Cassiterite was chosen for the separation studies as a typical example of an oxide mineral with acute slimes problems and whose improved recovery could be of economical importance.

Chapter 2. THE DISSOLVED AIR FLOTATION PROCESS

2. THE DISSOLVED AIR FLOTATION PROCESS

2.1. Introduction

The dissolved air flotation (DAF) process may be regarded as consisting of four fundamental stages: a) air dissolution in water, which controls air availability for flotation, b) pressure reduction, which induces microbubble formation, c) microbubble-particle attachment, which determines eventual particle flotation, and d) the recovery of the floated product. This Chapter will be devoted to describing each of these stages and the current understanding of the fundamentals of their operation. Factors related to the mechanism of bubble-particle attachment will be stressed, engineering and design factors associated with DAF being considered briefly in the section dealing with industrial applications of the process (section 2.4). Finally, previous attempts to float minerals through processes relying on gas precipitation from supersaturated solutions will be reviewed.

2.2. Air dissolution in DAF.

The theoretical amount of air available for flotation at atmospheric pressure is proportional to the gauge saturation pressure P* at which air has been dissolved into the water. If Henry's law is assumed to be valid for the air-water system, available air and gauge saturation pressure are related through equation 2.1 which, expressed as a function of volume of saturated water, is:

$$V_a = K \cdot P^* \qquad (2.1)$$

where V_a = theoretical volume of dissolved air available for flotation at atmospheric pressure per litre saturated water

P^* = gauge saturation pressure (above atmospheric)

K = solubility of air per liter water at atmospheric pressure (18.7 cm^3/l at 20^oC (68)).

At the gauge saturation pressures normally employed in DAF (175 - 420 KP_a, or 25 - 60 psig) the theoretical supply of air available for flotation at atmospheric pressure is of the order of 25 - 62 cm^3 per litre of saturator feed at 20^oC. In practice, the amount dissolved in water depends upon the efficiency of the air dissolution mechanism used.

The most common systems used in DAF for the dissolution of air in water at pressures greater than atmospheric are:

ii) Sparged air system, where compressed air is bubbled through diffusers or eductors into water contained in a saturator at constant saturation pressure. The air saturation efficiency of this system depends heavily on the air flow-rate and the saturation time.

ii) Air injection system, where water is introduced at the suction side of a centrifugal pump and mixed with the water by the shearing action of the impeller after which the mixture passes through a pressurized vessel to allow for complete air dissolution.

iii) Packed column system, where water is percolated through a saturator filled with a packing in a pressurized air atmosphere. No air is bubbled through the water. The efficiency of this system depends on the surface area per unit volume of packing.

Comparative studies (69) carried out on these systems showed that the packed saturator mechanism was the most efficient air dissolution mechanism, attaining air saturation values very close (90%) to the theoretical amounts predicted by Henry's law. This system, however, was unable to achieve these air dissolutions at pressures lower than 3 atmospheres (gauge) unless long water residence times in the saturator

were allowed.

Tests on the pump suction-air injection system indicated that its main shortcoming was that insufficient gas could be introduced because of air-locking in the pump and, therefore, air dissolution values obtained were only about 25% of the theoretical maximum amount. Full saturation can only be achieved with this system by introducing air in a supplementary fashion, e.g. by sparging air into the saturator (70).

Theoretical saturation values were only achieved by the sparged air system at the expense of high free air flow rates (over 70 l/min) and long water residence times in the saturator (greater than 40 min). By comparison full saturation was attained by the packed saturator system with a water residence time of about 1 min at a free air flow rate of 20 l/min for the same saturation pressure (69). The efficiency of the sparged air dissolution mechanism can be improved by introducing some agitation during saturation (71) and, in fact, for batch bench-scale unpacked saturators it is recommended that the unit is shaken during dissolution of air (67).

Measurements of the dissolved air content of DAF waters (72) have confirmed that an unpacked saturator could provide only 60 - 70% of the theoretical maximum amount of air, this, however, being readily provided by a packed saturator. Nevertheless, it has been claimed that various sparged air dissolution systems worked at over 90% efficiency (71)(64).

2.3. Bubble formation in DAF.

2.3.1. General considerations.

It is known that bubbles form most readily in supersaturated liquids as the result of the growth of minute masses of undissolved gas existing

on solid particles contained in all liquids. In the absence of undissolved gas, bubbles form only as the result of increases in the local density of dissolved gas or vapour embryos induced by the supersaturation of the liquid; this latter mechanism is usually referred to as 'de novo' nucleation and can be homogeneous (bubble formation in the bulk of the liquid) or heterogeneous (at solid/liquid or liquid/liquid interfaces). Thus, bubble formation caused by supersaturation of a liquid and commonly produced as a consequence of phenomena such as heating, acoustic cavitation or hydrodynamic cavitation, has its ultimate origin in these mechanisms.

The existence of pockets of undissolved gas attached to cracks or crevices in particles in the liquid or on the walls of the container was postulated by Harvey et al (73) to explain ordinary bubble formation phenomena. They proposed that these masses would act as nuclei for bubble formation through gas diffusion from the supersaturated solution into these stabilized gas cavities. Bubble formation through 'de novo' nucleation is expected to occur only in the absence of these easily activated Harvey nuclei. It has been shown both theoretically and experimentally (74)(75)(76) that a very high degree of supersaturation is required for bubbles to nucleate 'de novo'. For example, temperatures of around 300^{o}C are required to induce boiling water free from nuclei. The main evidence for the existence of Harvey nuclei is that when gas cavities are removed (by subjecting the system to high hydrostatic pressure, for example) much higher values of superheat, tensile strength or cavitation threshold are required to induce bubble formation in the same system. A more complete description of bubble nucleation mechanisms is offered in Chapter 8 where experimental work on flotation utilizing Harvey nuclei on minerals is reported.

It is commonly explained in the DAF literature that the phenomenon of bubble formation in DAF results from the air-supersaturation of the liquid produced by the pressure reduction involved in the process. However, the fact that water can withstand high degrees of supersaturation without showing bubble formation (77)(78) suggests that supersaturation is the mere thermodynamic prerequisite, and that for the excess dissolved air to form bubbles requires some additional conditions. The formation of microbubbles, or indeed, how dissolved air comes out of the supersaturated solution in DAF is important in so far as it determines the mechanism of flotation. In particular, the question of where bubbles start nucleating is crucial to determining the relative importance or even existence of the various mechanisms of bubble-particle attachment believed to occur in DAF.

2.3.2. Mechanism of bubble formation in DAF.

Microbubbles form in DAF as the result of cavitation of the high-pressure saturated water when it flows through devices causing sharp pressure drops. Cavitation has been mentioned as one mechanism for bubble formation (79) and experimental evidence has been provided by work carried out at this Department (80)(81). Further evidence about microbubble formation in the DAF process may be found indirectly, by considering that all DAF systems described in the literature include some kind of flow constriction or nozzle acting as the pressure reduction device between saturator and flotation cell. Nozzles or pressure reduction devices usually found are needle valves, single orifice plates and multiple hole plates. A more comprehensive review of nozzle design was given by Urban (80).

Cavitation produced as the consequence of hydrodynamic phenomena

has been extensively studied and reported in the literature (82). Cavitation of liquids due to flow across pipe or valve constrictions has been found to originate in pressure drops close to the vapour pressure of the liquid (83). In DAF, where the liquid is water with a high content of dissolved air, the formation of bubbles from cavitation at the pressure reduction nozzle is enhanced by diffusion of air from the now highly supersaturated water into the vapour cavities which would have otherwise re-dissolved downstream of the nozzle.

Studies on microbubble formation in DAF systems using single orifice plates (80) and Venturi-type constrictions (81) as pressure reduction devices have yielded the following conclusions:

a) There is a critical injection pressure below which no microbubble formation occurs in the given apparatus; this is the "cavitation inception pressure".

b) Cavitation inception pressures were found to depend on orifice diameter and dissolved air content of the water and to be independent of water surface tension (80).

c) Upon pressure reduction in the orifice, the vapour cavities need time to grow to microbubble size.

d) The flow regime downstream from the orifice is critical in determining bubble growth, and hence, bubble size.

e) The shape and size of the nozzle downstream from the orifice are fundamental in controlling flow regime and growth time.

f) Bubbles start forming in the orifice at the point of lowest pressure according to the Bernouilli equation.

With regard to the site of bubble nucleation in these systems two possibilities arise: bubbles may form from nuclei contained in the water, "stream nuclei", or from gas cavities deposited on the walls

of the particular pressure reduction device, "wall nuclei". There is evidence in the literature of bubble formation arising from the activation of both kinds of nuclei. Knapp (84) showed the existence of stabilized gas nuclei as acting mechanism for cavity formation when carrying out dynamic tests on smooth, precision-made, glass Venturi tubes which had been subjected to high hydrostatic pressure. In unpressurized water samples, cavitation occurred in the Venturi throat at pressures very close to the vapour pressure whereas all pre-pressurized samples required negative pressures (100 - 300 KP_a) to show cavitation. Furthermore, Knapp showed photographs of a bubble appearing at the 'vena contracta' of the Venturi in a pre-pressurized sample test which might be evidence of nucleation from stream nuclei as photographic evidence indicates that bubbles start forming at the walls of unpressurized Venturi tubes (85). Cavitation inception pressures have been determined (81) for smooth glass Venturi tubes and no differences were found with respect to the onset of cavitation inception when these tubes were subsequently roughened, or rendered hydrophobic, or both.

Urban (80) considered the case of flow through single orifice plate (see Figure 4.2(b)) and concluded that bubble nucleation occurred at Harvey nuclei on the leading edge of the orifice. He photographed cavitation at the orifice plate indicating that a cloudy region characteristic of cavity formation appeared at the edges of the orifice and not in the bulk flow. It was found that water quality did not have an effect on bubble number density or bubble size. Pre-pressurization of orifice plates did have an influence on microbubble number density but in the opposite direction to that expected. With pre-pressurized nozzles more bubbles were produced with both glass and brass orifices

which, however surprising, shows that Harvey nuclei play a role in bubble nucleation phenomena in DAF. Unfortunately, no measurements of cavitation inception pressures with pre-pressurized nozzles were made, nor any test with pre-pressurized water was carried out. Further, it was shown that increasing the plate thickness up to 5 mm did not have an effect on microbubble production whereas an increase of the number of orifices in the plate at constant flow rate, e.g. an increase in the total available perimeter for nucleation, did increase the number of bubbles produced.

It may be argued however, that by increasing the number of orifices in the plate, the flow pattern downstream from the nozzle was being changed, favouring microbubble formation. The fact that bubble diameter diminished with increasing number of orifices might be an indication of this kind of flow regime effect on the downstream environment for bubble growth. Moreover, the results of another work (86) indicated that the number of bubbles produced was dependent on the thickness of the plate and therefore on nuclei not only situated on the edge of the orifice; hydrodynamic effects, however, may also have influenced the results of this latter work. Indeed, measurements of bubble-number density are not a very reliable guide to estimating the site of bubble nucleation due to their dependence on water surface tension and on flow pattern characteristics in the nozzle (Appendix I). Homogeneous turbulence seems to form smaller and more numerous bubbles while sharply turbulent regions, like those at orifice plates, causing large cavities or eddies result in larger and less numerous bubbles due to coalescence and diffusion phenomena.

Hence, there is no definite proof as to which nuclei bubble growth starts from, although there is experimental evidence of the existence

and action of Harvey nuclei, whether "stream" or "wall". It is also clear that microbubbles start nucleating at the orifice and not in bulk solution in the flotation cell. It is expected, therefore that in DAF processes where only water is pressurized (effluent recycle systems) the suspended phase would have no influence on bubble nucleation. Regarding bubble nucleation sites, much greater information on the location of primary activation nuclei would be found by carrying out tests with various independent pre-pressurizations of the nozzle and water and measuring cavitation inception pressures instead of bubble-number density as the relevant parameter.

2.3.3. Bubble size in DAF.

Bubble size has been reported to depend on nozzle geometry and flow regime characteristics downstream from the constriction (Appendix I) (80)(81)(86). Upon pressure reduction, the nascient cavities surrounded by supersaturated water grow in solution before they are diluted in the flotation cell. But, for instance, if nozzle geometry and flow regime allow for the formation of large eddies in which these cavities may circulate, then there would be a time residence distribution in the nozzle giving rise to a large microbubble size distribution, and even more important, to the formation of big bubbles (1 - 2 mm) which have a deleterious effect on flotation performance and are wasteful of air (1 mm^3 of air gives 2 bubbles approximately 1 mm in diameter or 15000 bubbles of 50 μm in diameter). Conversely, it is found experimentally that if the nozzle allows too short a residence time then no microbubble formation takes place irrespective of water supersaturation (80)(81) (Appendix I).

The equilibrium diameter of a single bubble formed from super-

saturated solution has been studied theoretically by various authors (87)(88)(74). Thermodynamic treatments based on the change of the Helmholzt free energy (ΔF) for bubble formation from supersaturated solutions predict that ΔF is critical for bubbles of diameter d_c given by the Laplace equation:

$$\Delta F = \frac{\pi d_c^2 \gamma}{3} \qquad (2.2)$$

$$\text{with } d_c = \frac{4\gamma}{P_g - P_l} \qquad (2.3)$$

where γ = gas/liquid interfacial tension

P_g = pressure in the gas bubble

P_l = pressure in the liquid

It has been shown by those authors that this theoretical "equilibrium" diameter corresponds to an unstable system.

The size of bubble formed under the conditions prevailing in DAF was studied theoretically by Urban (80). Assuming mass conservation of each solute in the system, the validity of the Laplace equation for mechanical equilibrium of the bubble, and that the final concentration of dissolved gas is in equilibrium with its partial pressure in the bubble, he derived the following equation for a single solute (air) in terms of the DAF operation parameters:

$$P_l - P_v = \frac{P_o}{1 + \frac{H\pi d^3}{6nRT}} - \frac{4\gamma}{d} \qquad (2.4)$$

where P_l = pressure in the liquid

P_v = water vapour pressure in the bubble

P_o = saturation pressure of the liquid

γ = air/liquid interfacial tension

n = moles of water per bubble

d = bubble diameter

R = gas constant

T = temperature

H = Henry's law constant

Theoretical plots of equation 2.4 showed that there are two bubble equilibrium diameters when the pressure is reduced from P_o to P_1 = 101 kPa (1 atmosphere), of the order of 1 and 100 μm, respectively referred to as d_s and d_1. The question of which diameter will arise in practice was studied by thermodynamic stability analysis based on the entropy changes of the bubble/liquid system as a function of the diameter of a single bubble forming from supersaturated solution. Urban found that only the large equilibrium diameter was stable; bubbles departing slightly from the unstable diameter d_s would either dissolve or, if larger than d_s, grow to their stable size d_1. It was indicated, however, that this growth process is diffusion controlled and therefore slow; it was also predicted that a bubble of equilibrium diameter d_1 would become unstable if another bubble was introduced into the liquid (i.e. only <u>one</u> bubble would be stable at the equilibrium diameter d_1). Again, this process is diffusion controlled and would be expected to have little influence given the time scale of DAF experiments.

Urban showed that equation 2.4 reduces to equation 2.3 for the smaller, unstable, bubbles of equilibrium diameter d_s. The existence of two "equilibrium" sizes may account for most of the experimental observations concerning microbubble generation in pressure reduction devices; some experimental results interpreted by this theory are described in Appendix I.

2.3.4. Influence of DAF operation parameters on microbubble production.

Most experimental work on this problem has been confined to seeking a relationship between optimum flotation and air-to-solids mass ratio (A/S ratio) from which DAF equipment could be designed. Only two works have been published (80)(86) with more fundamental studies on the effect of operation variables on some basic microbubble production parameters.

The basic parameters that have been measured are mean bubble diameter, bubble-number density, the fraction of air released as bubbles, and the risetime of the microbubble swarm. The operation variables most usually considered at industrial level are saturation pressure (which determines eventual supersaturation of the water and the injection pressure at which this water is fed into the flotation chamber) and percent recycle (which controls the total amount of air added to the solids). On a laboratory scale, however, the pressure reduction device and injection pressure may be operation variables as well.

In their experiments, Takahashi, Miyahara and Mochizuki (86) varied pressure reduction characteristics, supersaturated water flowrate and saturator pressure. They used an unpacked saturator dissolving air via a sparger. The nozzles used as pressure reduction devices were single orifice plates of varying thickness (t = 0.2 - 5.0 cm) and diameter (D = 0.2 - 0.4 mm), and a needle valve. Few indications were given of the experimental procedure but mean bubble diameter was measured from photographs and the amount of air released from air flow rate measurements in the flotation vessel; the number of bubbles produced was calculated from the amount of air released and the mean bubble diameter.

Urban (80) measured all four basic microbubble production parameters

mentioned above using single orifice plates of constant thickness (t = 0.125 mm) and varying diameter (D = 0.7 - 2.02 mm). The apparatus he used is described in more detail in Chapter 4. The procedure was to make injections of high pressure air-saturated water into a beaker and take photographs of the microbubble swarm to determine bubble diameter and number. Microbubble rise times were determined visually and the amount of air released by the volumetric displacement of water, this latter method was inaccurate giving in some cases values higher than the theoretically possible. Urban considered the effect of orifice diameter, injection and saturation pressures, the volume of supersaturated water injected into the beaker (equivalent to percent recycle) and water surface tension.

The findings of these researchers and other related work have been summarized below in terms of microbubble parameters.

2.3.4.1. Mean diameter of microbubbles ($\overline{d}$). It was found that $\overline{d}$ depends inversely on saturation pressure as predicted theoretically. Increases in injection pressure or water flowrate slightly decreased the bubble diameter. The value of $\overline{d}$ was also lowered by a decrease in water surface tension. The dependence of bubble size on nozzle geometry was demonstrated in both investigations. Urban found that microbubble size depended quadratically on orifice plate diameter, $\overline{d}$ being minimum at about 1 mm orifice diameter. Takahashi et al found that an increase in plate thickness produced larger bubbles, an effect that diminished as saturation pressure was increased. In Urban's work, however, it was established that bubble diameter was independent of plate thickness for values of t up to 5.35 mm. These differing results may stem from the hydrodynamic conditions prevailing in each

nozzle and which may be shown by the thickness to orifice diameter ratio (t/D) range used in each work; Urban only worked with values of t/D up to 3.8 whereas Takahashi et al measured in the broader range t/D = 5-200.

It was found (86) that mean bubble diameter varied with sampling point in the flotation vessel, that is, bubbles grew as they rose up to the liquid surface. This increase in $\bar{d}$ may be interpreted as a consequence of the destabilization of "stable" equilibrium diameter bubbles which grow at the expense of smaller ones as discussed in section 2.3.3. Other possibilities, however, cannot be ruled out because of insufficient information about experimental procedures. Urban reported constant bubble size with sampling time but his sampling point was at 17 cm above the injection point compared to 99 cm in the flotation vessel used by Takahashi et al. Some degree of coalescence may also occur in the rising microbubble swarm (80)(81). It would be important for industrial DAF equipment design to determine whether bubble growth with height (or time) is a real effect because of its likely impact on flotation performance.

2.3.4.2. Bubble-number density (N_b). The pressure of saturation substantially increased the number of bubbles produced, as would be expected, due to the higher dissolved air content of the water. Bubble-number density was found to increase with higher water flow rates or injection pressures although the latter only occurred in the absence of surfactants. A decrease of the liquid surface tension also increased N_b, probably because of its action in preventing coalescence. Urban found that bubble-number density was a quadratic function of orifice diameter, passing through a maximum at values of D corresponding to minimum mean bubble diameter (at D = 1 mm). N_b was also found to be

directly proportional to the amount of supersaturated water injected into the cell.

Takahashi et al established relations for the variation of bubbles produced as a function of saturation pressure (P_o), supersaturated water flow rate (Q) and nozzle geometry expressed as the t/D ratio. Generally, they found that N_b was proportional to the degree of supersaturation and to the flow rate though in a different fashion for each nozzle. The relations they gave were:

for short nozzles, $N_b = 0.45 \times 10^4 \, (t/D)^{\frac{1}{2}} \, \left(\frac{P_o - P_a}{P_a}\right)^{3/2} Q^{\frac{1}{2}}$ (2.5)

$5 \leqslant t/D \leqslant 20$

for long nozzles, $N_b = 4.5 \times 10^4 \, (t/D)^{-\frac{1}{2}} \, \left(\frac{P_o - P_a}{P_a}\right)^2 Q$ (2.6)

$50 \leqslant t/D \leqslant 200$

and for the needle valve, $N_b = 1 \times 10^4 \, \left(\frac{P_o - P_a}{P_a}\right)^2 Q$ (2.7)

where P_a = atmospheric pressure.

Hence, for thin orifice plates the dependence of N_b on P_o and Q is less critical than for a thick plate or a needle valve. Orifice diameter has a different effect on microbubble production according to whether it is a short or long orifice plate; for short nozzles increases in diameter decrease the number of bubbles produced whereas for long ones it has the opposite effect. From the above equations it is possible to deduce that for constant supersaturation and flow rate, the number of bubbles produced decreases in the order short nozzle > needle valve > long nozzle. The inefficiency of the long (or thick) orifice plates of the kind used by Takahashi may be associated with both the absence of sharp pressure drops and the flow regimes developing at those values of t/D. Indeed, it has been shown (Appendix I) that by increasing its length sufficiently, no microbubbles are formed in a capillary tube

for saturation pressures up to 673 kPa (80 psig), in line with the previous discussion on microbubble formation.

2.3.4.3. Rise-time of microbubbles. The normal bubbles produced in DAF (50 - 100 μm size range) rise under laminar flow conditions in water at a velocity determined by Stoke's law. The time that the microbubbles take to rise a pre-determined height in the liquid or to disappear from solution after an injection of supersaturated water is defined as the rise-time. Some authors (79) have measured rise-times to give an indication of the size and amount of microbubbles generated under particular DAF conditions. Since microbubbles cannot be followed individually, what is noted is the degree of "milkiness" produced in solution after an injection of supersaturated water, and the time this "milkiness" takes to reach a certain level in the vessel under standard conditions. Some authors working on thickening of activated sludge by DAF measured the rate of rise of bubble-particle agglomerates for assessment of flotation performance (89) or design purposes (90).

Measurements of microbubble rise-times in water (80) established that for a given amount of dissolved air, rise-times are inversely proportional to microbubble size. The effect of bubble-number density on rise-time will depend on the fractional volume occupied by the bubbles since the displaced liquid will hinder upward movement. Variations of bubble-number density corresponding to 0.4 - 1.5% by volume showed no effect on rise-times (80). Therefore, within that fractional volume range, higher rise-times will predict greater densities of smaller bubbles (for a constant release of dissolved air).

2.3.4.4. Fraction of air released. This is the parameter that has

been most usually measured in the DAF literature but given its dependence on saturator and pressure reduction efficiency results are not easy to interpret. The experimental quantity commonly measured is the volume of air released as bubbles which, divided by the theoretical amount of dissolved air calculated from Henry's law, gives the fraction of air released. Therefore, the volume of air released should be expected to be directly proportional to the saturation gauge pressure as it determines the amount of excess dissolved air in water.

Indeed, Bratby and Marais (69) found that the amount of released air was a linear function of saturation pressures for values above 300 kP_a; below this pressure the dependence was not linear because, in the opinion of the authors, the air dissolution efficiency of the saturator was poor at low pressures. Urban (80) found that the volume of air released increased with saturation pressure but that the fraction of air released diminished. This latter effect may be related to inefficient air dissolution in the saturator or to a decrease in nozzle efficiency as saturation pressure rises. It is worth noting that Urban's measurements of released air gave erratic results and, as mentioned, some of them were greater than the theoretically expected values. Interestingly, he found that the volume of gas evolved depended slightly on the diameter of the orifice plate used as nozzle therefore giving evidence of nozzle efficiency being a factor in determining the fraction of air released.

Takahashi et al (86) also found that nozzles behaved differently in their ability to release air. For short nozzles the fraction of air released was quite high (above 80% of the theoretical amount) whereas for the long ones efficiency was much lower and decreased as the ratio t/D increased. Generally, nozzle efficiency, as measured

by the fraction of air released improved with high saturation pressures (greater than 300 KP_a); this was particularly so in the case of the needle valve tested. The fraction of air released was found to depend somewhat on supersaturated water flow rate as well, a result that would confirm the influence of flow regime on microbubble formation suggested earlier.

Zabel and Hyde (72) measured the dissolved air contents of the pressurized water in the saturator and the liquid in the flotation vessel after an injection had been made, the difference representing the actual amount of air liberated upon supersaturation. Since the dissolved air is measured in solution, this method allows the real saturation efficiency, as well as the efficiency of the nozzle, to be determined. Unfortunately, these workers did not publish a detailed description of their experiments but presented the quantity of air released as a function of saturator pressure. They showed results for two kinds of saturators, packed and unpacked. Volumes of released air from the unpacked saturator were much lower (around 50% of the theoretical value) than the packed unit ones which gave values close to the theoretical amount for pressures up to 300 kPa (gauge). The curves showed linear dependence of air released on saturator pressure up to pressures of about 250 - 300 KP_a, after which both curves flattened out. This behaviour, independent of saturator used, might indicate that the nozzle becomes inefficient with increased saturator pressure, showing the importance of nozzle design in the release of dissolved air.

The fact that nozzles are a factor in the release of dissolved air was previously established by Maddock (79) who tested five different needle valves with the result that only two could release about 100% of the dissolved air. Most investigators implicitly assume that the

pressure reduction system would release all the excess dissolved air when measuring the saturator efficiency. The theory and results discussed in this section on microbubble generation in DAF nozzles indicates that to consider the amount of released air a function only of the efficiency of the saturator in dissolving air might be a mistaken assumption.

2.4. Particle-bubble attachment in DAF.

This particular step of the DAF process has been the least studied of all. Vrablik (67) stated that attachment of bubbles to particles in DAF may be proceeded by three mechanisms, namely,

i) adhesion of a gas bubble to the suspended solids

ii) physical entrapment of rising air bubbles in floc structures

iii) "absorption" or "incorporation" of a gas bubble as the floc structure is formed.

It was pointed out by Vrablik that adhesion may be established as the result of collisions between bubbles and suspended solids or because of direct precipitation of the gas phase onto the solids.

No experimental work has been published on the actual mechanisms of bubble attachment for any DAF process. Given the importance of establishing conditions under which microbubbles are able to selectively attach to mineral particles, undertaking experimental work on the mechanism of bubble-particle attachment seems essential. The probability of existence of the three mechanisms is discussed below.

Adhesion of bubbles to particles as the result of collisions is the mechanism by which bubble-particle attachment takes place in conventional, dispersed air flotation (Chapter 1, sections 1.1 and 1.3). For bubble and particle to form a stable attachment on collision, the

formation of a contact angle between the bubble and the solid surface is essential. On the other hand, the phenomenon referred to as direct precipitation of air bubbles onto the solids may, theoretically, be the consequence of either heterogeneous 'de novo' nucleation, or formation of air bubbles from Harvey nuclei. Whichever the nucleation mechanism, the existence of a contact angle between the air bubble and the surface is inherent in bubble formation on the solid. Therefore, the role that adhesion plays in the mechanism of attachment can be studied by changing the hydrophobicity of the mineral surface.

The relative contributions of collision and air precipitation to the adhesion mechanism of attachment would be determined by the mechanism of bubble formation in the particular process under investigation. Collisions would be expected to be the major component in the effluent recycle systems where bubbles are generated away from the solids in the pressure release device as described in section 2.3.2. The possibility of air precipitation from supersaturated water playing the major part in bubble-particle attachment is most likely to occur in those systems where the full influent is pressurized. Under these conditions, air has the highest probability of nucleating during pressure reduction at sites on the surface of the suspended solids.

With regard to the occurrence of mechanisms ii) and iii), it may be deduced on the basis of their definition that a) they require an aggregation step and b) their relative contributions would depend on whether aggregation of the suspended solids takes place before or simultaneously with microbubble injection. Furthermore, these mechanisms of bubble-particle attachment do not rely on the surface properties of the solids but rather on the physical characteristics of the floc structure being formed. The mechanisms, as defined, are non-

selective and any floc structure capable of "trapping" microbubbles because of its surface irregularities would be expected to be floated regardless of the surface properties of the individual particles. In this regard, no industrial DAF operation has been reported in which surface-active agents are used as flotation aids. Conversely, there are very few DAF operations which do not employ reagents to induce the aggregation of the suspended phase. Even in those applications where destabilizing agents are not added (as in DAF of activated sludges), it is recognized that those sludges are naturally aggregated because they usually contain hydrolyzing metal cations (71).

The need for prior aggregation to obtain efficient DAF performance is widely acknowledged in the literature (91)(92)(93)(72). Polyelectrolytes and metal salts are commonly used to induce aggregation of the suspended solids. It is not clear, however, whether flocculation of the solid phase merely optimizes the performance of DAF as a solid/liquid separation process or is crucial in determining the attachment of bubbles to particles. If aggregation of the suspended phase was found to be critical for attachment to occur, then a requirement in a selective DAF process would be selective aggregation of the species of interest, in itself a major problem in a mixed mineral system.

Finally, the role of contact angle is unclear. Pearson and Shirley (94) found that the recovery of precipitated metal hydroxides by DAF was improved with the addition of a collector. Other authors explicitly state that the DAF method permits the flotation of hydrophilic particles (91)(95) although it is known that many of the influents treated by DAF carry small amounts of natural surface-active agents in solution (92)(96). It seems essential that the influence of hydrophobicity in the mechanism of bubble-particle attachment be studied as

an indispensable requirement for seeking ways whereby DAF can proceed selectively.

2.5. Industrial practice.

2.5.1. Applications.

Dissolved air flotation is now an established procedure in several solid/liquid separation processes. Lundgren (97) has classified its applications into the following categories: a) product recovery; b) water clarification; c) sludge thickening, and d) energy recovery. Some examples of applications of DAF in these areas are recorded below, operational details of specific average examples are shown in section 2.5.4.

i) Paper industry, which was the first to apply DAF (97) for treatment of paper machine white water and recovery of valuable fibres, water and heat.

ii) Meat packing and food processing industries, for recovery of fats and greases which may be reused as supplementary fuels (98).

iii) Petrochemical industry, for removal of oil from petrochemical plant effluents (65) and from oil refinery wastewaters (92).

iv) Metallurgical industry, for effluent treatment in metallurgical operations and steel mills for the removal of toxic and valuable metals (94).

v) Wastewater clarification is a chief application of DAF, being marginally superior to sedimentation because of improved algae recovery (99), lower capital costs and the production of sludges with a higher solids content (97).

vi) Sludge thickening, the production of sludges with higher solids content is the key reason for the utilization of DAF for sludge

thickening in municipal and industrial treatment (64).

2.5.2. Equipment.

With regard to air dissolution systems, packed saturators have steadily replaced the original pump suction system because of their higher air dissolution efficiency although there is extensive use of sparged-air saturators in the industry.

The most common pressure reduction devices are needle valves, back-pressure regulating valves, and specially made nozzles like the WRC Air Injection Nozzle, designed and patented by the Water Research Centre (100).

Flotation units are basically of two kinds, circular and rectangular. All designs aim, however, at attaining the maximum intimacy between wastewater feed and supersaturated water at the point of pressure release. The actual point of pressure release has not been found to be critical to flotation performance (70); however, Packham and Richards (91) suggested that it be remote from the area where the floated material is to be skimmed, to prevent disruption from free air bubbles escaping at the nozzle. Vrablik (67) reported a design for partial pressurization of the influent in which wastewater feed and the pressurized stream flow through concentric pipes which are arranged tangentially to the flotation cell. Van Vuuren et al (101) designed a circular cell for algae reclamation that combines flotation and sedimentation. The fully pressurized influent is fed at the bottom of the centre part acting as flotation cell contained in an outer part which also allows for sludge collection at its bottom. In the Komline-Sanderson rectangular units (64) widely used in the U.S. for sludge thickening, the sludge feed and the supersaturated recycle are mixed in an inlet chamber

prior to flotation in the whole unit. The flocculant, if required, is added in this inlet chamber.

Removal of floated material is critical in determining the quality of the treated effluent, continuous skimming being recommended for producing high-quality effluents (72). Disruption due to float skimming has been solved by Bratby and Marais (70) by installing vanes in the top of the flotation tank; they should be arranged radially for circular units or perpendicularly to the direction of the scraper for rectangular ones.

2.5.3. Design.

The primary consideration for designing a DAF process is whether the system will work on a full influent, partial influent or effluent recycle pressurization basis. Lately, the effluent recycle pressurization system has been consistently preferred because flocculated material tends to break up more easily in the influent pressurization systems. An advantage of these latter systems is that lower levels of water supersaturation, e.g. lower saturator pressures, are required for optimum flotation (70). As full influent pressurization may require an excessive saturator size to treat the whole feed, partial pressurization of the wastewater influent or recycle and pressurization of a portion of the clarified effluent may be adopted instead. The effluent recycle pressurization system has the disadvantage that the total hydraulic loading to the flotation unit is increased.

There are several methods in the literature (90)(102) for designing a full DAF plant from laboratory data. While it is accepted that data obtained from batch testing cannot be used to accurately design a DAF cell because of the many factors affecting batch flotation tests that

are not present in continuous operations (70), their use for evaluating the performance and dosage of flocculants has been recommended (72)(92). Hence, "jar" tests have been extensively used to predict a reagent's optimum dosage at full plant scale.

Usually, design procedures are aimed at calculating the dimensions of the flotation equipment, particularly the area of the flotation unit. Design methods have been proposed (70) which make allowance for the dimensions of the saturator and the height as well as the area of the flotation cell. Critical factors in design are: air-to-solids mass ratio (A/S), hydraulic flow rate (Q), solids loading rate (Q_s) and float solids concentration (C_f).

A DAF design has been proposed by Bratby and Marais (102) based on data obtained from continuous testing. They have applied their method to algae removal (93), activated sludge mixed liquor flotation (103) and to thickening of brown water sludges (104). Their design method considers both clarification and thickening purposes and it is characterized by three basic equations which contain six variables and eight constants. The variables they considered were: the effective downward velocity of the liquid, the air-to-solids mass ratio, the float solids concentration, the depth of float solids above and below water level, and the solids loading rate. They found that for an operation requiring clarification and thickening there were several combinations of the critical variables that would achieve the required float solids concentration, and therefore, they concluded that the optimum combination should be drawn from an economic analysis of how each variable influences the capital and operation costs of the particular DAF process studied.

Gulas et al (90) have proposed a design procedure based on batch

flotation tests for application to the thickening of activated sludges. Their design procedure considers the activated sludge properties but fails to take into account the proven solids loading rate factor. More practical aspects of DAF design may be found in the reviews of Packham and Richards (91) and Bratby and Mavais (70). The work carried out by the Water Research Centre on the use of DAF for water treatment (99)(105)(72) is illustrative of the design of factors influencing the flocculation stage of DAF.

2.5.4. Performance.

The factors influencing the performance of a DAF operation have been discussed in the preceeding sections. The influence of air-to-solids ratio, solids loading rate or flocculation on the performance indicator may be correlated with phenomena occurring at a microscopic level; it is beyond the scope of this work to make such a correlation. Rather, typical examples of flotation operations with data on the parameters affecting their performance will be shown. Table 2.1 lists ten examples of processing by DAF of the following influents:

1. Biologically treated oil refinery wastewater
2. Emulsified oil refinery wastewater at pilot plant scale
3. Oil refinery wastewater (recycle system)
4. Oil refinery wastewater (full influent pressurization system)
5. Chemical process industry wastewater (cosmetic manufacturer)
6. Thickening of activated sludge (Columbia Corp. Wallonsac, New York)
7. Thickening of activated sludge (City of Hamilton Wastewater Treatment Plant, Canada)
8. Raw domestic sewage at pilot plant scale (lime precipitation followed by DAF)
9. Food processing wastewater

Table 2.1. Performance of various DAF systems

Influent	Pressurization	Reagents(?) (mg/l)	Saturation pressure (kPa) (absolute)	Effluent Recycle	Air-to-Solids mass ratio	Hydraulic loading (m^3/m^2d)	Influent (mg/l)	Removal (%)	% Solids in float	Observations	Ref.
1	Recycle	50 Alum 4 Polymer	-	34%	0.67	40.9	50 SS 220 TOG	48 SS 96 TOG	5.2 SS 34 TOG		66
2	Recycle	15 Polymer	345	50%	-	110.0	747 oil	98.6oil 96 SS	50 oil	32 min floc flotation	92
3	Recycle	No	276	33%	-	134.5	270 oil	60 oil	-	23 min flotation time	106
4	Full	Yes	276-345		-	134.5	112 oil	65 oil	-	20 min flotation time	92
5	Full	No	-		0.007	93.0	5000 SS 450 TOG	25 SS 44 TOG	6.2 SS	Cost 0.03US /1000 gal	66
6	Recycle	40 Alum 0.5 Polymer	414-483		0.04	117.0	180 - 200 SS	95 SS	-	0.04US/ 1000 gal	64
7	Recycle	Polymer	435	15%	0.013	-	13200 SS	99 SS	5.4 SS	42% air sat. efficiency	71
8	Recycle	16 $FeCl_3$ 0.3 Polymer	451	50%		351.4	25.2 phosphorous 133 SS	98.5 phosphorous 100 SS		250mg/l $Ca(OH)_2$ 0.024US/ 1000 gal	108
9	Full	30 Alum 0.05 Polymer	- -		0.07	33.3	200 SS 1160 TOG	80 SS 69 TOG	2.9 SS 11 TOG		66
10	Recycle	175 Alum	310	18%	0.019	139.0	125 SS	90 SS	1 SS		107

SS = suspended solids; TOG = total oil and grease; Influents are described in Section 2.5.4.

10. Algae removal at pilot plant scale

2.6. Flotation of minerals by bubbles formed from supersaturated solutions.

2.6.1. Vacuum flotation

Vacuum flotation is the oldest example of mineral flotation by means of gas bubbles nucleating from supersaturated solution. In 1904 Elmore (109) patented a vacuum flotation cell; this method, however, was quickly superseded in the field of mineral processing by the rapid development of dispersed air flotation machines.

The major engineering problem encountered with vacuum flotation is the recovery of the floated products out of the low pressure region on a continuous machine.

Nevertheless, vacuum flotation has been extensively used on the laboratory scale for determining the incipient flotation conditions of minerals. Schuhman and Prakash (110) first introduced vacuum flotation to determine the effect of several activators on the flotation of quartz. Their experimental technique consisted of conditioning the minerals at various pH and activator concentration values in rotating cylinders after which a vacuum was applied and the degree of flotation recorded. Later, Joy et al (111) used a vacuum flotation technique to determine the limiting flotation conditions of various silicate minerals.

The application of vacuum to produce supersaturated solutions has been proposed by Lin (112) as a method of measuring contact angles in solution. The technique relied simply on vacuum to induce the formation of bubbles on the submerged surface of a mineral in the presence of a reagent solution. He reported that contact angle measurements on the quartz/dodecylamine system gave similar results

to the captive-bubble technique but with improved reproducibility because, it was claimed, the bubbles grew at specific sites on the surface.

More recently work on vacuum flotation has continued with a study of the kinetics of batch vacuum flotation (113) and theoretical and experimental work carried out by Huber-Panu and co-workers (114)(115) and Klassen (60). Huber-Panu et al (115) carried vacuum flotation tests out on various mineral mixtures (galena/quartz, blende/quartz, pyrite/quartz) and found that vacuum flotation gave better recoveries and grades than conventional flotation, particularly at the fine particle size ranges (smaller than 10 μm). They also found that the quality of the concentrate depended on the concentration of collector and frother, the degree of vacuum supersaturation applied and the pulp residence time in the cell. It was also shown that the kinetics of vacuum flotation were higher than those of dispersed air flotation and that the experimental results fitted their theoretical model well (114).

Klassen (60) summarized work carried out in the Soviet Union until 1960 concluding that the precipitation of gas from supersaturated solutions could be of use in mineral flotation by enhancing the recovery of fine mineral particles, improving the flotation of coarse size particles and by increasing the rate of flotation. Continuous vacuum flotation tests were reported on a finely ground barite ore (- 10 μm) with sodium oleate as collector, yielding substantially better barite grades and recoveries than conventional flotation in this fine particle size range.

Regarding the mechanism of bubble-particle attachment in vacuum flotation, it is believed (80) (Chapter 8) that bubbles grow on the

hydrophobic mineral surface as the consequence of air diffusion into pre-existing cavities filled with undissolved gas present in the solid. Bubbles may also be seen forming in the bulk solution (60) and therefore the possibility of some particles being captured on collision cannot be ruled out. Even though vacuum flotation requires some favourable surface conditions, aggregation of the particles has not been reported to be necessary although the formation of hydrophobic aggregates is usually observed in vacuum flotation tests (111)(116).

2.6.2. Dissolved air flotation

There have been few attempts to float minerals by DAF reported in the literature. Urban (80) attempted the separation of graphite from quartz by DAF as a corollary to his work on bubble formation in DAF. Shalih (116) tested the selectivity of the process for a range of mineral mixtures and Shimoiizaka et al (117) have recorded work on flotation of kaolinite with various reagents.

Urban carried out his flotation work in the apparatus described in Chapter 4 of this thesis. Supersaturated water was injected into a 2 g/l mineral suspension (50% synthetic graphite) after conditioning with reagents (polyethylene oxide, quebracho) at the required pH. Results showed that selectivity was achieved but only at the cost of very low graphite recoveries (20-30%). The interpretation of the results in terms of surface chemistry is difficult because no such measurements were carried out by Urban.

It seems difficult to relate Urban's results to a mechanism of bubble-particle attachment given the lack of information on the system. However, the importance of flocculation was underlined by the effect of polyethylene oxide concentration on graphite. The failure to

selectively float graphite from quartz might be ascribed to the failure to selectively flocculate the graphite. The effect of hydrophobicity is less clear as Urban found that the naturally hydrophobic graphite particles would not float on their own while a hydrophilic mineral like quartz would float well in the presence of polyethylene oxide (but only in tap water). It was concluded that the selectivity of DAF would depend on correctly controlling surface phenomena on the minerals and on their selective flocculation. Urban also concluded that froth behaviour and float stability in DAF required a special study.

Shimoiizaka et al (117) reported DAF of kaolinite with various reagents, namely, dodecylamine (pH 3.0 - 3.5), aluminium sulphate (pH 5.8 - 6.7) and a commercial flocculant, Separan NP10 (pH 3.5 - 3.7). They conditioned the mineral with the required reagent and then injected supersaturated water (150 ml) into a flotation cell containing the suspension (400 ml). These authors found that there was an optimum concentration for the DAF of kaolinite with dodecylamine and Separan NP10 above which flotation recovery decreased. With aluminium sulphate the recovery tended to plateau with increasing salt concentration. When no reagents were added kaolinite recovery was about 30%.

A comparison between dispersed and dissolved air flotation systems was also carried out by Shimoiizaka et al on the effect of solids concentration on recovery. With the dispersed air flotation system (Denver Sub A) optimum recovery was constant for the kaolinite/dodecylamine system over the range 0.2 - 1.0% solids whereas recovery decreased above 0.5% solids when using DAF. They also reported that at low concentrations of dodecylamine (less than 10^{-4} M) kaolinite recoveries were much higher with the DAF system than with the Denver cell. The

decrease of DAF recovery with increasing solids concentration was most drastic for Separan NP10 with which no flotation occurred over 0.3% kaolinite. Hence this work showed clearly that the process has limitations even in the case of the flotation of a single mineral. The lack of measurements of the kaolinite/solution interface in the presence of the reagents used prevents any correlation between the surface chemistry and the DAF of the mineral.

Shalih (116) attempted selective DAF of various fine mineral mixtures but the most extensive tests were carried out on the malachite/calcite and fluorite/calcite systems. He used vacuum flotation and Denver cell testing to determine the optimum flotation conditions for each system. It was reported that calcite, fluorite and quartz would float under vacuum only in the presence of suitable amounts of collector, while in the absence of collector no flotation would take place but many small bubbles would rise up. Interestingly, galena in the presence of potassium ethyl xanthate (KEX) showed no flotation behaviour under vacuum, the addition of a polymer made improvements in recovery but total flotation only occurred when KEX was replaced by dodecylamine as collector.

Most of Shalih's work on DAF was carried out in a batch single stage column. No work on microbubble formation in the system was reported. The mineral slurry was conditioned in a tank and them mixed with super-saturated water flowing through a nozzle, this mixture was then transported through 100 meters of plastic tubing of 3.6 mm diameter before entering the flotation column, where a subsequent addition of supersaturated water was made at the base of the column. The mineral particles were injected above the base of the column which was filled with water. Two saturators were used to provide supersaturated water to the mineral particles prior to and in the flotation column respectively. Air and

carbon dioxide were used more or less arbitrarily in both vacuum and DAF tests.

Shalih attempted the recovery of malachite from calcite with KEX as collector preceeded by sulphidization with sodium sulphide. Extensive tests of the system in the presence of various modifiers yielded no selective separation of the minerals by DAF. The addition of oleic acid plus quebracho as modifier did not improve malachite flotation although malachite floated well in the presence of oleic acid in vacuum flotation tests. Tests on less complicated systems like fluorite/calcite or even galena/quartz also failed; nor could galena be floated by DAF in the presence of KEX or a cationic collector (Armac C) which led Shalih to speculate on the effect of the mineral's specific gravity on particle-bubble attachment in DAF. Other conclusions he arrived at were that flocculation of the mineral particles in the column was essential for DAF to be successful, and that DAF tests on a batch basis were not representative because of the changing chemical environment to which the particles were subjected. More extensive tests were carried out with a multi-stage flotation column with facilities for rougher, scavenger and cleaner stages. These tests also failed to attain selectivity for the malachite/quartz and galena/quartz systems with a number of reagents.

The work of Shalih has many shortcomings but it illustrates the complexities involved in recovering minerals by DAF; mixtures which would separate with relative ease in dispersed-air flotation were not floated by this process. The three works reviewed indicated that the mineral surface characteristics were important in DAF and that selective flocculation was a prerequisite for the process to act selectively in finely-divided pulps; none of them, however, stated unambiguously under

which conditions the DAF-produced microbubbles would attach themselves selectively to a mineral surface.

2.7. Summary.

a) Despite the widespread use of dissolved air flotation in solid/liquid separations, little research has been carried out into the fundamental aspects of the process. Examples of industrial DAF operations have been given and equipment, design and performance factors have been briefly discussed.

b) Microbubbles form in the DAF process as the result of sharp pressure drops imposed on the pressurized water at the pressure reduction nozzle. Microbubble formation also depends on factors associated with nozzle geometry and flow regime. It is unclear whether bubbles start forming from nuclei situated on the nozzle or contained in the liquid.

c) Theoretical studies of the equilibrium size of bubbles formed from supersaturated solutions have been briefly outlined. Theoretical studies of the equilibrium of bubbles formed under the conditions prevailing in DAF predict the formation of bubbles of a size which agrees well with experimental data. The influence of the DAF operation parameters on microbubble production characteristics has been discussed.

d) The probability of occurrence of the various mechanisms of particle-bubble attachment proposed in the literature has been discussed. The role of aggregation of the suspended phase and of the contact angle are unclear. Work on dissolved air flotation of minerals has been reviewed; no successful selective separations have been reported.

e) Elucidation of the mechanism of bubble-particle attachment in DAF is an inescapable prerequisite for rationalizing selective separations. The mechanism of attachment in DAF may be studied by correlating the flotation behaviour of a solid with phenomena occurring at the solid/liquid interface. The use of a well-characterized mineral surface as model solid may be useful for correlation purposes.

Chapter 3. THE OXIDE MINERAL/AQUEOUS SOLUTION INTERFACE

3. THE OXIDE MINERAL/AQUEOUS SOLUTION INTERFACE

3.1. Introduction

The dissolved air flotation studies were carried out using finely-divided oxide minerals (quartz, cassiterite) as model solids, the mechanism and performance of the process being correlated with phenomena occurring at the oxide mineral/aqueous solution interface. Generally, the dissolved air flotation of quartz and cassiterite was correlated with their electrical double layer properties, the adsorption of surface-active agents which acted as collectors for these minerals and the stability of their suspensions. Therefore, the basic principles governing these interfacial phenomena at the oxide mineral/aqueous solution interface have been briefly outlined in this Chapter. In addition, a short literature survey on the surface properties and flotation of cassiterite is included. The surface chemistry of quartz is discussed in Chapter 5 in connection with the results of this work.

3.2. Electrical phenomena at the oxide mineral/aqueous solution interface.

Oxide minerals are characterized by the hydration of their surface caused by the multimolecular adsorption of water vapour (5). Upon rupture of an oxide, bonds are broken and the exposed surface atoms hydroxylate in an attempt to complete their coordination shell. The presence of hydroxyl groups on the surface of a number of oxide minerals has been detected by infrared spectroscopy studies (118).

When the oxide mineral is immersed in aqueous solution, an electrical charge originates on its surface due to the adsorption or desorption of hydrogen ions from the hydroxylated surface, viz

$$MOH_{(s)} + H^+_{(aq)} \rightleftharpoons MOH_2^+{}_{(s)} \quad (3.1)$$

$$MOH_{(s)} \rightleftharpoons MO^-_{(s)} + H^+_{(aq)} \quad (3.2)$$

Where M is the metal ion on the oxide surface and the subscripts denote surface and aqueous species. From these charging mechanisms it follows that H^+ and OH^- ions act as potential-determining ions for oxide minerals. Parks and de Bruyn (119) have proposed an alternative charging mechanism involving the surface adsorption of charged hydroxo complexes formed by the partial dissolution of the oxide. However, as the formation of these complexes is also pH-dependent it is not possible to distinguish between both surface charging mechanisms and, therefore, the total surface charge (σ_o) of an oxide mineral is usually defined as

$$\sigma_o = F(\Gamma_{H^+} - \Gamma_{OH^-}) \quad (3.3)$$

where Γ_{H^+}, Γ_{OH^-} = surface excess or deficiency of hydrogen and hydroxyl ions per unit area

F = Faraday constant

Thus the surface charge can be experimentally determined by measuring the difference of the adsorption desntities of the potential-determining ions.

An important double layer parameter for minerals is the point of zero charge (PZC). The PZC is defined as the negative logarithm of the activity of the potential-determining ion at which the net surface charge is zero ($\sigma_o = 0$). Thus for oxides, the point of zero charge occurs at a characteristic pH which has been postulated to depend on the cationic charge and its radius (120).

The surface charge of the mineral particle induces orientation of the ions in solution forming a counter charge thus maintaining electroneutrality. The distribution of charges on the surface and in

the solution is called the electrical double layer of the particle. The charge distribution in solution is referred to as the diffuse part of the double layer or as the Gouy layer. Theoretical treatments regarding the structure of the double layer were formulated independently by Gouy (121) and Chapman (122), further modifications being introduced by Stern (123) and Grahame (124).

The electrochemical double layer of a particle may be considered as consisting of three parts (125):

i. The surface layer whose charge (σ_o) is given by equation 3.3 for an oxide.

ii. The Stern layer, which is the region between the surface and the plane of closest approach of hydrated counter ions, located at a distance δ from the surface. Stern considered that specifically adsorbed ions would also be situated at this plane but Grahame supplied evidence that these ions would lose part of their hydration shells upon adsorption and therefore would approach the surface at a distance closer than δ. He proposed that the Stern layer would be constituted by the inner Helmholtz plane (IHP), centre of specifically adsorbed, dehydrated ions, and the outer Helmholtz (OHP), location of the hydrated counter ions, coinciding with Stern's plane. Specific adsorption is defined generally as adsorption that depends on the nature rather than merely on the charge of the ion.

iii. The diffuse or Gouy layer, extending from the OHP outwards into the solution. The charge in the diffuse layer (σ_d) is considered to consist of point-like ions distributed according to a Boltzmann relationship.

As the system is electrically neutral it follows that

$$\sigma_o + \sigma_\delta + \sigma_d = 0 \qquad (3.4)$$

with σ_δ = charge density in the Stern layer; in the absence of specific adsorption σ_δ is zero.

This model of the double layer has been schematized in Figure 3.1 showing also the potential drop across the double layer in the absence and in the presence of specific adsorption.

The potential difference between the surface and the bulk solution (usually referred to as the surface potential) is for the case of non-polarizable, reversible electrodes given by the Nerst equation:

$$\psi_o = \frac{kT}{z_i e} \ln \frac{a_i}{a_{i(PZC)}} \qquad (3.5)$$

where ψ_o = double layer potential

a_i = activity of the potential-determining ion i

$a_{i(PZC)}$ = activity of the potential-determining ion i at the PZC

k = Boltzmann constant

e = electronic charge

T = absolute temperature

z_i = valency of potential-determining ion i

which for the case of oxide minerals becomes:

$$\psi_o = 2.303 \frac{kT}{e} (PZC - pH) \qquad (3.6)$$

Nevertheless, equation 3.6 is considered to be valid only near the PZC (126).

The double layer potential is constituted by a potential difference in the Stern layer and a potential drop across the diffuse layer. According to the Gouy-Chapman theory the potential drop for the diffuse part of a flat double layer constituted by ions of a symmetrical

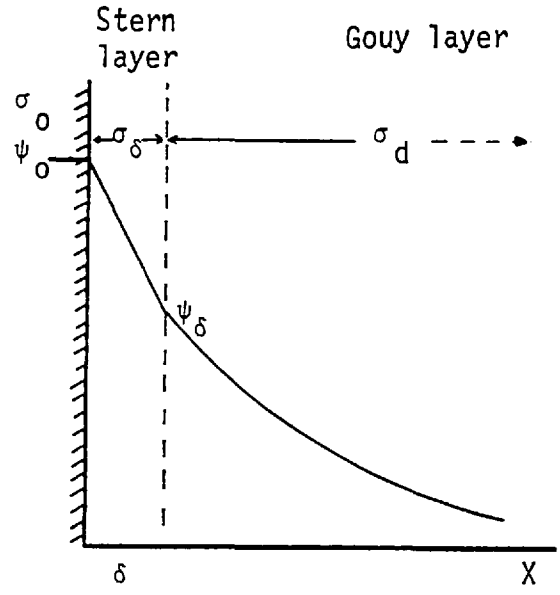

(a) no specific adsorption

$\sigma_\delta = 0$

$\sigma_o = \sigma_d$

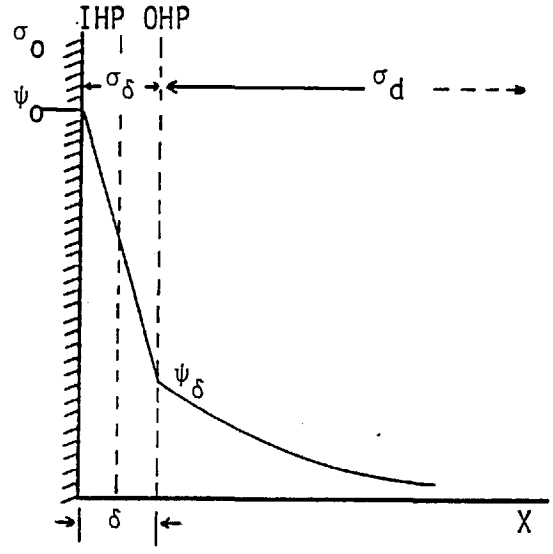

(b) specific adsorption

$|\sigma_\delta| < |\sigma_o|$

$\sigma_o = -(\sigma_\delta + \sigma_d)$

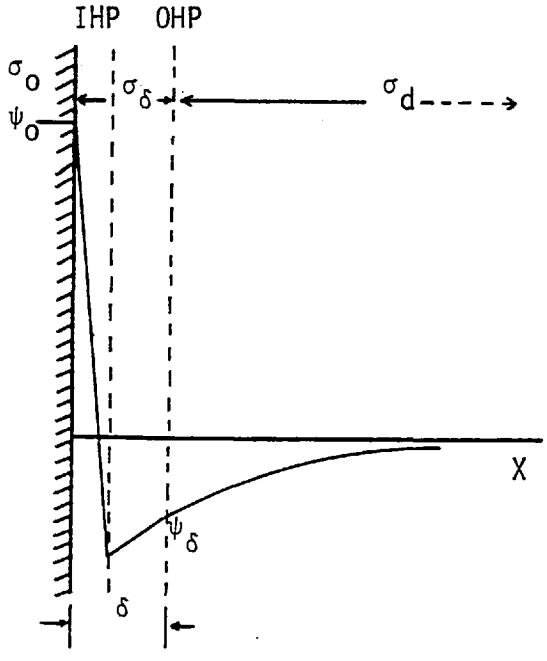

(c) superequivalent specific adsorption

$|\sigma_\delta| > |\sigma_o|$

$\sigma_o = -(\sigma_\delta + \sigma_d)$

Figure 3.1. Stern-Grahame model of the electrical double layer at the solid/liquid interface

electrolyte is given by

$$\psi_{(x)} = \frac{2kT}{ze} \ln \frac{1 + \gamma \exp(-\kappa x)}{1 - \gamma \exp(-\kappa x)} \qquad (3.7)$$

with

$$\gamma = \frac{\exp(ze\psi_\delta/2kT) - 1}{\exp(ze\psi_\delta/2kT) + 1}$$

and

$$\kappa = \left(\frac{8\pi e^2 n z^2}{\varepsilon kT}\right)^{\frac{1}{2}} \qquad (3.8)$$

where $\psi_{(x)}$ = diffuse layer potential at a distance x from the Stern plane

ψ_δ = potential at the Stern plane

κ = Debye-Hückel parameter (its reciprocal is taken as a measure of the 'thickness' of the diffuse layer)

n = ionic concentration in the bulk solution

ε = dielectric constant of liquid

Charge and potential are related for a flat diffuse layer through

$$\sigma_d = \left(\frac{2n\varepsilon kT}{\pi}\right)^{\frac{1}{2}} \sin h \left(\frac{ze\psi_\delta}{2kT}\right) \qquad (3.9)$$

At low potential values (ψ_δ < 25 mV) equations (3.7) and (3.9) become respectively:

$$\psi_{(x)} = \psi_\delta \exp(-\kappa x) \qquad (3.10)$$

$$\sigma_d = \frac{\varepsilon\kappa}{4\pi} \sigma_\delta \qquad (3.11)$$

showing clearly that the Stern potential determines the characteristics of the diffuse part of the double layer and <u>not</u> the surface potential (ψ_δ).

The only experimentally measurable potential in the double layer of an oxide mineral is the electrokinetic or zeta-potential (ζ). The

zeta-potential is the potential at the plane of shear between the particle and the solution when the two move with respect to each other. The exact location of the slipping plane is not known but it is customary to assume that it coincides with the OHP ($\zeta = \psi_\delta$). Calculations of zeta-potentials from electrophoretic mobilities is discussed in section 4.2. From electrokinetic measurements it is possible to obtain isoelectric point (iep) of an oxide mineral; the iep is the negative logarithm of the potential-determining ion activity corresponding to zero zeta-potential.

The PZC and the iep coincide only in the absence of specific adsorption. If ions adsorb specifically, the PZC and the iep are shifted in opposite directions (125).

Corrections introduced to this basic model of the double layer take into account the 'discreteness of charge' effect in the IHP (127) and the different value of the medium permittivity in the Stern layer due to the structuring of the solvent near the solid surface (128).

3.3. Collector adsorption at the oxide mineral/aqueous solution interface

The mechanism of adsorption of flotation collectors at the mineral/solution interface has been the subject of various studies (129)(130)(131). These works have shown that collector adsorption by oxide minerals is determined by their electrical double layer properties and by specific interactions arising from the surface affinity for the collector ion. These studies have also shown, using electrokinetic measurements, that collector ions adsorb specifically in the Stern layer of the oxide mineral.

The adsorption density of ions adsorbed in the Stern layer is

given by the Stern-Grahame equation (124):

$$\Gamma_i = 2rC\exp(-\Delta G^0_{ads}/RT) \quad (3.12)$$

where Γ_i = adsorption density of ions at the plane i in the Stern layer

r = radius of adsorbed ion

C = bulk ionic concentration

ΔG^0_{ads} = free energy change of adsorption

The free energy change of adsorption is made up of various contributions, namely,

$$\Delta G^0_{ads} = \Delta G^0_{elec} + \Delta G^0_{spec} \quad (3.13)$$

where ΔG^0_{elec} is the electrostatic contribution to the total free energy change associated with transferring a collector ion from the bulk solution to a plane of potential ψ_i in the Stern layer, viz

$$\Delta G^0_{elec} = zF\psi_i \quad (3.14)$$

The term ΔG^0_{spec} groups the specific contributions to the adsorption free energy change. These contributions may arise from chemical bond formation between the collector and the adsorbant (ΔG^0_{chem}), hydrogen bond formation (ΔG^0_h), collector and surface solvation effects (ΔG^0_{solv}), association between hydrocarbon chains of the adsorbed collector ions at the interface ($\Delta G^0_{CH_2}$). Thus, it is considered that

$$\Delta G^0_{spec} = \Delta G^0_{CH_2} + \Delta G^0_{chem} + \Delta G^0_h + \Delta G^0_{solv} + \ldots \quad (3.15)$$

$\Delta G^0_{CH_2}$ depends on the chain length of the collector ion and has been calculated assuming:

$$\Delta G^0_{CH_2} = n\phi \quad (3.16)$$

with n = number of carbon atoms in the collector chain

ϕ = free energy change associated with the removal from water of one mole of CH_2 groups.

Fuerstenau (132) considers that collector adsorption is physical

(physisorption) when the free energy term is made up only of electrostatic and hydrophobic contributions, that is,

$$\Delta G^{o}_{ads} = zF\psi_i + n\phi \qquad (3.17)$$

although true physical adsorption is generally considered to occur when only van der Waals forces of attraction are operating in the adsorption mechanism (133).

Fuerstenau and his associates have found that adsorption of alkyl amines at the quartz/water interface, and alkyl sulphates and sulphonates at the alumina/water interface (134 - 138) is of a physical nature as described by equation 3.17. They have proposed a model of adsorption based on electrokinetic, adsorption and contact angle measurements. At low surfactant concentrations the ions adsorb as counter ions in the diffuse part of the double layer while at higher concentrations they associate through hydrophobic bonding of the hydrocarbon chains in two-dimensional aggregates (hemimicelles) in the Stern layer. Above the surfactant concentration at which hemimicelle formation occurs, the zeta-potential decreases sharply (indicating that specific adsorption is taking place) while the adsorption density and the contact angle experience a steeper increase. Eventually, the zeta-potential reverses and adsorption continues to occur with a repulsive contribution from ΔG^{o}_{elec}.

Collector adsorption is considered to be chemical (chemisorption) when there is a specific reaction affinity between collector and the metallic ion of the oxide mineral leading to the formation of a new surface compound. Examples of chemisorption phenomena on oxide minerals are the adsorption of dithizone on zinc oxide minerals (27) and the adsorption of salicylaldehyde on cassiterite (139). Another kind of chemisorption mechanism involves chemical affinity between the

polar head of the collector and groups on the mineral surface plus hydrophobic bonding due to surfactant chain association; this mechanism is typical of the adsorption of long-chain carboxylates on oxide minerals, e.g. adsorption of oleic acid on hematite (140).

According to the model proposed by Fuerstenau, physical adsorption at the oxide/water interface can occur only if an ionic surfactant and the mineral surface are opposedly charged. Conversely, collector chemisorption may be characterized by the adsorption of collector ions at surfaces of like charge. Han, Healy and Fuerstanau (141) have proposed that adsorption at the PZC of an oxide mineral, as measured by electrokinetic methods (i.e. the iep), is an evidence of chemisorption of the surfactant on the surface. In a later paper (142), a model was proposed for the distribution of the surface charge of oxides showing that near the PZC there is a distribution of neutral, positive and negative sites; no mention was made, however, of how this site distribution would affect the adsorption or electrokinetic behaviour of oxide minerals.

Cases and co-workers have adopted another approach, considering adsorption at the solid/liquid interface as a condensation process on either a homogeneous or a non-homogeneous surface; similar to adsorption at the solid/gas interface (143 - 145). This approach has been criticized on thermodynamic grounds because it assumes that entropic effects are the same both in adsorption from solution and from the gaseous state. However, water molecules displaced during collector adsorption significantly increase the entropy of the solid/solution system (4). The model of Cases is also somewhat limited in relating physico-chemical phenomena occurring at the solid/solution interface with the adsorption behaviour of collectors.

3.4. Phenomena at the solid/liquid interface associated with the aggregation of mineral suspensions

Minerals dispersed in aqueous solution may exhibit the properties of either lyophobic colloidal dispersions or of suspensions, depending on their stability behaviour in solution. Suspensions are unstable systems because of particle sedimentation under the action of gravity forces. Colloids, on the other hand, are subjected to Brownian movement and are stable dispersions if the net interaction of the surface forces between particles prevents them from aggregating.

The surface forces intervening in the aggregation of two colloidal particles are London-van der Waals attractive forces, electrostatic repulsive forces arising from the overlapping of like-charge electrical double layers and repulsive forces arising from solvation, adsorbed layers, etc. (246). A quantitative theory of the stability of lyophobic colloids was formulated independently by Derjaguin and Landau (146) and Verwey and Overbeek (147) on the basis of the interaction between van der Waals and electrical double layer forces considered as a function of inter-particle distance. This theory is usually referred to as the DLVO theory. An important feature of colloidal systems is their sensitivity to destabilization by small additions of electrolyte; the action of an electrolyte is to reduce the range of the electrostatic repulsive forces to such a distance that the shorter range attractive forces may prevail and aggregation occur. The range of the electrostatic repulsive forces depends on the characteristics of the diffuse part of the double layer and therefore a reduction in either the potential ψ_δ or the thickness of the diffuse layer diminishes the repulsive forces. In addition to electrolytes, colloidal dispersions may be destabilized by addition of compounds which adsorb at the solid/

liquid interface through diverse mechanisms; examples of destabilizing agents are ionic surfactants (148), hydrolyzing metal ions (149) and polymeric and macromolecular compounds (150).

Recently a distinction has been made between two kinds of aggregation processes, coagulation and flocculation (151). Coagulation is destabilization brought about by a reduction of the repulsive electrostatic forces upon addition of inert electrolyte. Coagulation is said to be 'slow' when only a fraction of the collisions leads to aggregation and 'rapid' if every collision is effective. Furthermore, when the aggregation process occurs only through Brownian collisions between the particles the term perikinetic coagulation is used whereas if hydrodynamic shear is responsible for the collisions the particle aggregation process is referred to as orthokinetic coagulation.

Flocculation is defined as aggregation produced by the bridging action of high molecular weight polymeric compounds. The mechanism of flocculation and the adsorption of polymeric flocculants have been extensively reviewed by various authors (150)(152)(153). Flocculated aggregates (flocs) are larger and settle faster than those formed by electrolyte coagulation. They also show different rheological properties such as visco-elasticity at low shear and irreversible breakdown at high shear rates (154). Flocculation can also proceed through perikinetic and orthokinetic collisions.

Aggregation by hydrolyzing metal ions can combine features of both, coagulation and flocculation, as destabilization is brought about by a reduction of the repulsive electrostatic forces and at certain pH values the precipitated hydroxide may exert a bridging action between particles. This process, as well as destabilization induced by ionic surfactants, will be referred to as coagulation in this work.

Colloidal dispersions and suspensions are characterized by their respective particle size ranges but a clear cut-off does not exist for the upper size limit of the colloidal range. Kitchener has pointed out that colloidal phenomena do not disappear at any particle size limit but persist (in diminishing importance) up to at least 10 μm (155).

Mineral suspensions are polydispersed (and polymineralic) and some have a large number of very fine particles. These fine particles although unstable in suspension in the long term, show colloidal properties when considered in the short term. There is no quantitative theory at present to describe the stability behaviour of these polydispersed systems. However, it is possible to make use of the short term 'stability' for studying the aggregation behaviour of mineral suspensions. This can be done by comparing their relative stability in the presence of various compounds which adsorb at the mineral/solution interface.

Suspensions may show perikinetic coagulation (as all small particles undergo Brownian motion) but more important at these particle sizes (> 1 μm) is orthokinetic coagulation produced either by collisions between large sedimentary particles and smaller suspended ones, or through particle collisions caused by velocity gradients in a fluid (156). As with colloids, mineral suspensions may be destabilized by reducing the repulsive electrostatic forces or by the addition of polymeric flocculants. Indeed, the recovery of valuable slimes has been attempted through processes relying on the selective destabilization of a single mineral component in the suspension. Selective coagulation showed several practical problems (157) but selective flocculation was carried out successfully for various model systems (158)(159)(160).

The aggregation of mineral suspensions in the presence of ionic surface-active agents (such as flotation collectors) has been widely

reported in the literature (164). Little work has been carried out to correlate aggregation of mineral suspensions by flotation collectors with phenomena occurring at the solid/solution interface. However, the works of Ottewill and co-workers on destabilization of model colloidal systems by cationic and anionic surface-active agents (161) (162) and that of Somasundaran et al (163) on colloidal alumina destabilized by an anionic surfactant, indicate that aggregation proceeds from a reduction of the electrostatic repulsive forces caused by the specific adsorption of the surfactant ions. Also of interest are studies on the aggregation of galena particles by ethyl xanthates (36) and on 'shear flocculation' of scheelite by oleic acid (165).

3.5. The surface properties and the flotation of cassiterite

The surface of cassiterite in aqueous solution has amphoteric properties of the kind described in section 3.2 for oxide minerals. The presence of hydroxyl groups and molecular water bonded to stannic oxide surfaces has been detected by infra-red spectroscopy (166) and water vapour adsorption studies (167). The charging mechanisms of the cassiterite surface in aqueous solution were studied by Edwards and Ewers (168) and Jaycock, Ottewill and Tar (169). The latter authors proposed that cassiterite was positively charged in acid media due to adsorption of hydrogen ions whereas in alkaline media it became negative due to ionization of the surface hydroxyl groups. Thus, schematically,

$$SnOH + H^+ \rightleftharpoons SnOH_2^+ \qquad (3.18)$$

$$SnOH \rightleftharpoons SnO^- + H^+ \qquad (3.19)$$

The point of zero charge and the isoelectric point of cassiterite have been measured by various authors. Table 3.1 summarizes the results.

Table 3.1. Measurements of the PZC and the iep of cassiterite by various authors

Sample	Method	iep	PZC	Reference
synthetic	electrophoresis	4.5		(170)
natural	electrophoresis	7.3		(170)
synthetic	electrophoresis, titration	4.4	5.4	(169)
natural	streaming potential	4.7		(173)
natural	suspension pH changes		5.5	(174)
natural	electrophoresis	4.0		(175)
natural	streaming potential	4.5		(28)

These results show that cassiterite may adsorb both anionic and cationic collectors depending on the pH value and indeed, it is readily floated by alkyl sulphates and alkyl amines at the positive and negative side of the PZC respectively. The selective flotation of cassiterite from tin ores, however, is beset with problems. The difficulties in obtaining efficient, selective separations of cassiterite by flotation arise from the following factors:

a) Cassiterite may be associated with as much as 10 or 15 other minerals in a tin ore; some of these minerals are oxides with similar surface properties. Other minerals may be damaging because they release ions which may precipitate the collector or activate other minerals in the gangue.

b) The relative chemical inertness of cassiterite, which results in low specificity of the collector for the mineral surface and subsequently in the low selectivity of cassiterite flotation.

c) The presence of impurities in cassiterite minerals which have

significant effects on their flotation behaviour, either by increasing or reducing their floatability. Impurities may consist of ionic substitutions in the crystal lattice, minute inclusions of other phases or surface coatings.

Factor c) is very important because, apart from its influence in the flotation behaviour, contamination may change the surface properties of the mineral and the mechanism of adsorption of collectors at the cassiterite/solution interface. This factor may be the cause of the large number of irreproducible results found in the literature on cassiterite flotation.

Trahar has reviewed research into the flotation of cassiterite until 1964 (176) and showed that most of the work had been done with carboxylate and alkyl sulphate collectors. Investigations on the adsorption of alkyl sulphates on stannic oxide led to different conclusions with respect to the effect of pH on adsorption (168)(169) although the flotation of cassiterite by these collectors is strongly pH-dependent (168) (177). Johansen, O'Connor and Buchanan studied in a series of publications (170 - 172) the electrokinetic properties of stannic oxide; they showed that sodium cetyl sulphate adsorbed strongly at acid pH values causing the zeta-potential to reverse sign.

The flotation of cassiterite by oleic acid and the role of various activators has been studied by Gaudin, Schuhman and co-workers (178 - 181). Data on the mechanism of adsorption of oleic acid on cassiterite are few and contradictory. Schuhman and Prakash (181) reported flotation of a synthetic sample (using a vacuum flotation technique) over the pH range 2 to 12 whereas Polkin et al (183) found that pure stannic oxide was not floatable by oleic acid. Goold (182) also reported poor floatability of reagent grade SnO_2 by oleic acid and very low adsorption

(≃ 1% of a theoretical monolayer) at pH 9. However, when this SnO_2 sample was recrystallized it floated well under the same conditions. Infra-red studies carried out by Polkin and associates (183) showed that oleic acid adsorbs only below pH 5 on pure stannic oxide; nevertheless, when the sample was activated by various cations (Fe^{+3}, Cu^{+2}, Pb^{+2}) the spectra showed that oleic acid chemisorbed on the oxide at pH 6.0. Further tests on flotation of activated samples revealed the important role of certain crystalline impurities in enhancing flotation by the carboxylic acid collector.

The main conclusion of Trahar's review in 1964 was that more specific collectors for cassiterite had to be developed if tin was to be recovered by flotation. Indeed, the increase in tonnage of tin ore treated by flotation has been accompanied by the development of new collectors for cassiterite (and also by the technological advance of the tin smelting industry which has made it possible to treat lower grade concentrates). According to Moncrieff and Lewis (34), the collectors now used industrially for the flotation of cassiterite are sulfosuccinamates, phosphonic acid and arsonic acid collectors.

Wottgen (184)(185) studied the cassiterite/phosphonic acid system in detail and on the basis of adsorption measurements and infra-red studies concluded that phosphonic acid was adsorbed specifically forming a surface compound with tin. It was also shown that selectivity and recovery were dependent on the chain length of the collector, and that the pH range in which the phosphonic acid collectors floated cassiterite was related to their dissociation constants. Adsorption of phosphonic acids was optimum at pH 2, decreasing drastically at pH values above 4, although surface coverage remains significant up to neutral values of pH. Flotation tests on tin ores with heptyl phosphonic acid showed

that this collector is effective between pH 3 - 7. Collins (187) tested the flotation ability of several collectors on various cassiterite minerals and tin ores finding that phosphonic acids gave the best overall selectivity.

The adsorption of arsonic acid collectors has also been claimed to occur via a chemisorption mechanism. Polkin et al (193) based their claim on studies of the precipitation of tin (Sn^{+4}) by p-tolyl arsonic acid, carrying out infra-red spectroscopy on the compounds formed. They found that a reaction occurred between hydrated compounds of Sn^{+4} and the arsonic acid and that spectra of the reaction between the collector and stannic oxide were analagous to those found in the precipitation studies. Adsorption of p-tolyl arsonic acid on stannic oxide decreased with increases in pH and more drastically for 'less hydrated' samples. Collins (187) reported that although these collectors are highly selective, they are very expensive, toxic and they are required in high concentrations.

Data on the interactions at the cassiterite/sulfosuccinamate solution interface are scarce and except for some electrokinetic and flotation experiments carried out by Zambrana et al (175)(186) little is known about the system. These researchers have shown that sulfo-succinamate floats natural cassiterite in the pH range 1 - 8 and that selective flotation from a synthetic cassiterite/quartz mixture is possible in alkaline media if cassiterite is activated by lead. This collector has been used industrially in Bolivia at pH 2.3 and in Cornwall, England, at pH 5.6 (34).

An important problem in the selective flotation of cassiterite by these three collectors is that all of them react strongly with iron. This can mean the suppression of flotation via collector precipitation

if the iron concentration is high and also the activation of cassiterite if it is present on the mineral surface. Many authors believe (183)(188) that the flotation of cassiterite by these collectors (and oleic acid) at neutral to alkaline pH values is possible only because of the presence of lattice impurities, particularly iron. The surface chemistry of cassiterite and the mechanism of adsorption of collectors will be discussed again in Chapter 6 in connection with the results of this work.

Other collectors claimed to be specific for cassiterite are hydroxamic acids (29), phosphoric acids (183) and salycylaldehyde (26). The addition of a non-ionic surfactant has been proposed to improve the floatability of cassiterite by sulfosuccinamate collectors (28) and a modified polyacrylamide has been used to selectively flocculate cassiterite from synthetic binary mixtures.

Chapter 4. EXPERIMENTAL

4. EXPERIMENTAL

4.1. Materials

4.1.1. Minerals

"Optically clear" Brazilian quartz rock crystals were hand-selected, crushed and the -2.63 mm + 150 μm fraction leached in hot concentrated hydrochloric acid until no iron was detected in solution by atomic absorption spectrophotometry. The crystals were then washed with double distilled water until no trace of chloride was found by a silver nitrate spot test. The sample was dried at 110°C, dry-ground in 100 g batches for 50 minutes in a Tema vibrating agate mill and then mixed and stored in glass bottles in a vacuum dessicator.

A sample of the ground quartz was passed through a Warman M5 Cyclosizer and was found to have the following size distribution:

Table 4.1. Size distribution of quartz sample

Size (μm)	% Wt Undersize
43.2	96.5
32.1	85.3
23.4	71.1
16.6	59.1
13.6	52.6

The specific surface area of the sample was 1.7±0.1 m^2/g. Specific surface areas were measured on the Quantachrome Corp. "Monosorb" surface area analyser which uses a single point adsorption method.

A semiquantitative X-ray fluorescence scan was carried out on the quartz to determine its purity and gave the following results:

Table 4.2. XRF analysis of quartz samples

Major (5%)	Inter (0.5-5%)	Minor (0.05-0.5%)	Trace (0.05%)
Si	Nil	Nil	Ca (50 ppm) K, Fe (both 10 ppm)

The cassiterite sample consisted of Nigerian cassiterite lumps showing inclusions of quartz and mica as major visible contaminants. This sample was hand-crushed to -1.18 mm, screened and split into size fractions. The -75 μm material was discarded. The +75 μm fractions were subjected to dry magnetic separation followed by gravity concentration on a Superpaner. The resulting cassiterite concentrate was deslimed, cleaned with methanol and warm sodium hydroxide, and then thoroughly washed with double distilled water. The -105 +75 μm material was selected for Hallimond tube flotation tests. The rest of the sample was dry-ground in 50 g batches for 50 min in a Tema vibrating agate mill after which it was stored dry in a vacuum dessicator. This final sample was found to have a specific surface area of 3.18 ± 0.12 m^2/g.

The size distribution of the sample was determined independently by Coulter Counter analysis and wet microsieve screening. The results given in Table 4.3 show that the majority of the cassiterite was below 30 μm.

Table 4.3. Size distribution of cassiterite sample

Size (μm)	% Wt Undersize
30	98.1
20	89.9
10	74.1
4.4	49.5
2.1	28.4

A semiquantitative X-ray fluorescence scan and a quantitative chemical analysis were performed on the sample. The results shown below indicate that the sample contained over 93% tin as SnO_2.

Table 4.4. XRF analysis of cassiterite sample

Major (>5%)	Inter (0.5-5%)	Minor (0.05-0.5%)	Trace (<0.05%)
Sn	Nb, Ta	Ca, Fe	S, Cl, K, Mn Zn, W, Zr

Table 4.5. Chemical analysis of cassiterite sample

SnO_2	93.75 ± 0.20
Ta_2O_5	3.22 ± 0.04
Nb_2O_5	0.84 ± 0.04
Fe_2O_3	0.762± 0.003
CaO	0.54 ± 0.01

Chemical grade stannic oxide was used in some experiments. A XRF scan carried out on the powder showed aluminium as the only and very minor contaminant (0.05 - 0.5%). The specific surface area of this powder was 7.65 ± 0.19 m^2/g. All XRF scans and the cassiterite sample chemical analysis was carried out by the Imperial College Analytical Services Laboratory.

4.1.2. Reagents

Dodecylamine and sodium dodecylsulphate were selected as cationic and anionic surfactants respectively. Aeropromoter 845 kindly supplied by the Cyanamid Co. was chosen as an example of a commercial collector

for cassiterite. Dodecylammonium chloride solutions were prepared by dissolving weighed amounts of BDH dodecylamine in water acidified with HCl. 'Chemically pure' sodium dodecylsulphate was supplied by B. Newton Maine Ltd.; the critical micelle concentration (CMC) determined by solution conductivity measurements to be 8.10×10^{-3} M which agrees well with values reported in the literature (190).

According to the manufacturers, Aeropromoter 845 (A845) is a 35 ± 1.5% solution of tetrasodium N-(1,2 dicarboxyethyl)-N-octadecylsulfo-succinamate, a branched long chain anionic surfactant whose structural formula is

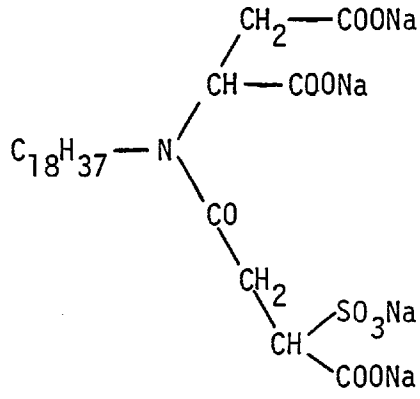

Conductivity measurements of A845 solutions indicated that the CMC occurred at a concentration of 560 mg/l. The CMC value given by the manufacturers is 600 mg/l.

Other reagents used in this work are described below:

- N100, supplied by BTI, a nonionic polyacrylamide flocculant
- C150/23, supplied by BTI, a cationic polyacrylamide flocculant
- Polyethyleneimine, supplied as a 50% solution by BDH ($-CH_2-NH-CH_2-$)
- Precipitated silica, supplied by BDH.

All other reagents used were of 'Analar' grade including the HCl and NaOH which were used for pH adjustment. All glassware was cleaned first with chromic acid and then with warm nitric acid and ethanol.

High purity water was used throughout this work. It was prepared in all Pyrex glass still by passing distilled water through a mixed bed ion exchange resin, followed by an activated charcoal bed and then by re-distillation. The purified water was stored in a glass vessel vented to atmosphere via an activated charcoal filter. The conductivity of this water averaged 3.0×10^{-6} ohm^{-1} cm^{-1} and bubble persistence tests showed that it was free from surface-active impurities.

4.2. Electrokinetic studies

4.2.1. Electrophoresis

The electrical phenomena associated with the oxide mineral/ liquid interface have been discussed and the influence of the particle charge in determining the adsorption of surfactants, or the stability of colloidal systems has been stressed. It is of great importance, therefore, to determine the electrical double layer properties of an oxide mineral when studying its flotation or stability behaviour in the presence of a surfactant.

Electrokinetic measurements are one of the techniques available for providing information on the charge distribution in the electrical double layer surrounding a particle (191). The relationship between the electrokinetic or zeta-potential and electrical double layer phenomena has been the subject of many reviews in the literature (192) (128)(193).

The zeta-potential, the potential at the plane of shear between the solid and liquid phases, can be determined indirectly by the micro-electrophoresis technique which is particularly suitable for fine mineral particles (194). Thus when an electrical field is applied to a mineral suspension the particles migrate towards the electrode bearing a charge

opposite to that of the particles. The velocity of migration of the particles under unit potential gradient is called the electrophoretic mobility and is related to the zeta-potential through the Helmholtz-Smoluchowski equation (191) as modified by Henry (195):

$$u = \frac{v}{E} = \frac{\varepsilon \zeta}{6\pi\eta} f(\kappa a) \qquad (4.1)$$

where u = electrophoretic mobility

v = velocity of particle

E = electric field strength

ζ = zeta-potential

ε = permittivity

η = viscosity

a = radius of particle

κ = reciprocal Debye-Hückel length

The function $f(\kappa a)$ was introduced by Henry to account for the double layer retardation effect and takes values between 0.75 and 1.5 depending on the size and shape of the particles as well as on their orientation with respect to the applied electric field.

Further corrections have been introduced to account for the effect of surface conductivity (196), relaxation (197)(198), and viscosity and permittivity changes with field strength (199)(200) on the electrophoretic mobility. Later Wiersema, Loeb and Overbeek (201) developed a model for the electrophoretic mobility of a spherical colloidal particle considering retardation, relaxation and surface conductivity (outside the surface of shear) effects. They solved the differential equations without approximations using a computer and gave a full range of numerical solutions for the relations between u, ζ and κa. Their results showed that the relaxation effect was most important between $0.2 < \kappa a < 50$ and

that its magnitude had been overestimated by Overbeek and Booth. They also confirmed the validity of Henry's equation at low zeta-potentials and for high κa values.

4.2.2. Experimental procedure

Electrophoretic mobilities were determined in a Rank Bros. micro-electrophoresis apparatus using a flat cell. Generally, suspensions were prepared by adding small amounts of the mineral (≈25 mg) to a 50 ml solution at the required pH and then conditioning for 10 min. The suspension was added to the cell and the velocity of the particles was measured by timing 10 particles at each stationary level in both directions. For the quartz/dodecylamine chloride system the mobilities were measured from samples taken from the suspensions that were used in the stability tests.

The electrophoretic mobility was calculated from the equation:

$$u = \frac{v}{V/L} \left(\frac{\mu m\ sec^{-1}}{volt\ sec^{-1}}\right) \qquad (4.2)$$

where V = applied potential

L = effective interelectrode distance = RKA ≡ constant (this work = 8.12 cm)

A = cross sectional area of the cell

R = resistance across cell

K = specific conductivity of solution

Uncertainties associated with the absolute value of κa in most of these electrokinetic studies have lead to the results being presented as electrophoretic mobilities reather than as zeta-potentials. Where zeta-potential values are given, unless otherwise stated, they have been calculated from equation 4.1 taking $f(\kappa a)$ as 1.5; that is, its

value for $\kappa a >> 1$ (128). Equation 4.1 may then be written in a more convenient way to calculate zeta-potential values:

$$(\text{at } 25^{o}C) \quad \zeta = 12.83\, u \quad (mV) \qquad (4.3)$$

where u is in $\mu m\ sec^{-1}/volt\ cm^{-1}$.

4.3. Adsorption measurements

4.3.1. Experimental procedure

Adsorption densities were determined by the difference between the initial amount of surfactant in solution and that measured after adsorption on the mineral had taken place. The adsorption tests were carried out by shaking a quantity of mineral in a known volume of surfactant solution at a fixed pH for a pre-determined time. After this conditioning the final pH was recorded and the solids separated by centrifuging. The residual concentration of surfactant was determined spectrophotometrically. The conditions used for each system studied are given in Table 4.6.

Table 4.6. Experimental conditions used in adsorption measurements

System	Solid (g)	Solution volume (ml)	Equilibration time (h)
Quartz/DAC	1	100	18
Cassiterite/SDS	2	25	0.5
SnO_2/SDS	3	50	0.5

DAC = dodecylammonium chloride; SDS = sodium dodecyl sulphate

At a given initial concentration, no differences in adsorption

density were found for cassiterite and SnO_2 for equilibration times between 15 min and 2 hours.

4.3.2. Dodecylamine analysis

The concentration of dodecylamine in solution was determined by complexing the amine with an acidified alcoholic solution containing a sulphanapthelein indicator, bromocresol green, and then extracting the complex into chloroform (202).

The indicator was prepared by dissolving 0.1 g bromocresol green in 60 ml ethanol, acidifying the solution with 0.5 ml concentrated sulphuric acid and diluting with water to 100 ml. In each determination 5 ml DAC solution were reacted with 1 ml of the indicator solution in 5 ml distilled water followed by the addition of 5 ml chloroform. The mixture was then inverted rapidly 100 times and the chloroform separated and its colour determined at 416 μm in a Perkin Elmer 124 Double Beam Spectrophotometer. Fig. 4.1 shows the calibration curve obtained in the determination of DAC in solution by this procedure.

4.3.3. Sodium dodecyl sulphate analysis

The concentration of SDS in solution was measured using the method of Gregory for anionic surface-active agents (203). The SDS solution was reacted with copper(II) triethylenetetramine in an alkaline medium of monoethanolamine to give a complex which was extracted into an isobutanol-cyclohexane mixture. Addition of diethylammonium diethyl-dithiocarbamate to the extracted complex produced a colour which was analysed in a Perkin Elmer 200 Spectrophotometer at 435 μm.

The reagents were prepared as follows:

Copper(II) triethylenetetramine: 25 g copper(II) nitrate trihydrate was

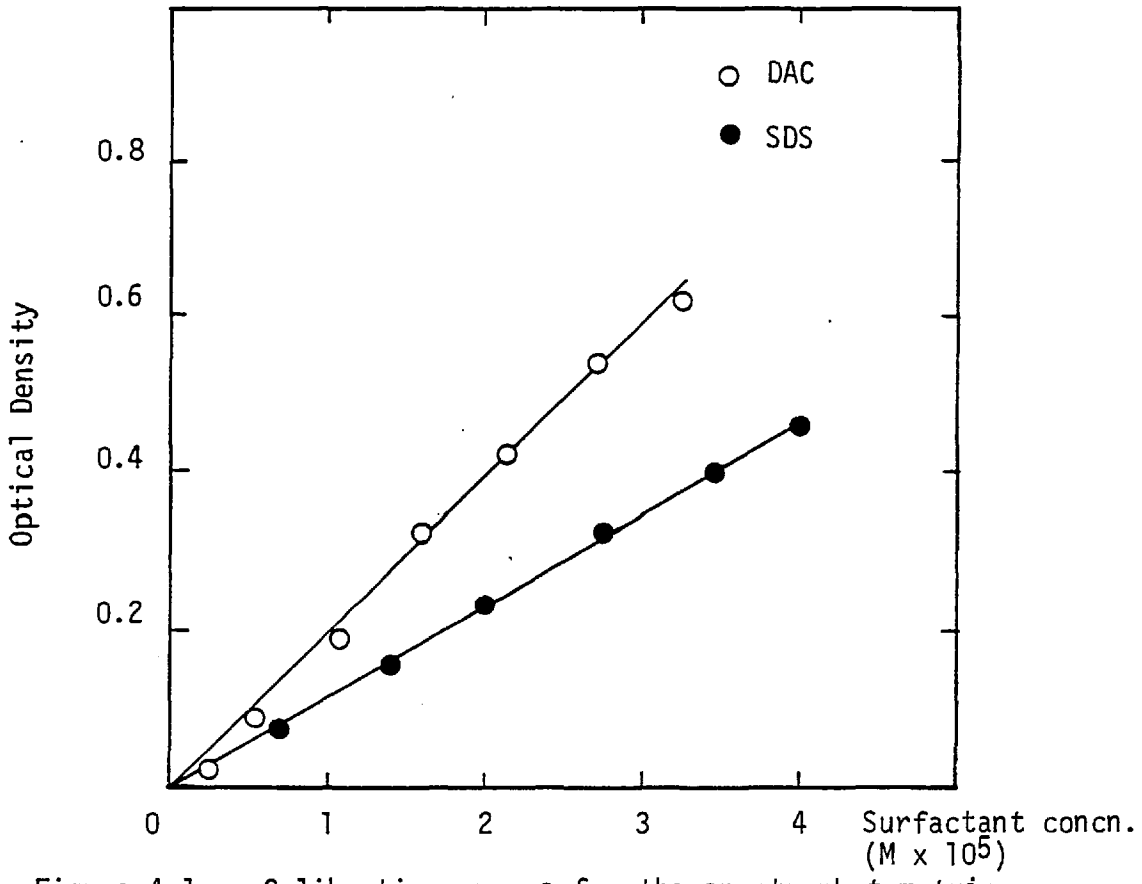

Figure 4.1. Calibration curves for the spectrophotometric determination of dodecylamine (DAC) and sodium dodecylsulphate (SDS)

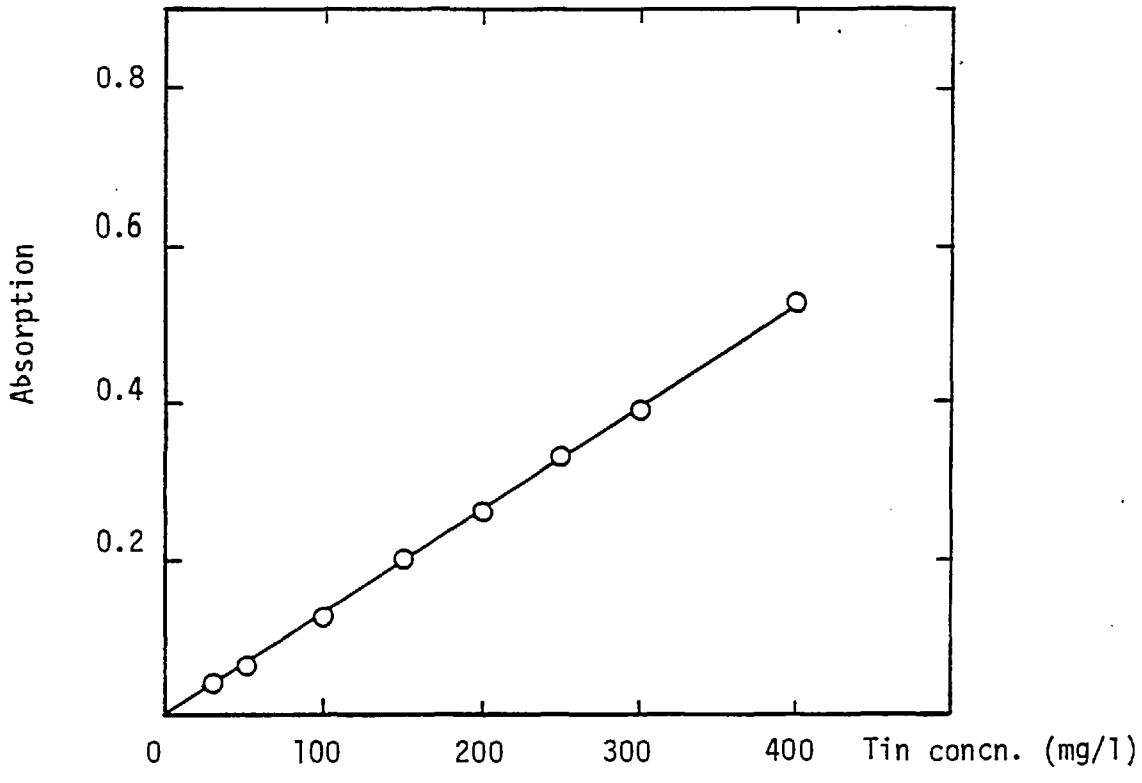

Figure 4.2. Calibration curve for the determination of tin by atomic absorption spectroscopy

dissolved in 125 ml water and a solution containing 16.25 g triethylene-tetramine in 125 ml water was slowly added. A solution containing 250 ml monoethanolamine in 250 ml water was then added and the whole made up to 1 l with double distilled water.

Isobutanol-cyclohexane extractant: 200 ml isobutanol was mixed with 800 ml cyclohexane.

Diethylammonium diethyldithiocarbamate: 0.5 g diethylammonium diethyl-dithiocarbamate was dissolved in 25 ml isobutanol. This solution was freshly prepared every two days.

An analysis involved the addition of 5 ml copper complex and 10 ml extractant to 25 ml of the SDS solution. After rapidly inverting the mixture 100 times, the organic phase was separated from the aqueous phase and mixed with two drops of carbamate solution. The sample was left to stand in the dark for 15 minutes and then its optical density was determined in the spectrophotometer. The calibration curve for SDS is shown in Figure 4.1.

4.4. Tin analysis

Recoveries and grades of tin achieved in the dissolved air flotation tests were obtained by determining the tin content of the flotation concentrates according to a method developed by Bowman (204). The method involves the sublimation of tin in the concentrate as tin iodide followed by dissolution in warm hydrochloric acid and analysis by atom absorption spectrophotometry in a nitrous oxide-acetylene flame.

In a determination 200 mg of the dried concentrate sample were weighed into a long pyrex test tube and mixed with 2 g of ammonium iodide crystals. The end of the tube was then rotated in and out of a flame until the sublimate ceased to condense on the walls of the tube.

20 ml of 2N HCl were added and the tube was kept in a bath at 65°C for 20 minutes to allow for complete dissolution of the tin iodide. The solution was cooled and then diluted to a known volume with 2N HCl. This solution was analysed in the nitrous oxide/acetylene flame of a Hilger and Watts Atomspek 1700 atomic absorption spectrophotometer at 235.5 μm.

Standard tin solutions containing ammonium iodide and hydrochloric acid at the same concentrations present in the sample solutions were used for calibration. A calibration curve for the determination of tin is shown in Figure 4.2. Analysis was carried out mainly in the region 50 - 200 mg/l. The low sensitivity of tin analysis by atomic absorption is determined by the low emission intensity of hollow cathode lamps containing tin (205).

Bowman claims recoveries of 99% for the ammonium iodide method. Nixon (205) found that even though this method gave slightly higher recoveries than the alkaline fusion method (206) recoveries were of the order of 94%. In this work the method was found to give recoveries of tin of 96.6 ± 0.9%. The reproducibility of results was very good giving variations of less than 1.5% relative.

4.5. Suspension stability studies

4.5.1. Determination of suspension stability

The theory of the stability of dispersed systems has been outlined and the relationship between aggregation of the dispersed phase and dissolved air flotation discussed. One of the aims of this work was to obtain quantitative information on this relationship which made it necessary to determine the stability of mineral suspensions under the conditions used for the dissolved air flotation tests.

A quantitative determination of suspension stability poses problems stemming from both the lack of a quantitative theory of coagulation for polydisperse systems and experimental difficulties (155). Nevertheless, empirical methods have been developed, mainly aimed at yielding information on the particular process for which aggregation is required, but from which it is also possible to measure relative degrees of aggregation of the suspended phase.

The determination of effectiveness of flocculation of fluorite by several methods was compared by Slater and Kitchener (207). They concluded that turbidity measurements of the supernatant liquid after standard conditions of stirring and settling were simple, quick and superior to refiltration rate measurements. Kitchener, in a recent review (155), recommended that the test closest to the required process should be used.

For the purpose of these studies, measurements of relative changes in stability as a function of a given variable were carried out by determination of the turbidity of the supernatant liquid.

4.5.2. Experimental procedure

Stability tests were carried out in 1 l beakers fitted with variable speed stirrers and under standard experimental conditions for each mineral/reagent system.

In a particular test the mineral was dispersed in double distilled water at the required pH, the reagent was added and the suspension conditioned at a fast stirring rate. The stirrer was then switched to slow stirring for some period after which the suspension was left to stand. Following this standing period a 60 ml sample from the supernatant liquid was syphoned off at a fixed depth (25 mm) and its turbidity

rapidly determined. Turbidimetric measurements were made in a EEL Absorptiometer with a neutral density filter, using distilled water as a blank. This experimental procedure is similar to 'jar testing' used in laboratory wastewater flocculation tests (208).

The sensitivity of the method for a particular mineral/reagent system was improved by varying the duration of the different stages of the test outlined above. This implied that only qualitative comparisons could be made between different systems regarding their stability properties. The duration of the stability test stages for each system are given in Table 4.7. In all tests a total suspension volume of 800 ml was used with either 0.4 g or cassiterite or 0.5 g of quartz.

Table 4.7. Experimental conditions in the suspension stability studies

	Fast stirring		Slow stirring		Standing
System	Time (min)	rpm	Time (min)	rpm	Time (min)
Quartz/DAC	5	200	15	100	5
Quartz/FS	1/6	200	5	100	5
Quartz/PEI	5	200	15	100	10
Flocculation[a]	1-2	200	5	100	5
Cassiterite[b]	5	400	10	150	15

FS: ferric sulphate; PEI: polyethyleneimine; a: quartz or cassiterite/flocculant; b: cassiterite/SDS or A845.

4.6. Dissolved air flotation studies

4.6.1. General

Experimental techniques and apparatus used in laboratory scale dissolved air flotation (DAF) differ widely, ranging from very simple batch bench-scale apparatus to quite sophisticated systems. The techniques applied depending mainly on the particular process being investigated and the kind of information required.

Batch bench-scale DAF tests were deemed acceptable for the purpose of studying the conditions for selectivity in DAF since it was likely that selectivity should ultimately lie with suspended phase properties rather than with equipment or microbubble characteristics. The fact that the main emphasis of this study was directed to the surface chemistry aspects of flotation by dissolved air implied that the parameters of the DAF system would have to be constant. Bearing this in mind it was decided to utilize the equipment, with a few minor modifications, with which M.R. Urban studied the mechanism of bubble formation in dissolved air flotation at the Mineral Resources Engineering Dept. of Imperial College (80).

4.6.2. Apparatus

The apparatus consisted of a saturator connected to the flotation cell through a pipe containing the pressure reduction nozzle (Figure 4.3).

The saturator used for air dissolution was a 3.5 l epoxy-coated pressure vessel (Figure 4.3 (a)) that withstood pressures of up to 791 kPa (100 psig). Air was dissolved in water at high pressure by bubbling compressed air (supplied in cylinders by the British Oxygen Corporation) under pressure into distilled water in the saturator.

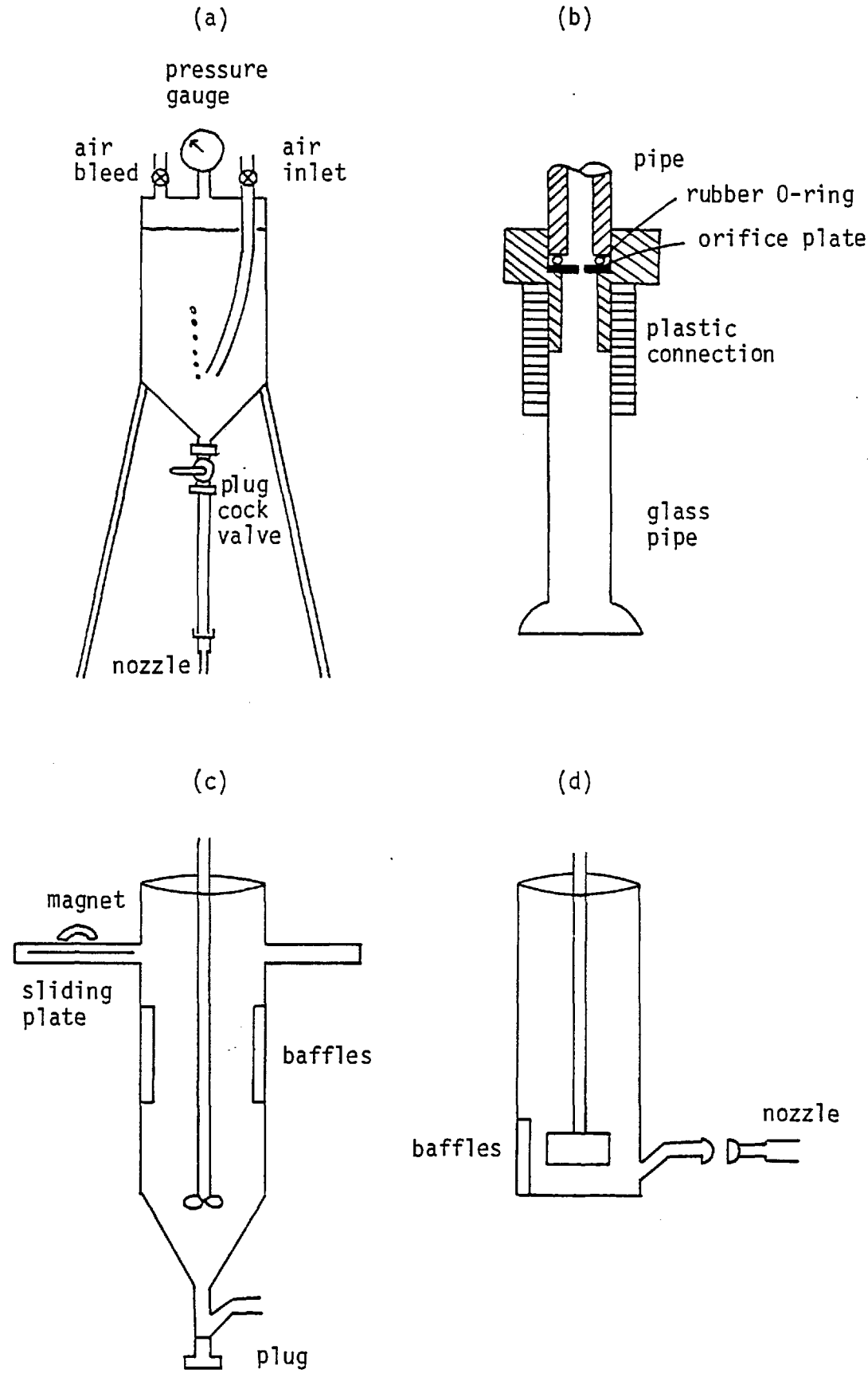

Figure 4.3. Schematic diagrams of (a) saturator, (b) pressure reduction nozzle, (c) Urban's cell, and (d) cell designed in this work

Equilibrium was attained by using air flowrates in excess of 10 l/min for periods of 30 minutes.

The pressure reduction device consisted of a 2 mm-thick brass plate with a single orifice (1 mm diameter) mounted in a nozzle between the saturator and flotation cell (Figure 4.3 (b)).

The two flotation cells used are shown schematically in Figure 4.3 (c) and (d). Urban's cell was only used for studies on the mechanism of bubble-particle attachment in DAF (Chapter 5). Urban reported problems in obtaining a stable froth containing the floated material and, therefore, his cell design included a sliding plate to "cut off" the suspension from the froth (80). Urban's cell proved to be unnecessarily elaborate since froth stability problems were overcome in this work (see Chapter 8). It was also found that Urban's conical design for the lower part of the cell was disadvantageous for flotation purposes.

The new cell shown in Figure 4.3 (d) had the advantage of reproducing the shear conditions predominant in the stability tests. It was also easy to clean and handle. Four baffles (0.5 x 8.0 cm) were incorporated at the bottom of the cell for the separation studies (Chapter 7).

4.6.3. Experimental procedure

DAF tests procedure consisted of four consecutive steps as follows: a) suspension conditioning, b) microbubble injection, c) flotation, and d) recovery of floated material.

Suspensions were prepared by dispersing 0.5 g of mineral in water in the flotation cell (1 l total volume). Conditioning of the suspension followed the procedure adopted in the stability tests for the particular

mineral/reagent system, with microbubble injection taking place at the end of the slow stirring period.

Microbubble production was accomplished by opening the plug valve and injecting 100 ml saturated water into the cell through the orifice plate. The pressure reduction over the plate caused the release of excess dissolved air as microbubbles which mixed into the suspension. Supersaturated water was usually injected at the gauge saturation pressure (e.g. the pressure at which air was dissolved) which, unless otherwise stated in the text, was 377 kPa (40 psig). When an injection pressure different to that of saturation was required, it was performed by removing the bubbling tube from the saturator and adjusting the pressure in the saturator just before the injection. Changes in the dissolved air content of the water, either by opening the saturator to atmospheric pressure or by diffusion when adjusting saturator pressure, are negligible (80)(209). The experimental data of Urban (80) show that under the conditions used in this work the microbubbles had a mean bubble diameter of 50 μm, their number density was 40 - 80 bubbles/mm^3 and their rise-time was about 240 s. Measurements of the microbubbles rise-time carried out in this work agreed very closely with those obtained by Urban.

The flotation stage commenced after microbubble injection had taken place. In all tests reported in Chapter 5 flotation occurred under quiescent conditions, flotation time being 4 min. Later, during the cassiterite flotation studies, it was discovered that slow stirring (25 - 50 rpm) during microbubble injection improved recovery. Therefore, those flotation tests were carried out under slow stirring conditions for 4 min and then left to stand for 2 minutes. Flotation times were determined from the rise-time of the microbubbles formed in the DAF

apparatus (240 s).

After the flotation time had elapsed the floated material was recovered by suction. This product was filtrated under vacuum using Whatman glass fibre GF/F filter paper capable of retaining particles above 0.7 μm. The filtrate was then dried, weighed and analysed.

RESULTS

Chapter 5. STUDIES ON THE MECHANISM OF BUBBLE-PARTICLE ATTACHMENT IN DISSOLVED AIR FLOTATION

5. STUDIES ON THE MECHANISM OF BUBBLE-PARTICLE ATTACHMENT IN DISSOLVED AIR FLOTATION

5.1. Dissolved air flotation of the quartz/dodecylamine system

5.1.1. Electrokinetic studies at the quartz/solution interface

The electrophoretic mobility of quartz in aqueous solution was determined in distilled water and at constant ionic strength as a function of pH. The results (Figure 5.1) showed that quartz was negatively charged down to pH values around 2.4. A measurement carried out at pH 2.4 and with 10^{-2} M NaCl indicated that the majority of the particles had a zero electrophoretic mobility at this pH. This is in good agreement with the value of the isoelectric point that may be extrapolated from the mobility/pH curves.

The curves show that the electrophoretic mobility of the quartz particles increased linearly with pH up to neutral values where it became almost constant and then increased slightly again at alkaline pH values. The increase in mobility at high pH values was higher in distilled water than at constant ionic strength. At pH values below 7, the electrophoretic mobility decreased at high ionic strength in agreement with theoretical considerations (191).

Ageing the samples for 24 hours did not have a substantial influence on the electrophoretic mobility of the quartz particles, in disagreement with the findings of other researchers (158)(210). Measurements of the electrophoretic mobility of a quartz sample at pH 7.0 and 10^{-2} NaCl over a period of seven days gave a constant value, within experimental error. Nevertheless, all experimental work on quartz was carried out on samples aged for 24 hours.

The effect of dodecylammonium chloride (DAC) concentration on the

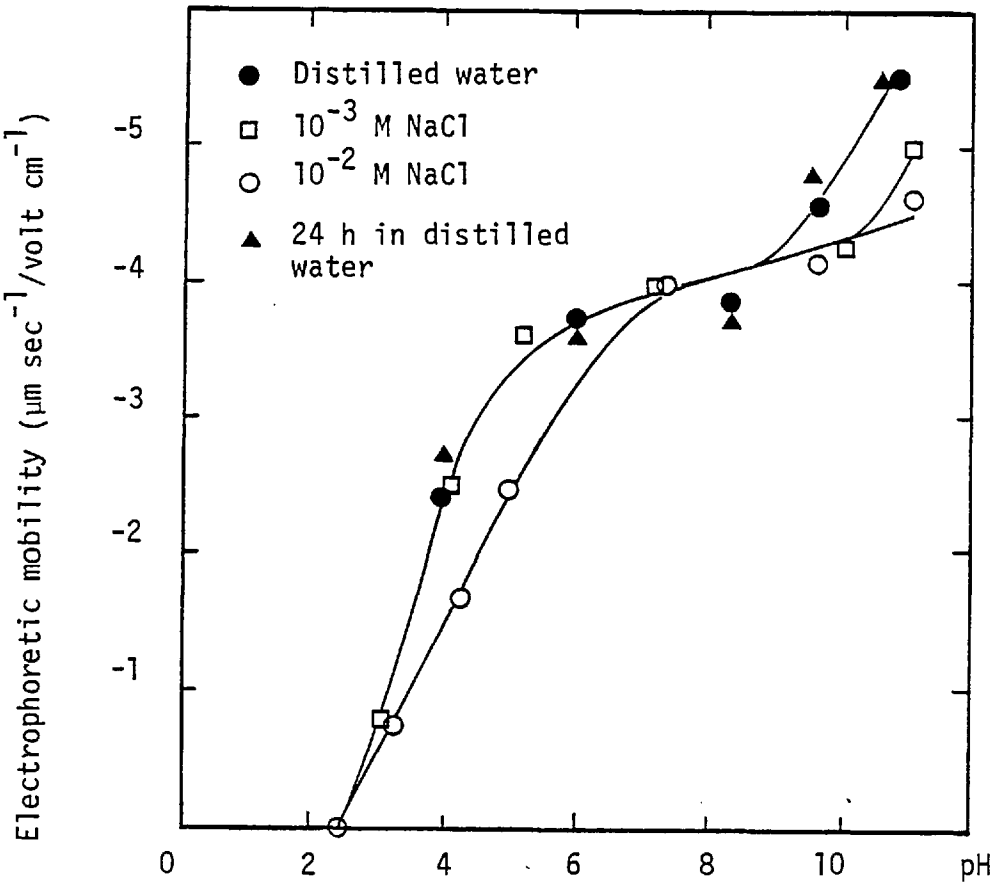

Figure 5.1. Electrophoretic mobility of quartz in aqueous solution as a function of pH

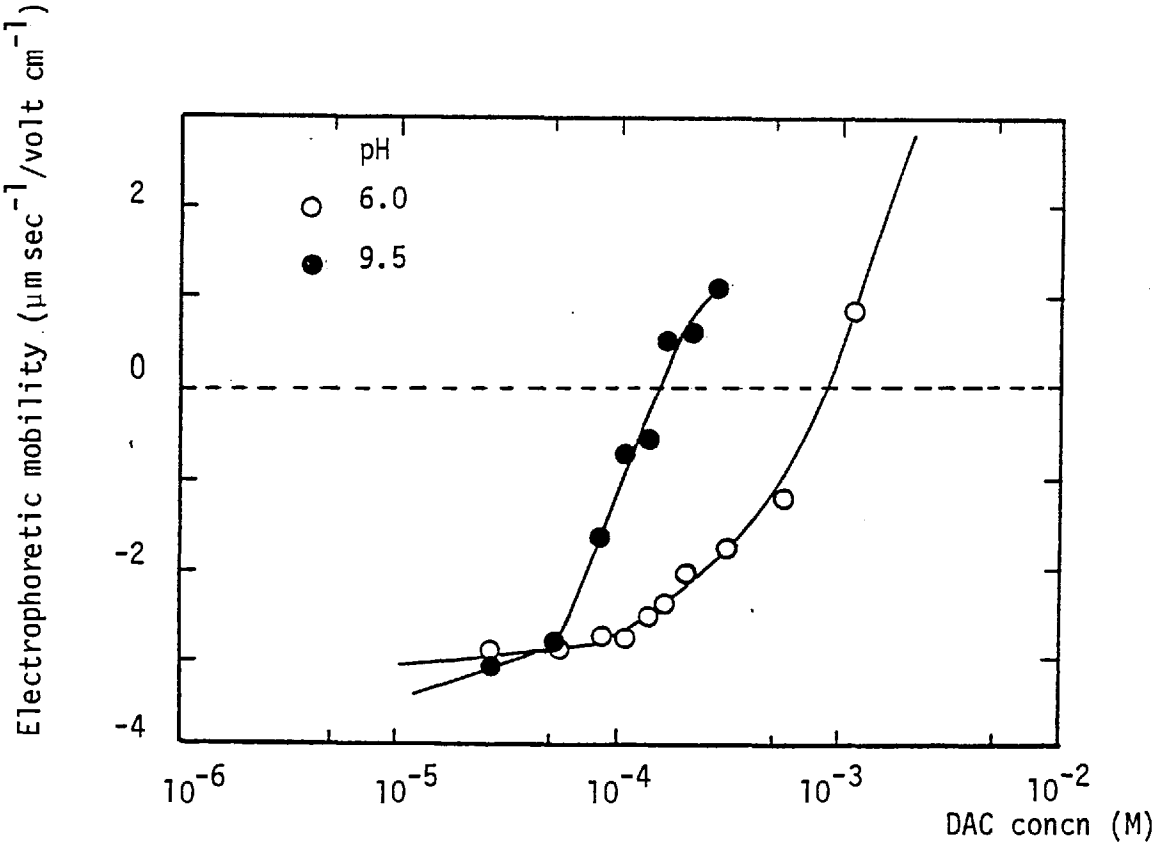

Figure 5.2. Electrophoretic mobility of quartz in the presence of dodecylamine at two pH values

electrophoretic mobility of quartz at pH values of 6.0 and 9.5 is presented in Figure 5.2. The curves show two distinct sections, namely, a section where the mobility is relatively constant with increases in the DAC concentration and, above a critical surfactant concentration, a second section where small increases in the DAC concentration caused a sharp decrease in the mobility and eventually charge reversal. The shape of the mobility/DAC concentration curves is very similar to those obtained by various authors for this system (134)(210)(211). The DAC concentration at which there is an abrupt decrease in the mobility will be referred to as the critical hemimicelle concentration (C_{HMC}) following the suggestion of Gaudin and Fuerstenau (134). The C_{HMC} is that surfactant concentration at which specific adsorption in the Stern layer begins to occur due to hydrocarbon chain interactions. The values of the C_{HMC} at pH 6.0 and 9.5 were about 10^{-4} and 5×10^{-5} M DAC respectively.

The DAC concentration at which the zeta-potential was reversed (the point of zeta-potential reversal, or pzr) depended on the pH value, a lower DAC concentration being required at the higher pH value. The pzr occurred at 1.5×10^{-4} M DAC for pH 9.5 and at 8.5×10^{-4} M DAC for pH 6.0. At pH 9.5, for surfactant concentrations above about 2×10^{-4} M, the slope of the mobility curve tended to decrease again indicating the existence of a third region. This region of the mobility/DAC concentration curves has been associated with the precipitation of the free amine (211). At this pH value precipitation of the amine molecule occurs at a DAC concentration of about 3×10^{-4} M (Figure 5.9), roughly coinciding with the beginning of the third region.

5.1.2. Stability of quartz suspensions in the presence of dodecylamine

Measurements of the supernatant transmittance of quartz suspensions

in distilled water showed no light transmittance in the pH range 4 - 11 over a period of 18 hours. At pH 2.0, the suspension underwent coagulation but at a slow rate (2% transmittance at 3 h, 72% after 18 h).

Tests on the stability of quartz suspensions in the presence of dodecylamine were carried out at various pH values. Figure 5.3 shows the effect of DAC concentration on the transmittance of quartz suspensions at pH 6.0 and 9.5. Depending on surfactant concentration and pH value the cationic surfactant acted as a destabilizing agent for quartz, inducing the aggregation of the particles into small but visible flocs (less than about 1 mm). The maximum supernatant transmittance values were associated with fast rates of particle aggregation and the formation of flocs exhibiting rapid rates of settling during the standing period. Conversely, optical transmittances of less than 10% corresponded to very small flocs and turbid suspensions showing dense and persistent hazes after the standing period.

Figure 5.3 also indicates that the range of DAC concentrations over which the quartz suspensions were destabilized was narrower at the higher pH value and that smaller concentrations of surfactant were required to cause particle aggregation at that pH. The critical effect of pH on the stability of quartz suspensions in the presence of dodecylamine is also demonstrated in Figure 5.4. Other tests were carried out at pH 10.9 and 9.5 in the presence of 10^{-4} M DAC to determine the reversibility of aggregation with respect to pH. The results showed that although the suspensions tended to redisperse when the pH was lowered to 6, some degree of aggregation still remained after 20 minutes.

The shape of the transmittance/DAC concentration curves indicates that after the destabilizing effect of DAC, further increases in concentration induced the redispersion of the aggregates and the restabilization

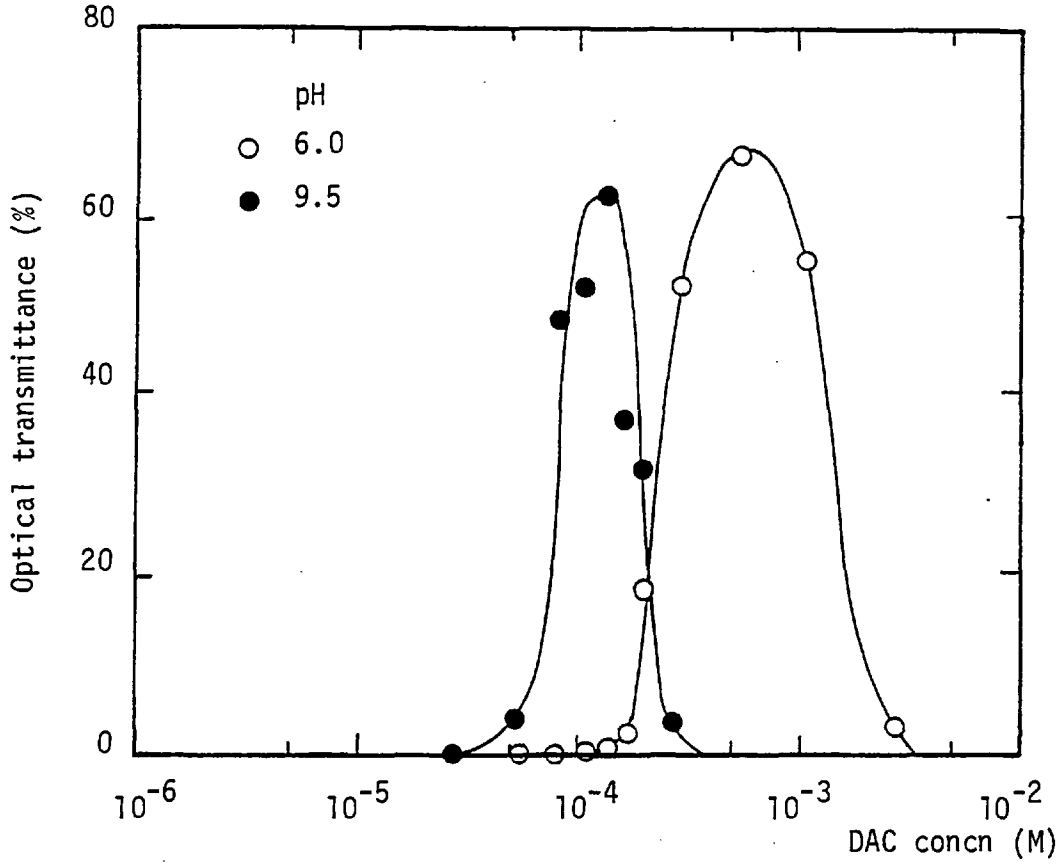

Figure 5.3. Stability of quartz suspensions as a function of dodecylamine concentration for two pH values

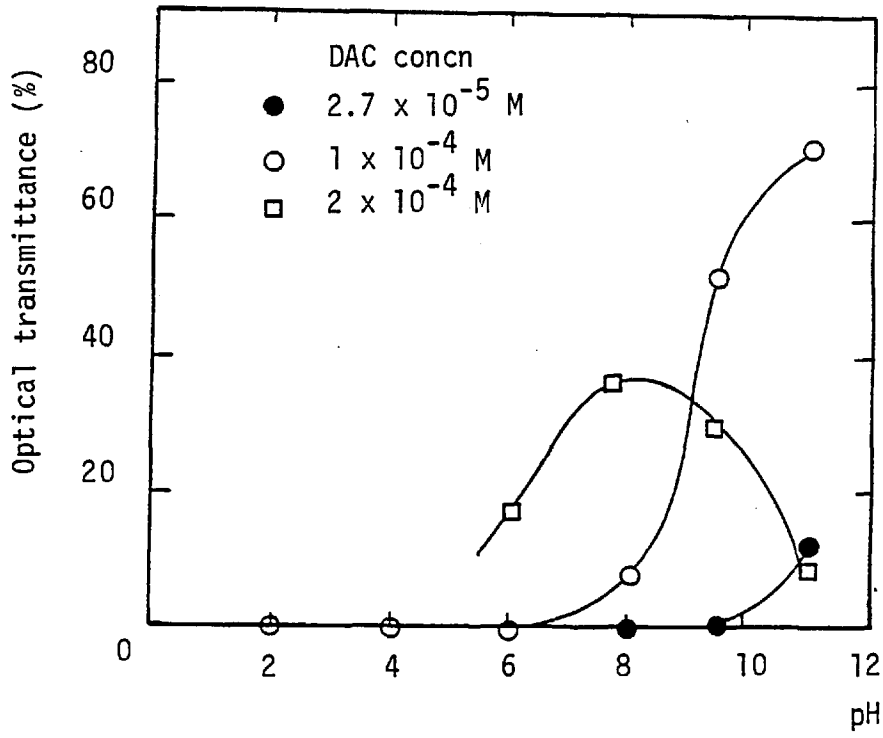

Figure 5.4. Stability of quartz suspensions as a function of pH for various dodecylamine concentrations

of the quartz suspensions. From these curves it is possible to extrapolate 'critical coagulation concentrations' (ccc) and 'critical stabilization concentrations' (csc), analogous to coagulation of colloidal systems by hydrolyzing metal ions (149). The extrapolated values of these parameters are presented in Table 5.1 together with the corresponding values of the electrophoretic mobility.

Table 5.1. Electrophoretic mobility of the quartz/DAC system at the critical coagulation and critical stabilization concentrations

pH	ccc (M)	mobility m sec^{-1}/volt cm^{-1}	csc (M)	mobility m sec^{-1}/volt cm^{-1}
6.0	1.8×10^{-4}	-2.3	2×10^{-3}	+2.75
9.5	6.5×10^{-5}	-2.4	2.4×10^{-4}	+1.0

The ccc values shown in Table 5.1 indicate that destabilization of the quartz/DAC system proceeded at much lower concentrations than would be expected for a 1:1 electrolyte (between 0.05 - 0.15 M (212)). Also, the ccc values corresponded to DAC concentrations higher than the critical hemimicelle concentrations and occurred at approximately the same value of the electrophoretic mobility (and possibly of the zeta-potential) for both pH values. It is also significant that maximum coagulation occurred at DAC concentrations in the region of the pzr and that the restabilization region occurred at positive (but different) values of the electrophoretic mobility.

These results suggest that the stability behaviour of quartz suspensions in the presence of dodecylamine is determined by the specific

adsorption of the cationic surface-active agent at the quartz/solution interface and by its subsequent influence on the potential energy of interaction between quartz particles.

5.1.3. Adsorption measurements of dodecylamine on quartz

A few measurements of the adsorption density of dodecylamine on quartz were carried out at pH values of 6.0 and 9.5 covering the range of initial DAC concentrations corresponding to the regions of rapid coagulation. The measurements were carried out at room temperature and the resulting isotherms have been plotted in Figure 5.5.

The results showed that the adsorption density of dodecylamine on quartz is dependent upon pH and equilibrium surfactant concentration. Higher adsorption densities were detected at pH 9.5 than at pH 6.0 for the same equilibrium concentration. At pH 6.0, the adsorption isotherm of DAC on quartz showed three different regions according to equilibrium surfactant concentration:

a) at low DAC concentrations, a region where adsorption density increases little with DAC concentration,

b) a second region at about 10^{-4} M DAC characterized by a sharp upturn in slope indicating a marked increase of adsorption density with a small increase in DAC concentration,

c) and at about 1.5×10^{-4} M DAC, a third region where the slope of the isotherm decreases again as a closely-packed vertically orientated monolayer is approached (assuming 20 A^{o2} per dodecylammonium ion (213)).

A similarly shaped sigmoidal isotherm has been reported for this system by Ball and Fuerstenau (214).

The adsorption isotherms at pH 9.5 showed only two regions:

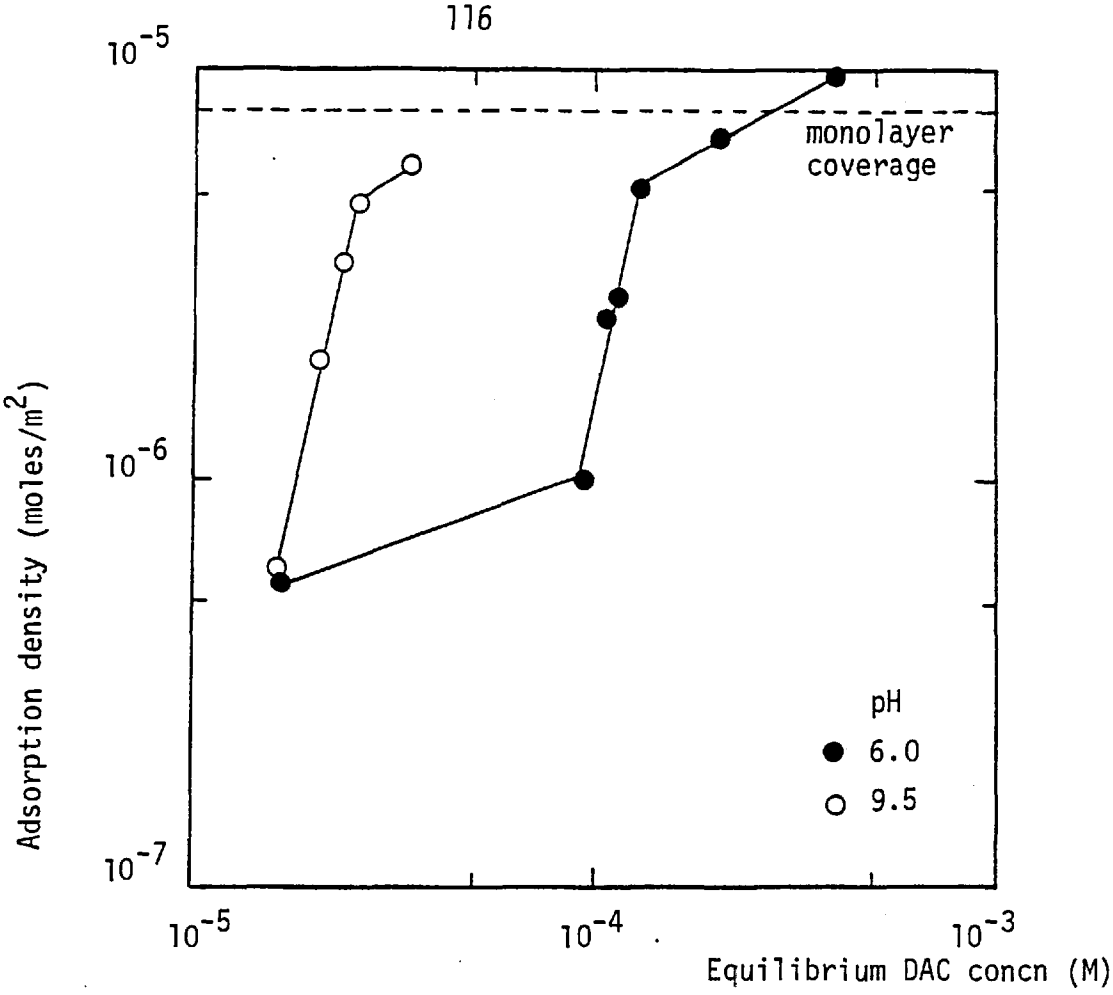

Figure 5.5. Adsorption measurements of dodecylamine on quartz at two pH values

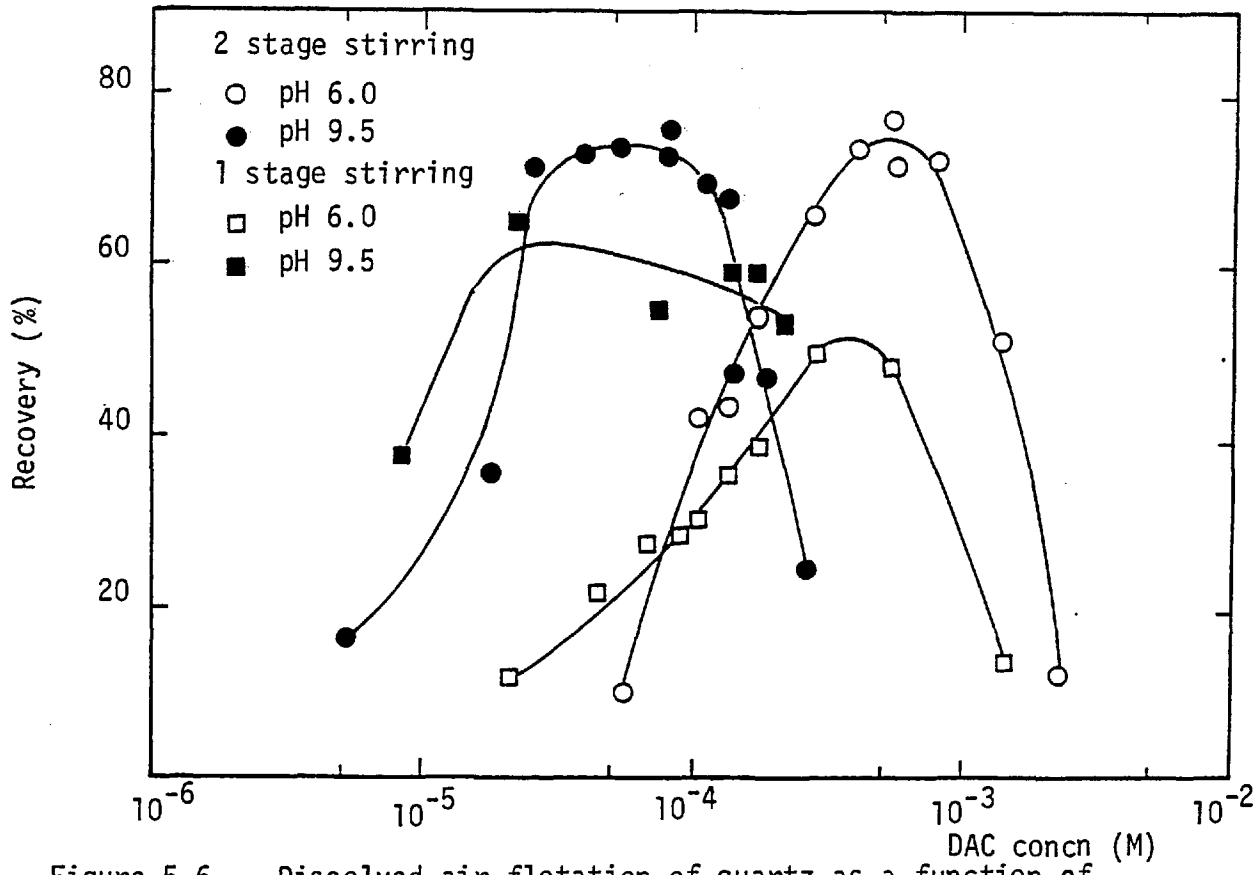

Figure 5.6. Dissolved air flotation of quartz as a function of dodecylamine concentration

a) a region where adsorption density increased very rapidly with DAC concentration,

b) a second region above 2.5×10^{-5} M DAC where the slope of the curve decreased as monolayer coverage was approached.

No measurements were carried out below 10^{-5} M DAC because of limitations imposed by the analytical method. Li and de Bruyn (211) have reported isotherms of DAC on quartz at alkaline pH values of similar shape to that obtained in these measurements at pH 9.5.

The adsorption isotherms of DAC on quartz have not been measured with an adequate number of points to consider them complete, but since the data obtained were in good agreement with those presented in the literature it was thought unnecessary to include more points.

5.1.4. Dissolved air flotation studies

Quartz in distilled water did not float over the pH range 2.4 - 9.5 and the addition of a frother (amyl alcohol) did not alter this situation When dodecylamine was added quartz floated well depending on pH and surfactant concentration as shown for two sets of experimental conditions in Figure 5.6.

The curves (2-stage stirring) showed that lower DAC concentrations were required at pH 9.5 to induce the recovery of quartz by dissolved air flotation than at pH 6.0. They also demonstrate that there was a range of surfactant concentrations for optimum mineral recovery and that an overdosage of DAC led to the suppression of recovery by DAF. The recovery/DAC curves are similar in shape to those described in the stability studies and indeed, a very close correlation between DAF and coagulation was established.

The importance of the aggregation of quartz particles is also

reflected by the effect of the conditioning period on DAF recovery. The '2-stage' period was identical to the experimental routine followed in the coagulation tests; on the other hand, the '1-stage' conditioning allowed only the fast stirring period prior to microbubble injection. The latter technique lead to smaller aggregates and reduced coagulation of suspensions, subsequently leading to lower DAF recoveries. It is interesting to note, however, that maximum flotation recoveries occurred at roughly the same collector concentration for both conditioning procedures.

It was found that large aggregates were not floated well by the microbubbles and this was reflected in the maximum value achieved for quartz recovery (about 80%). Coarse particles and big flocs tended to settle out and accumulate at the bottom of the cell, showing very little floatability upon microbubble injection although bubbles did attach. However, after some time (30 min - 1 h) some of these flocs could be observed rising through the liquid, being lifted by one or more of those attached bubbles. This observation is important as it constitutes experimental evidence of the growth of bubbles in the solution and therefore, evidence of some degree of liquid supersaturation after the injection of the microbubbles.

The relationship between dissolved air flotation and the phenomena occurring at the quartz/solution interface in the presence of DAC may be seen in Figures 5.7 and 5.8. The figures represent the correlation between DAF, optical transmittance, electrophoretic mobility and adsorption density as a function of surfactant concentration at pH 6.0 and 9.5. The DAF, transmittance and mobility results have been plotted against the initial DAC concentration; these parameters were all measured under equivalent experimental conditions (cf. Chapter 4).

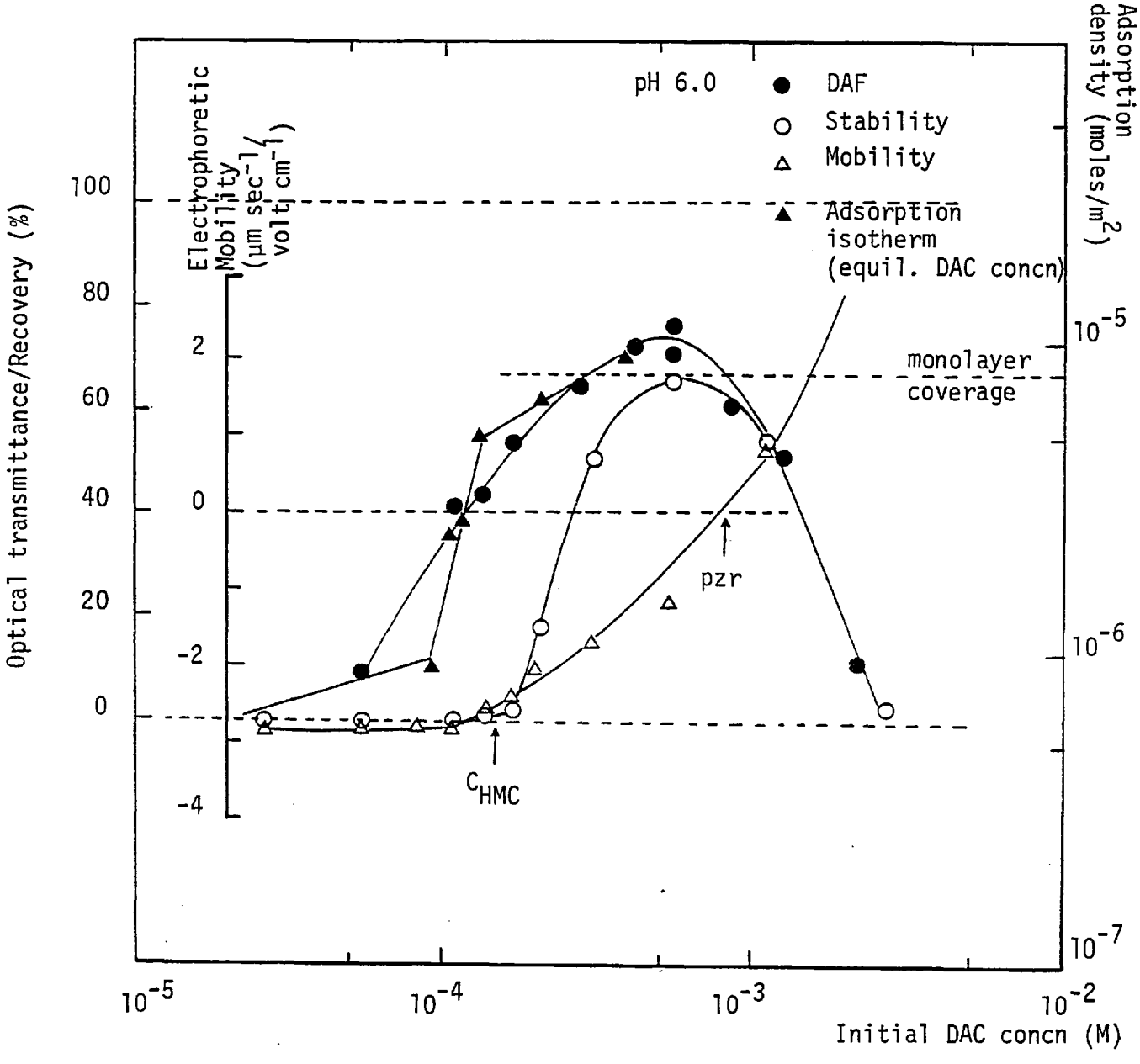

Figure 5.7. Dissolved air flotation, suspension stability, electrokinetic and adsorption measurements on quartz at pH 6.0 in the presence of dodecylamine

The adsorption results have been plotted as adsorption isotherms, that is, against equilibrium DAC concentrations. However, the results indicated that the various measurements shown in Figure 5.7 (pH 6.0) need be only slightly shifted towards lower DAC concentrations to correspond with equilibrium concentrations, whereas at pH 9.5 the shift is expected to be higher due to the greater adsorption obtained.

At pH 6.0, low floatability (less than 50% recovery) of quartz particles is associated with the region in which dodecylammonium ions adsorb without changing the electrophoretic mobility of the particles (similar to the behaviour of an indifferent electrolyte at low concentrations (134)), with stable quartz suspensions and with collector adsorption densities of less than 10% of monolayer coverage. The region of maximum flotation recovery (over 50%) occurred at DAC concentrations above the C_{HMC} and correspond with marked increases in the aggregation of quartz suspensions and in the adsorption of DAC on quartz. Maximum DAF recovery coincided with the DAC concentration of maximum coagulation, corresponded to an adsorption density of about monolayer coverage and lay close to the point of zeta-potential reversal. According to the results of Smith (215), the equilibrium contact angle at this DAC concentration is about 30^{o}. For surfactant concentrations above the pzr, both DAF and coagulation decreased rapidly while the electrophoretic mobility continued to increase, indicating that surfactant adsorption was occurring above the pzr. This region occurred above monolayer coverage and two-liquid flotation tests (with cyclohexane as the oil phase) indicated that the particles were increasingly hydrophilic, no extraction being found at 4×10^{-3} M DAC. This would suggest that above the pzr the dodecylammonium ions adsorb with the polar head pointing towards the solution as suggested by Jaycock and Ottewill (130).

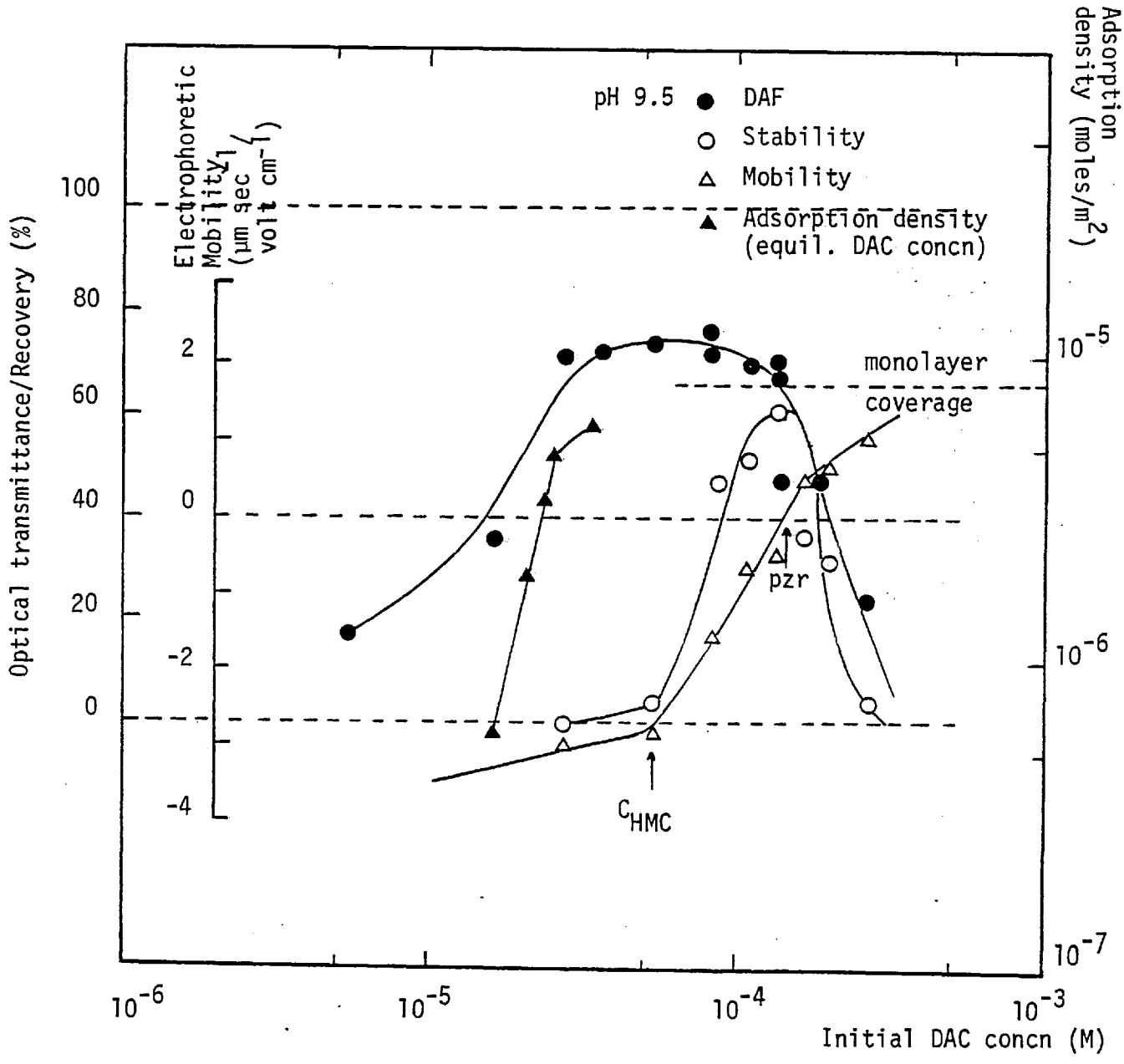

Figure 5.8. Dissolved air flotation, suspension stability, electrokinetic and adsorption measurements on quartz at pH 9.5 in the presence of dodecylamine

At pH 9.5, recoveries of less than 50% occurred at DAC concentrations below the C_{HMC} and the quartz suspensions showed zero transmittance in the stability studies. Surfactant adsorption in this region may be estimated from the isotherm to be approximately between 5 - 15% of monolayer coverage. Maximum DAF recoveries occurred for DAC concentrations between the C_{HMC} and the pzr, thus various degrees of coagulation were associated with a constant level of flotation recovery. Surfactant adsorption probably increased in this region to above monolayer coverage at the pzr and so it would appear that there was a minimum level of hydrophobicity for DAF to be maximum. The results of Smith (215) show that the equilibrium contact angle varies in this region between 30^{o} and 70^{o}. The higher levels of hydrophobicity reported for the quartz/dodecylamine system at alkaline pH values have been attributed to the coadsorption of neutral molecular amine, which exceeds 10^{-6} M at total DAC concentrations over 2×10^{-5} M (Figure 5.9)(215). Above the pzr, DAF and coagulation decreased and the electrophoretic mobility increased but less markedly as the solubility limit of the cationic species was reached (3×10^{-4} M at pH 9.5). Two-liquid flotation tests carried out in this region gave erratic results but 'no extraction' was detected at about 10^{-3} M DAC. It is also interesting to note that the DAC concentration indicating the suppression of flotation (about 5×10^{-4} M) corresponded with the CMC of the surfactant at this pH value and with the limiting flotation concentration obtained by other workers (216).

5.1.5. Discussion

The studies described in the previous sections revealed firstly, that the recovery of mineral particles by dissolved air flotation was possible and secondly, that the flotation could be correlated with the

interfacial properties of the mineral/collector system.

The negative electrophoretic mobilities measured for quartz in aqueous media were consistent with the presence of a negatively charged quartz surface due to the dissociation of hydrogen ions from the surface silanol groups. The isoelectric point obtained for quartz at pH 2.4 is within the range of values quoted in the literature for this oxide (217).

The electrokinetic and adsorption measurements on the quartz/dodecylamine system agreed well with research carried out on this system by other workers (218)(210)(211). These measurements were consistent with the model proposed by Gaudin and Fuerstenau (134) for the adsorption of dodecylamine on quartz. According to the model, at low surfactant concentrations the ions adsorb in the diffuse part of the double layer through electrostatic attraction for the surface until a critical DAC concentration is reached (the C_{HMC}). Above the C_{HMC}, the ions adsorb specifically through hydrophobic bonding interactions between the hydrocarbon chains and associate into two-dimensional patches in the Stern plane.

The stability behaviour of quartz suspensions in the presence of dodecylamine followed the pattern described by other authors for negatively charged sols in the presence of cationic surface-active agents (161)(219). Destabilization is induced by the lowering of the electrostatic double layer repulsion forces due to the neutralization of charged sites by the adsorbed surfactant. Hence, the stability minimum occurs in the vicinity of the pzr and restabilization of the suspensions occurs due to the superequivalent adsorption of the surfactant above the pzr which increases the repulsive electrostatic forces.

Surfactant concentration and pH were confirmed to be the most

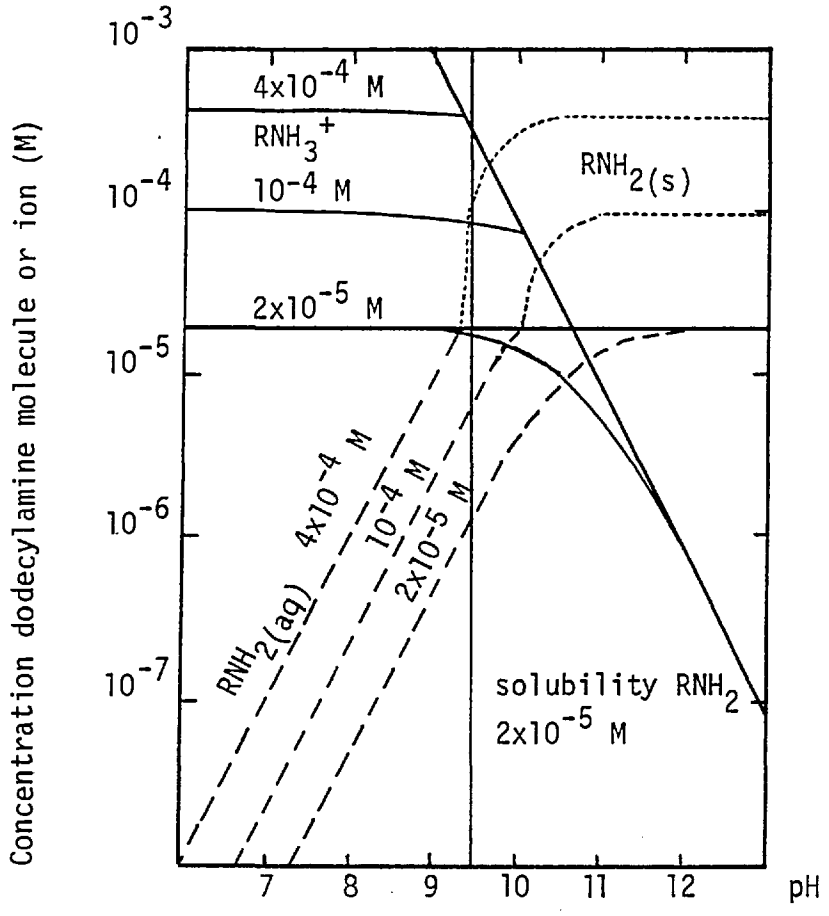

Figure 5.9. Concentration of dodecylamine species in solution as a function of pH for various total amine concentrations

important parameters governing the interfacial behaviour of the quartz/dodecylamine system. The influence of pH arises from the fact that: a) H^+ and OH^- are potential-determining ions for quartz and therefore pH determines the surface potential and coulombic attraction of DAC ions for the quartz surface, and b) as primary amines are weak bases the pH value determines the degree of ionization of the surfactant. Dodecylamine ionizes in water according to the reactions (220):

$$RNH_{2(aq)} + H_2O \rightleftharpoons RNH_3^+ + OH^- \qquad K = 4.3 \times 10^{-4} \qquad (5.1)$$

$$RNH_{2(s)} \rightleftharpoons RNH_{2(aq)} \qquad K = 2 \times 10^{-5} \qquad (5.2)$$

The concentrations of dodecylamine ion and molecule in solution have been represented in Figure 5.9 as a function of pH on the basis of equations 5.1 and 5.2. The influence of surfactant concentration on

the various interfacial phenomena studied is basically explained by the change of adsorption mechanism with increasing DAC concentration. Furthermore, the critical hemimicelle concentration is dependent upon a combination of factors including pH, total surfactant concentration and the ratio of neutral to charged species in solution.

The results of the dissolved air flotation studies showed quartz flotation to be closely associated with both surfactant adsorption and coagulation of the dispersed phase. Thus, good recoveries of quartz by dissolved air flotation were obtained when the adsorption density of dodecylamine on quartz was approximately between 10 - 100% of a closely-packed vertically oriented monolayer of DAC ions (assuming 20 A^{o2} for the cross sectional area of an adsorbed DAC ion). For adsorption densities below about 10% monolayer coverage the particles showed only slight floatability. On the other hand, the suppression of quartz recovery by DAF was associated with increasing hydrophilicity probably due to the reversed orientation of the adsorbed DAC ions at high surfactant concentrations.

It would appear, therefore, that adhesion mechanisms relying on the establishment of an air bubble/mineral surface contact angle are important in the attachment mechanism of the dissolved air flotation process. Having established a relationship between DAF and surfactant adsorption, the question of the influence of coagulation in the attachment mechanism remains to be explained. With the exception of some results at pH 9.5, where at low DAC concentrations significant recoveries occurred for stable quartz suspensions, the domains of the DAF and coagulation regions coincided almost exactly. There are various kinetic factors that might explain the importance of aggregating the dispersed phase for DAF operations but their discussion is not

relevant unless it is shown that coagulation is not a prerequisite for DAF to occur. The influence of the aggregation of the dispersed phase on the attachment mechanism was studied by carrying out DAF tests on a number of hydrophilic aggregated systems, the results of which are presented in the next section.

5.2. Dissolved air flotation of various aggregated systems

5.2.1. Dissolved air flotation of the quartz/iron(III) system

It is known that hydrolyzing metal ions such as iron or aluminium have destabilizing properties on colloids and suspensions, their action depending upon the pH, the metal concentration and the surface area of the solids (149). Stability tests were carried out on the quartz suspensions in the presence of iron(III) with the view of their further recovery by dissolved air flotation.

Preliminary tests, carried out in the pH range 5 - 8 using iron(III) as the ammonium ferric sulphate salt, gave best optical transmittance at pH 7.0 and subsequent work was carried out at that pH value. The effect of metal ion concentration on the stability of quartz suspensions is presented in Figure 5.10. For iron concentrations above 5×10^{-5} M floc formation was very rapid, being noticeable around 40 seconds after the salt addition. At those concentrations the flocs were relatively large, their size increasing with increases in coagulant concentration. The flocs appeared as irregular three-dimensional networks showing an open and loose structure. The supernatant solutions were transparent and colourless and the sedimented flocs exhibited the reddish colour of ferric hydroxide. No restabilization was observed with respect to iron concentration increases for values up to 1.25×10^{-3} M.

These observations are consistent with the experimental results

reported by other researchers on destabilization of colloidal systems by hydrolyzing metal ions (149)(221)(222). At pH 7.0, a probable mechanism of destabilization would be the primary adsorption of hydrolyzed iron(III) species on the negatively charged quartz particles, followed by their coating with colloidal precipitated ferric hydroxide (the predominant species at this pH) and the aggregation of the particles in bigger hydroxide flocs.

The recovery of quartz by DAF as a function of iron(III) concentration was studied at pH 7.0 and the results are shown in Figure 5.10 (open triangles). The results showed that quartz recovery varied between 60 - 85% for the metal concentration range 10^{-5} - 10^{-3} M; below 10^{-5} M, recovery decreased markedly to nil at about 10^{-6} M paralleling the decrease in coagulation of the suspension. At concentrations above 10^{-5} M Fe(III), the large and reddish-coloured flocs floated massively, levitated by the 'milky' cloud of microbubbles formed upon the injection of supersaturated water. The floated material formed a thick layer at the top of the flotation cell which remained stable unless disturbed. A certain portion of the solids, however, consisted of large flocs which were not floated by the microbubbles.

The possibility of flotation occurring as the result of a 'carry-over' effect was explored by carrying out DAF tests in a different way. The tests were carried out in the coagulation beakers by injecting the supersaturated water from above after the flocs had settled down, thus the mixing between flocs and bubbles was ensured without the presence of an upward current of liquid as happens in the DAF cell. The results of these tests, shown as black triangles in Figure 5.10, indicated that DAF of quartz/iron(III) flocs was a genuine effect.

The fact that intrinsically hydrophilic flocs could be floated by

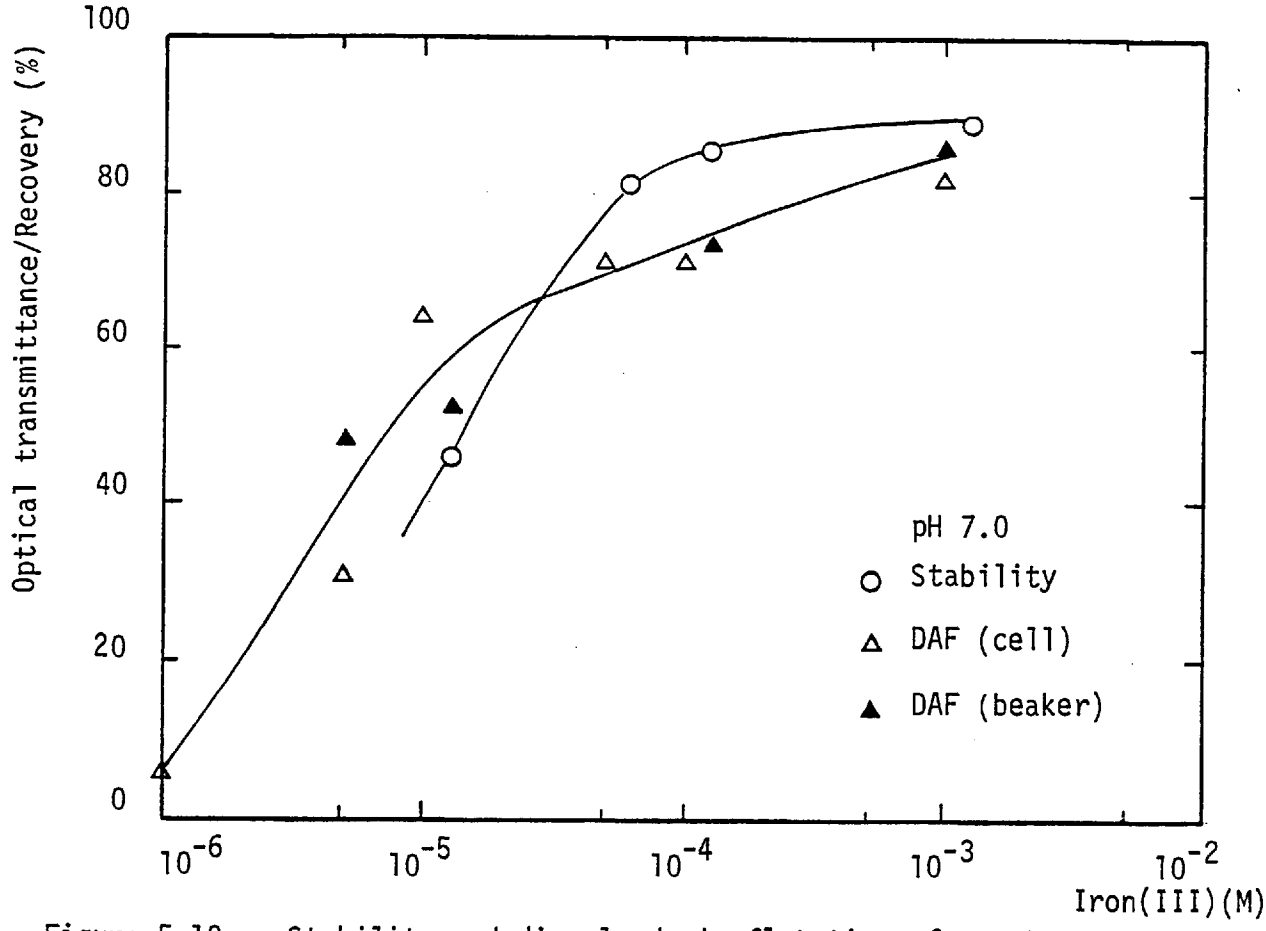

Figure 5.10. Stability and dissolved air flotation of quartz as a function of iron(III) concentration at pH 7.0

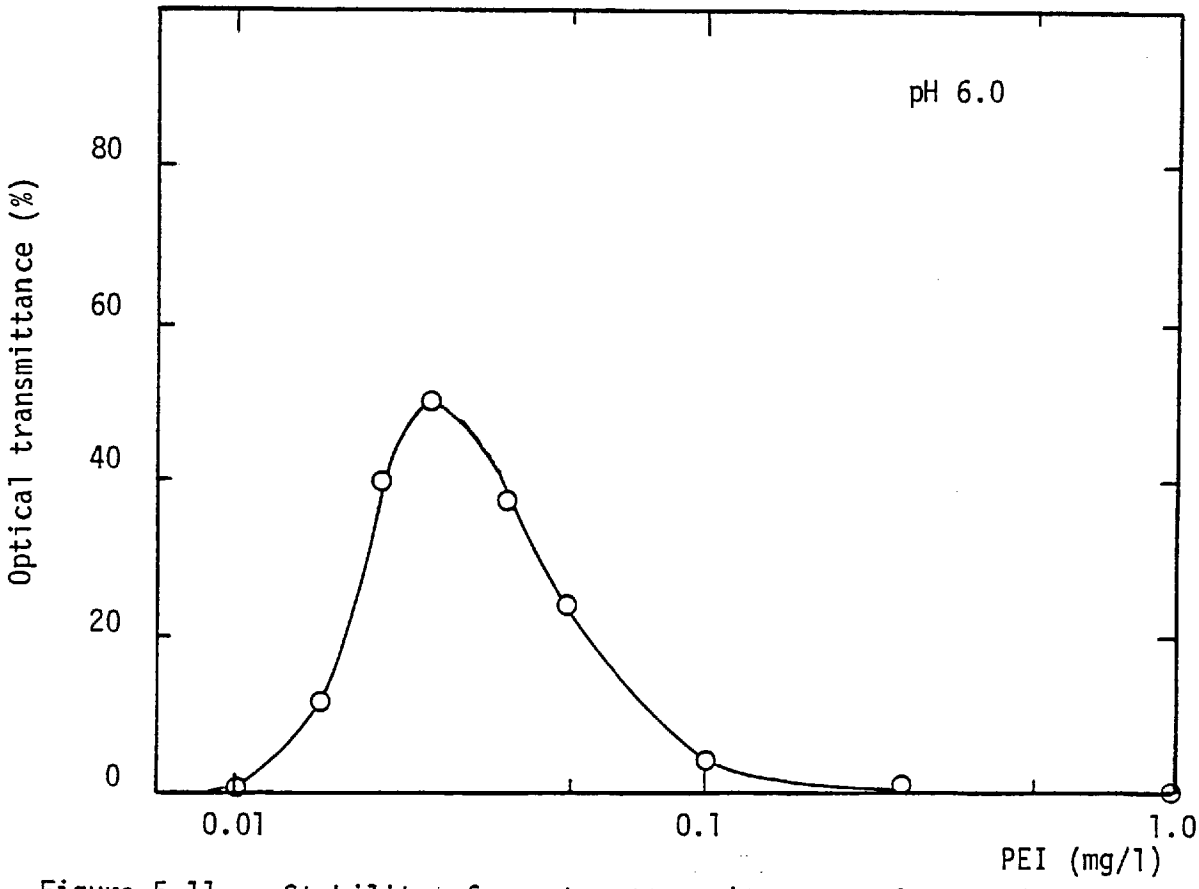

Figure 5.11. Stability of quartz suspensions as a function of polyethyleneimine concentration at pH 6.0

the DAF microbubbles and the correlation between DAF and coagulation being corroborated by these results, tended to suggest that aggregated systems could always be floated by DAF irrespective of the flocs' surface properties. However, as the flocs would bear the surface properties of ferric hydroxide, tests were carried out to determine the degree of hydrophilicity of these flocs.

The tests consisted of putting the freshly prepared quartz/ferric flocs into contact with water supersaturated with air (2.7 atmospheres supersaturation), the reasoning being that if the flocs were hydrophobic air would precipitate out of solution and nucleate as bubbles on their surface (these tests are very sensitive to the hydrophobicity of the flocs and were used extensively to determine the nucleation behaviour of bubbles from supersaturated solutions in Chapter 8). The results of these tests demonstrated that the quartz/ferric hydroxide flocs prepared from 'Analar' reagents and usually 'pure' laboratory conditions, exhibited a few but not negligible amount of hydrophobic spots where bubbles could nucleate, grow and eventually lift some individual floc structure. Thus, it would appear that the reagents were not free from organic contamination that might have provided sites for microbubble attachment.

The purification of the reagents to produce hydrophilic flocs was considered but not pursued further given the results obtained in a similar work carried out at the Department (81). Those results indicated that the flotation of 'very pure' ferric hydroxide flocs by microbubbles generated by an electrolytic flotation cell was very irreproducible but followed a pattern according to the purity conditions of the reagents. When using freshly prepared reagents (triple distilled water containing less than 0.02 ppm total organic carbon, especially

prepared ferric sulphate and sodium carbonate treated for the removal of organic matter) no flotation was obtained whereas if the same reagents were stored for a few days or handled repeatedly they would yield total flotation.

It seems remarkable that the degree of contamination introduced by bacterial growth or handling could induce the floatability of ferric hydroxide flocs. The only plausible explanation for this behaviour lies with the physical structure of these flocs which may enhance their ability to induce the attachment of microbubbles. Hence, the flocs 'woolly' structure with their branches extending into the solution would provide a large interfacial area which would facilitate microbubble collisions and attachment. Since the density of the flocs is low only a small number of hydrophobic spots might suffice to induce flotation.

A survey of the literature on flotation of various solids coagulated by hydrolyzing metal ions showed the following common factors:

a) The floatability region of the solids corresponds closely with the region where they are destabilized by the metal ion as was found in this work (72)(92)(223 - 226).

b) The flotation recovery of the aggregates is dependent upon bubble size, large bubbles being inefficient (227)(228).

c) The role of hydrophobicity is unclear, some authors added a collector (224)(228), while others floated flocs of unspecified surface characteristics but likely to be contaminated (72)(92), and others floated hydroxide flocs in conditions similar to this work (225).

These results and those reported in this work suggest that dissolved air flotation of flocs produced upon the precipitation of metal hydroxides occurs as the result of a combination of factors including hydrophobicity, floc structure and coagulation which has not been completely elucidated.

5.2.2. Dissolved air flotation of the quartz/polyethyleneimine system

Dissolved air flotation tests were carried out on the quartz/polyethyleneimine system as it was suggested that the quartz particles would aggregate in a different floc structure in the presence of this cationic polyelectrolyte.

Indeed, coagulation tests carried out in the presence of polyethyleneimine (PEI) showed that the resulting flocs were very small and of a 'compact' structure. Remarkably low concentrations of PEI were required to destabilize the quartz suspensions which then showed very slow rates of clarification. The small size of the quartz/PEI flocs resulted in slow rates of settling and low values for the optical transmittance of the supernatant solutions compared to the previous studies. However, the transmittance of the quartz suspensions in the presence of PEI is not indicative of weak coagulation, being due to the physical characteristics of the flocs. Measurements of optical transmittance after allowing for longer standing times (2 h) gave values of about 80% transmittance.

Figure 5.11 shows the effect of PEI concentration on the optical transmittance of quartz suspensions at pH 6.0. The curve shows that the ccc for this system occurred at about 0.015 mg/l PEI above which the system underwent strong aggregation, maximum values being obtained between 0.025 and 0.05 mg/l. The curve further shows that increase in the PEI concentration produced the restabilization of the suspension, stability being obtained for PEI concentrations in excess of 1.0 mg/l for a period of 18 hours.

These results agree well with the studies carried out by Dixon, La Mer et al (229) on the flocculation of silica by polyethyleneimines of various molecular weights. These authors showed that PEI adsorbed

through electrostatic attraction for the negatively charged silica surface and reversed the sign of the electrophoretic mobility of the particles, the PEI concentration for optimum refiltration rate corresponding to the pzr of the particles. Dixon et al (229) proposed that above the PEI concentration that causes charge reversal, destabilization occurred via polymer bridging between the particles. However, Lindquist and Stratton (230) argued that the bridging mechanism occurs only at high pH values (above pH 9). Both sets of researchers agreed that the restabilization of the silica/PEI system was due to the high electrostatic repulsion between the positively charged particles. Restabilization of the silica/PEI system took place only in the presence of high molecular weight polymers (1000 - 32,000)(229). As the destabilization of silica by PEI occurred primarily through the reduction of the electrostatic repulsive forces, the phenomenon will be referred to as coagulation in this work.

Dissolved air flotation studies carried out on the quartz/PEI system under conditions of good particle aggregation (0.02 - 0.08 mg/l PEI) showed that these flocs were not floated by the microbubbles, flotation recoveries being of the order of 5 - 10%. After microbubble injection into the cell, the flocs were observed rising to the top and then falling down in a circulation pattern typical of non-floating flocs (81). It was thought that this behaviour may have been due to the lack of a persistent froth and DAF tests were performed with the addition of amyl alcohol and Dowfroth 250 as frothers. However, neither of them substantially improved the floatability of the suspensions, the recoveries varying between 10 - 20%.

To confirm that the non-flotation behaviour of these quartz/PEI flocs was due to their hydrophilicity, two-liquid flotation tests were

carried out on flocs formed with 0.04 mg/l PEI (using cyclohexane as the oil phase). The tests indicated that the flocs had strong affinity for the aqueous medium, the oil phase remaining clear. Thus, there was definite proof that hydrophilic aggregated systems were not floated by the microbubbles produced by the dissolved air flotation process.

If the adsorption mechanism of PEI on quartz is analogous to that found on silica the pzr would be expected to occur in the vicinity of the PEI concentration indicating maximum coagulation, and above this concentration the quartz particles would be expected to be positively charged and liable to adsorption of negatively charged ionic species. Consequently, DAF tests were performed on the quartz/PEI system at 0.04 and 0.08 mg/l PEI in the presence of 8.7×10^{-5} M of an anionic surfactant (sodium dodecyl sulphate). At the lower PEI concentration, the DAF recovery was raised to 28% and at 0.08 mg/l PEI the flocs showed considerable flotation yielding a recovery of 53%.

The dissolved air flotation studies carried out on the quartz/polyethyleneimine system demonstrated that the process can act selectively by not floating aggregates which are hydrophilic. The tests further showed that flotation of the same aggregates could be achieved if a reagent which might confer hydrophobicity to their surface was added.

5.2.3. Dissolved air flotation of the silica/polymeric flocculant system

The previous studies showed that hydrophilic flocs were not floated by DAF but since the PEI flocs were very small the influence of floc structure on the attachment mechanism of microbubbles was not elucidated. It was therefore decided to carry out a few DAF tests with hydrophilic

flocs whose structure and size could facilitate microbubble collision.

The system chosen for these tests was BDH precipitated silica and a cationic polyacrylamide flocculant (C150/23). Precipitated silica was chosen as the solid phase since flocculation of quartz by this polymer resulted in the formation of small flocs. BDH precipitated silica is a hydrophilic, fully hydrated silica with a high surface coverage of silanol groups and its properties are well documented in the literature (231). Preliminary flocculation tests showed that additions of 5 mg/l of the cationic polymer to a 0.05% silica dispersion at pH 5.5 resulted in the formation of big flocs ($\geq$ 1 cm) exhibiting 'loose' structures. Experiments with bubble nucleation from air supersaturated solutions gave no bubble formation on these flocs confirming their hydrophilicity.

The results of DAF tests carried out under 'very clean' conditions (extensively cleaned glassware, freshly prepared reagents, surfactant-free double-distilled water) indicated that these flocs were non-floatable. However, when the flocs were prepared in single distilled water (which showed slight bubble persistence upon shaking) they showed a variable degree of floatability which sometimes resulted in complete flotation. Additions of 5.4×10^{-5} M dodecylamine to the preformed flocs resulted in their complete flotation. When Aerosil silica (silica rendered hydrophobic by reaction with dimethyl dichlorosilane (231)) was used instead of the precipitated sample, good flotation of the flocs was obtained.

The results outlined in the flotation of flocculated silica confirmed that hydrophilic flocs are non-floatable by dissolved air flotation. However, they also confirmed that large and open floc structures lower the minimum hydrophobicity requirements for microbubble

attachment and DAF to occur.

5.2.4. Dissolved air flotation of the silica gel/cationic surfactant system

DAF tests on hydrophilic floc particles were continued on silica gel 'flocs'. A weak silica gel was prepared* by acidification of a dilute sodium silicate solution (about 60% SiO_2) to pH 5 followed by its further dilution in distilled water at the 'gel point'. Suspensions containing about 0.1% silica were used in the flotation tests. The silica gel particles were irregularly shaped and of a soft texture but appeared less woolly and much more rigid than the ferric hydroxide flocs. They were also capable of withstanding greater shear forces than the quartz/ferric hydroxide flocs without disintegrating. The maximum size of these silica flocs was about 5 mm.

Dissolved air flotation tests of gel particles in single distilled water and in the presence of amyl alcohol showed no floatability behaviour whatsoever. However, the addition of 6.7×10^{-5} M dodecylamine at pH 8.0 resulted in the massive flotation of the silica flocs in a froth layer from which some detachment occurred only after 20 minutes. An increase of the pH value to 9.5 for the same DAC concentration resulted in strong flotation and no floc detachment from the froth. Some large silica gel particles did not tend to float. DAF experiments carried out at pH 5.5 in the presence of another cationic surfactant (2.5 mg/l CTAB) also gave good flotation showing slight froth detachment but an increase in the surfactant concentration (25 mg/l) produced strong flotation with the formation of a stable froth. Electroflotation tests carried out on the silica gel/CTAB system gave similar results (81).

These tests confirmed that hydrophilic silica particles were not

* Prepared by Dr. J.A. Kitchener

floated by the microbubbles generated by the dissolved air flotation system even though their size gave an increased opportunity for bubble-particle collision. These particles also showed less sensitivity to water contamination than either ferric hydroxide or polymer flocculated silica, both of which showed some degree of floatability in single distilled water.

5.3. Discussion

The mechanism of bubble-particle attachment in dissolved air flotation

The dissolved air flotation studies carried out on a well-characterized oxide mineral/collector system and on destabilized systems of various physical and chemical characteristics, indicated the significant factors in the mechanism of bubble-particle attachment in the DAF process.

The results obtained in the DAF studies showed that particles or flocs which were hydrophilic would not be floatable by DAF. Nevertheless, if the dispersed phase was rendered hydrophobic by the addition of a surface-active agent, it would be easily floated by the microbubbles. Thus, the establishment of a contact angle between the solid phase and the air bubble appears as the determinant factor in the attachment mechanism.

The mechanism of bubble-particle attachment in dissolved air flotation is therefore very similar to that occurring in conventional, dispersed air, flotation systems (Chapter 1), hydrophobic particles being collected by bubbles upon collisions. The possibility of bubble-particle attachment occurring as the result of direct air nucleation onto the hydrophobic particles rather than upon bubble-particle collisions was studied (Chapter 8) and found not to be of importance

in this DAF system (and probably in all DAF systems where the microbubbles are formed at pressure reduction devices, i.e. effluent recycle pressurization systems).

The main difference between the attachment mechanisms in dispersed and dissolved air flotation systems arises from the relative size of bubbles and particles. Thus, while in conventional dispersed air flotation the particles are 'captured' by much bigger rising bubbles, the inverse occurs in dissolved air flotation systems. In DAF, the particles are usually aggregated in flocs comparable to or larger than the microbubbles and it is these flocs that require to 'capture' the necessary microbubbles to achieve floatability. This also implies that in a dissolved air flotation system the probability of bubble-particle collisions is higher than in a conventional flotation machine (for the same amount of air).

The possibility of entrapment of bubbles in floc structures as a mechanism of bubble-particle attachment in DAF has been suggested in the literature but no experimental evidence has been supplied (67). Two entrapment mechanisms have been suggested, namely, the trapping of rising microbubbles in floc structures and the absorption or incorporation of microbubbles in growing flocs. Then a prerequisite for these mechanisms is the presence of suitable floc structures and their existence may be proved by floating hydrophilic flocs.

The results of experiments on flocculated systems (section 5.2.3) which encouraged bubble entrapment indicated that hydrophilic flocs do not 'trap' microbubbles. The possibility of flotation through purely physical entrapment mechanisms is even less likely in real DAF operations due to the degree of agitation prevailing in those cells.

However, the fact that a slight degree of hydrophobicity or contamina-

tion could induce the flotation of certain floc structures does point to the floc characteristics having some influence on the attachment mechanism. Thus, because of their higher interfacial area and lower density, larger flocs required only a few localized hydrophobic 'sites' to induce microbubble attachment compared with smaller aggregates.

Hydrophobic 'spots' may develop on the floc structure as the result of adsorption of surface-active agents contained in the water or from reagent contamination. The first possibility is the most likely in DAF operations where anionic surfactants are usually present in the wastewater. A recent study (96) indicated that MBAS measurements (methylene blue active substance, a measure of the anionic surface-active agent concentration) of various influents in DAF plants gave amounts fluctuating between 0.4 - 2 mg/l and some were even higher (35 mg/l). It is then conceivable that flocs produced by precipitated metal hydroxides and polymeric flocculants in the aqueous environment of DAF operations would contain hydrophobic sites.

The results of dispersed air microflotation studies (bubble size about 50 μm) also show that a collector is required to float particles aggregated by hydrolyzing metal ions (224)(228) but in very small amounts (1 mg/l lauric acid for 5×10^{-4} M aluminium sulphate). Also of interest is the deleterious effect of increasing bubble size on the recovery of ferric or alum hydroxide flocs (227)(228). Cassell et al (228) found that only slight increases in bubble size (from 50 to 100 μm) caused the suppression of flotation at constant surfactant concentration. This behaviour is not completely understood as it cannot be explained only in terms of the rupture of flocs upon bubble-particle collisions.

The studies carried out on various hydrophilic aggregated systems in section 5.2 demonstrated that the aggregation of the dispersed phase

does not determine the mechanism of bubble-particle attachment in DAF. The effects of aggregating the dispersed phase are basically an increase in the effective 'particle' size and a reduction in the total number of 'particles' to be recovered.

An increase in particle size affects the kinetics of the DAF process. Larger particle sizes result in higher probability of bubble-particle collisions and therefore in an increased collection efficiency of the bubble. This in turn will lead to a higher flotation rate (see section 1.3). A reduction of the total number of suspended particles through particle aggregation influences the efficiency of the process. Simple calculations show that the amount of air required to float unflocculated particles is too high to be efficiently (and economically) provided by the DAF process.

Dispersed air microflotation studies have also indicated that unflocculated material requires more air (223)(224). Hence, flotation times of 20 min or longer were required to recover 50% of the unflocculated particles (at a 20 ml/min gas flow rate) whereas when aluminium sulphate was added 5 minutes flotation time sufficed to achieve total recovery. These results and those obtained in this work emphasise that the role of particle aggregation is to improve the efficiency and the kinetics of the flotation process when the gas phase consists of very small bubbles.

Selective recovery of minerals by dissolved air flotation

Since the mechanism of bubble-particle attachment in DAF occurs via the capture of microbubbles by hydrophobic particles or flocs, the establishment of a contact angle at the air/mineral interface seems to be the theoretical condition for the selective recovery of minerals by

dissolved air flotation. Thus, the selective flotation of a hydrophilic mineral from a suspension would imply the selective adsorption of a collector on the mineral surface just as in mineral separations by conventional flotation processes.

However, the fact that the particles must have some degree of aggregation for efficient mineral recovery by a DAF system poses a problem as selective aggregation processes for particles in suspension are not well developed. The addition of polymeric flocculants or hydrolyzing metal salts is not acceptable for selective flotation as these reagents adsorb unselectively.

It would appear that the most selective way of inducing the aggregation of the valuable mineral particles is via the destabilizing action of the collector itself, as has been shown for the quartz/dodecylamine system. In this way, collectors would accomplish a two-fold objective upon adsorption: they would render the mineral surface hydrophobic and they would bring about selective aggregation of the valuable particles. Therefore, operations aimed at the selective recovery of minerals by dissolved air flotation would have to make allowance for physico-chemical and design conditions that permit the selective aggregation of the valuable mineral particles.

The studies on dissolved air flotation of quartz in the presence of dodecylamine showed that the floatability regions of a mineral can be predicted from basic surface chemistry studies at the mineral/solution interface in the presence of the collector. Of particular importance would be the determination of the regions in which the mineral suspensions are destabilized in the presence of the collector as they tend to coincide with the regions in which DAF of the mineral occurs.

Chapter 6. THE SURFACE CHEMISTRY AND DISSOLVED AIR FLOTATION OF CASSITERITE

6. THE SURFACE CHEMISTRY AND DISSOLVED AIR FLOTATION OF CASSITERITE

Studies on the dissolved air flotation of cassiterite in the presence of two anionic collectors (sodium dodecyl sulphate and a sulphosuccinamate-based commercial product) were carried out to establish suitable conditions for the selective separation of this mineral by the DAF process. The flotation behaviour of cassiterite in the presence of these collectors was correlated with other interfacial phenomena and studies were carried out on the mechanism of adsorption of these surfactants on cassiterite and on a stannic oxide sample.

6.1. Studies on the cassiterite/sodium dodecyl sulphate system

6.1.1. Electrokinetic studies

Measurements of the electrophoretic mobility of cassiterite in distilled water (Figure 6.1) indicated that the isoelectric point (iep) of cassiterite occurred at pH 4.2. This value is within the range of ieps reported by other workers (cf. Table 3.1). For pH values below the iep the mobility was positive and increased very markedly with decreasing pH whereas above the iep the dependence on pH was less marked. The influence of pH on the electrophoretic mobility of cassiterite confirmed the potential-determining role of hydrogen and hydroxyl ions for this oxide mineral.

The effect of the sodium dodecyl sulphate (SDS) concentration on the mobility of the cassiterite particles at constant pH value is presented in Figure 6.2. The curves show that the mobility is a function of surfactant concentration and depends strongly on pH. They also show that the SDS concentration required to bring the zeta-potential to zero (pzr) increased with decreasing pH.

For pH values below the iep (pH 2.0 and 3.0 curves) the mobility

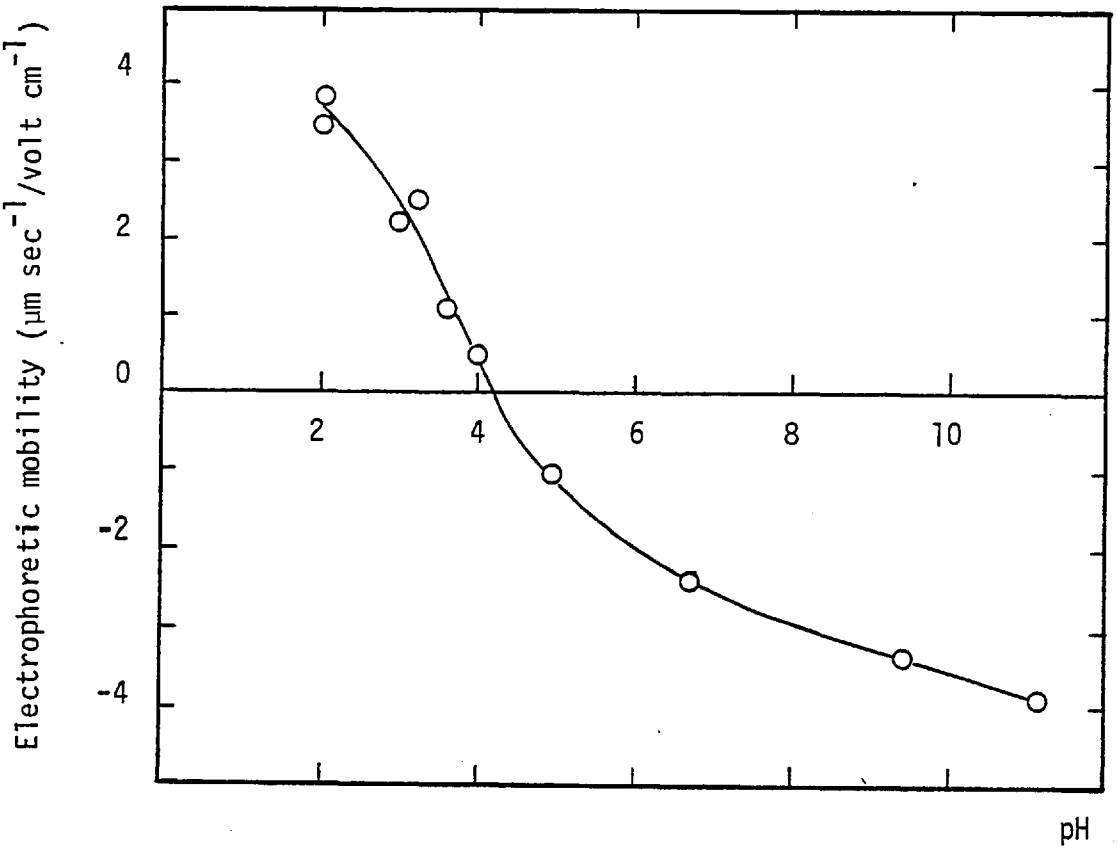

Figure 6.1. Electrophoretic mobility of cassiterite in distilled water as a function of pH

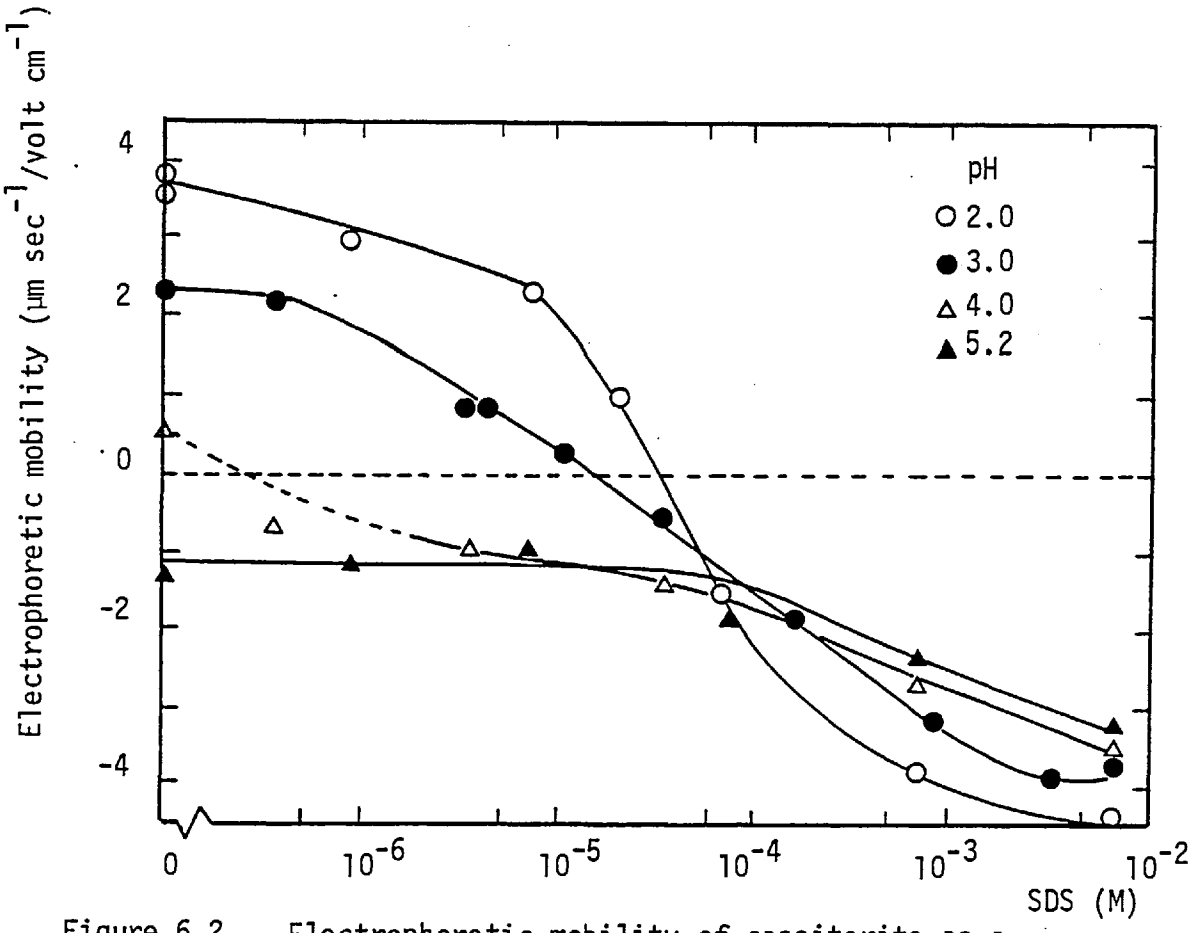

Figure 6.2. Electrophoretic mobility of cassiterite as a function of SDS concentration for various pH values

curves are very similar to those reported for the adsorption of long-chain electrolytes on oxide minerals (132). Thus, the curves show three distinct regions:

i) A region where the mobility is relatively constant with respect to SDS concentration and where adsorption would occur as the result of ion exchange in the diffuse part of the double layer.

ii) A region where the mobility decreases steeply with SDS concentration and within which charge reversal occurred. The predominant mechanism of adsorption in this region would be hydrophobic bonding between the hydrocarbon chains of the surfactant leading to the formation of hemimicelles in the Stern layer. The surfactant concentration at which the abrupt change in electrophoretic mobility occurs has been termed the critical hemimicelle concentration (C_{HMC}) (134).

iii) A region where the mobility tends to a constant value.

Although the shape of both curves is similar, the range of SDS concentrations which characterize each region is different. Thus, for instance, at pH 3.0 the region of hemimicellization (region ii) extends over SDS concentrations covering 3 orders of magnitude (from 10^{-6} to about 2×10^{-3} M) whereas at pH 2.0 it only occurs between approximately 10^{-5} and 10^{-3} SDS. Also, the C_{HMC} value increases with decreasing pH.

At a pH value near the iep of cassiterite (pH 4.0), minute concentrations of surfactant (less than 10^{-6} M SDS) were sufficient to bring about charge reversal and specific adsorption. For a pH value of 5.2 the mobility was constant up to about 3×10^{-5} M SDS and, as at pH 4.0, then increased with increasing SDS concentration, showing that adsorption of SDS was taking place under conditions of negative Stern potential. Other workers (172)(169) have reported a similar electrokinetic behaviour

for the stannic oxide/alkyl sulphate system at pH values above the iep.

The experimental data of Figure 6.2 have been replotted in Figure 6.3 to show the influence of pH on the electrophoretic mobility of cassiterite in the presence of SDS. The curves show that the iep of cassiterite is shifted towards more acid pH values as the SDS concentration is increased, indicating that adsorption of SDS ions is occurring at the iep of the mineral. The mobility/pH curves indicate that charge reversal occurs first at pH values near the iep but above 10^{-5} M SDS the mobility is negative over all pH values. The change in the shape of the mobility/pH curves with increasing SDS concentration is associated with specific adsorption occurring at higher surfactant concentrations for the lower pH values.

It has been postulated (141) that for a surfactant to adsorb at the iep of an oxide mineral there must be some kind of specific affinity other than electrostatic between adsorbate and adsorbent (cf. section 3.2). To test the possibility that chemical interactions between the mineral surface and the polar head of the surfactant might be contributing to the adsorption of SDS at the iep of cassiterite, a few mobility measurements were carried out on cassiterite in the presence of dodecylammonium chloride (DAC). The results (Figure 6.3) indicated that the cationic surfactant also adsorbed at the iep of cassiterite shifting it towards alkaline pH values. Furthermore, the influence of pH on the mobility of cassiterite particles at constant DAC concentration was quite similar to that in the presence of the alkyl sulphate, if allowances are made for the different charges of surface and surfactant in this case. De Cuyper and Gutiérrez (173) obtained analogous results in their electrokinetic studies of the cassiterite/DAC system. Stratton-Crawley (35) carried out an electrokinetic study of the rutile/

alkyl sulphate system and also reported very similar results to those obtained in this work for the cassiterite/SDS system.

Tests were carried out to determine the reversibility of the mobility/SDS concentration curves by diluting or washing cassiterite suspensions conditioned with SDS. Results indicated that the surfactant was easily washed off the mineral surface and that the resulting cassiterite particles exhibited mobility values very close to those expected. This tends to confirm that the specific affinity of SDS for the cassiterite surface was not of a chemical nature.

Some authors (169) have suggested that the adsorption of SDS on stannic oxide is influenced by the ionic strength of the solution and Ahmed and Maksimov (174) have postulated that chloride ions may adsorb specifically on an SnO_2 surface. Measurements of the electrophoretic mobility were therefore carried out in the presence of SDS at constant ionic strength (10^{-2} M) with KCl and KNO_3 as supporting electrolytes. When KNO_3 was used the pH was adjusted with nitric acid. The results (Figure 6.4) indicated that at both pH values tested (2.0 and 3.0) the influence of the ionic strength consisted only of reducing the absolute value of the electrophoretic mobility in region i) of the mobility curves (in agreement with theoretical considerations and other experimental results (232)). In the region of hemimicellization, little difference was observed with respect to the curves obtained in the absence of constant ionic strength. An exception was the results at pH 3.0, where slightly higher mobilities were recorded in the presence of 10^{-2} M KCl. It would also appear that both electrolytes had little effect on the pzr at both pH values. On the basis of these electrokinetic measurements it was concluded that the ionic strength and the kind of electrolyte did not have a substantial influence on the

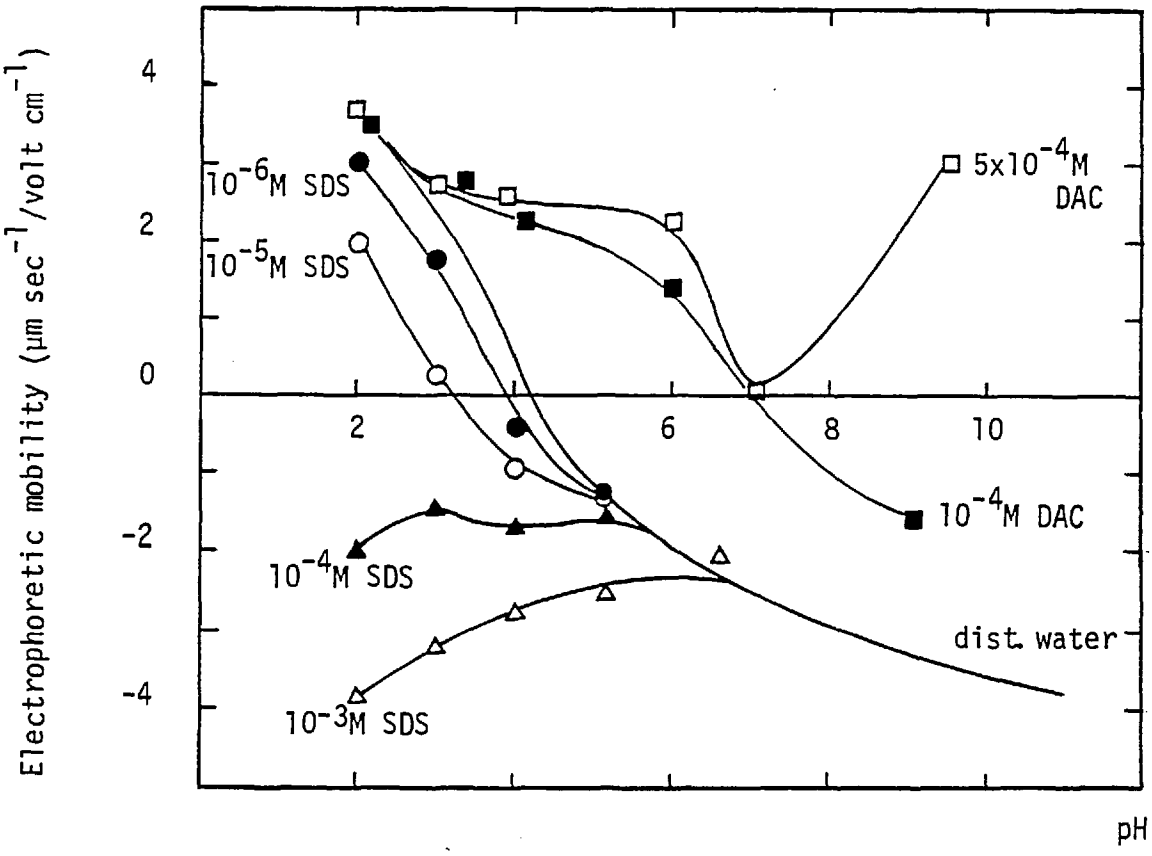

Figure 6.3. Electrophoretic mobility of cassiterite as a function of pH for various concentrations of SDS and dodecylamine (DAC)

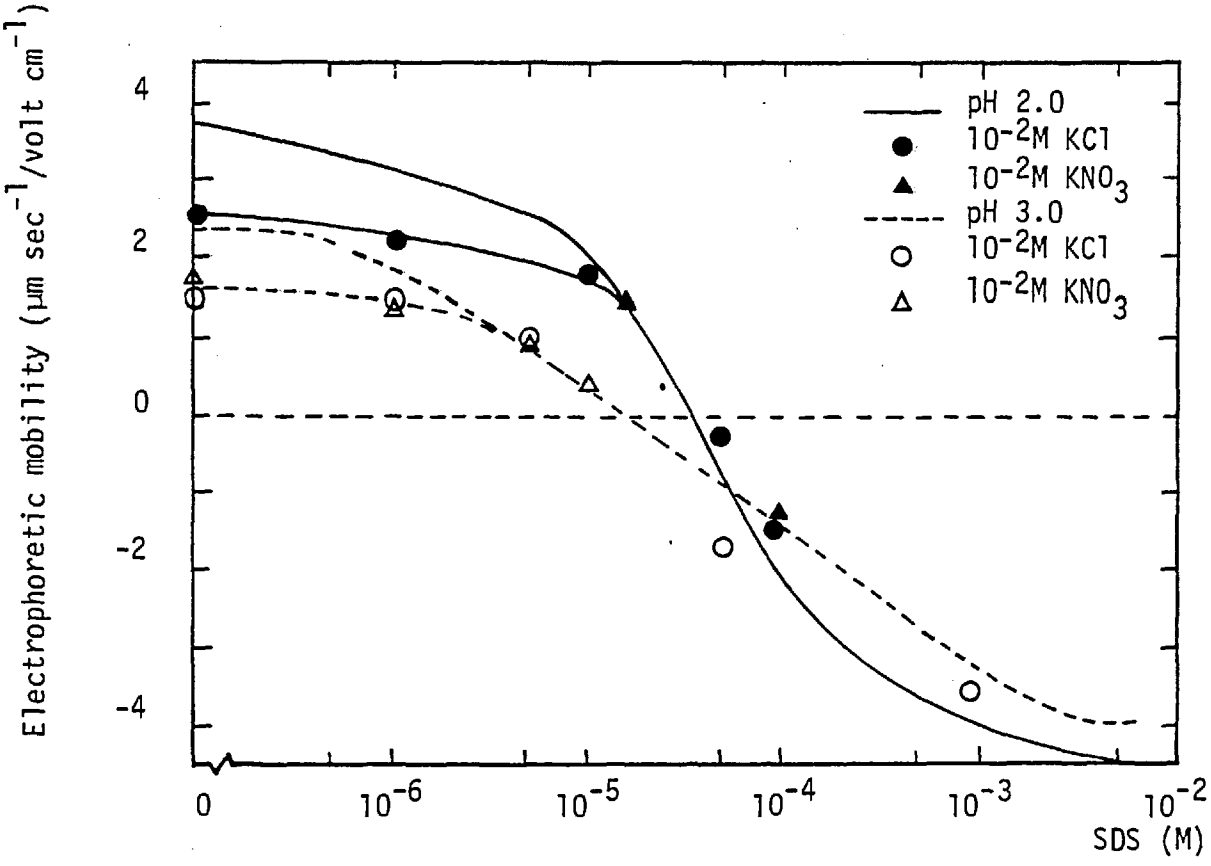

Figure 6.4. Effect of ionic strength and supporting electrolyte on the electrophoretic mobility of cassiterite in the presence of SDS

adsorption of the alkyl sulphate on cassiterite.

6.1.2. Stability measurements

Measurements of the stability of cassiterite suspensions in distilled water as a function of pH showed that they were unstable only at the isoelectric point of the mineral. In the presence of sodium dodecyl sulphate the destabilization regions of cassiterite suspensions depended upon surfactant concentration and pH value. Figure 6.5 shows the destabilization regions for the cassiterite/SDS system at 3 pH values below the iep; cassiterite suspensions showed stable behaviour at all pH values above the iep irrespective of SDS concentration.

The figure shows that the instability regions of cassiterite are determined by surfactant concentration and to a certain extent by pH. At pH 4.0 the destabilizing effect of SDS on cassiterite extends up to 10^{-3} M whereas at pH 2.0 it occurs between 2×10^{-5} and 10^{-3} M SDS. The smallest destabilization region occurred at pH 3.0 where it covered the range 8×10^{-5} - 7×10^{-4} M SDS. For all pH values the optimum level of aggregation was at SDS concentrations between 1.5 - 3.0×10^{-4} M. At 5×10^{-4} M SDS the degree of aggregation of cassiterite suspensions diminished notably and complete restabilization was attained over 10^{-3} M SDS.

The cassiterite suspensions destabilized yielding small, pale brown coloured aggregates with relatively fast settling rates. At the optimum aggregation concentrations the suspensions still exhibited a haze which prevented the supernatants from recording transmittance values higher than 60%.

To elucidate the mechanism of destabilization of SDS on cassiterite the % transmittance values were plotted against the corresponding value

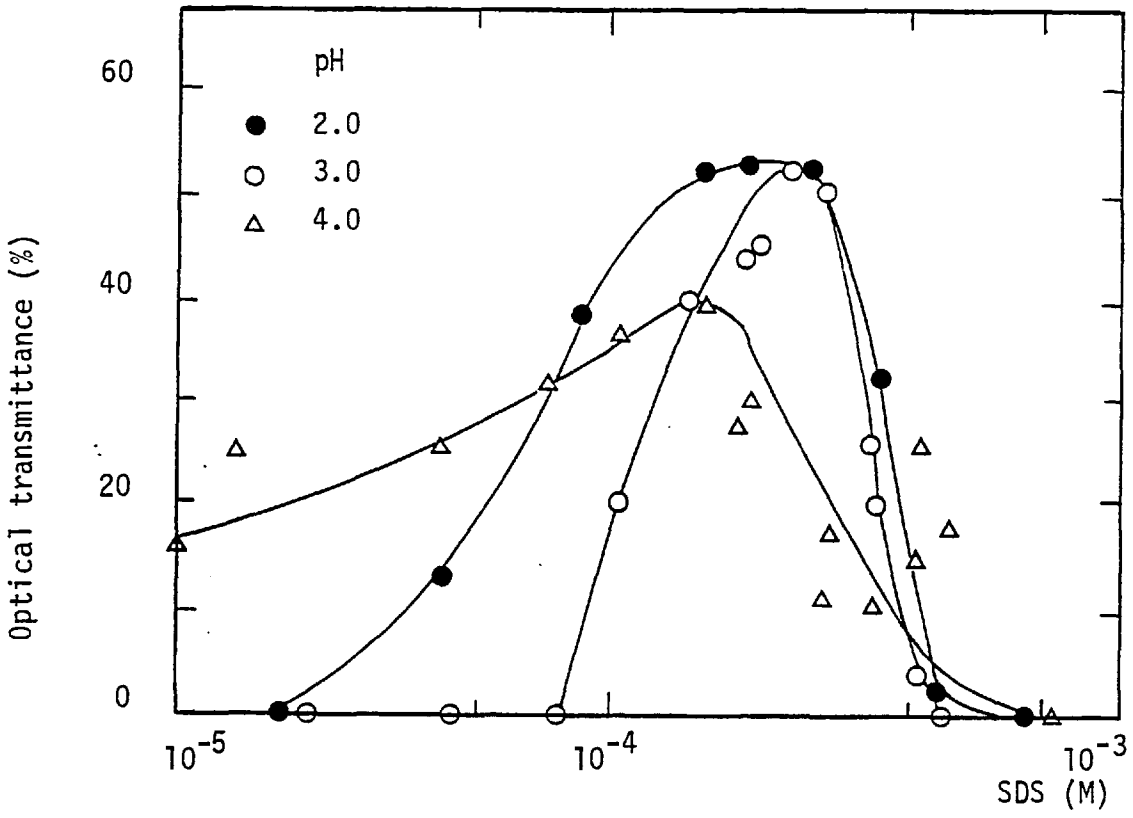

Figure 6.5. Stability of cassiterite suspensions as a function of SDS concentration for various pH values

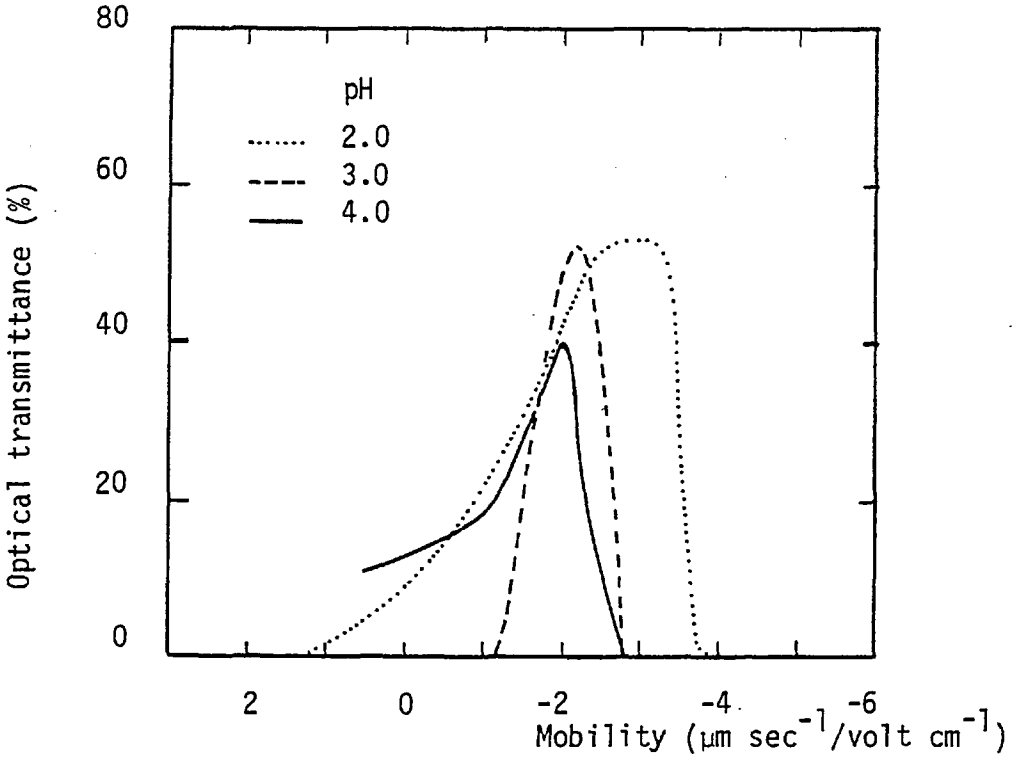

Figure 6.6. Stability of cassiterite suspensions in the presence of SDS as a function of the electrophoretic mobility for various pH values

of the electrophoretic mobility (Figure 6.6). The curves at pH 2.0 and 4.0 show that the onset of destabilization of cassiterite suspensions was associated with a decrease in the electrophoretic mobility of the particles to values near neutrality. At pH 3.0, however, the suspensions showed no light transmittance at the pzr and destabilization occurred only at negative values of the electrophoretic mobility. This behaviour is probably associated with a slower rate of coagulation at the pzr than at higher SDS concentrations, since when supernatant transmittances were measured after longer standing times (30 min) the coagulation region broadened towards lower surfactant concentrations.

Maximum degrees of destabilization were achieved at negative values of the electrophoretic mobility at all pH levels. This behaviour may also be related to the rate of coagulation as the interparticle collisions could be more effective when a certain degree of surfactant adsorption had occurred. Restabilization of the suspensions was associated with high zeta-potential values. Hence, restabilization occurred at pH 3.0 for a mobility value of about -2.7 $\mu m\ sec^{-1}/volt\ cm^{-1}$ which corresponds to a zeta-potential of about -35 mV (assuming $\kappa a = 150$). At pH 2.0, the suspensions restabilized at $u = 3.8\ \mu m\ sec^{-1}/volt\ cm^{-1}$ which can be estimated to correspond to a zeta-potential of about -49 mV (assuming $\kappa a = 450$).

The correlation between stability behaviour and electrophoretic mobility of cassiterite in the presence of SDS would indicate that the destabilizing effect of this anionic surfactant is primarily the result of a reduction in the electrostatic repulsive forces between the particles. The low surfactant concentrations ($< 10^{-4}$ M SDS) needed to cause suspension destabilization by this 1-1 electrolyte are further proof that this reduction arises from the specific adsorption of the alkyl sulphate on

the cassiterite surface and not from double layer compression effects. The restabilization of the cassiterite suspensions would appear to occur as the result of the increase in the double layer repulsive forces due to the superequivalent adsorption of the surfactant. However, the fact that maximum aggregation occurred at negative values of the zeta-potential and that high values of the zeta-potential were required to redisperse the aggregates would suggest that the destabilizing action of ionic surface-active agents is not a simple mechanism, in agreement with the suggestions of other authors (162)(163).

6.1.3. Adsorption measurements

The adsorption isotherms of sodium dodecyl sulphate on cassiterite at pH 2.0 and 3.0 are presented in Figure 6.7 on a logarithmic scale. Some measurements carried out at pH 1.4 are also shown in this figure. The adsorption measurements were all performed at a room temperature of $19 \pm 1^{o}C$.

The curves indicate that adsorption of SDS on cassiterite is a pH dependent process, higher surfactant adsorption densities being obtained at the more acid pH values. As the effect of decreasing pH is to increase both potential and charge on the mineral surface, it would appear that the adsorption mechanism is influenced by the electrostatic attraction between surface and surfactant ions.

The adsorption isotherms showed a S-2 shape according to the classification of Giles (233). The S shape is commonly associated with the adsorption of mono-functional ions which have moderate intermolecular attraction for the surface and which adsorb in competition with the solvent molecules for the adsorbant sites. The sigmoidal shape is also characteristic of the adsorption of long-chain surfactants on oxide

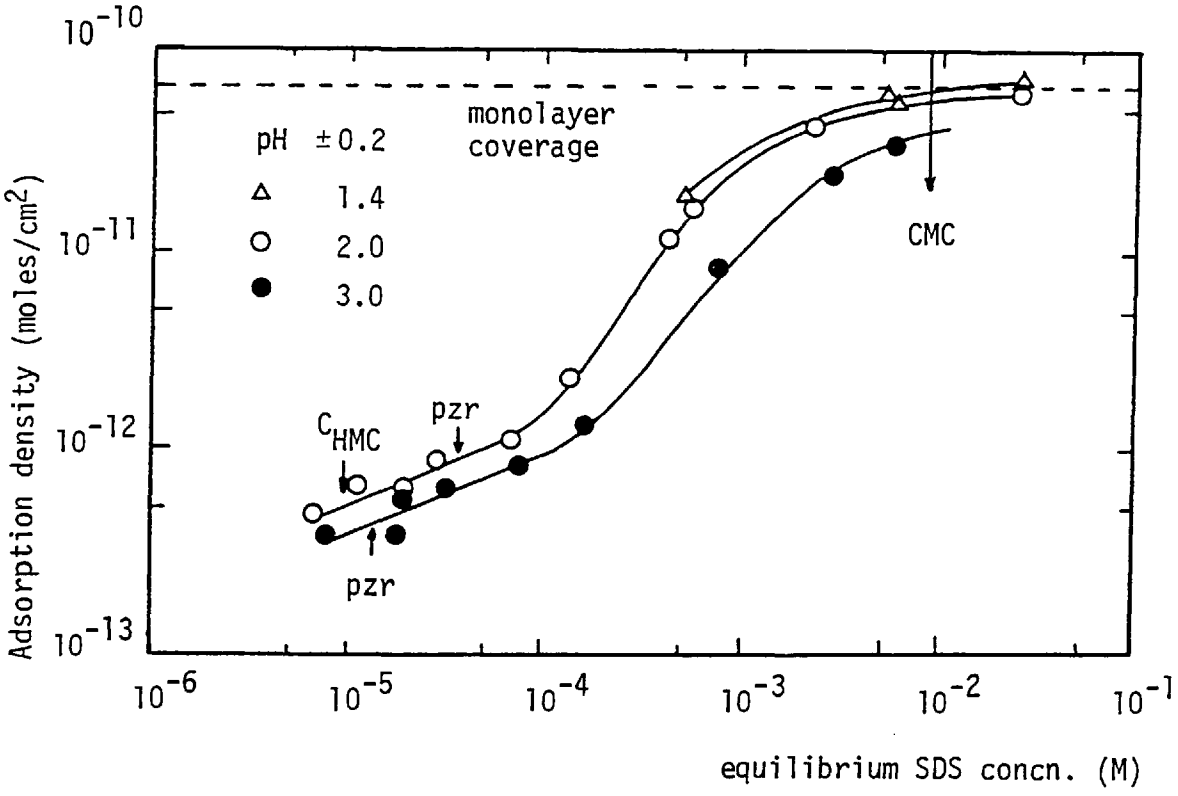

Figure 6.7. Adsorption isotherms of sodium dodecyl sulphate on cassiterite at various pH values

minerals (132). Both adsorption isotherms showed three adsorption regions, namely,

I. A linear region at low SDS concentrations, where adsorption does not increase significantly with equilibrium surfactant concentration. This section of the isotherm had a slope of 0.5 for both pH values.

II. A region where adsorption increases markedly over a small range of SDS concentrations. The slope of the linear part of this section was again similar for both pH values (1.5 and 1.2 for pH 2.0 and 3.0 respectively).

III. A third region where the curves tended to level off as saturation was reached, this occurred near the critical micelle concentration (CMC) of SDS. At pH 1.4 and 2.0, the adsorption density at saturation corresponded with a close-packed, vertically oriented

monolayer of SDS ions each occupying an area of 0.25 mm^2 (25 A^{o2}).

Fuerstenau and co workers (134)(137) have proposed that the initial section of these isotherms is associated with adsorption through an ion exchange mechanism in the Gouy layer. They have also proposed that the surfactant concentration marking the steep rise in adsorption density (the beginning of region II) corresponds to the critical hemimicelle concentration extrapolated from electrokinetic measurements, that is indicating the onset of adsorption through hydrophobic chain associations in the Stern layer. Once the pzr has been reached the slope of the adsorption isotherm curve should decrease. Experimental evidence to support this model has been supplied from studies carried out on the quartz/alkyl amine (134)(235) and alumina/alkyl sulphonate systems (137) (234).

In order to compare these isotherms with the model proposed by Fuerstenau et al, the SDS concentrations at which the C_{HMC} and the pzr occurred in the electrokinetic measurements have been marked with arrows in Figure 6.7. No C_{HMC} value is marked on the isotherm at pH 3.0 since it occurred at very low SDS equilibrium concentrations (4×10^{-6} M) where the adsorption of SDS could not be measured because of limitations imposed by the analytical technique.

The arrows show that at both pH values there was little correlation between the electrokinetic and adsorption results, the C_{HMC} and pzr having no apparent relationship with the regions of the adsorption isotherm. Furthermore, the isotherms showed that for SDS concentrations above the pzr, where adsorption occurs under a negative Stern potential the curves did not exhibit a decrease in their slope; on the contrary, above a certain SDS concentration (about 10^{-4} M) the adsorption density increased more steeply (region II).

At both pH values, region I and the pzr occurred at low adsorption density values suggesting that the ionization of the mineral surface was not very high. Assuming that each surfactant ion attaches to one charged site, the total number of charged sites on the surface may be estimated from the value of the adsorption density at the pzr. Table 6.1 presents the results of such calculations; 100% surface coverage has been assumed to correspond to a monolayer of SDS ions each occupying an area of 0.25 mm^2.

Table 6.1. Data for the adsorption of SDS on cassiterite at the pzr

pH	pzr (M)	adsorption density ($moles/m^2$)	surface coverage (%)	number of charged sites (cm^{-2})	area per adsorbed ion (nm^2)
2.0	3.4×10^{-5}	8.7×10^{-8}	1.31	5.24×10^{12}	19.08
3.0	1.5×10^{-5}	4.4×10^{-8}	0.66	2.65×10^{12}	37.73

The figure of 5.24×10^{-2} charged sites per cm^2 (pH 2.0) is low compared to other results reported in the literature. Based on the results of Wakamatsu and Fuerstenau (234) for the alumina/dodecyl sulphonate system at pH 7.2 (iep at pH 9.1), a similar calculation gave 4.82×10^{13} charged sites at the pzr with an area of 2.08 nm^2 per adsorbed ion. Ottewill and Watanabe (162) calculated 1.94×10^{13} active sites/cm^2 for the AgI/SDS system at pAg 3.0 (iep at pAg 5.4). In the present system, a pH increase from 2.0 to 3.0 decreased the number of active sites on the cassiterite surface by half.

The adsorption isotherms were reversible, independent of equilibration time over 15 minutes and independent of the amount of solids. These results together with the electrokinetic studies would suggest

that the adsorption mechanism is not of a chemical nature. From the adsorption studies reported in this section it is only possible to conclude that the adsorption free energy term is made up of electrical and hydrophobic contributions.

6.1.4. Dissolved air flotation studies

Dissolved air flotation tests on cassiterite in the presence of SDS at various pH values (Figure 6.8), showed that flotation only occurred below the iep and that cassiterite recovery was higher for the more acid pH values. Also, cassiterite recovery by DAF increased at all pH values with an increase in SDS concentration.

The dependence of DAF of cassiterite on pH and surfactant concentration may also be seen in Figure 6.9 where DAF recovery has been plotted as a function of SDS concentration for various pH values. The results showed that larger flotation areas and higher recovery values were obtained for the lower pH values. The shape of the curves is similar to that obtained for the quartz/dodecylamine system, the recovery reaching a maximum and then decreasing rapidly with increases in surfactant concentration.

A comparison with Figure 6.5 indicates that the regions of dissolved air flotation agreed closely with the destabilization regions obtained for cassiterite suspensions in the presence of the alkyl sulphate. However, at pH 4.0 no substantial flotation occurred below 10^{-4} M SDS, although the cassiterite suspensions were coagulated. This result is in agreement with the attachment mechanism proposed for DAF in Chapter 5, i.e. a certain level of hydrophobicity is the main requirement for DAF to occur.

A correlation between all surface phenomena investigated in the

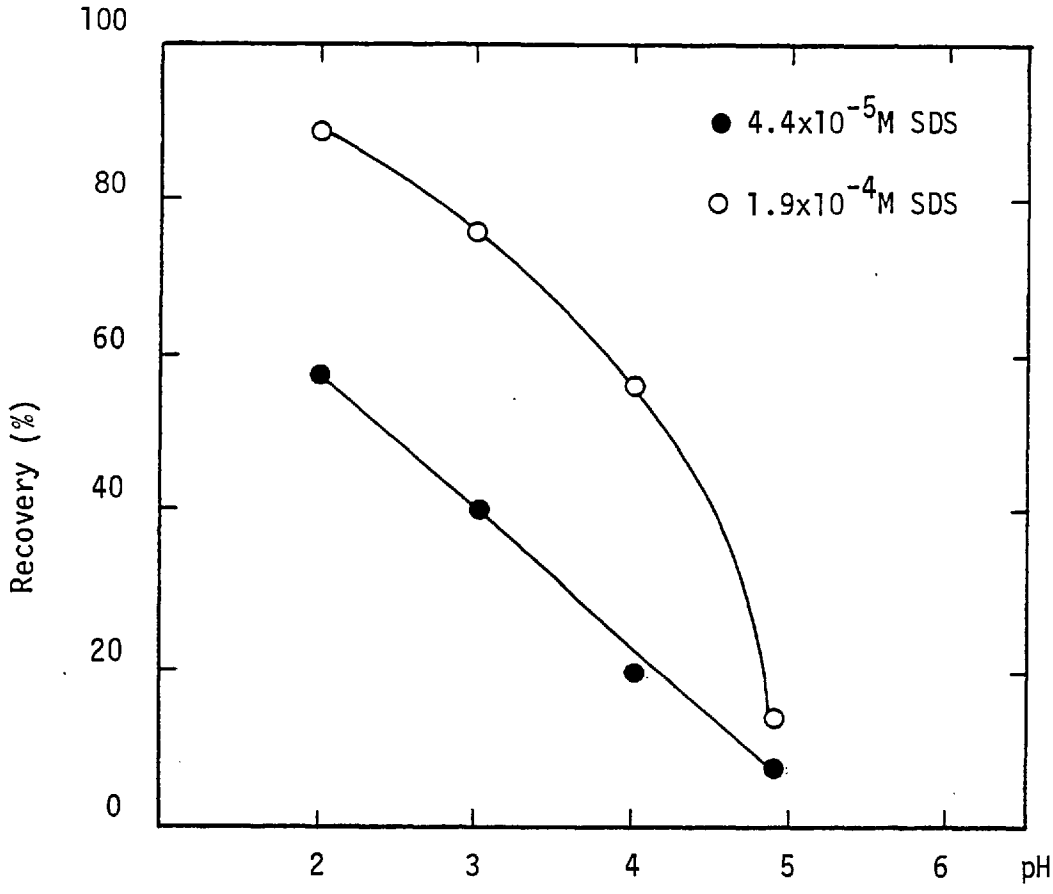

Figure 6.8. Dissolved air flotation of cassiterite as a function of pH for two SDS concentrations

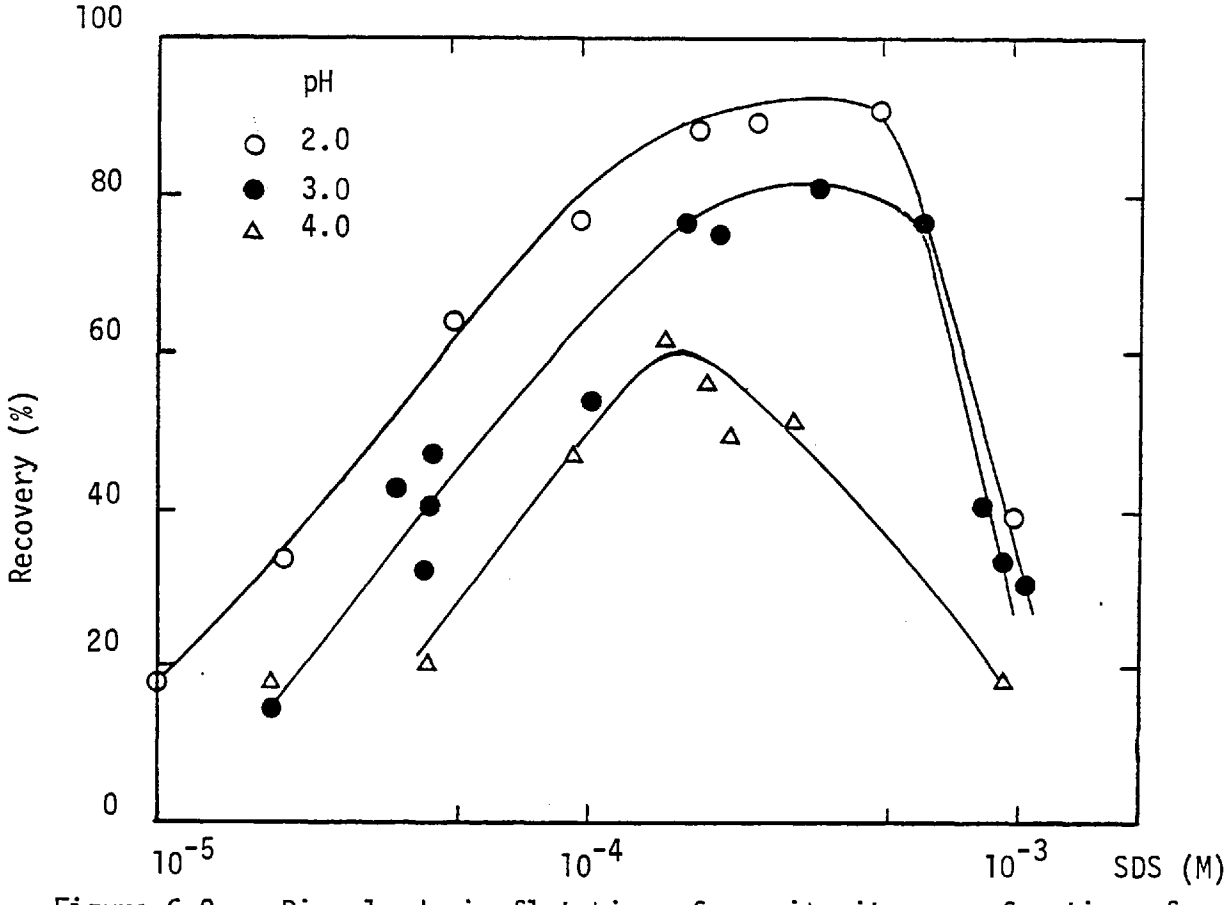

Figure 6.9. Dissolved air flotation of cassiterite as a function of SDS concentration at various pH values

cassiterite/SDS system at pH 2.0 is presented graphically in Figure 6.10. The SDS concentration is strictly an equilibrium concentration only for the adsorption measurements but as the levels of SDS adsorption have been found to be very low, no great discrepancy exists between the initial and equilibrium SDS concentrations. The electrophoretic mobility results have been drawn with the negative values in the upper part of the scale to improve clarity.

The correlations shown in Figure 6.10 may be discussed in terms of three DAF regions:

1) A region of rapid flotation from 8×10^{-6} to 10^{-4} M SDS which was characterized by a low level of collector adsorption (below 2.6% of a monolayer) and, above 2×10^{-5} M, by rapid suspension destabilization by the surfactant. This region also corresponds closely with the region of hemimicellization as extrapolated from the electrophoretic mobility curve. Maximum flotation did not occur at the pzr for this system, probably because of the low level of collector adsorption at that SDS concentration.

2) The maximum flotation recovery region ($1 - 6 \times 10^{-4}$ M SDS) was associated with region II of the adsorption isotherm (2.6 - 27% of monolayer coverage) and with variable degrees of aggregation of the cassiterite particles (from the optimum at 10^{-4} M to about 3% transmittance at 6×10^{-4} M SDS). The mobility was negative in this region (-2 to -3.5 $\mu m\ sec^{-1}/volt\ cm^{-1}$).

3) A region between 6×10^{-4} - 2×10^{-3} M SDS where flotation recovery fell rapidly with small increases in surfactant concentration and where the cassiterite suspensions showed restabilization above 9×10^{-4} M SDS. In this region both the electrophoretic mobility and the adsorption isotherm tended to level off. The adsorption

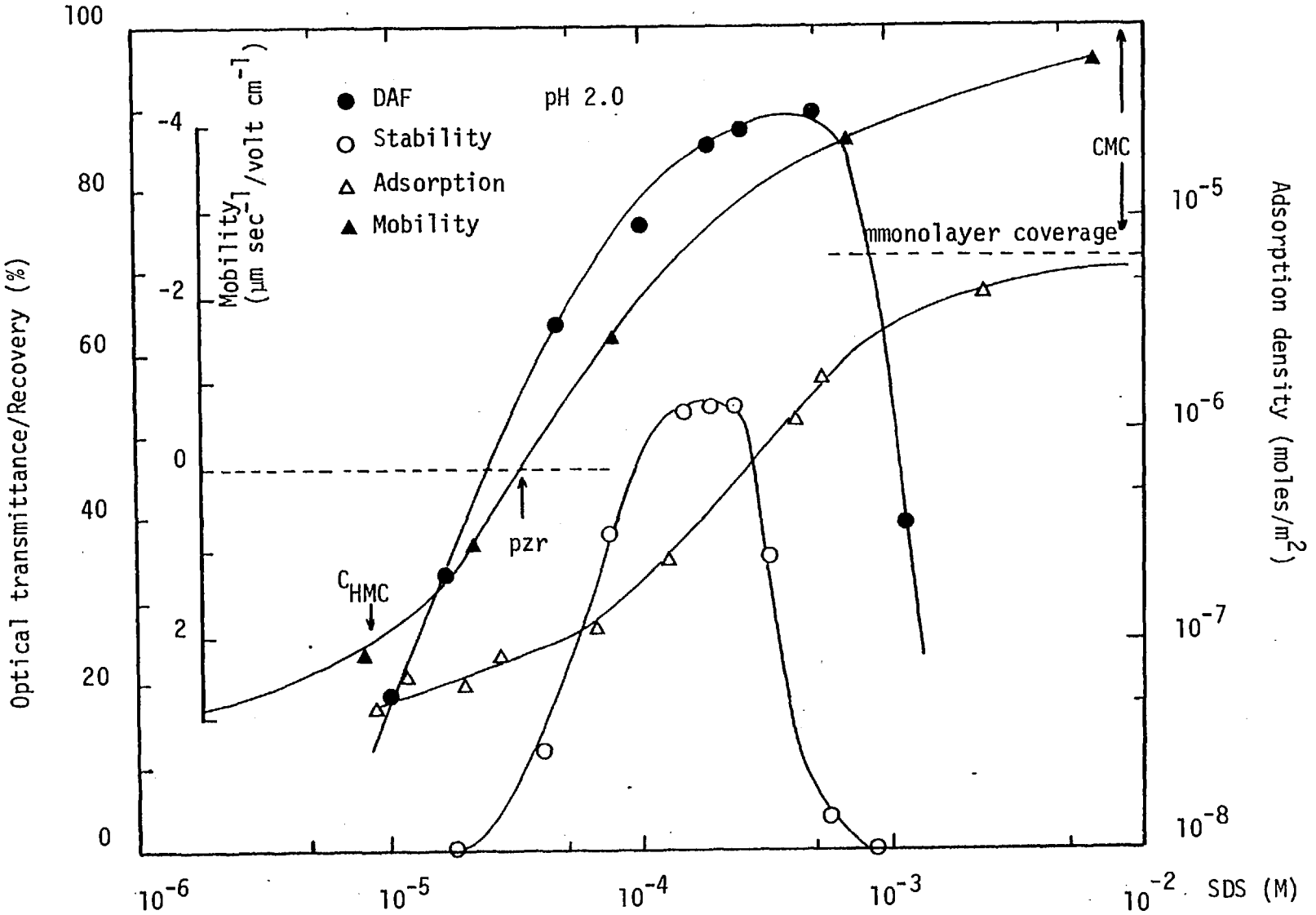

Figure 6.10. Dissolved air flotation, suspension stability, electrokinetic and adsorption measurements on cassiterite in the presence of SDS at pH 2.0.

density at 2×10^{-3} M SDS was about 63% of monolayer coverage

A broadly similar correlation may be made for the cassiterite/SDS system at pH 3.0.

It is also apparent that the regions of maximum recovery (region 2 of the DAF results) at pH 2.0 and 3.0 corresponded with rapidly increasing surfactant adsorption. In addition, the subsequent suppression of flotation is associated with the saturation of the cassiterite surface. Thus, it would appear that region II of the SDS adsorption isotherm is a region of increased hydrophobicity whereas region III is characterized by increasing hydrophilicity.

6.2. Studies on the stannic oxide/sodium dodecyl sulphate system

Electrokinetic and adsorption measurements were carried out on a stannic oxide sample of high purity in order to compare the results with those obtained on the natural cassiterite sample.

6.2.1. Electrokinetic studies

Measurements of the electrophoretic mobility of stannic oxide (SnO_2) in distilled water gave an isoelectric point at pH 4.0 (Figure 6.11). Measurements of the fast pH change upon addition of SnO_2 to double distilled water at various initial pH values can indicate the position of the PZC of the oxide (236). Results showed that pH decreased at alkaline and neutral values but no change was detected at pH 4.2 and below. This would suggest that the iep and PZC lay close to each other. The electrophoretic mobility of stannic oxide as a function of pH was found to be almost identical to that of cassiterite.

The effect of the concentration of SDS upon the electrophoretic mobility of SnO_2 is shown in Figure 6.12 for pH values above and below

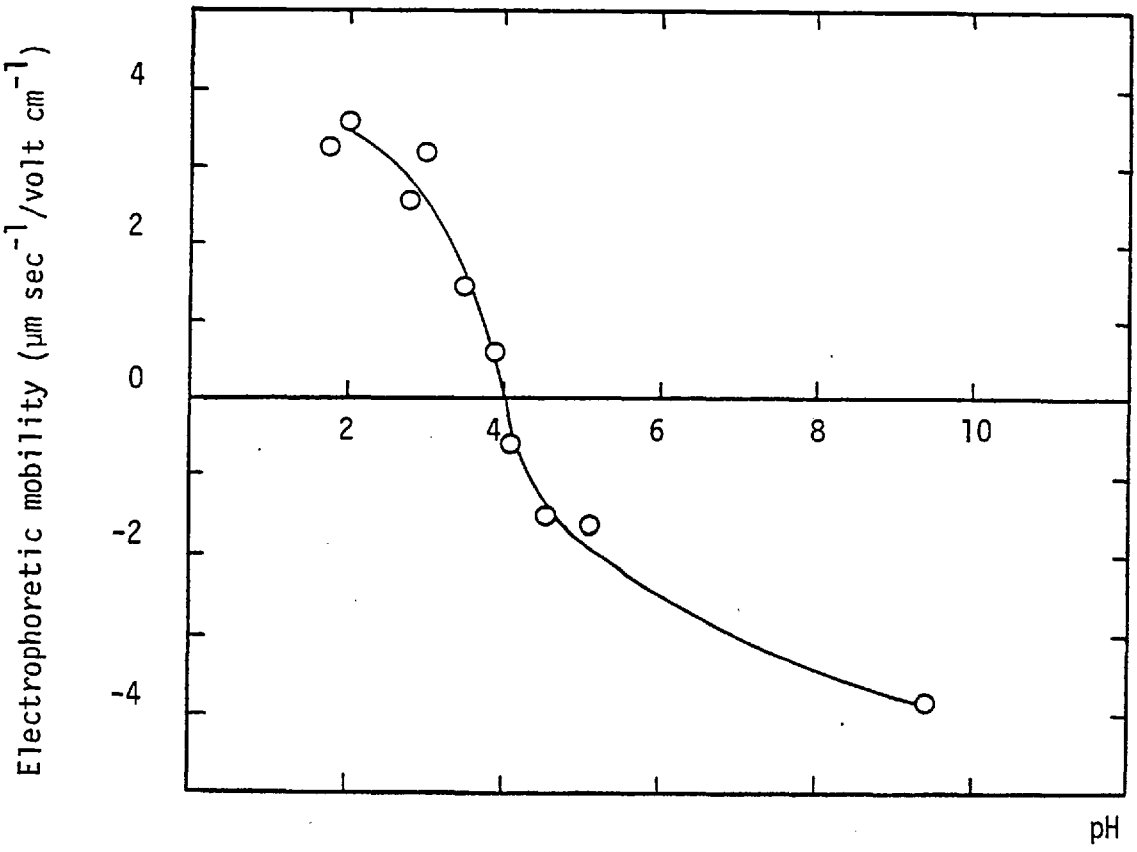

Figure 6.11. Electrophoretic mobility of stannic oxide in distilled water as a function of pH

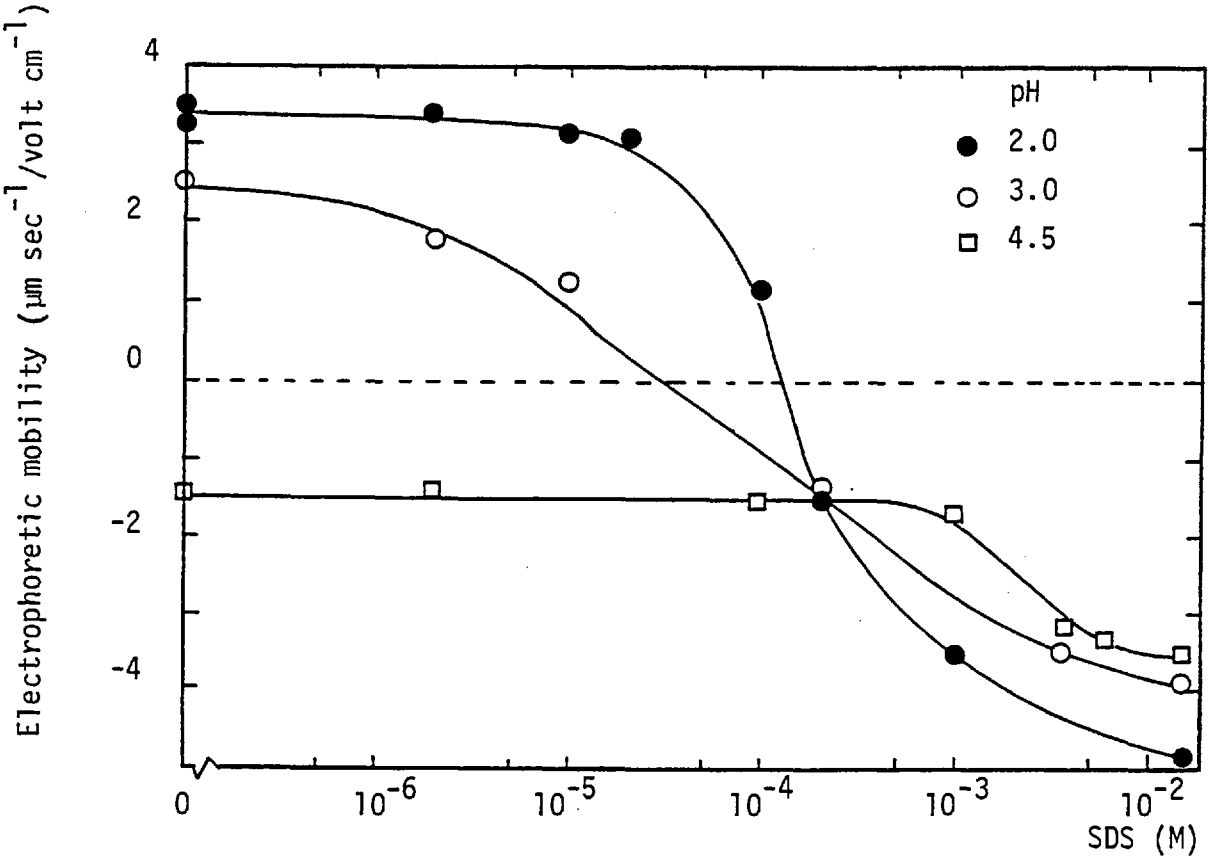

Figure 6.12. Electrophoretic mobility of stannic oxide as a function of SDS concentration for various pH values

the iep. The effect of the alkyl sulphate on the electrokinetic behaviour of the oxide is very similar to that exhibited by the natural sample (Figure 6.1). Note that adsorption was also found at the iep of this sample.

6.2.2. Adsorption measurements

The adsorption isotherms of SDS on stannic oxide at 19 ± 1°C at pH values above and below the iep are presented in Figure 6.13. As with cassiterite, the adsorption isotherms were reversible and independent of the amount of solids and of the equilibration time. For SDS concentrations above 10^{-3} M larger amounts of solids had to be used to obtain reproducible results (between 10 - 25 g depending on the pH value). The isotherms have been plotted on a log-log basis to show the detail of the low concentration region.

The figure shows that the adsorption of SDS on stannic oxide is a function of the pH value, the adsorption density increasing as the pH decreases. Comparing these isotherms with those obtained for the cassiterite/SDS system (Figure 6.7), it appears that at each pH value larger adsorption densities were recorded on the natural sample than on the synthetic material. The shape of the isotherms was also different at each pH value measured.

The adsorption isotherm at pH 2.0 exhibited the three-region shape characteristic to the S-2 curves, and more particularly, to the adsorption of ionic surface-active agents on oxide minerals. This isotherm gave a better correlation with the electrokinetic results than its equivalent for cassiterite. Thus, region I of the isotherm (up to 4×10^{-5} M SDS) is linear and roughly corresponds to the section of the electrophoretic mobility curve associated with adsorption of SDS through

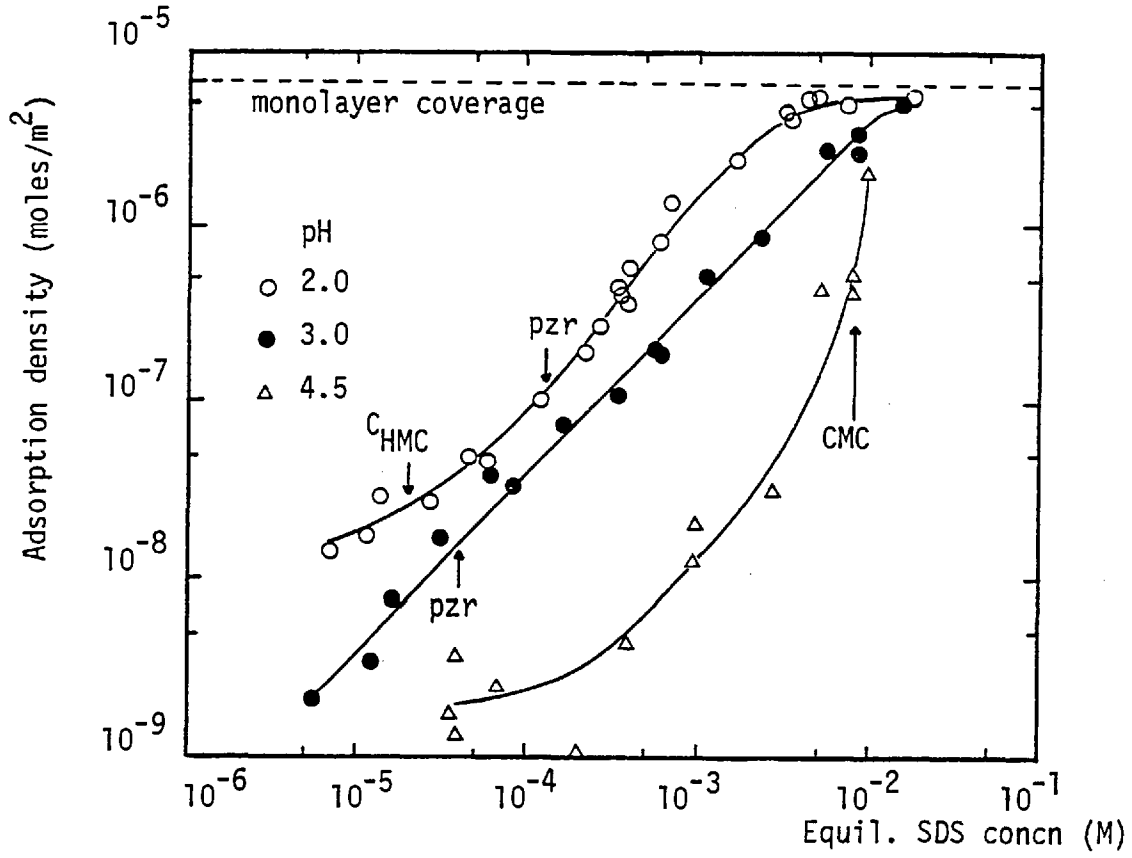

Figure 6.13. Adsorption isotherm of SDS on stannic oxide at various pH values

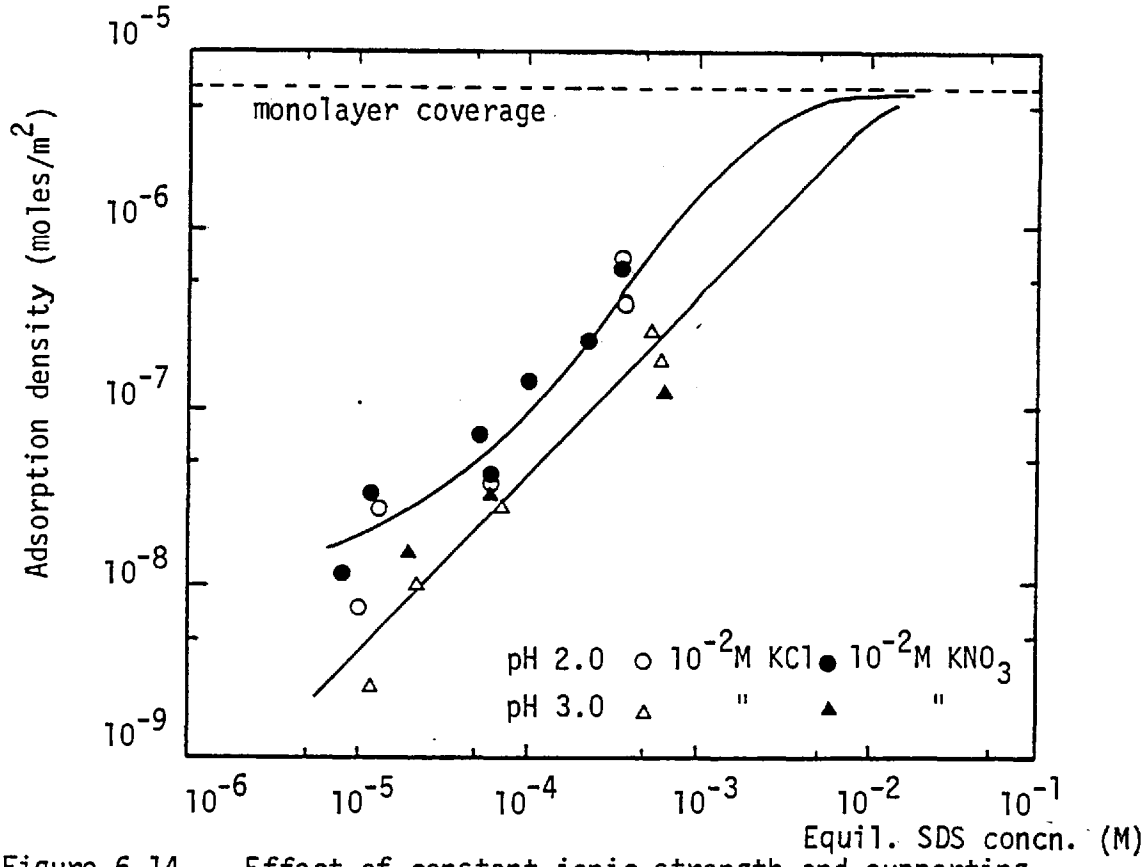

Figure 6.14. Effect of constant ionic strength and supporting electrolyte on the adsorption isotherm of SDS on stannic oxide

ionic exchange in the diffuse layer. The slope of the linear section of the isotherm is 0.65. For SDS concentrations over 4×10^{-5} M, a marked increase in adsorption density with surfactant concentration occurred which extended up to abour 10^{-3} SDS. This second region of the isotherm closely corresponds with the hemimicellization region of the electrokinetic studies. The value of the C_{HMC} extrapolated from the mobility curve was 2×10^{-5} M SDS which compares well with 4×10^{-5} M which marks the beginning of region II of the isotherm. Over 10^{-3} M SDS, the adsorption tended to reach saturation as the CMC of the surfactant was approached and the adsorption plateau corresponded to an adsorption density of 6×10^{-6} moles/ m^2 (90% of monolayer coverage). The electrophoretic mobility also tended to level off within this region. The pzr occurred within region II of the isotherm at 1.4×10^{-4} M SDS, above this concentration no decrease in the slope of the isotherm was observed.

The adsorption isotherm at pH 3.0 showed a remarkable linearity over the range of SDS concentrations tested. The isotherm may be described by the equation:

$$\log \Gamma = \log K + n \log C \qquad (6.1)$$

where $\log K = -3.37$ and $n = 1.0$, are the parameters of the isotherm at pH 3.0. Γ and C represent the adsorption density in moles/m^2 and the surfactant molar equilibrium concentration respectively. The pzr occurred at an equilibrium concentration of 4×10^{-5} M SDS and had no influence on the shape of the isotherm. The C_{HMC} estimated from the electrokinetic studies (about 10^{-6} M SDS) occurred below the detection limit of the experimental technique and therefore its influence on the adsorption isotherm could not be evaluated. The linear section of the isotherm ends slightly over the CMC of the adsorbate (8.1×10^{-3} M SDS) leading to a saturation plateau at about 5×10^{-6} moles SDS/m^2 which

corresponds to 75% of a monolayer of SDS ions each occupying 0.25 nm^2.

The adsorption isotherm of SDS on stannic oxide at pH 4.5 exhibited a S-1 shape according to Giles' classification (233). The S-1 shape indicates a similar adsorption mechanism to the S-2 isotherm but saturation is not attained. At this pH value above the iep of the oxide, adsorption was very low up to a SDS concentration of 10^{-3} M above which the adsorption density increased steeply with increasing surfactant concentration. There was no sign of an adsorption plateau for SDS concentrations up to the CMC and above this value the adsorption measurements were very irreproducible. The adsorption behaviour of SDS above the iep correlates well with the electrokinetic results as the SnO_2 mobility also changes above 10^{-3} M SDS, becoming more negative. In this case, however, the electrophoretic mobility tended to a plateau at about 10^{-2} M SDS.

Few adsorption isotherms have been reported for the stannic oxide/alkyl sulphate system in the literature. Edwards and Ewers (168) obtained sigmoidally shaped isotherms for cetyl sulphate and found that adsorption was higher for the more acid pH values. On the other hand, Jaycock, Ottewill and Tar (169) obtained a linear isotherm for SDS in the pH range 2.86 - 4.17, this isotherm being almost identical to that obtained at pH 3.0 in this work. Based on their results, Jaycock et al proposed that the adsorption mechanism of SDS on SnO_2 was via ion exchange with chloride ions on the surface. To evaluate this possibility and the influence of constant ionic strength, adsorption measurements were carried out in the presence of 10^{-2} M KCl and of 10^{-2} M KNO_3 (pH adjusted with HNO_3 in these experiments). The results are shown in Figure 6.14.

The figure shows that a greater dispersion of results was obtained

at constant ionic strength. Nevertheless, the trend was that neither the ionic strength nor the presence of the chloride ions had much influence on the adsorption of SDS on stannic oxide.

Analogously to the cassiterite/SDS system, the number of charged sites on the stannic oxide surface can be calculated at each pH value assuming that each surfactant ion attaches to a charged site at the pzr. The results of the calculations are presented in Table 6.2.

Table 6.2. Data for the adsorption of SDS on stannic oxide at the pzr

pH	pzr (M)	adsorption density ($moles/m^2$)	surface coverage (%)	number of charged sites cm^{-2}	area per adsorbed ion nm^2
2.0	1.4×10^{-4}	1.2×10^{-7}	1.81	7.23×10^{12}	13.84
3.0	4×10^{-5}	1.7×10^{-8}	0.26	1.02×10^{12}	97.66

The data in Table 6.2 show that as in the case of the cassiterite sample, a very low level of surfactant adsorption was needed to neutralize the charged surface sites. The calculations show that at pH 3.0 there is a charged site per 97.66 nm^2 (9766 A^{o2}) and that as the pH is lowered away from the iep, the ionization of the surface increases to about a charged site per 13.84 nm^2.

6.3. Studies on the cassiterite/Aeropromoter 845 system

Electrokinetic, stability and dissolved air flotation studies were carried out on cassiterite in the presence of Aeropromoter 845, a commercial product used widely in industry for cassiterite flotation. According to the manufacturers (Cyanamid Co. Ltd.) this product is a

solution of sodium octadecyl sulphosuccinamate, a branched anionic surfactant on which various commercial collectors for cassiterite are based, e.g. Aerosol 22 (237). It was thought that these measurements would provide more information on the adsorption mechanism on cassiterite which could then be compared with the results obtained on the cassiterite/SDS and stannic oxide/SDS systems.

6.3.1. Electrokinetic studies

Measurements of the electrophoretic mobility of cassiterite particles in the presence of Aeropromoter 845 (A845) at various pH values gave a set of curves identical to those obtained with the cassiterite and stannic oxide samples in the presence of SDS (Figure 6.15). These experimental data have been plotted in Figure 6.16 to show the effect of pH upon the mobility of cassiterite particles.

The effects of surfactant concentration and pH on the electrokinetic properties of cassiterite in the presence of the sulphosuccinamate collector were found to be the same as those detailed in section 6.1.1. for the behaviour of cassiterite in the presence of the alkyl sulphate surfactant. The most important effects were that surfactant adsorption increased with decreasing pH value and that adsorption occurred above the iep of the mineral, the upper pH value being determined by the collector concentration.

However, the surfactant concentrations at which the significant electrophoretic phenomena (C_{HMC} and pzr) occurred in this system were substantially lower than with SDS. Thus the pzr values occurred at 0.6, 0.1 and 0.02 mg/l A845 for pH 2.0, 3.0 and 4.0 respectively, which corresponded to 3.2×10^{-7}, 5.4×10^{-8} and 1.0×10^{-8} M for the sulphosuccinamate surfactant (assuming A845 is a 35% solution of

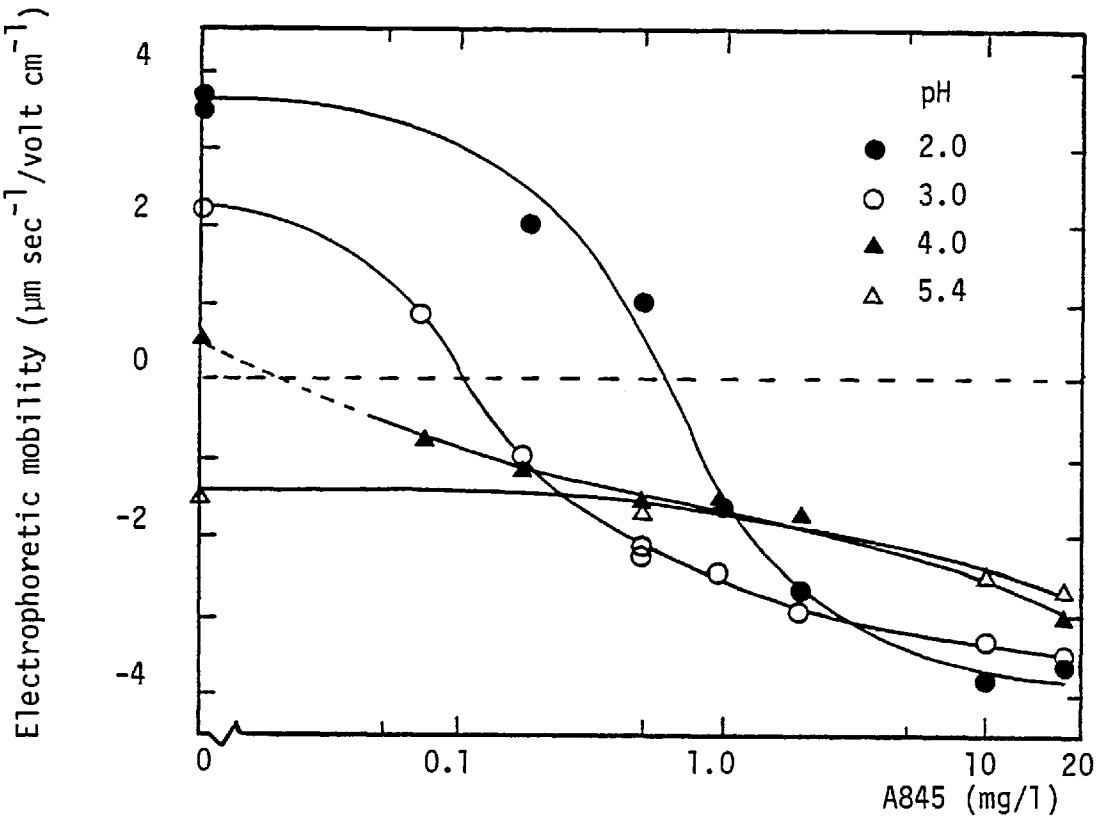

Figure 6.15. Electrophoretic mobility of cassiterite as a function of Aeropromoter 845 concentration for various pH values

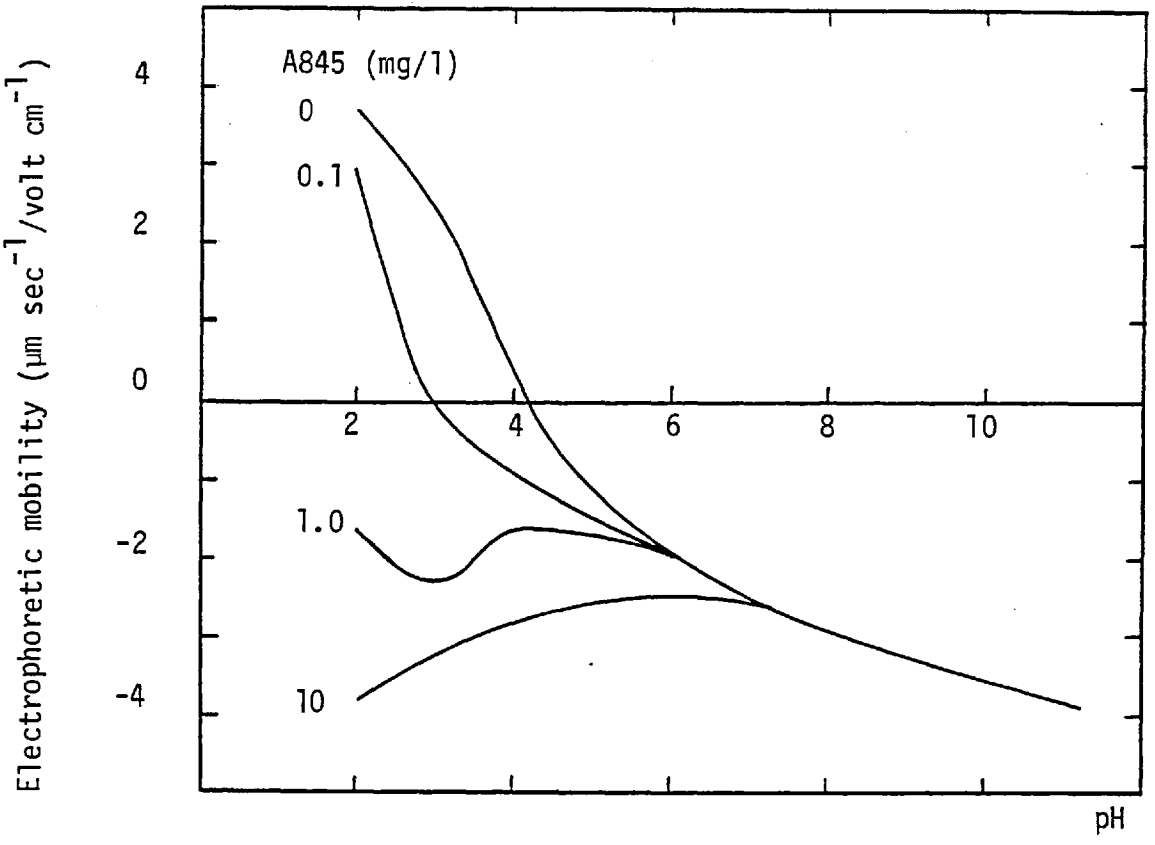

Figure 6.16. Electrophoretic mobility of cassiterite as a function of pH values for various concentrations of Aeropromoter 845

sulphosuccinamate of molecular weight 653). The pzr values in the presence of SDS were between 4×10^{-5} and 3×10^{-7} M for the same pH values (cf Figure 6.2). The lower concentrations required to produce charge reversal in the case of the A845 collector is probably due to the longer hydrocarbon chain of the sulphosuccinamate. The effect of increasing the chain length for a homologous series of surfactants is to reduce both the critical hemimicelle concentration and the point of zeta-potential reversal (235)(35).

Tests similar to those reported on the cassiterite/ SDS system were carried out to assess the reversibility of collector adsorption in this system. The results showed that A845 was easily washed off the cassiterite surface and the mobility/log C curves were reversible upon dilution of the suspensions.

6.3.2. Stability measurements

The stability of cassiterite suspensions in the presence of A845 is shown as a function of concentration at pH values below the iep in Figure 6.17. No suspension destabilization occurred at pH values above the iep.

The shape of the destabilization regions was very similar to that found for SDS (compare Figures 6.5 and 6.17) indicating that excesses in A845 concentration led to suspension restabilization. Surfactant concentration and pH were the determining variables for particle aggregation to occur. The correlation between stability and the electrophoretic mobility of cassiterite in the presence of A845 is presented in Figure 6.18. Figures 6.17 and 6.18 clearly demonstrate that the destabilizing mechanism of A845 on cassiterite suspensions is very similar to that described for the cassiterite/SDS system in section 6.1.2.

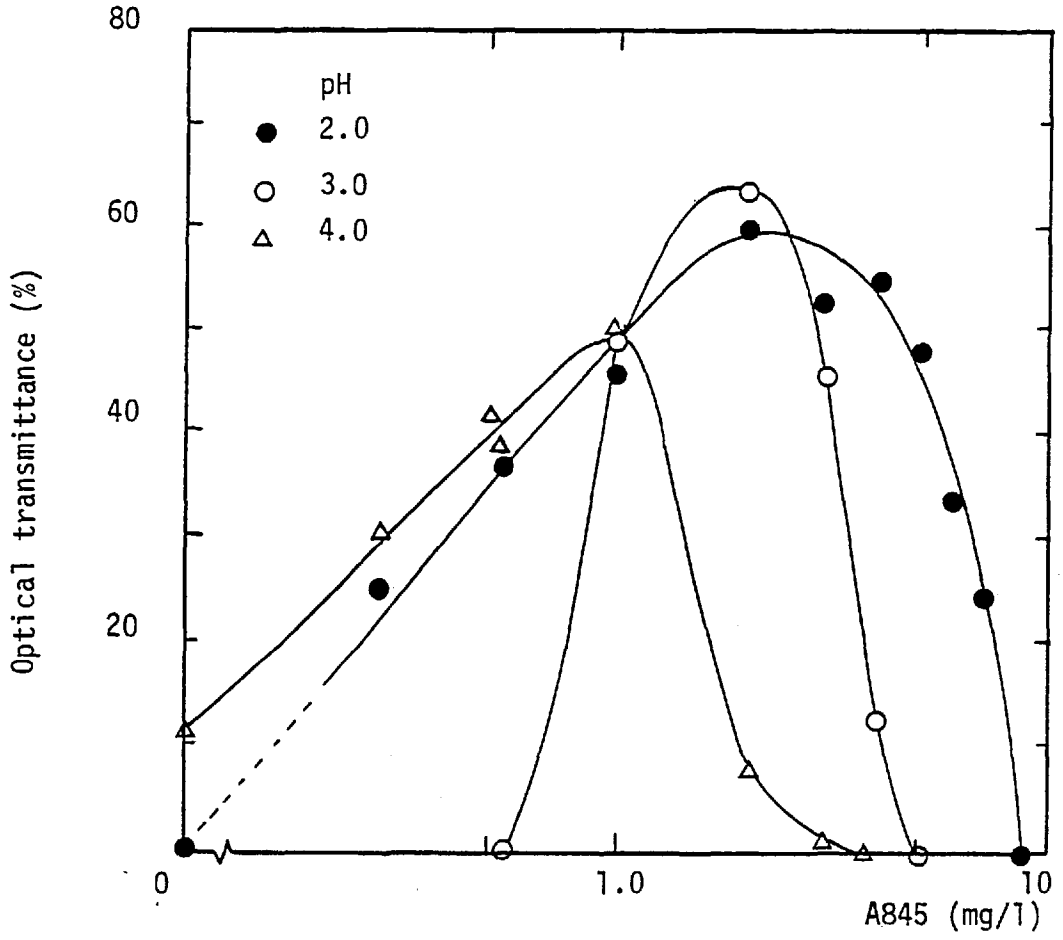

Figure 6.17. Stability of cassiterite suspensions as a function of Aeropromoter 845 concentration at various pH values

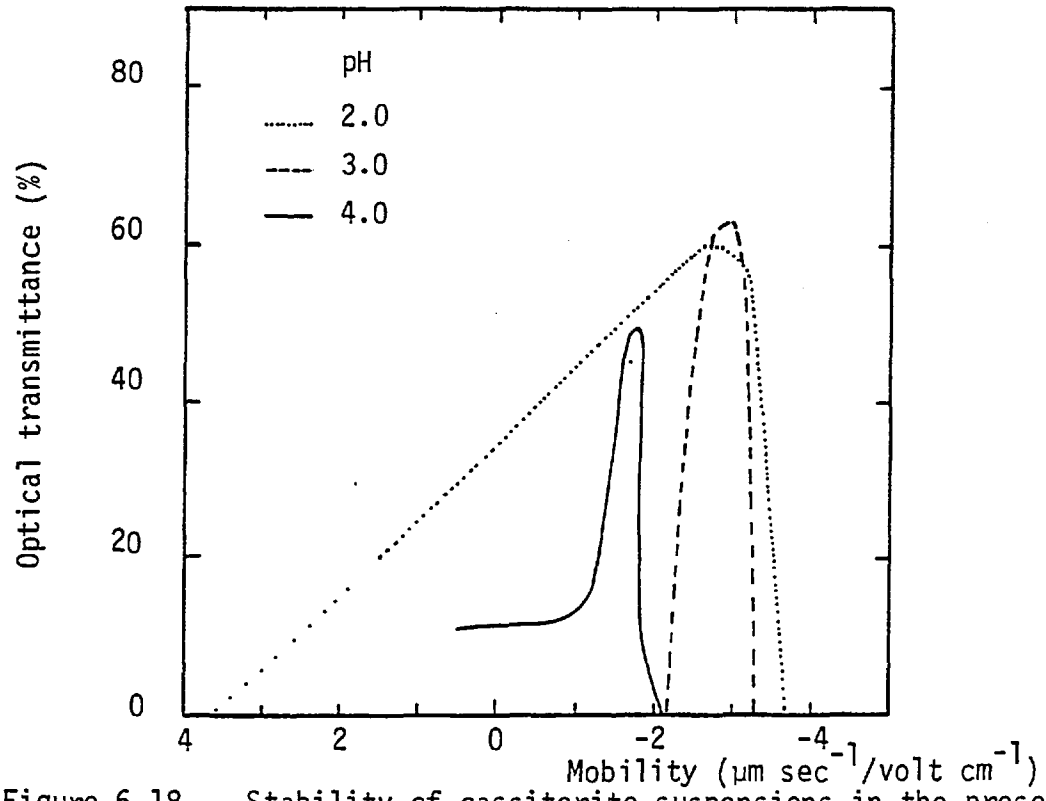

Figure 6.18. Stability of cassiterite suspensions in the presence of Aeropromoter 845 as a function of the electrophoretic mobility at various pH values

The optical transmittance measurements indicated that suspension restabilization occurred at all pH values for A845 concentrations in excess of 10 mg/l (5.4×10^{-6} M sulphosuccinamate). At pH 2.0, however, complete redispersion of the aggregates was observed only above 20 mg/l A845. The low sulphosuccinamate concentrations involved in causing destabilization of cassiterite suspensions are in line with those obtained by other authors working with ionic surface active agents of comparable chain length (161)

6.3.3. Dissolved air flotation studies

The effect of pH on the dissolved air flotation of cassiterite with A845 as collector is depicted in Figure 6.19 for 3.0, 6.0 and 10.0 mg/l A845. The curves show that flotation decreased drastically above the iep of cassiterite (pH 4.2), no cassiterite recovery being obtained at pH 5.0. On the other hand, recovery increased as the pH was lowered away from the iep.

The effect of A845 concentration on the DAF behaviour of cassiterite is shown in Figure 6.20 for various pH values below the iep. The curves were similarly shaped to those obtained in the presence of the alkyl sulphate and exhibited a three-region division characteristic of DAF curves. Optimum recovery was pH dependent, 4 - 7 mg/l A845 for pH 2.0 and 4.0, and 2 - 4 mg/l at pH 3.0. No significant recoveries were obtained below and above 0.6 and 15.0 mg/l A845 respectively.

The DAF and coagulation regions of cassiterite in the presence of Aeropromoter 845 are presented in Figure 6.21. The correlation indicates that at low A845 concentrations both regions roughly coincided for pH 2.0 and 3.0 but at pH 4.0 there was no flotation even though the particles were coagulated. At high collector concentrations there was significant

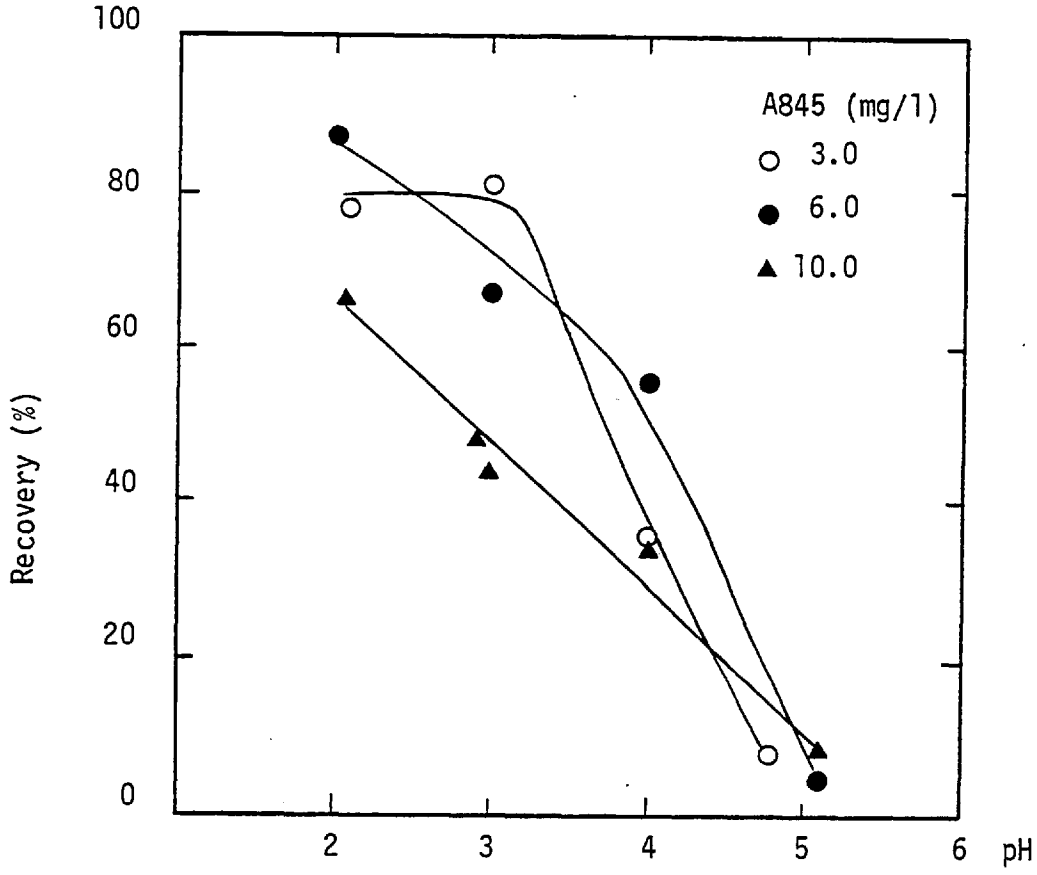

Figure 6.19. Dissolved air flotation of cassiterite as a function of pH for various Aeropromoter 845 concentrations

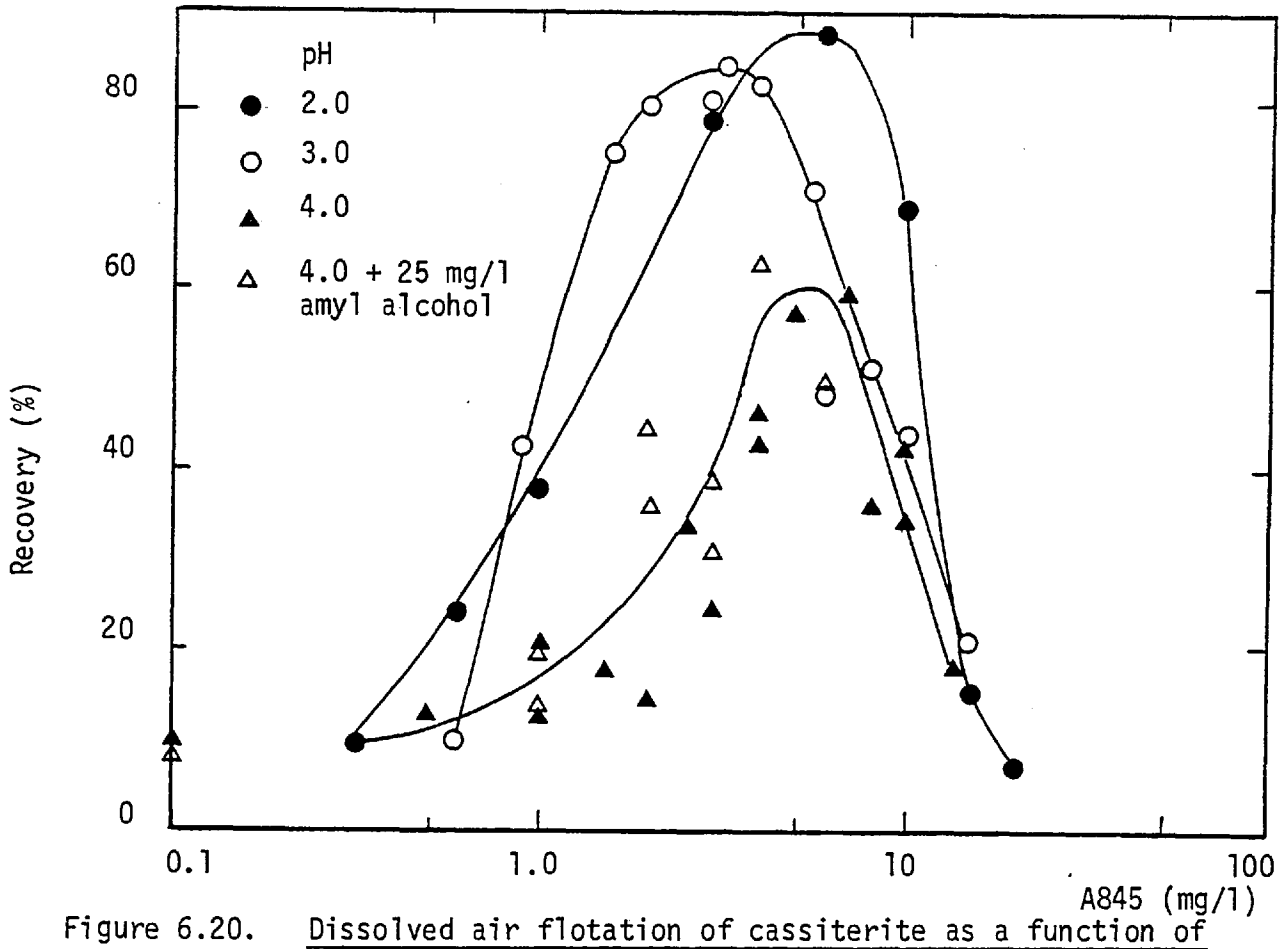

Figure 6.20. Dissolved air flotation of cassiterite as a function of Aeropromoter 845 concentration for various pH values

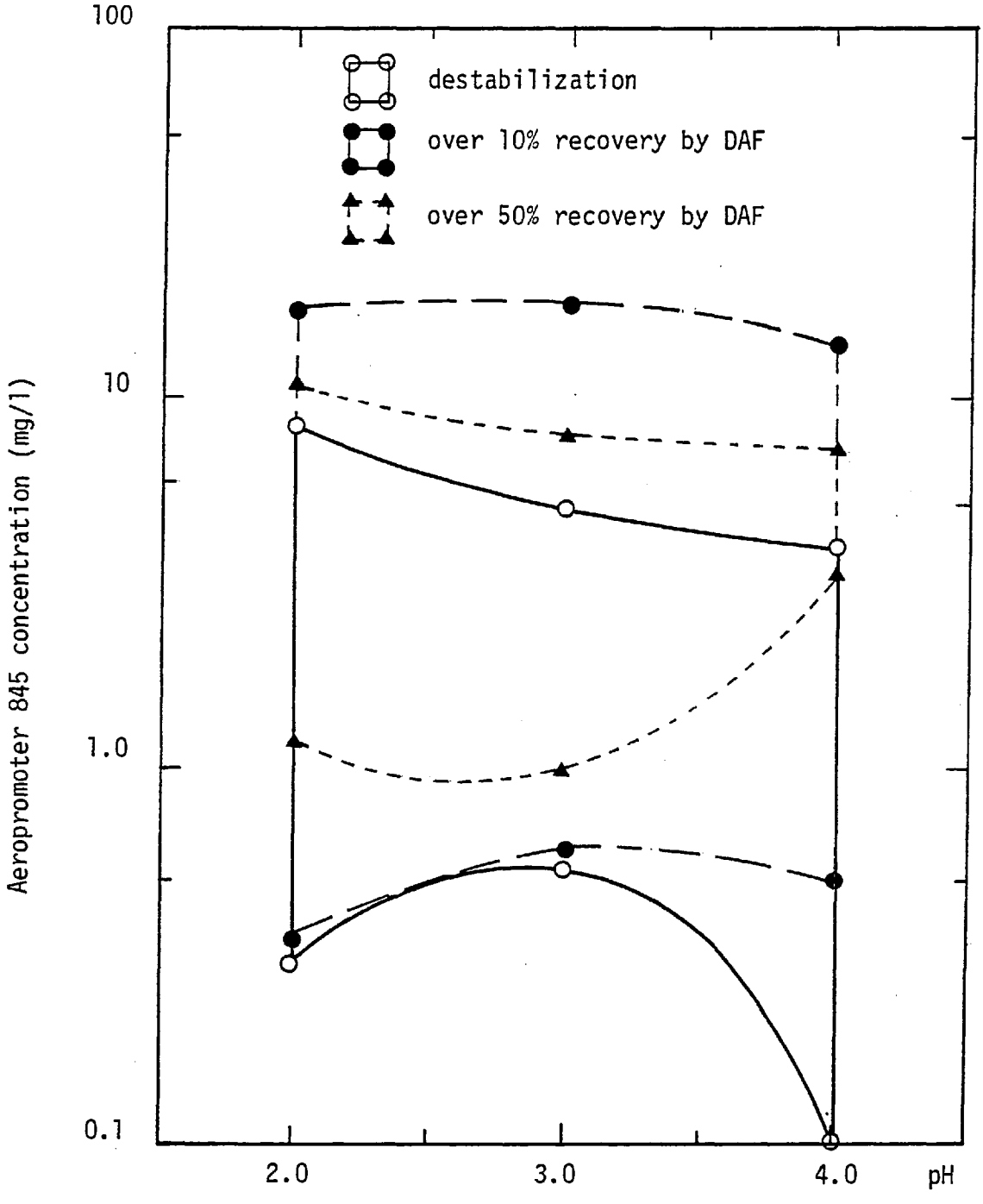

Figure 6.21. Destabilization and dissolved air flotation regions for the cassiterite/Aeropromoter 845 system

flotation outside the destabilization region for all pH values. Thus, it would appear that the degree of hydrophobicity of the mineral particles was the determinant condition for DAF to proceed.

In the absence of any adsorption results with which to correlate the DAF behaviour of cassiterite (A845 solutions could not be analysed by Gregory's method (203)), the electrokinetic phenomena may serve as a guide to establish a relationship between DAF and collector adsorption. Thus, at pH 2.0 and 3.0, cassiterite flotation occurred only within the hemimicellization region and for A845 concentrations well above the pzr. Conversely, the suppression of DAF was associated at both pH values with collector concentrations at which the electrophoretic mobility tended to level off. These results would appear to demonstrate that the higher part (above the pzr) of the hemimicellization region is a region of high hydrophobicity.

At pH 4.0 the range of concentrations yielding maximum DAF corresponded with the section of the mobility curve between 4 and 10 mg/l A845. Therefore, it would seem that the increased adsorption of collector shown by the electrokinetic measurements results in an increase of the hydrophobicity of the mineral particles. Nevertheless, the experimental observations indicated that further additions of collector brought about the suppression of flotation, presumably through the cassiterite surface becoming increasingly hydrophilic.

6.4. Discussion

The cassiterite surface

The electrokinetic properties exhibited by cassiterite particles in aqueous solution were consistent with the proposed mechanism of surface ionization, namely, the adsorption-desorption of hydrogen ions from

surface SnOH groups (169). The potential-determining role of pH on oxide mineral surfaces was also confirmed by the dependence of the electrophoretic mobility of cassiterite on the pH value.

Experiments on the electrokinetic behaviour of a synthetic stannic oxide sample showed an almost equivalent behaviour to that exhibited by the natural cassiterite sample, indicating that the impurities contained in the latter did not have an appreciable influence on its electrokinetic properties. The shape of the mobility/pH curves for both samples were similar to others reported in the literature (170)(238), slightly higher values being recorded at the acid side of the iep and the electrophoretic mobility tending to a constant value at alkaline pH values.

It has been pointed out that calculations of the number of active sites on both samples gave low values compared with results reported in the literature for oxides and ionic solids at comparable concentrations of the potential-determining ions. The range of values calculated for cassiterite and SnO_2 at pH 2.0 and 3.0 ($1 - 7 \times 10^{12}$ active sites) was equivalent to an active site per 13 - 97 nm^2. Kittaka et al (167) have shown that the amount of chemisorbed hydroxyl groups on the surface of a chemically precipitated stannic oxide sample varied between 2.6 - 12 OH groups per nm^2 depending on the heat treatment of the sample. Assuming that there were 2.6 OH groups/nm^2 and that all active sites corresponded to charged hydroxyl sites, then it follows that there was a charged OH group per 34 - 252 OH groups. This corresponds to a ionization of the surface hydroxyl groups of the order of 3 - 0.4% depending on the sample and the pH value. If the surface was more hydroxylated (say 12 OH groups /nm^2) a similar calculation shows that only 0.6 - 0.09% of the hydroxylated groups were charged.

The degree of surface ionization calculated from the adsorption

studies depended upon the sample and the pH value, decreasing in the order

SnO_2 (pH 2.0) > Cassiterite (pH 2.0) > Cassiterite (pH 3.0) > SnO_2 (pH 3.0)

which is consistent with the notion that the surface sites become progressively neutralized as the iep of the oxide is approached (in the absence of specific adsorption).

The surface charge of cassiterite and SnO_2 was calculated at pH 2.0 and 3.0 from the adsorption results. The values (Table 6.3) were in fairly good agreement with those obtained from the electrokinetic measurements using double layer theory (see Appendix II for details).

Table 6.3. Surface charge of cassiterite and stannic oxide at pH 2.0 and 3.0 calculated from electrokinetic and adsorption results

Sample	pH	$\sigma_{o\ elect}$ ($\mu C/cm^2$)	$\sigma_{o\ ads}$ ($\mu C/cm^2$)
Cassiterite	2.0	1.28	0.84
"	3.0	0.24	0.42
Stannic oxide	2.0	1.16	1.16
" "	3.0	0.26	0.16

These observations are discussed further in the next section in connection with the mechanism of adsorption.

The adsorption mechanism of anionic collectors on cassiterite

The results presented in the preceeding sections indicated that the mechanism of adsorption of alkyl sulphate and sulphosuccinamate collectors is primarily by coulombic attraction of the surfactant ions

for the opposedly charged surface, and that over a certain concentration adsorption occurs purely through hydrophobic bonding of the surfactant in the Stern layer. No evidence was obtained to support adsorption mechanisms involving chemisorption of the collectors on the cassiterite or stannic oxide surfaces. Hence, according to the classification discussed in Chapter 3, the adsorption mechanism would appear to be of a physical nature.

The electrostatic and hydrophobic contributions to the adsorption mechanism of these anionic collectors on cassiterite have been clearly demonstrated by the dependence of the electrokinetic, adsorption, stability and dissolved air flotation behaviour of the oxide upon pH and surfactant concentration.

The influence of pH on the adsorption mechanism arises from the role of hydrogen and hydroxyl ions in determining the surface potential and charge of the mineral surface (cf. section 3.2), and therefore the electrostatic attraction between surface and surfactant ions. On the other hand, the increased levels of hydrophobicity and adsorption detected at surfactant concentrations over the pzr of the oxide/surfactant solution system revealed the contribution of hydrophobic bonding to the adsorption mechanism. Calculations of the free energy change associated with this adsorption mechanism showed it to be comparable with the decrease in free energy corresponding to the removal of a hydrocarbon chain from aqueous solution (see below).

Alternative mechanisms of adsorption of alkyl sulphates on synthetic stannic oxide samples have been put forward by Edwards and Ewers (168) and Jaycock, Ottewill and Tar (169). The former authors proposed that cetyl sulphate adsorbed through an ion exchange mechanism with hydroxyl ions on the surface. They supplied results showing that

when SnO_2 was added to sodium cetyl sulphate solutions at acid pH values the solution pH increased. This was taken as evidence of the release of OH^- ions from the oxide surface. This effect was also observed in this work but was dependent upon surfactant concentration, significant pH increases being observed only at high alkyl sulphate concentrations. It is, therefore, probable that the observed increase in pH occurs only for concentrations well over the pzr and that it is due to the adsorption of hydrogen ions into the diffuse layer as counter-ions (no supporting electrolyte was used by the authors in their experiments). As the increase in pH was the only proof supplied and no evidence of the chemisorption of cetyl sulphate on SnO_2 was obtained, the proposed mechanism may be discarded.

Jaycock et al (169) proposed that adsorption occurred as the result of ionic exchange with chloride ions on the oxide surface. They based this suggestion on results showing the adsorption of SDS to be independent of pH value in the range 2.86 - 4.2. The exact location of the Cl^- ions on the surface was not indicated by the authors but it is assumed that they are referring to chloride ions acting as hydrated counterions in the diffuse layer. The possibility of an exchange of SDS ions with chemisorbed Cl^- ions on the surface is tantamount to postulating a chemical interaction between the surface and surfactant and was explicitly discarded by the authors (the chemisorption from solution of Cl^- ions on cassiterite has been proposed by Ahmed and Maksimov (174) but other authors have considered it to be doubtful (239)). The possibility of Cl^- ions being specifically adsorbed at the inner Helmholzt plane was not revealed by the electrokinetic studies reported in this work (at 10^{-2} M KCl) where the presence of Cl^- or NO_3^- ions made little difference to the effect of SDS on the electrophoretic mobility of the

cassiterite particles.

If the ionic exchange mechanism of Jaycock et al (169) refers to hydrated chloride counter ions it is then in agreement with the electrostatic adsorption mechanism proposed in this work, i.e. ionic exchange in the diffuse layer. However, it is clear that the ionic exchange mechanism cannot account for SDS adsorption above the pzr. In this region the Cl^- ions are no longer counterions and therefore, the proposed ionic exchange mechanism is unable to explain the whole of the adsorption process.

Han, Healy and Fuerstenau (141) have suggested that the mechanism of adsorption of long chain surfactants at the oxide/water interface may be deduced from the shape of the electrophoretic mobility/pH curves. Surfactant chemisorption at the mineral surface is indicated in their model by a shift of the iep with increasing surfactant concentration. The shape of the mobility/pH curves obtained in this work for the cassiterite/SDS, cassiterite/sulphosuccinamate, cassiterite/dodecylamine and stannic oxide/SDS, is equivalent to those which, according to the classification of Han et al, would involve a chemisorption mechanism of surfactant adsorption on this oxide mineral. Since no experimental evidence was found to support a chemisorption mechanism of adsorption of these surface-active agents on cassiterite on stannic oxide, it would appear that relying only on electrokinetic measurements to ascertain the adsorption mechanism of surfactants at the oxide/water interface might lead to erroneous conclusions.

However, the shape of the mobility/pH curves and the adsorption results obtained in this work showed that surfactants adsorbed at the iep of cassiterite and stannic oxide, and that they also adsorbed at pH values above the iep, depending on the concentration. This behaviour

has also been reported by other authors. Hence, Jaycock (238) reported the adsorption of a cationic surfactant (dodecyl pyridinium chloride) at pH values below the iep and Jaycock et al (169) the adsorption of an anionic surfactant (SDS) above the iep of stannic oxide. The results of de Cuyper and Gutiérrez (173) show that dodecylamine adsorbed at the iep of cassiterite but not at the iep of siderite (pH 7.3). Zambrana et al (175) reported the adsorption of SDS and Aerosol 22 (a sulphosuccinamate similar to the Aeropromoter 845 used in this work) at and above the iep of cassiterite. Other systems in which surfactant adsorption at the iep has been reported and no claim of a chemisorption mechanism has been made were (i) hematite in the presence of SDS and dodecylamine (213), and (ii) rutile in the presence of various alkyl sulphates and CTAB (35).

Thus, it would seem that although specific adsorption at the iep of cassiterite, stannic oxide and other oxide minerals does not appear to be the effect of a chemisorption mechanism, some explanation is needed for the adsorption of surfactant ions on certain oxide minerals under conditions of (overall) neutrality or electrostatic repulsion.

The adsorption isotherms of SDS on cassiterite and SnO_2

The adsorption isotherms of SDS on cassiterite and stannic oxide showed a sigmoidal shape below the iep (except the isotherm at pH 3.0 for SnO_2) which is characteristic of the adsorption of ionic surfactants on charged solids (130)(132). Nevertheless, the three regions characterizing S-2 isotherms have been found to correspond with different phenomena depending on which adsorbent has been used to study surfactant adsorption. Hence, for the adsorption of a cationic surfactant on silver iodide (130) the pzr occurred within the first region which was

linear and extended up to monolayer coverage, above monolayer coverage the surfactant adsorbed in multilayers at almost constant surfactant concentration (region II) and attained saturation (region III) at surfactant concentrations in the vicinity of the CMC. On the other hand, for the adsorption of an anionic surfactant on alumina (234) it was found that the first region was linear and extended up to the C_{HMC}, above this concentration adsorption increased markedly up to the pzr (12% of a monolayer) after which surfactant adsorption decreased and region III (saturation) began to develop.

In the present case, the regions of the adsorption isotherm on cassiterite and stannic oxide show features of both the cases outlined above. The particular characteristics of these isotherms are discussed below.

Region I. For SnO_2 this region is associated with an adsorption mechanism based on ionic exchange with Cl^- ions on the diffuse double layer. The slope of this section (0.65) is in good agreement with other experimental values reported in the literature (213)(234). For cassiterite, however, the situation is less clear as both the C_{HMC} and the pzr occurred within this region without apparently having any effect on the slope of this section of the isotherm. The specific adsorption of SDS on cassiterite may be evaluated from considerations of the Stern-Grahame equation (cf. section 3.2) since the adsorption density is low:

$$\Gamma_i = 2\, r\, C \exp\left(-\Delta G^0_{ads}/RT\right) \qquad (6.2)$$

which is equivalent to

$$\frac{-\Delta G^0_{ads}}{RT} = \frac{\ln \Gamma_i}{2rC} \qquad (6.3)$$

but according to eq. 3.13 and 3.14

$$\Delta G^{o}_{ads} = \Delta G^{o}_{elec} + \Delta G^{o}_{spec} = zF\psi_i + \Delta G^{o}_{spec} \quad (6.4)$$

and at the pzr, $\Gamma_i = \Gamma_o$, $C = C_o$ and $\psi_i = 0$, so that equation 6.3 becomes

$$\frac{-\Delta G^{o}_{spec}{}^{*}}{RT} = \frac{\ln \Gamma_o}{2rC_o} \quad (6.5)$$

with $\Delta G^{o}_{spec}{}^{*}$ = specific free energy of adsorption at the pzr

Γ_o = adsorption density at the pzr (moles/cm^2)

C_o = surfactant concentration at the pzr (moles/cm^2)

r = radius of the adsorbed ion, 2.8×10^{-8} cm for a desolvated SDS ion

Furthermore, the value of ϕ, the free energy change associated with the removal of one mole of CH_2 groups from aqueous solution, may be calculated assuming that

$$\Delta G^{o}_{spec}{}^{*} = G^{o}_{CH_2} = n\phi \quad (6.6)$$

with n = 12 for SDS. Table 6.4 shows the value of ΔG^{o}_{spec} calculated at the pzr of cassiterite and stannic oxide for two pH values.

Table 6.4. Calculated values of ΔG^{o}_{spec} and ϕ for cassiterite and stannic oxide at the pzr

Sample	pH	C_o (moles/cm^3)	Γ_o (moles/cm^2)	$-\Delta G^{o}_{spec}{}^{*}$	$-\phi$
Cassiterite	2.0	3.4×10^{-8}	8.7×10^{-12}	8.43RT	0.71RT
"	3.0	1.5×10^{-8}	4.4×10^{-12}	8.56RT	0.71RT
Stannic oxide	2.0	1.4×10^{-7}	1.2×10^{-11}	7.33RT	0.61RT
" "	3.0	4×10^{-8}	1.7×10^{-12}	6.63RT	0.55RT

The values calculated for G^{o}_{ads} at the pzr for cassiterite (about 20.5 kJ/mol at 20°C) are within the range of values quoted for physical mechanisms of surfactant adsorption (4). The values calculated for ϕ are within those quoted in the literature (240) for free energy changes associated with the transfer of surface-active agents to various interfacial states (between -0.6 and -2.0 RT). Values of ϕ obtained from zeta-potential and flotation results are of the order of -1.0 RT for the free energy change of hemimicellization (240). It is therefore proposed that for cassiterite at the pzr there are hydrocarbon chain interactions between adsorbed SDS ions but these are not completely removed from aqueous solution. The mode of orientation of surfactant ions at the solid/liquid interface is probably angled as suggested by Jaycock and Ottewill (130), with some taking up a horizontal position at the pzr as the surface-solvent attractive forces are most weakened when the surface charge has been neutralized.

Region II. For SnO_2 at pH 2.0, the beginning of this region approximately corresponded with the critical hemimicelle concentration obtained from the electrokinetic studies and therefore above this concentration hydrophobic association of the surfactant chains is expected to occur. The pzr occurred some way above the C_{HMC} and at this concentration the calculated values of G^{o}_{spec}* and ϕ were respectively -7.33 and -0.61 RT which were somewhat lower than those found for cassiterite. Above the pzr, the slope of the adsorption isotherm did not decrease as it would have been expected if close correspondence with the model of surfactant adsorption on other oxides had occurred (132).

For cassiterite, the upward break marking the beginning of region II occurred at a similar adsorption density for both pH values ($\simeq 1 \times 10^{-7}$ moles/m^2, around 1.8% of a monolayer). In this region, adsorption occurred

under conditions of negative Stern potential, that is, against the repulsion of the electrostatic forces between surface and surfactant ions. The fact that this repulsive force did not show up in the slope of the isotherms and, on the contrary, the adsorption density increased with surfactant concentration clearly implies that the free energy of adsorption increases (is more negative) with surfactant concentration. The only possibility for this to occur if ΔG^{o}_{ads} is made up of electrostatic and hydrophobic contributions, is through an increase (more negative) of the free energy change associated with hydrophobic bonding ($\Delta G^{o}_{CH_2}$), so that

$$\frac{d(\Delta G^{o}_{CH_2})}{dc} < 0 \qquad (6.7)$$

The variation of $\Delta G^{o}_{CH_2}$ with concentration expresses the fact that in region II the removal from aqueous solution of CH_2 groups in the hydrocarbon chain increases with increasing adsorption density. The increase in adsorption (and of $\Delta G^{o}_{CH_2}$) in this region would qualitatively appear to be a function of both adsorption density and bulk surfactant concentration. Wakamatsu and Fuerstenau (234) consider that complete removal of the hydrocarbon chain is only possible at monolayer coverage and Fuerstanau (135) has found that hydrophobic associations occur at bulk surfactant concentrations of the order of 1/100 of the CMC. As $\Delta G^{o}_{CH_2} = n\phi$, the variation of $\Delta G^{o}_{CH_2}$ with surfactant concentration may be interpreted as an increase in the number of CH_2 groups (n) removed from aqueous solution through hydrophobic associations on the mineral surface (234), or, alternatively, as the increase (more negative) of the free energy change associated with the adsorption (or removal from aqueous solution) of the surfactant hydrocarbon chain (ϕ).

Thus, the observed increase in adsorption density in this region may be due to the effect of a rearrangement of the adsorbed surfactant ions on the surface, permitting SDS ions to be more completely abstracted from the aqueous phase upon adsorption. It is likely that the surfactant ions adsorb in this region on uncharged sites existing in the vicinity of ionized sites, the whole process appearing as adsorption in clusters around ionized sites. The fact that dissolved air flotation was maximum in region II would further suggest that the orientation of the adsorbed ions is such that it gives rise to increased hydrophobicity. Orientation of the adsorbed species with the polar head pointing towards the solution would therefore be unlikely.

Region III. The decrease in adsorption density with surfactant concentration exhibited in this region is probably associated with $\Delta G^{o}_{CH_2}$ attaining its maximum value ($\simeq$ -12 RT, about -1.0 RT per CH_2 group) and with the electrostatic repulsive forces beginning to show up. The saturation plateau depended slightly on the pH value and varied between 105 - 75% of a close-packed, vertically oriented monolayer of SDS ions each occupying an area of 0.25 nm^2 for pH values between 1.4 and 3.0.

All the isotherms indicated that saturation was attained as the critical micelle concentration of the surfactant and monolayer coverage were approached. The influence of the CMC upon adsorption is consistent with the proposal that the surfactant ions adsorbed through hydrophobic bonding in the second region, since above the CMC the surfactant hydrocarbon chains would tend to associate in the bulk solution rather than on the mineral surface.

The hydrophilicity of the cassiterite surface at SDS concentrations within this region would indicate that adsorption of the surfactant ions

occurred with the polar head in the direction of the solution. Thus, at saturation the surface presents an adsorbed bilayer with (mostly) reversedly orientated surfactant ions as suggested by various authors (130)(241).

The remarkable linearity of the adsorption isotherm of SDS on stannic oxide at pH 3.0 has been the subject of controversy in the literature (242), but these results confirmed the earlier finding of Jaycock et al (169). Nevertheless, when the isotherm is coupled with the electrokinetic results it is clear that the adsorption mechanism proposed by these authors to justify its linearity (ionic exchange between Cl^- and SDS ions) is not tenable.

The critical hemimicelle concentration exhibited by SDS on SnO_2 at pH 3.0 during the electrokinetic studies was of the order of 10^{-6} M SDS and, therefore, any region in which adsorption proceeds through ionic exchange in the diffuse layer would be expected to show up below that concentration.. With the colorimetric technique used in this work only adsorption densities of about 8×10^{-6} M SDS could be measured but Jaycock et al (169) measured SDS adsorption densities down to 10^{-6} M SDS and found the isotherm to be linear down to that concentration. The data of Table 6.4 show that the pzr, ΔG^{o}_{spec} was -6.63 and ϕ was -0.55 RT, just about the minimum value measured for the free energy change associated with the removal of a hydrocarbon chain from the aqueous phase (240).

No explanation can be offered at present for the linearity of the adsorption isotherm at pH 3.0, and for the general lack of correlation observed between the adsorption and electrokinetic measurements on cassiterite compared with results on other oxide minerals. It is interesting to note, however, that the order in which the adsorption

isotherms tended to correlate with the electrokinetic measurements was similar to that reported for the ionization of the surface, i.e. the best correlation was obtained for the more charged surface (SnO_2 at pH 2.0, calculated from the adsorption data).

The adsorption isotherm of SDS on stannic oxide at pH 4.5 (i.e. above the iep) shows marked adsorption over a small range of surfactant concentrations without reaching saturation. This behaviour has been attributed to a 'phase' change (130), 'salting-out' (35), solute capillary condensation and surfactant precipitation (126). This phenomenon may also be due to preliminary adsorption on 'active sites' followed by hydrophobic bonding at high surfactant concentrations. The nature of these 'active sites' is not clear at present but the fact that many researchers have found specific adsorption at and above the iep of cassiterite and stannic oxide would lend support to their existence.

The dissolved air flotation of cassiterite with anionic collectors

The results obtained in this work showed that the recovery of very fine cassiterite particles by dissolved air flotation was possible and that it depended upon the surface physico-chemical properties of the oxide.

Dissolved air flotation (DAF) of cassiterite by the anionic collectors used in this work was dependent on pH and collector concentration. No recovery could be obtained with any of the surfactants used at pH values above the iep of cassiterite. In addition, substantial rates of recovery could only be attained at pH values lower than 3.0, the highest occurring at the most acid pH value tested (pH 2.0). These results are consistent with the proposed mechanism of adsorption for these collectors.

The concentration of SDS and A845 at a particular pH determined the

recovery of the oxide mineral by DAF. At every pH value investigated there was only a small range of collector concentrations where recovery by DAF was maximized, an overdosage leading inexorably to the suppression of flotation.

For the commercial reagent (A845) flotation was completely depressed for concentrations over 20 mg/l at all pH values. However, cassiterite flotation in Hallimond tube with sulphosuccinamate collectors has been reported to occur at concentrations as high as 100 mg/l (175)(186). Hallimond tube flotation tests carried out on this cassiterite sample with 62.5 mg/l A845 did show complete recovery in the pH range 2 - 8.5. The increase in the upper limit of flotation for both surfactant concentration and pH value, under conditions of coarser cassiterite particles and air bubbles, is not totally understood.

The DAF results on both the cassiterite/SDS and the cassiterite/A845 systems are in good agreement with the proposed mechanism of bubble-particle attachment in DAF. Thus, the main prerequisite for DAF to occur was a level of collector adsorption that rendered the particles hydrophobic. Cassiterite suspensions which were hydrophilic or showed very low surfactant adsorption were not floated even though they were destabilized. The importance of the surface chemical parameters of the mineral on DAF was also shown by the fact that maximum recovery did not occur at the point of zeta-potential reversal (pzr) for any pH value. This was a consequence of the pzr occurring at very low surface coverages (less than 1.6% monolayer) and therefore there was not sufficient hydrophobicity at the pzr for bubble-particle attachment to occur.

The DAF results outlined in this Chapter provided a good basis for selection of the conditions under which DAF of cassiterite from quartz was carried out. The regions of flotation for pH-collector concentration

combinations having been determined, selective separations of artificial cassiterite/quartz mixtures by DAF could be attempted.

Chapter 7. STUDIES ON THE SEPARATION OF CASSITERITE FROM QUARTZ BY DISSOLVED AIR FLOTATION

7. STUDIES ON THE SEPARATION OF CASSITERITE FROM QUARTZ BY DISSOLVED AIR FLOTATION

The use of dissolved air flotation for the selective separation of fine mineral particles was tested on suspensions prepared with mixtures of cassiterite and quartz. With these two oxide minerals a small range of pH values existed within which selective separations may have been possible with anionic collectors. The separation studies were carried out with the aim of exploring the possibilities of the DAF process rather than with the objective of optimizing the recovery and selectivity of a particular separation example. Thus, these studies were concerned basically with (a) separations under the same conditions used for cassiterite in the previous DAF studies, (b) study of the response of the DAF process to modifications in the surface chemistry of the cassiterite/quartz/solution system, and (c) study of the effect of various parameters of the DAF operation on the separation of the minerals.

7.1. Separation studies in the presence of anionic collectors

Primary tests were performed on quartz to see whether it would respond to dissolved air flotation in the presence of the anionic collectors used, Aeropromoter 845 and sodium dodecyl sulphate. The results showed that quartz was not floated by SDS at any pH value and that in the presence of A845 a very slight degree of flotation ($\simeq$ 15% recovery) was exhibited at pH 2.0 only.

Preliminary separation experiments were carried out at pH 3.0 on the basis of 1:1 cassiterite/quartz mixtures and 1 g/l total solids with A845 as collector, following the experimental routine described in section 4.6.3. These tests showed that while the optimum recovery

was between 60-75%, the grade of the floated product remained virtually unchanged. It was also observed during the tests that a degree of particle aggregation occurred prior to flotation. These observations suggested that heterocoagulation between the opposedly charged cassiterite and quartz particles could be taking place during the conditioning period before collector addition. Subsequent tests were, therefore, carried out changing the order in which collector addition and pH adjustment were made in the conditioning stage, the collector being added before the pH was adjusted to its flotation value. The rest of the experimental procedure remained unchanged.

The effect of A845 concentration on the separation of cassiterite by DAF at pH 2.0, 3.0 and 4.0 is shown in Figures 7.1, 7.2 and 7.3 respectively. The effect of pH on tin recovery and concentrate grade is represented in Figure 7.4 at a constant A845 concentration of 6 mg/l. All tests were carried out using 0.5 g cassiterite plus 4.5 g quartz (feed grade 7.38% Sn) giving a total of 0.5% solids concentration. Some tests were carried out at pH 2.0 with suspensions of the same feed grade (7.38% Sn) but containing only 0.1% solids. The feed grade has been marked in the figures with a horizontal dashed line.

The results show that the highest tin recoveries were obtained at pH 2.0 and 3.0 (60-65%) and that the best selectivity was achieved at pH values above 3.0 where enrichment ratios of about 4 were recorded (28% Sn concentrate grade). The best overall result was at pH 3.0 in the range 4 - 8 mg/l A845 where recoveries fluctuated between 65-30% and the concentrate grade between 15-30% Sn respectively. It is significant that the optimum pH lies halfway between the isoelectric points of cassiterite and quartz.

The shape of the Sn recovery curves at pH 2.0 and 3.0 was very

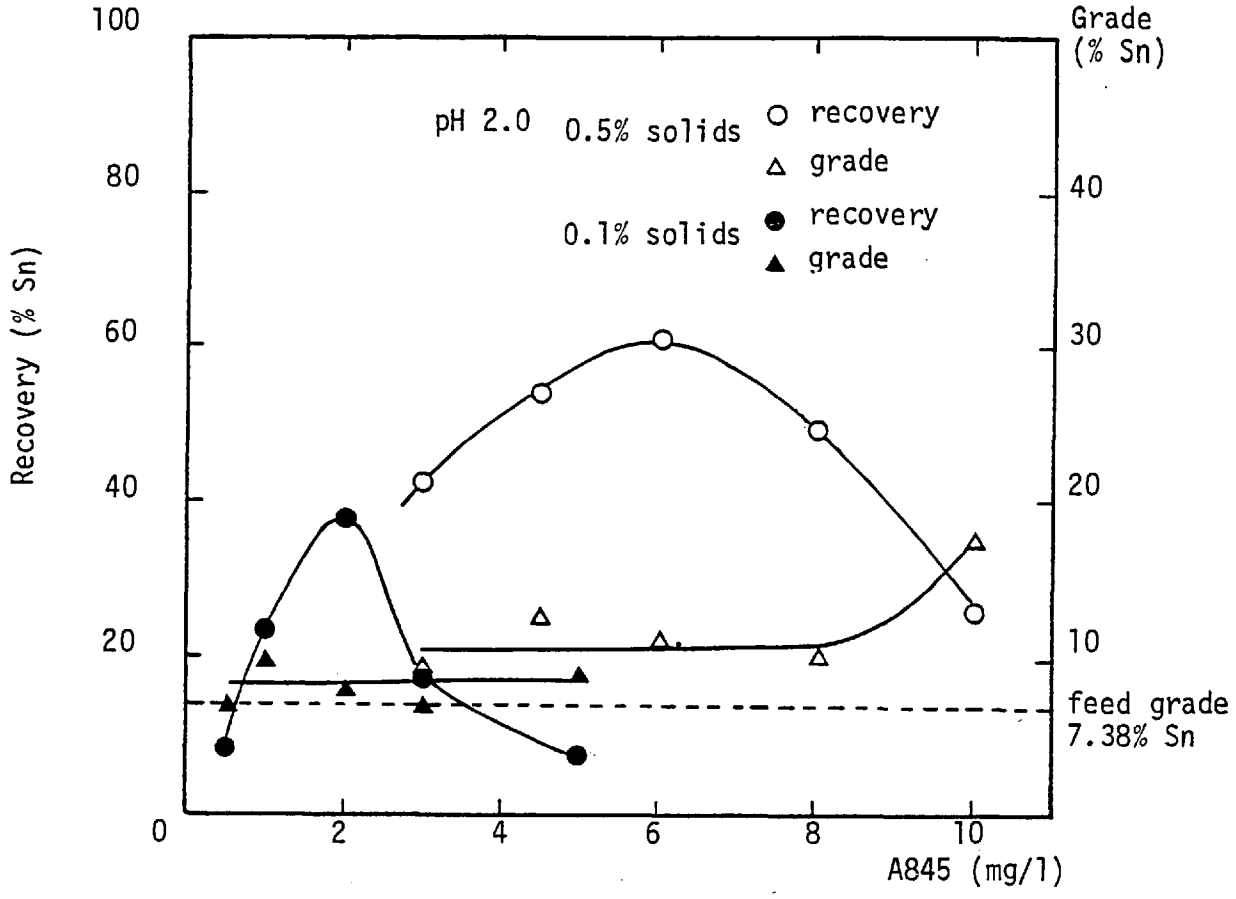

Figure 7.1. DAF of cassiterite from quartz as a function of Aeropromoter 845 concentration at pH 2.0 for two solids concentrations

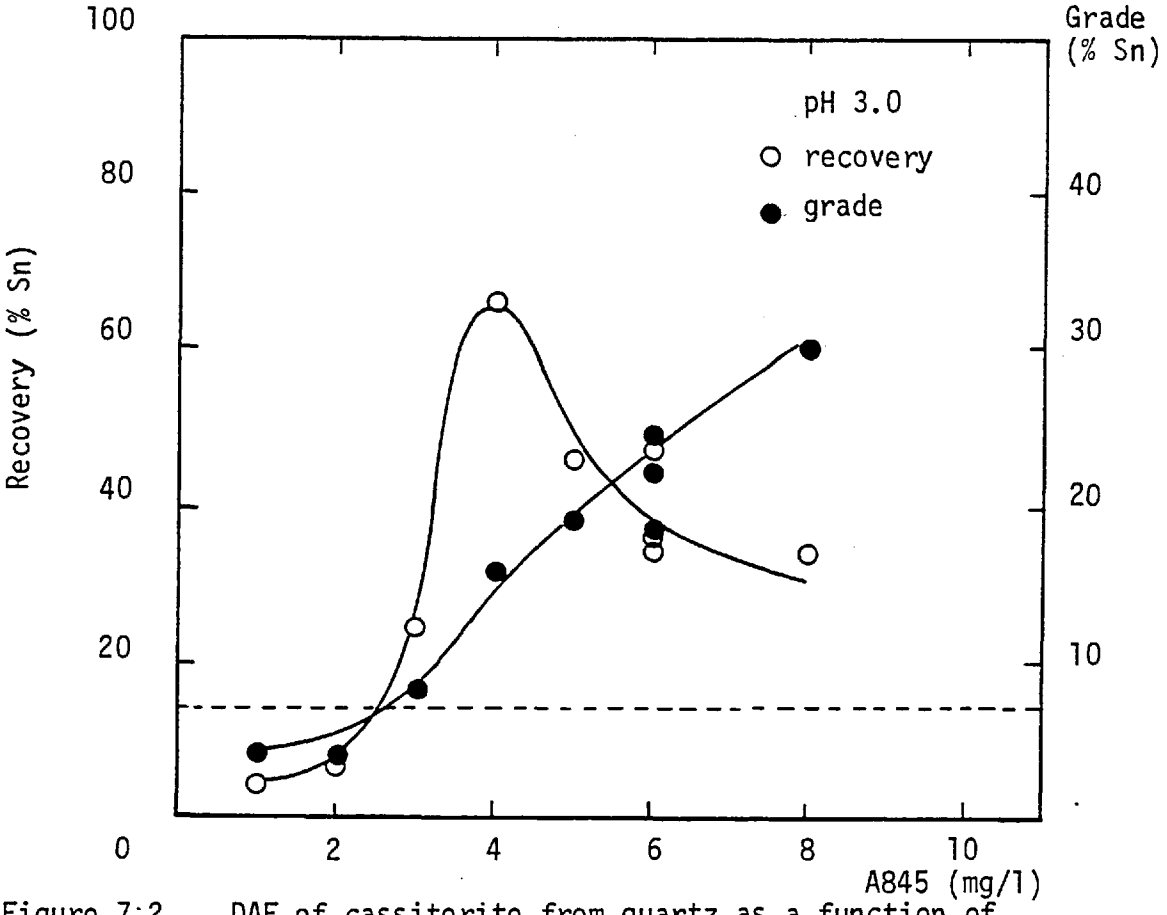

Figure 7.2. DAF of cassiterite from quartz as a function of Aeropromoter 845 concentration at pH 3.0

similar to those obtained previously for the DAF of single cassiterite in the presence of this collector (see Figure 6.20). Indeed, the collector concentrations corresponding to maximum tin recovery in the separation tests coincided almost exactly with those which gave maximum cassiterite recovery in the previous studies on the single mineral. At A845 concentrations above the optimum, the recovery of cassiterite from the mixed mineral suspensions decreased substantially, also in agreement with the DAF behaviour of the single mineral.

The concentrate grade increased with increases in the pH value and the collector concentration. The influence of pH probably arises from its effect on the charge of quartz particles, the negative charge increasing with pH value thus reducing the chances of collector adsorption or heterocoagulation with cassiterite particles and therefore resulting in a 'cleaner' concentrate. The concentrate grades obtained at high collector concentrations and at pH 4.0 are considered to be overestimates as some of the floated material was collected in the froth prior to flotation. This was possible because of the formation of a mineralized froth layer as air was entrapped into the suspension due to the high stirring rate applied during the conditioning stage. When the introduction of air was prevented by using better stirring conditions, the mineralized layer disappeared and the grade of the concentrate diminished. Nevertheless, the overall effect of pH and surfactant concentration was still observed (see Figure 7.6 and below).

The results of the tests carried out at a lower solids concentration (0.1% solids) indicated that both tin recovery and grade were lower than at 0.5% solids (Figure 7.1). Also, lower A845 concentrations were required to achieve optimum recovery. These results would suggest that the concentration of valuable fine particles is a variable to be optimi-

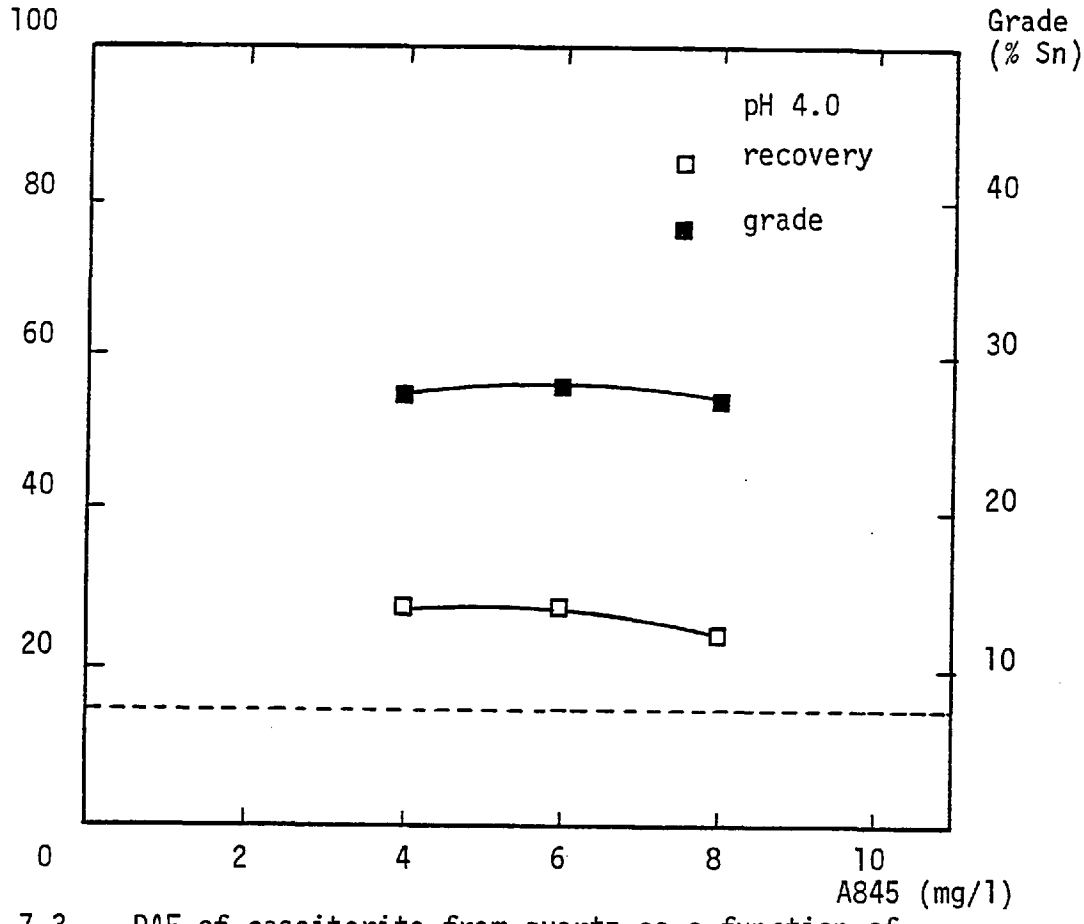

Figure 7.3. DAF of cassiterite from quartz as a function of Aeropromoter 845 concentration at pH 4.0

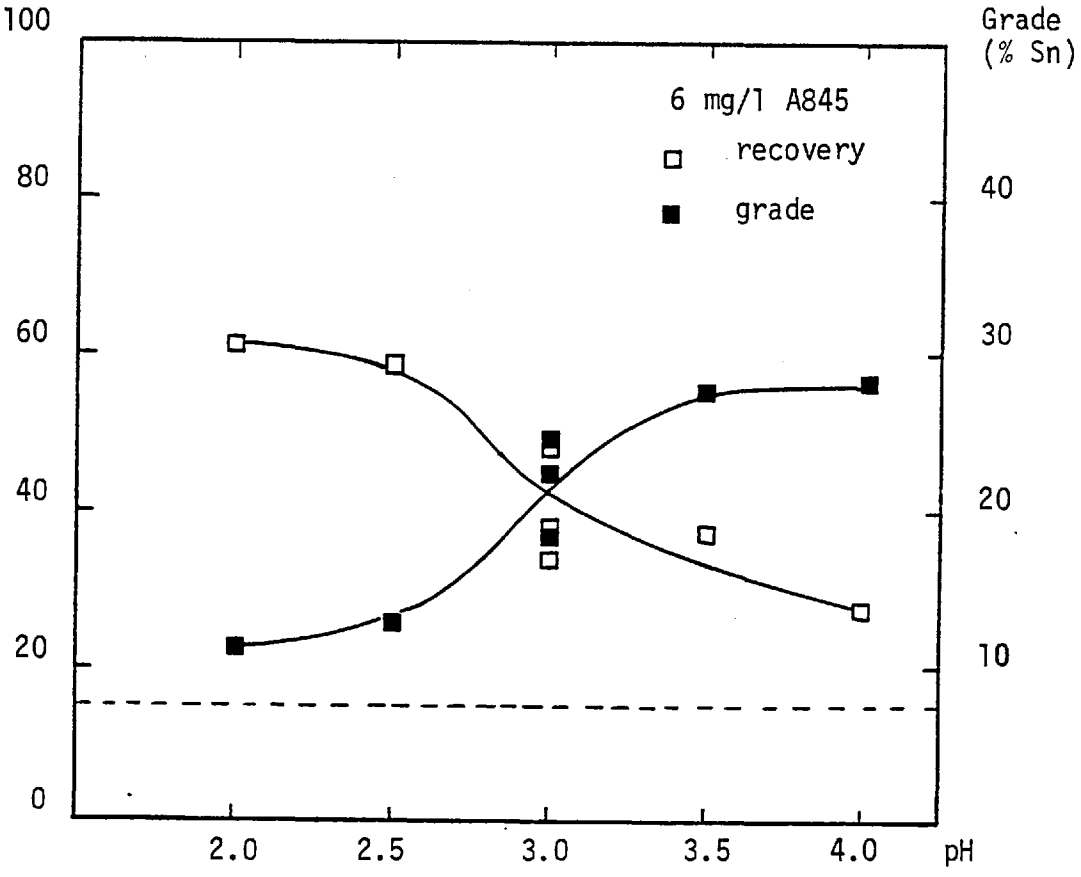

Figure 7.4. DAF of cassiterite from quartz as a function of pH in the presence of 6 mg/l Aeropromoter 845

zed in selective DAF operations.

Separation tests were carried out at pH 3.0 using sodium dodecyl sulphate as collector and the results are presented in Figure 7.5. The curves showing tin recovery and grade followed the same trend as reported for the sulphosuccinamate collector; maximum tin recovery occurring at the SDS concentration at which maximum DAF of cassiterite was observed previously (Figure 6.9). The values obtained for tin recovery and concentrate grade in the presence of SDS were equivalent to those obtained with the commercial collector and, therefore, further DAF studies on the separation of cassiterite were carried out using Aeropromoter 845 as collector.

During these tests it was noticed that a portion of the solids settled out and accumulated at the bottom of the cell without mixing with the microbubbles. Four baffles were therefore incorporated into the flotation cell with the purpose of improving the mixing conditions. The results of separation tests carried out in the baffled cell at pH 3.0 in the presence of the sulphosuccinamate collector are shown in Figure 7.6. No substantial change occurred compared with the results reported previously in Figure 7.2. However, no formation of mineralized froth occurred prior to flotation and therefore the results obtained in the baffled cell represented 'true' flotation by the DAF microbubbles. All subsequent separation tests were carried out in this baffled cell.

An important factor in the separation tests was the physical recovery of the floated product as it effectively imposed a constraint on the maximum concentrate grade. Extraction of floated material was by the vacuum suction method and a volume of about 50 - 100 ml was removed from the top of the cell. This constituted the 'floated product'. If the 4.5 g of quartz particles were fully dispersed the extracted volume

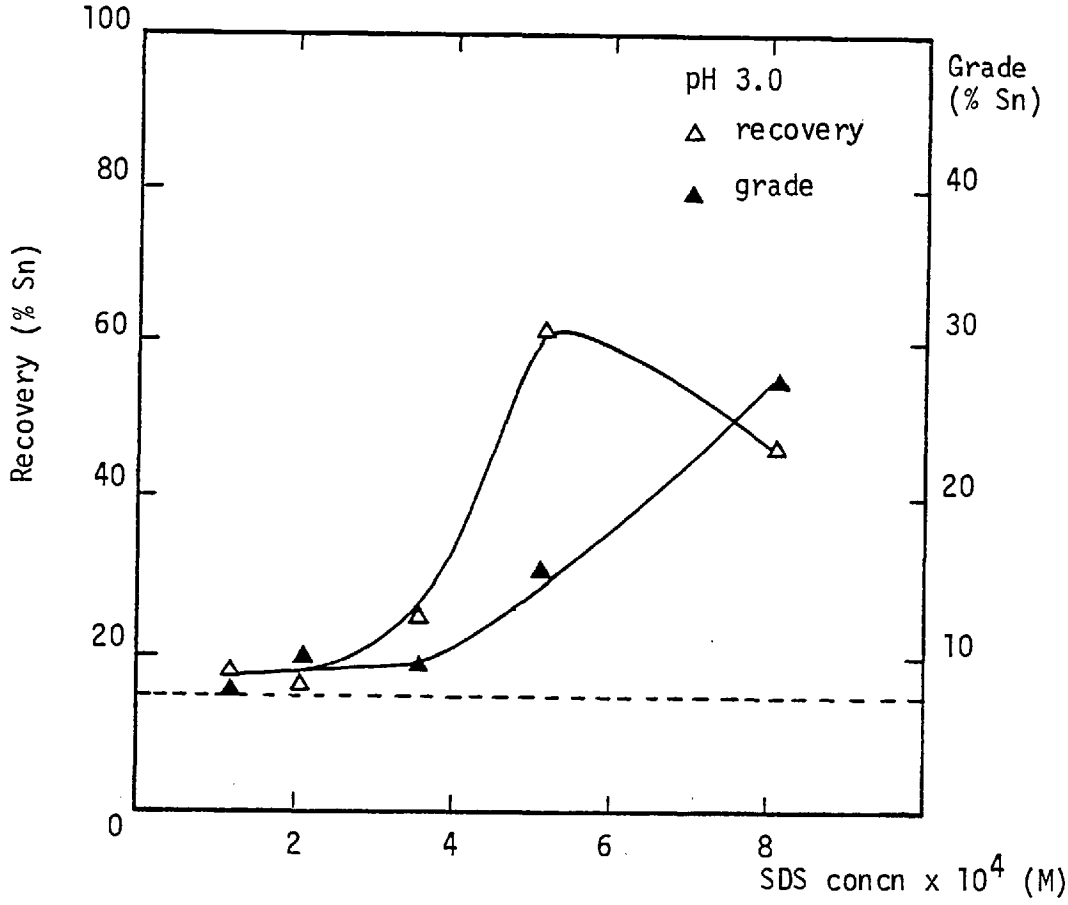

Figure 7.5. DAF of cassiterite from quartz as a function of sodium dodecylsulphate concentration at pH 3.0

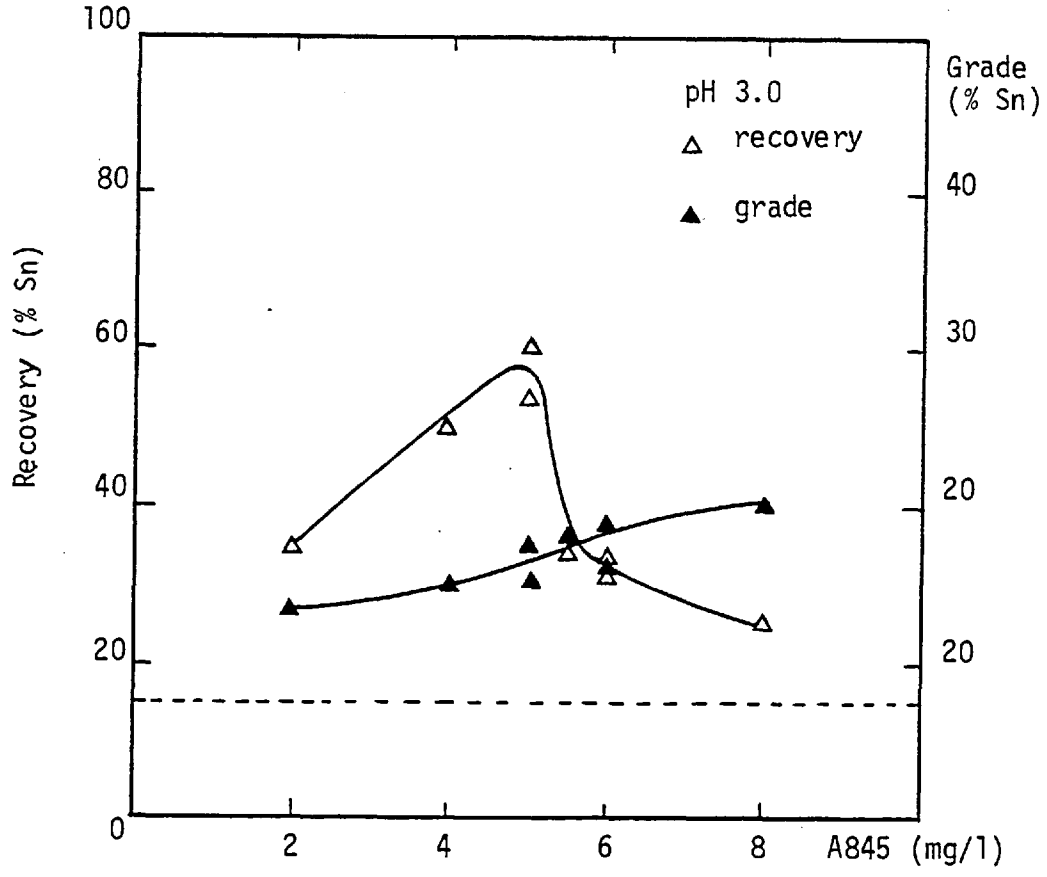

Figure 7.6. DAF of cassiterite from quartz in the baffled cell as a function of Aeropromoter 845 concentration at pH 3.0

would contain at least 200 - 300 mg of quartz, which, even if the whole 500 mg of cassiterite were recovered, would result in a maximum concentrate grade of 46 - 53% Sn. Hence, the recovery of the floated material was carried out attempting the removal of only the mineralized froth produced upon flotation and not a fixed volume of liquid. This method led, of course, to higher levels of variability in the results.

7.2. Separation studies in the presence of oil/collector emulsions

The studies on the separation of cassiterite from cassiterite/quartz mixtures were continued by testing the effect of the addition of a neutral oil on recovery and grade. The addition of oils in various forms has been claimed to improve the performance of the dispersed air flotation process in the fine particle range (31).

The oil used was laboratory grade kerosene supplied by BDH. The oil was added as an emulsion in the collector solution at various collector/oil ratios. The collector used was Aeropromoter 845. A separation test carried out at pH 3.0 in the presence of 100 mg/l kerosene and without the addition of A845 indicated that no flotation of cassiterite particles occurred when the oil was added in the absence of collector.

Figures 7.7 and 7.8 show the effect at pH 3.0 of varying simultaneously the addition of collector and oil at constant (1:4 and 1:8) collector/oil concentration ratios. The results indicated that in the presence of the 1:4 emulsion tin recovery increased slightly at A845 concentrations greater than 5 mg/l, and no improvement on concentrate grade was obtained over the tests in the absence of oil (Figure 7.6). However, when the concentration of oil was increased in the emulsion (1:8 collector/oil) a substantial increase in Sn recovery occurred (75 - 80%) over the range of collector concentrations tested (4 - 10 mg/l).

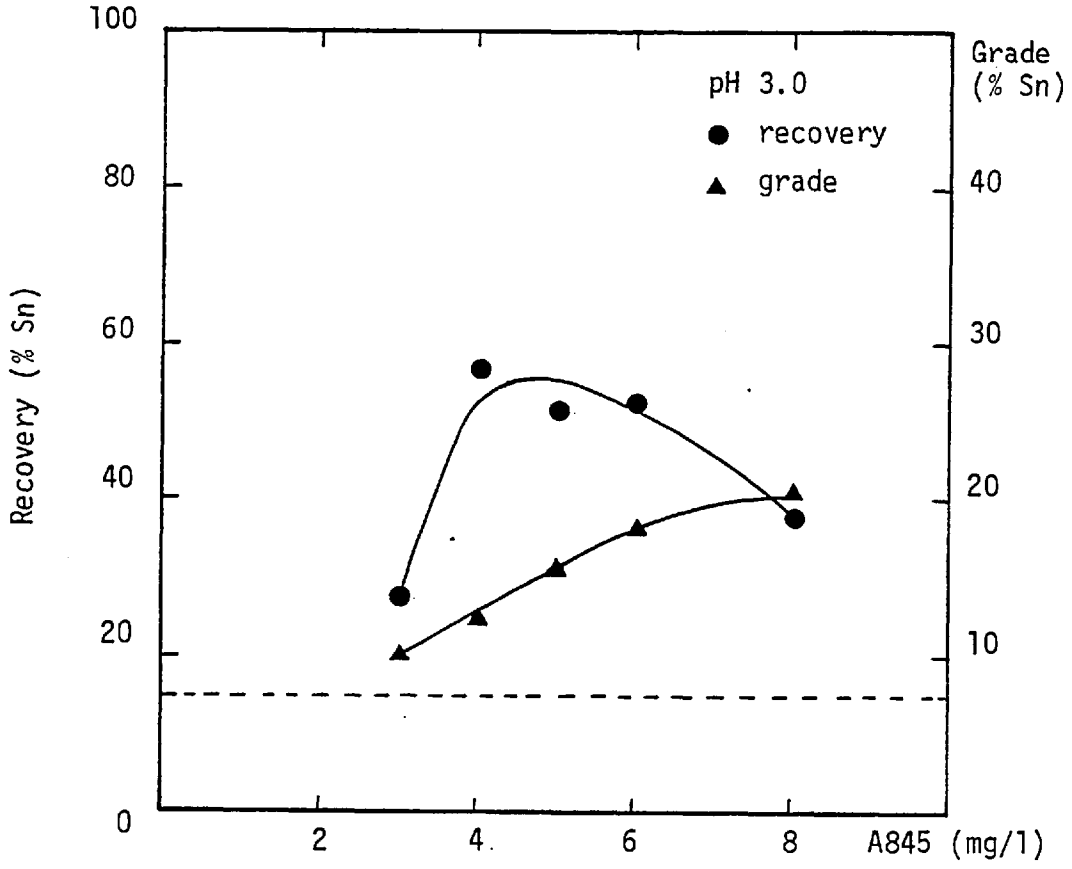

Figure 7.7. DAF of cassiterite from quartz in the presence of a 1:4 Aeropromoter 845/kerosene emulsion at pH 3.0

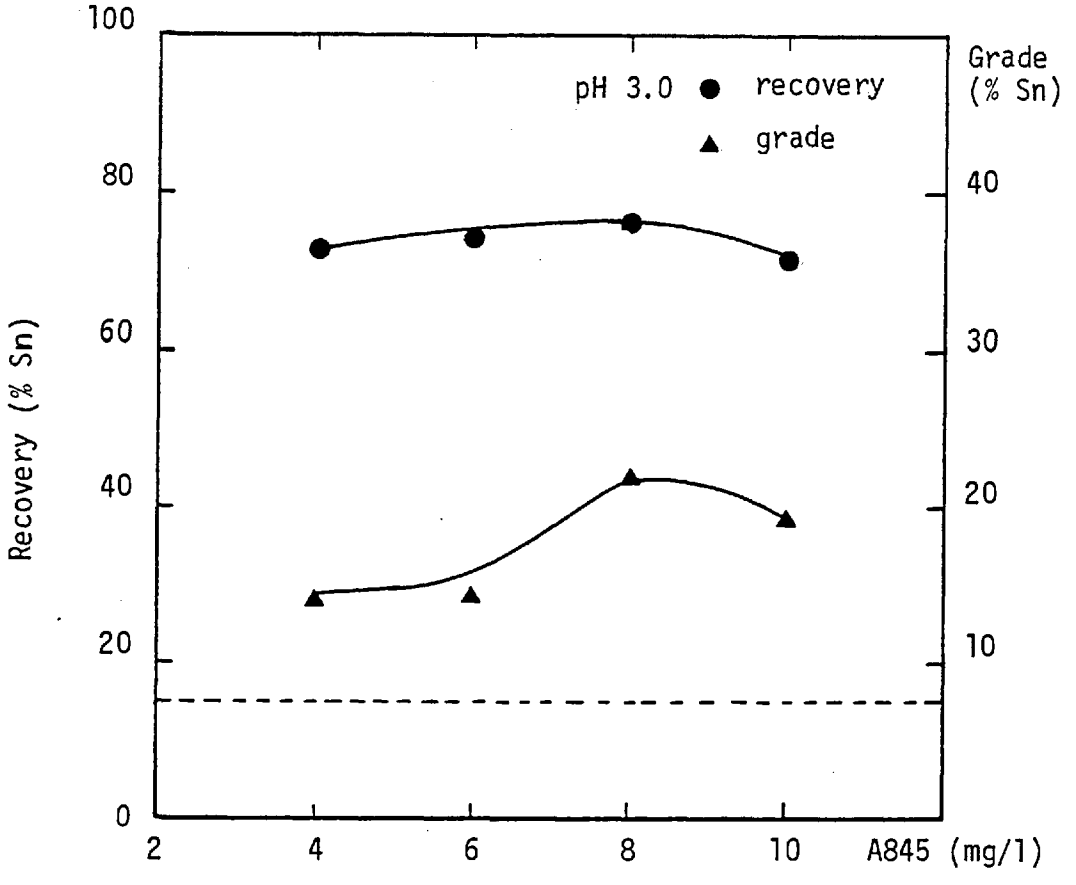

Figure 7.8. DAF of cassiterite from quartz in the presence of a 1:8 Aeropromoter 845/kerosene emulsion at pH 3.0

The concentrate grades obtained were marginally superior to those obtained with the 1:4 emulsion and in the absence of oil.

The addition of the oil resulted in the alteration of the physical characteristics of the cassiterite flocs. They became much bigger and more 'lumpy' aggregates which, unlike in the absence of kerosene, could be observed forming and rising through the suspension. The increase in floc size with oil concentration was also observed in tests carried out on cassiterite alone at pH 3.0 with 4 and 32 mg/l A845 and kerosene respectively (a 1:8 emulsion). When the collector concentration was increased to 8 mg/l (and 64 mg/l kerosene) the floc size increased but some degree of redispersion started to occur. A DAF test carried out on this latter suspension gave 85.1% recovery. In the absence of oil the suspension exhibited no light transmittance and a DAF recovery of about 50% at the same collector concentration (see Figures 6.17 and 6.20). Thus, it would appear that the influence of the oil was to increase the collector concentration domains of both coagulation and dissolved air flotation of cassiterite.

As kerosene had a beneficial effect on the separation of cassiterite by dissolved air flotation, the influence of the oil dosage in the emulsion was determined at constant collector concentrations. The effect of kerosene concentration on the separation of cassiterite is presented in Figure 7.9 for a constant A845 concentration of 4 mg/l. The curves show that tin recoveries increased with oil concentration up to 32 mg/l kerosene and thereafter remained constant with increasing oil dosage. Conversely, concentrate grades were constant up to 32 mg/l kerosene and then increased with oil concentration attaining a value of 36.6% Sn at 120 mg/l kerosene; this grade corresponded to an enrichment ratio of 5 for an oil emulsion in which collector and oil were in a

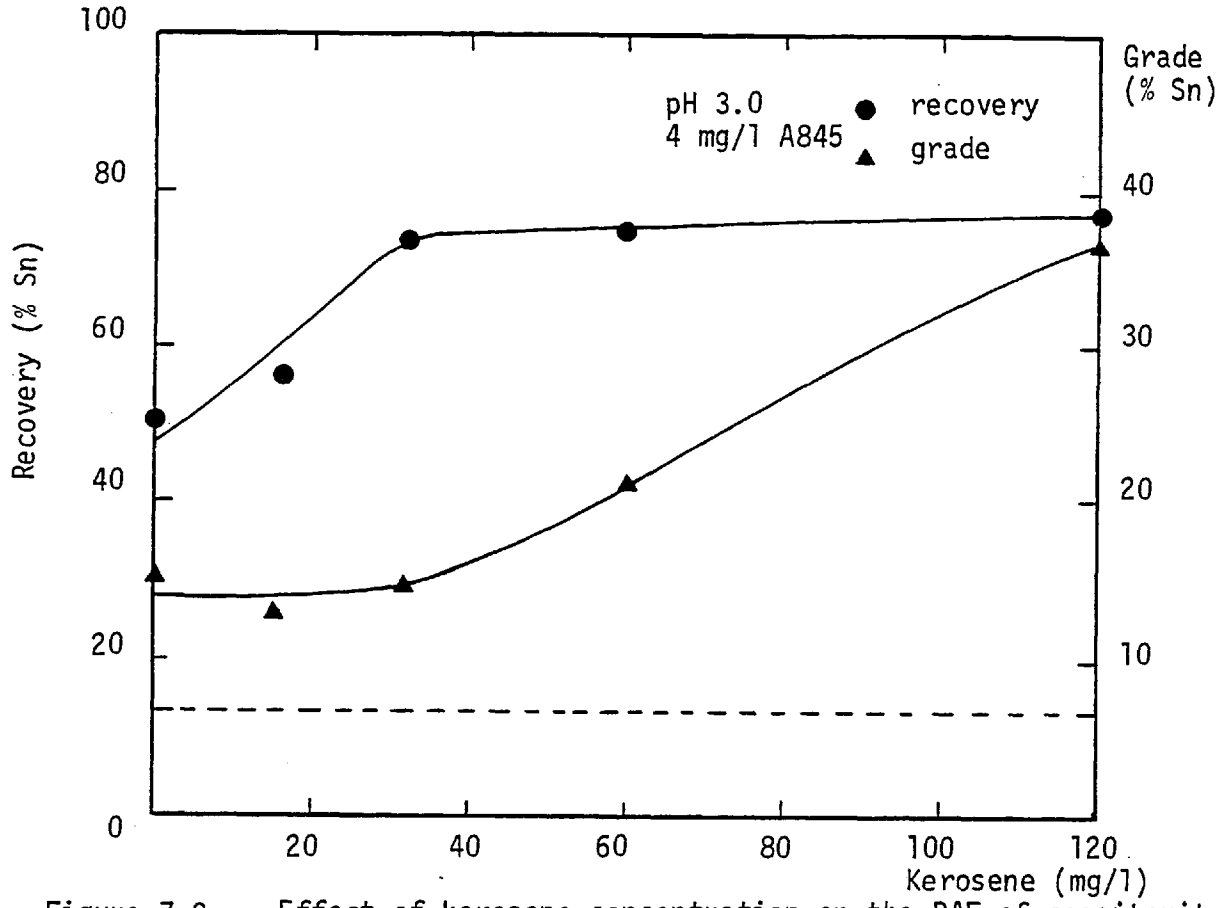

Figure 7.9. Effect of kerosene concentration on the DAF of cassiterite from quartz with a kerosene/A845 emulsion at 4 mg/l A845

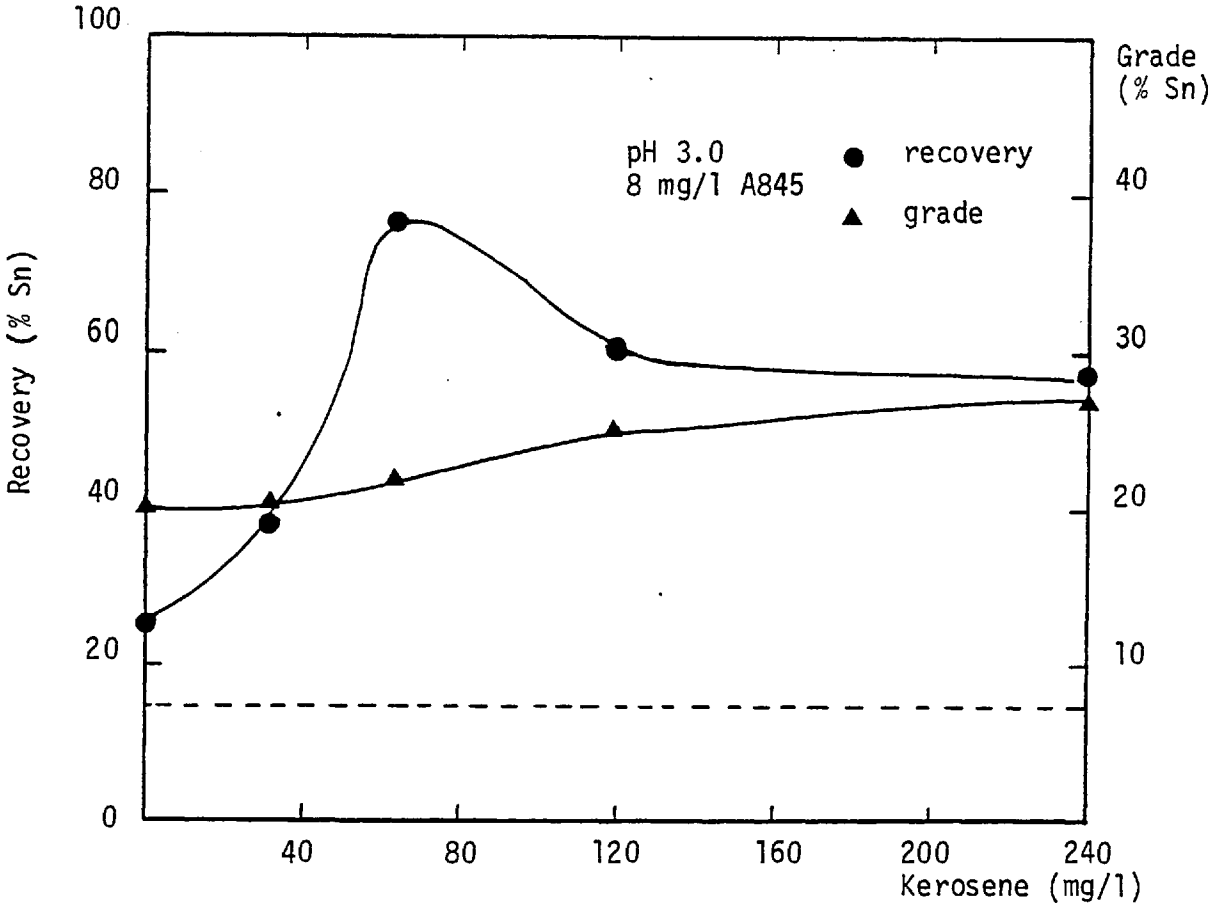

Figure 7.10. Effect of kerosene concentration on the DAF of cassiterite from quartz with a kerosene/A845 emulsion at 8 mg/l A845

concentration ratio of 1:30.

When the concentration of the sulphosuccinamate collector was raised to 8 mg/l A845, the effect of oil concentration was found to be somewhat different to that observed at the lower collector concentration. Hence, Figure 7.10 indicates that tin recovery increased up to 75% at about 60 mg/l kerosene and then decreased with increases in oil concentration, achieving a constant value (60%) in the range 120-240 mg/l kerosene. The grade of the floated product was only slightly influenced by the oil dosage, varying between 20% Sn in the absence of oil to 27% Sn at 240 mg/l kerosene.

Various interesting effects were noticed during these tests. At 4 mg/l A845, the increase in concentrate grade was partly associated with a better recovery of the floated product as this tended to agglomerate at the top of the cell. No similar effect was observed in the tests at 8 mg/l A845. The decrease in recovery observed at 8 mg/l collector concentration for oil additions in excess of 60 mg/l corresponded with the formation of large and dense aggregates too heavy to be floated by the DAF microbubbles. This decrease in recovery may have been partly caused by the lack of a persistent froth at high oil concentrations.

A series of separation tests were carried out to study the effect of pH in the presence of the emulsion. The tests were performed with a 1:8 collector/oil emulsion at a A845 concentration of 6 mg/l. The results showed (Figure 7.11) that the addition of the oil resulted in an overall increase in cassiterite recovery within the pH range 2 - 4 compared with the results in the presence only of the sulphosuccinamate (Figure 7.4). Following the trend established in the DAF studies of cassiterite, recoveries were higher at the more acid pH values and tended to decrease as the pH approached the iep of cassiterite. The effect of

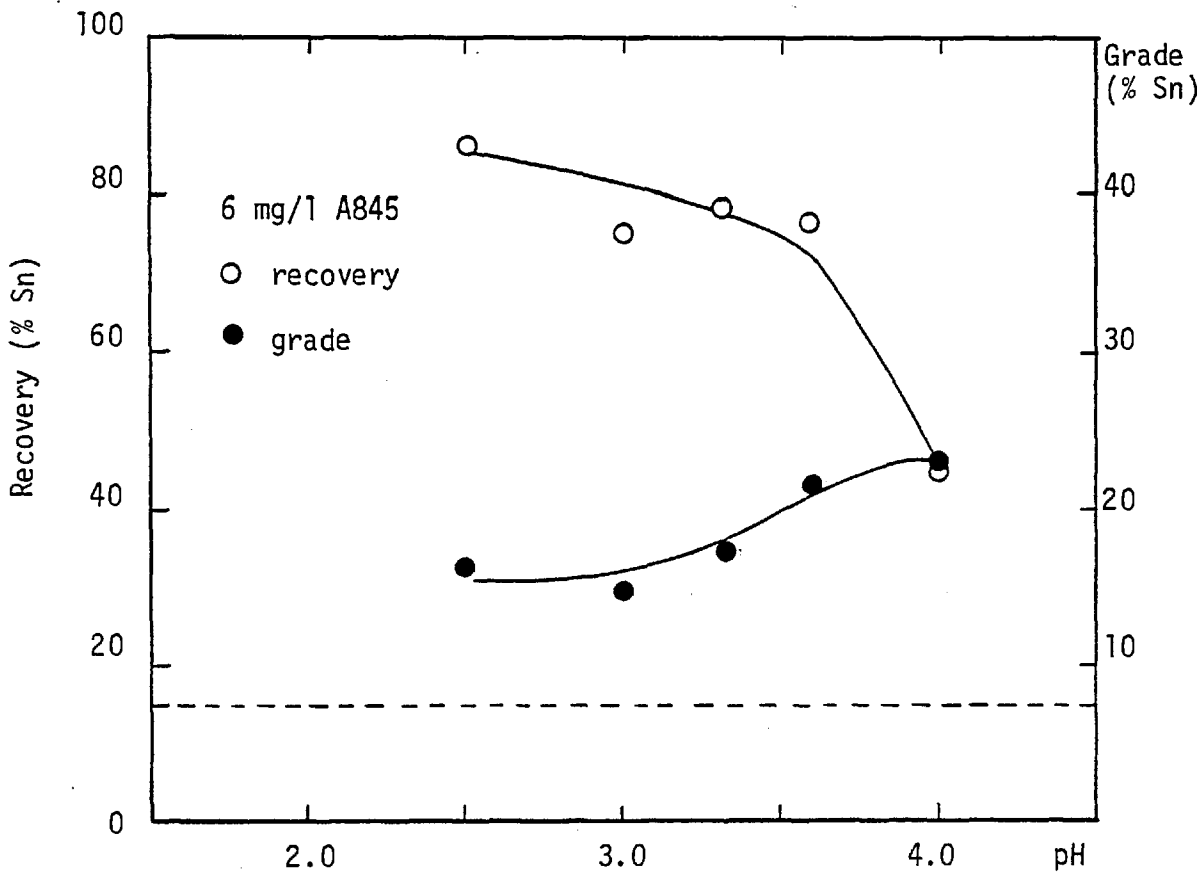

Figure 7.11. DAF of cassiterite from quartz as a function of pH in the presence of a 1:8 A845/kerosene emulsion

pH on concentrate grade in the presence of the emulsion was much less marked than on recovery, a slight increase of only 2% Sn being recorded over the whole range of pH values tested. It would seem, therefore, that the influence of the oil was to increase the effective pH range over which good tin recoveries could be obtained by DAF, this resulting in improved selectivity of the separation as concentrate grades became higher with increasing pH value.

A recent survey of the literature (35) indicated that the role of the neutral oil in emulsion flotation is a subject of controversy. However, these results were generally consistent with the 'sweeping-penetration' model of Mackenzie (243) for the interaction between oil drops and mineral particles. Thus, the results of the separation studies in the presence of the emulsion indicated that (a) the oil exerted only a supplementary action to that of the collector, and (b) the influence of the neutral oil was primarily determined by the collector concentration.

7.3. Influence of various parameters on the separation studies

7.3.1. Effect of the addition of a modifier

Studies on the separation of cassiterite by DAF were carried out in the presence of a modifier for quartz. Fluoride has long been used in mineral separations involving quartz and although its role in those separations is not clear (220), it has been shown to adsorb on quartz below pH 4.5 (244). Therefore, separation experiments were conducted at pH 3.0 in the presence of sodium fluoride to see whether it had any influence on the selectivity of the DAF separations.

The experiments were carried out with Aeropromoter 845 in the absence and presence of kerosene. The sodium fluoride used (NaF) was 'Analar' BDH and was added to the suspensions before the collector.

The results are shown in Figure 7.12 for 5 mg/l A845 and in Figure 7.13 for 4 mg/l A845 and a 1:8 emulsion.

The curves show that the general effect of the concentration of sodium fluoride was to increase the grade of the floated product but at the expense of the tin recovery. The curves also show that these effects were more drastic in the absence of the oil. Hence, the concentrate grade increased only to about 20% Sn with 4 mg/l NaF ($\simeq 10^{-4}$ M) with a decrease in recovery to 43% whereas in the presence of kerosene a similar decrease in Sn recovery was only produced with the addition of 40 mg/l NaF ($\simeq 10^{-3}$ M) but the concentrate grade was nearly 30% Sn.

The addition of fluoride, therefore, depressed the recovery of both minerals but cassiterite was floated preferentially over quartz. The mechanism by which cassiterite flotation is depressed in the presence of the modifier is not clear but, given the positive mineral charge and the relative concentrations of fluoride (10^{-4} - 10^{-3} M) and sulpho-succinamate ($\simeq 2 \times 10^{-6}$ M), competition for the cassiterite surface sites could be a possibility. Since the presence of the oil was shown to make cassiterite more resistant to the depressing action of fluoride, some tests were conducted with higher oil concentrations in the emulsion. The results of those tests are shown in Table 7.1 together with the data previously obtained in the absence of sodium fluoride. Also shown is a test carried out at a higher collector concentration (8 mg/l).

The data presented in Table 7.1 show very clearly that an increase in the oil concentration can counterbalance the depressing effect of fluoride on cassiterite recovery yielding at the same time a concentrate of high tin grade. It may also be noted that an increase in the collector concentration at roughly constant oil concentration in the emulsion resulted in an increased grade ($\simeq$ 42% Sn) with only a small loss

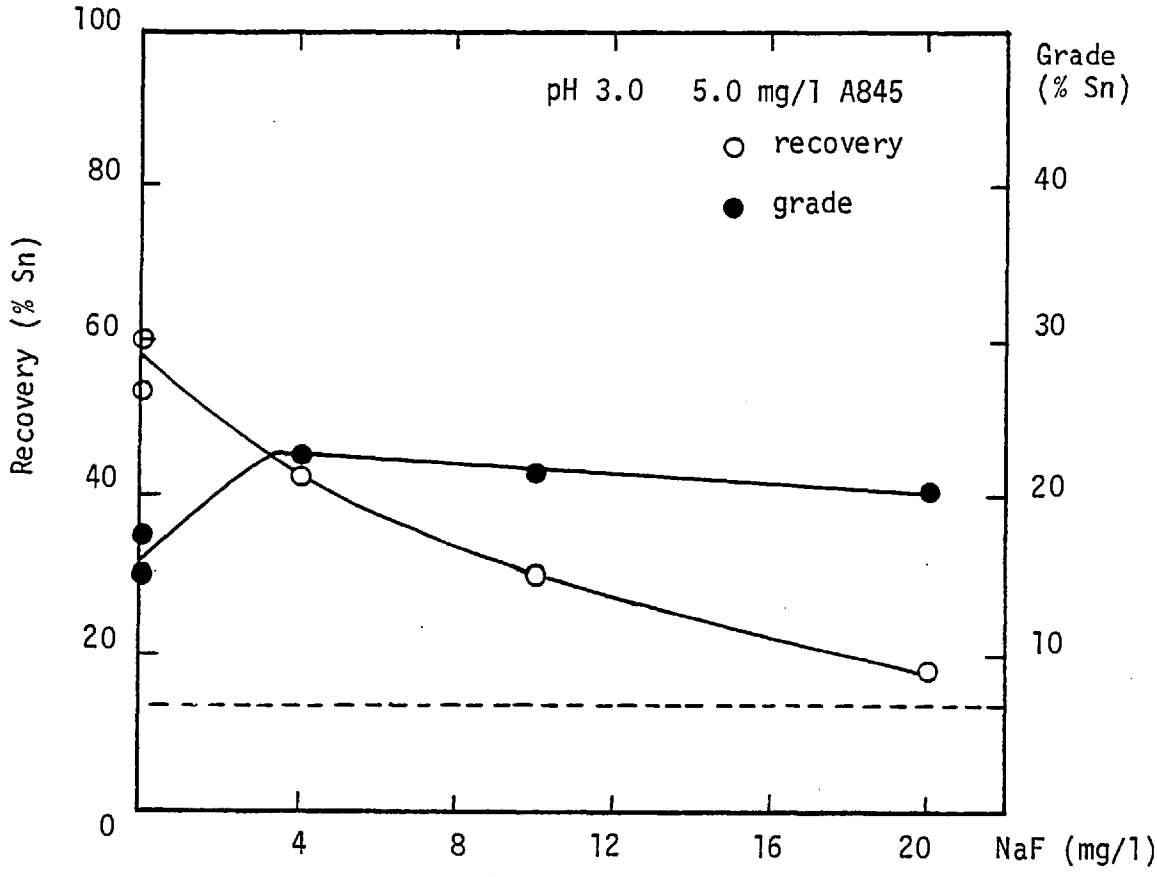

Figure 7.12. DAF of cassiterite from quartz in the presence of Aeropromoter 845 as a function of sodium fluoride concentration

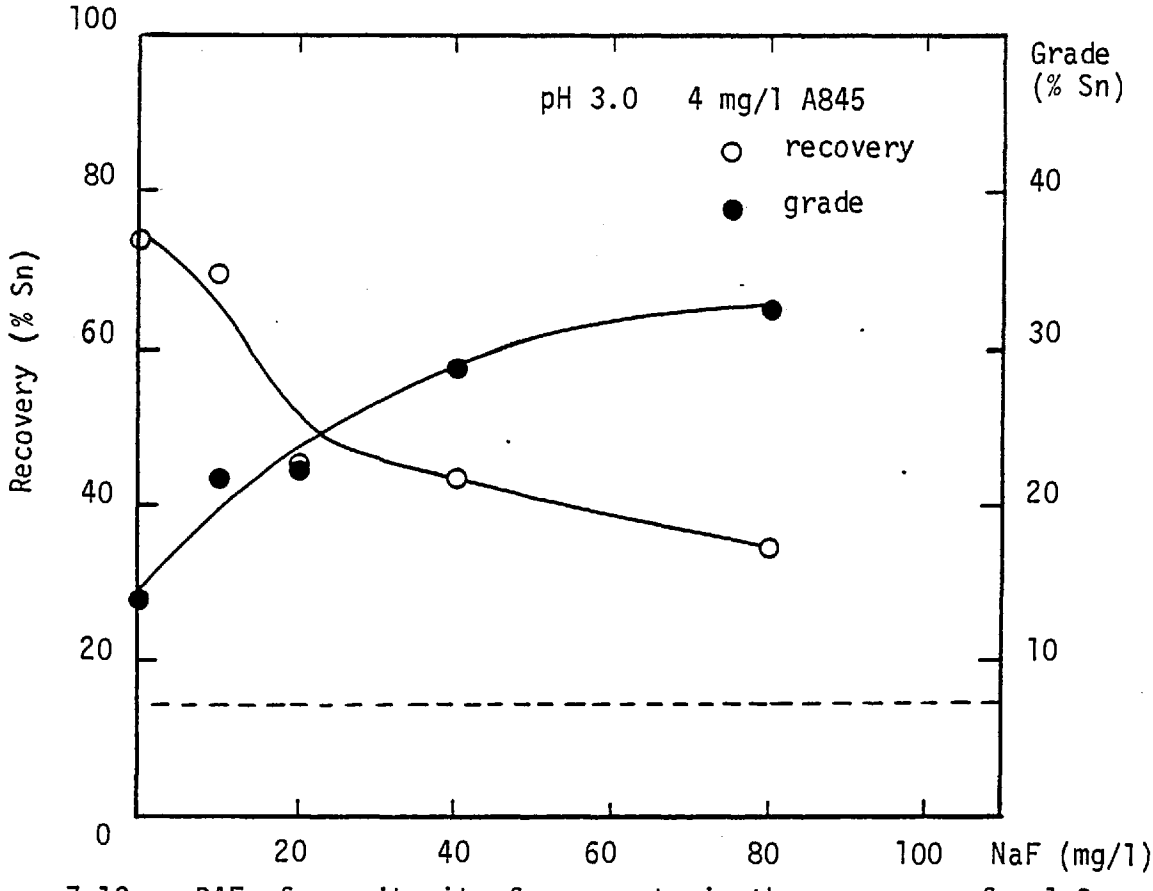

Figure 7.13. DAF of cassiterite from quartz in the presence of a 1:8 A845/kerosene emulsion as a function of sodium fluoride concentration

in tin recovery. A comparison with the concentrate grades obtained in the absence of sodium fluoride demonstrates the role of the modifier in boosting selectivity.

Table 7.1. Effect of sodium fluoride on the separation of cassiterite by DAF at pH 3.0 with various kerosene/A845 emulsions

	Without NaF		With 40 mg/l NaF	
Emulsions	Recovery (% Sn)	Grade (% Sn)	Recovery (% Sn)	Grade (% Sn)
4.0 mg/l A845 plus				
. 32 mg/l kerosene	73.5	14.2	43.9	29.2
. 60 mg/l kerosene	74.7	21.8	71.0	31.7
8.0 mg/l A845 plus				
64 mg/l kerosene	77.2	22.0	65.6	41.7

The mechanism by which fluoride depresses quartz flotation is not at all clear. However, any physically adsorbed sulphosuccinamate ions would be readily displaced by fluoride ions (due to their higher affinity for the quartz surface) and consequently higher concentrate grades would be obtained if quartz flotation was occurring via adsorption of A845. A decrease in the heterocoagulation of the particles due to fluoride (and SiF_6^{-2}) ions increasing the negative Stern potential of the quartz is another possibility.

7.3.2. Effect of rate of stirring during microbubble injection

It has already been mentioned in section 7.1 that mixing conditions in the flotation cell are a critical factor in dissolved air flotation.

A test was therefore conducted to evaluate the influence of the rate of stirring during the stage of microbubble injection on the separation of cassiterite by DAF.

The test was carried out at a stirring rate of 150 rpm (the same used in the slow stirring conditioning stage) at pH 3.0 and in the presence of 4 mg/l A845 and 32 mg/l kerosene. The results obtained are presented in Table 7.2 together with those obtained at 50 rpm (the stirring rate used throughout these tests).

Table 7.2. Effect of stirring rate during microbubble injection on the separation of cassiterite by DAF

Stirring rate (rpm)	Concentrate (mg)	Sn in Conc. (mg)	Recovery (% Sn)	Grade (% Sn)
50	1912.5	271.29	73.5	14.2
150	884.7	261.21	70.8	29.5

The results indicated that the higher rate of stirring doubled the concentrate grade while keeping the tin recovery high, thus confirming that stirring is a variable which must be optimized in selective DAF. The result obtained was equivalent to having increased the oil concentration 3 times and showed a better selectivity than the use of 40 mg/l sodium fluoride.

A higher rate of stirring during microbubble flotation would result in (a) higher probability of bubble-particle collisions and subsequent attachment, (b) higher shear rates imposed on microbubble-floc aggregates, and (c) higher rate of detachment of the floated material from the froth. Of these, factors (b) and (c) seem the most likely to be responsible for

an increased grade in the floated product since the higher stirring rate would have probably exerted a 'cleaning' action upon both the froth and the flocs. Thus, it could be assumed that the approximately 1 g of quartz particles which did not 'float' at 150 rpm are associated with 'carry-over', froth entrainment and similar non-selective 'flotation' mechanisms.

7.3.3. Effect of a cleaner DAF stage

The studies reported in this Chapter have demonstrated that cassiterite separations of the order of 75 - 80% may be obtained by dissolved air flotation operations performed on a single stage basis. However, it is envisaged that the selective recovery of a mineral by this method would involve the introduction of additional dissolved air flotation stages. The influence of the introduction of a second DAF stage was therefore studied to determine possible effects on concentrate grade and tin recovery.

The second (cleaner) DAF test was carried out by redispersing and refloating the concentrate obtained from a previous test. The experimental conditions were as follows:

- Rougher (1st) stage : pH 3.0; emulsion containing 6 mg/l A845 + 48 mg/l kerosene; 20 mg/l NaF; usual experimental procedure.
- Cleaner (2nd) stage : dispersion of rougher concentrate in 1 l water for 4 min at 100 rpm; pH ≃ 4.0 - 5.0 (no addition of acid); no addition of collector.

The results of using a cleaner stage are shown in Table 7.3.

Table 7.3. Effect of a cleaner stage on the separation of cassiterite by DAF

Stage	Concentrate (mg)	Sn in Conc. (mg)	Recovery (% Sn)	Grade (% Sn)
Rougher	1884.6	275.7	74.7	14.6
Cleaner	403.0	237.1	64.2	58.8

Hence, the addition of a cleaner stage permits the production of a final concentrate with nearly 60% tin at a recovery of 64% Sn. This represents an overall enrichment ratio of 8. It was very interesting to note that the strong and highly hydrophobic aggregates formed in the rougher stage did not require a further addition of collector to induce strong microbubble attachment. In fact, the recovery of the single cleaner stage may be estimated to be of the order of at least 86%. These observations would suggest that perhaps only a gentle washing or dilution of the rougher concentrate would result in a substantial increase in concentrate grade.

7.3.4. Effect of higher solids concentration

It was established in previous tests (section 7.1) that the separation of cassiterite by DAF was less efficient at low solids concentration than at the 0.5% at which these studies have been conducted. The effect of a higher concentration of solids on the separation of the minerals was studied using a suspension of 2.5% solids. The feed grade of these suspensions was lowered to 1.48% Sn to keep the concentration of cassiterite particles in the suspension constant (0.5 g cassiterite/24.5 g quartz).

The results of tests carried out at pH 3.0 in the presence of

emulsions containing 4 mg/l A845 and varying amounts of kerosene indicated that the separation of cassiterite by dissolved air flotation was greatly hindered at this higher concentration of solids. Modifications in the experimental procedure were made by varying the amount of air introduced to the system, and using higher collector concentrations (Table 7.4). The tests were all carried out at pH 3.0 and in the presence of 40 mg/l sodium fluoride.

Table 7.4. Effect of 2.5% solids concentration on the separation of cassiterite by DAF for various conditions of microbubble injection

Emulsion	Gauge sat. Pressure (psig)	Volume SSW* Injected (ml)	Recovery (% Sn)	Grade (% Sn)
6 mg/l A845+98 mg/l K*	40	100	4.9	3.8
" +48 "	80	100	18.6	10.1
8 mg/l A845+64 mg/l K	40	100	20.2	12.0
" + "	40	200	14.2	9.1
" + "	80	100	38.5	13.2

* K = kerosene; SSW = supersaturated water

It can be seen that although a higher saturation pressure did increase the recovery of tin it failed to equal the efficiency obtained at 0.5% solids. The selectivity of the operation was however quite high as enrichment ratios of the order of 6 and over were attained. As the introduction of more air bubbles through a larger volume of supersaturated water did not have a substantial effect on the parameters of

the operation, it is thought that part of the improvement in using 80 psig saturation pressure must come from the correspondingly higher injection pressure used (80 psig). Indeed, a higher injection pressure resulted in a greater level of mixing at the bottom of the flotation cell where large amounts of solids settled out in a compact layer. This sedimented layer was not easily dispersed as tests on the effect of stirring rate during microbubble injection showed no improvement on tin recovery.

The data shown in Table 7.4 indicate that an increase in collector concentration favoured the selective separation of cassiterite by DAF. The effect of collector concentration in a 1:8 emulsion is shown in Figure 7.14; the tests were conducted at 80 psig gauge saturation pressure with 100 ml injections of supersaturated water.

The figure shows that optimum recovery was obtained at 8 mg/l A845 but the optimum grade occurred at a higher concentration (10 mg/l). The selectivity obtained was good considering that it was obtained in a single stage DAF operation; the levels of recovery, however, were not acceptable. It is worthwhile noting that the range of collector concentrations over which cassiterite separation by dissolved air flotation occurred did not increase substantially over that found in the DAF studies at a lower solids concentration (Figure 7.7).

An optimization of the separation of cassiterite by DAF at 2.5% solids was not pursued further but these studies make it possible to predict that areas where improvement of the results may occur are:

i) increases in the oil concentration in the emulsion in the range of collector concentrations between 6 - 10 mg/l A845

ii) increases in the stirring rate during the slow conditioning and microbubble injection stages

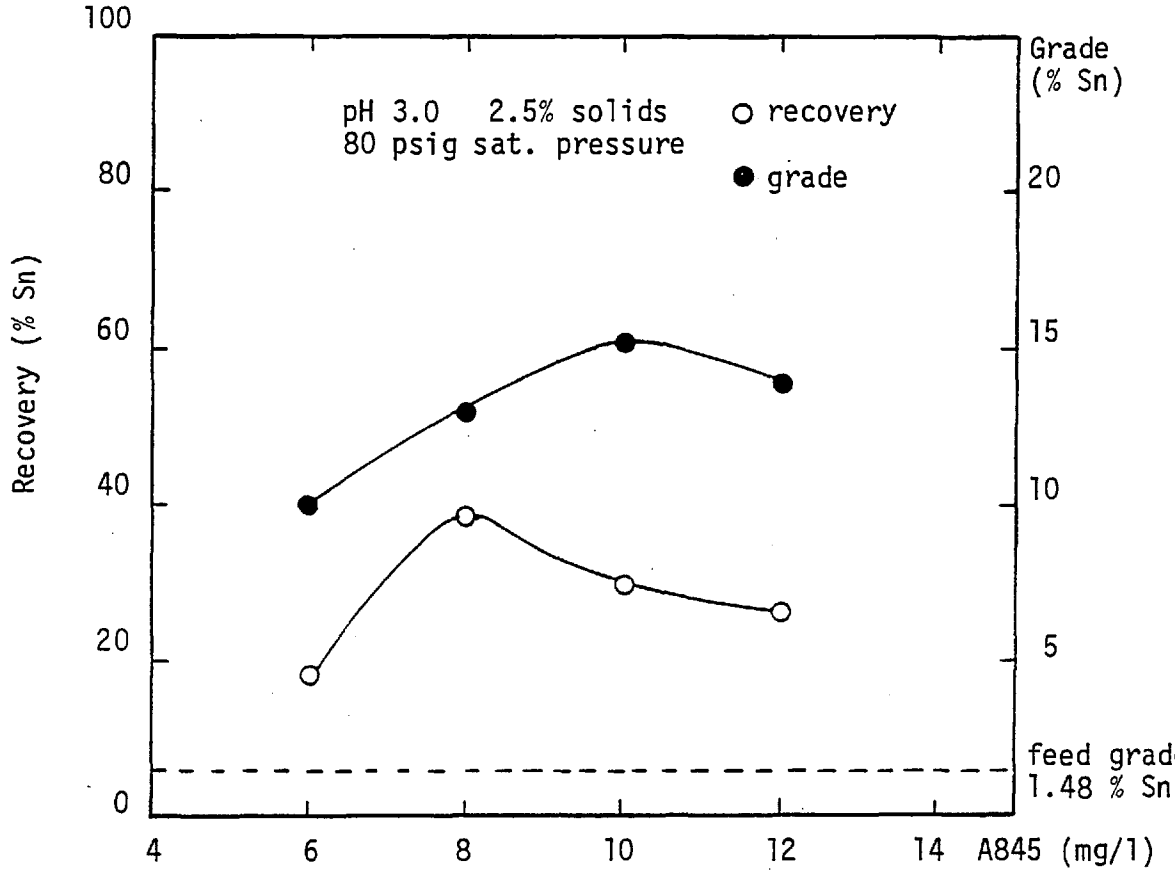

Figure 7.14. DAF of cassiterite from quartz at 2.5% solids in the presence of a 1:8 A845/kerosene emulsion

iii) optimum dosage of sodium fluoride.

Nevertheless, it is thought that the limiting capacity for efficient use of the flotation cell was being attained at 2.5% solids and therefore that further improvements should be brought about through the modification of parameters such as cell design and experimental procedures.

7.4. Discussion

The results of the studies carried out on the separation of cassiterite from cassiterite/quartz mixtures by dissolved air flotation suggest that this process can be successfully used to selectively separate fine mineral particles from suspension. Thus, for a 0.5% solids suspension containing 7.38% Sn, concentrates of about 37% Sn grade could be obtained at a 75% Sn recovery in a single-stage DAF test. If a second DAF stage was used, the concentrate grade increases to about 60% Sn for an overall recovery of around 70%. These results correspond to enrichment ratios of 5 and 8.1 respectively; the maximum attainable enrichment ratio in these cases was 10.6 (as cassiterite has 78.76% Sn). Higher tin enrichment ratios of about 10 were recorded in tests carried out at higher solids concentration (2.5%) and lower feed grades (1.48% Sn) but the recovery of tin was decreased to about 40% under these conditions.

The recoveries obtained in the DAF separation studies are even higher if it is considered that the maximum recovery of cassiterite alone by DAF at pH 3.0 was only about 85% (Figure 6.20). Therefore, the 75% recoveries obtained in the DAF separation studies amount in real terms to about 85% since not all cassiterite particles could be floated (this phenomenon is reported in Chapter 8).

The recovery of fine cassiterite particles by dissolved air flotation compares quite well with other methods reported in the literature.

Claus et al (189) carried out selective flocculation tests on synthetic and natural cassiterite samples mixed with quartz using a modified polyacrylamide flocculant. They used 1% solids suspensions containing 26.3% Sn and obtained very good grades (71% Sn) but low recoveries for the synthetic SnO_2 sample (usually about 45%). With the cassiterite mineral for suspensions of 15% solids, the flocculated material exhibited a grade of 16.5% Sn (a tin enrichment of 20) but at a tin recovery of only 11%.

On the other hand, Zambrana et al (245) conducted liquid-liquid extraction tests on a finely-ground tin ore (1.5% Sn). These tests were performed using oil drops (gasoline) to float a pulp (2% solids) previously conditioned with a collector (Aerosol 22, a sulphosuccinamate collector equivalent to the Aeropromoter 845 used in this work). These authors obtained rougher concentrates analysing 4.5% Sn for a tin recovery of about 80%. These results represented a tin enrichment of 3. A single cleaning stage brought the tin enrichment to about 6 and a second cleaning stage increased it to 9 (13.5% Sn), the tin recoveries however exhibited dropped to 75 and 58% respectively.

The most important variables found in these DAF separation studies were pH value and the dosage of the various reagents used. This is a direct consequence of the more general conclusion that the recovery and selectivity of the separations was basically determined by the surface properties of the mineral components in suspension. Thus, like in dispersed air flotation, without a close control of the surface chemistry of the suspended minerals no selective separations by dissolved air flotation are feasible. Therefore, it is proposed that previous attempts to selectively use DAF to separate minerals (80)(116) have failed because of the insufficient study of surface chemical factors.

Furthermore, these results (together with those in Chapter 6) have also shown that the separation behaviour of the valuable fine particles can be studied and predicted very accurately from basic surface chemistry and DAF studies on the single mineral.

The recovery of fine cassiterite particles by selective dissolved air flotation was essentially a function of the same variables obtained in the DAF tests on the single mineral. Hence, the hydrophobicity of the cassiterite particles and their degree of aggregation in suspension proved to be the most important parameters influencing tin recovery in the selective DAF tests. This was also shown by the improvement in recovery produced upon the addition of a neutral oil, since this resulted in increased hydrophobicity and aggregation of the cassiterite slimes.

The selectivity of the dissolved air flotation process, on the other hand, appeared to be related to the respective surface properties of the suspended particles and to parameters of the DAF operation. Thus the evidence supplied by studies on the separation of cassiterite from quartz suspensions indicated that the following factors may have exerted a detrimental action on the selectivity of the separations:

i) Collector adsorption on quartz particles. The fact that the sulphosuccinamate ions adsorbed on quartz was shown by the slight increase in flotation of quartz particles near the iep of the mineral in the presence of this collector.

ii) Heterocoagulation of the quartz and cassiterite particles. This factor was observed to occur under conditions of electrostatic attraction between both kinds of particles. This factor may also be expected to occur when the cassiterite particles are negatively charged (due to superequivalent collector adsorption) as the potential energy of interaction is determined by the particles

with the lower Stern potential (246) and at pH 3.0 quartz would exhibit the lower (negative) Stern potential value.

iii) Stirring conditions in the DAF cell. It was shown that when flotation occurred under quiescent conditions the mechanical entrapment of quartz particles into the floated product was favoured. A higher rate of stirring during the injection of the microbubbles resulted in a higher concentrated grade probably through the detachment of entrained quartz particles from the froth.

iv) The recovery of the floated product. This parameter is important insofar as the grade of the concentrate is a measure of the selectivity with which a DAF separation is carried out. The method of recovery of the floated product was found to have the concentrate grade under these experimental conditions and its influence should be expected to be greater the higher the concentration of solids.

The physical characteristics of the flocs are also important in selective DAF given the influence of the stirring rate on the selectivity of the process. The possibility of adding small amounts of non-polar oils is therefore of interest as the oil would strengthen the bonding between hydrophobic particles producing a floc of much higher resistance to hydrodynamic shear.

Other factors that should be taken into account in future selective DAF operations involve the modification of design variables. In particular, a modified batch dissolved air flotation cell should provide better microbubble-particle contact near the point of microbubble injection; cell designs which have solved this problem may be found in the literature (89).

But the factor that would contribute most to boosting both recovery and selectivity in DAF, would be the use of a highly specific collector for the particular mineral to be recovered. This collector would have to fulfil a further requisite in that it must be capable of inducing the destabilization of the valuable mineral particles. Thus, in the case of cassiterite, it is considered that the use of a, say, phosphonic acid collector would result in more selective separations than those obtained with the sulphosuccinamate collector.

The results of these studies indicated that while the recovered cassiterite particles were very fine (75% below 10 μm) and were separated from suspensions which would have been normally discarded in a conventional floation plant, they were not floated as 'fine' particles but as aggregates of larger size. The size of these aggregates is crucial in selective DAF operations. They cannot be too large as the microbubbles would not be able to float them. On the other hand, dispersed particles would require an enormous amount of air which would be difficult to provide economically. It is interesting to note that in the recovery of cassiterite particles by oil drops (245) the formation of aggregates has also been found to be beneficial. Whether the larger bubbles produced in dispersed air flotation machines would perform better under the experimental conditions used in this work is a question that remains to be answered.

These studies have indicated the technical feasibility of separating finely-divided minerals in suspension by the dissolved air flotation process. The results have shown that the process compares well in terms of recovery and selectivity with other processes claimed to recover very fine cassiterite particles. These studies have also pointed out the areas where the performance of selective DAF operations may be

expected to improve. The testing of the DAF process for the separation of valuable minerals from finely-divided ores would therefore be recommended, to assess the full capability of the process in a mineral processing context.

Chapter 8. OTHER ASPECTS OF DISSOLVED AIR FLOTATION OF MINERAL PARTICLES

8. OTHER ASPECTS OF DISSOLVED AIR FLOTATION OF MINERAL PARTICLES

8.1. Introduction

The experimental work reported in this chapter concerns (a) the influence of several parameters on the recovery of minerals by dissolved air flotation, and (b) the flotation of mineral particles through bubbles nucleating from supersaturated solution. Experiments dealing with part (a) are reported in section 8.2 together with a brief summary of results obtained throughout this work on froth stability in DAF. The results shown in section 8.2 were obtained in systems generally under constant surface chemical conditions which ensured the floatability of the dispersed phase. The tests were carried out on cassiterite or quartz suspensions. In section 8.3, the question of whether particle-bubble attachment may proceed through bubbles forming from supersaturated solutions was subjected to an experimental study.

8.2. The influence of various parameters on the recovery of mineral particles by dissolved air flotation

8.2.1. Stability of the floated product

It has been observed by other investigators (80)(116) that the recovery of the floated product in DAF can be difficult because of variable froth stability. Moreover, in section 7.1 it was shown that the method used to recover the floated product may also influence the selectivity of DAF operations. In addition, in dissolved air flotation used for solid/liquid separations the recovery of the floated material is also an important factor in the efficiency of the process (see section 2.5.2)(99).

Throughout this work the stability of the froth was observed to

vary but to follow well defined patterns. Generally, low floatability of the solids corresponded with a froth which would show little persistence and considerable detachment with time or if disturbed. Hydrophobic particles would float forming a thin, rigid layer of floated material of high stability with both time and physical stresses. In the presence of hydrophilic solids at high concentrations of surface-active agents, the formation of a very persistent two-phase froth was observed. Table 8.1 summarizes the behaviour observed for the floated product in some of the systems studied throughout this work.

From these observations it is possible to conclude that the hydrophobicity of the mineral particles determined, to a large extent, the consistency of the floated product and the ease with which it could be recovered. The stabilizing effect of mineral particles in the formation of three-phase froths in conventional flotation has been widely documented in the literature (1)(2)

Thus, given the high stability of the floated product under conditions of optimum mineral recovery by dissolved air flotation, it would appear that froth stability would not be a problem in DAF of minerals and that the problems experienced by other authors esteemed from the lack of hydrophobicity of the floated phase.

8.2.2. The effect of stirring

Three stages of stirring were normally employed in the dissolved air flotation studies:

i) fast stirring, to disperse the solid phase and to mix the reagents rapidly.

ii) slow stirring, to induce good floc formation.

iii) stirring during microbubble injection, to produce good mixing

Table 8.1. Stability of the floated product for various solid/solution systems

System	Frother	Stability	Observations	Section
Quartz/polyethyleneimine	Dowfroth 250 amyl alcohol	Fluid froth of little persistence	No flotation of quartz observed	5.2.2.
Silica/polyacrylamide flocculant	-	Little, flocs fall back easily if disdisturbed or after some time	Variable degree of floation according to type of water used	5.2.3.
Quartz/ferric	-	Flocs formed stable scum with little detachment		5.2.1.
Cassiterite/A845	amyl alcohol (pH 4.0)	Persistent fluid froth; over certain A845 concentration mineralized froth	Frother addition made no difference to DAF recovery	6.2.4.
Cassiterite/SDS	-	Formation of a very stable, rigid layer of floated material	Persistent froth, no detachment occurred	6.4.3.
Cassiterite/A845 kerosene emulsion	-	Very stable floated product at medium collector concentrations	If oil dosage increased less froth	7.2

conditions between microbubbles and particles during the flotation stage.

Of these, experimental evidence showed stages ii) and iii) to exert substantial influence upon the recovery of mineral particles by DAF.

Hence, in Chapter 5 (Figure 5.6) it was shown that the net effect of suppressing the slow stirring stage was to decrease the DAF recovery of quartz in the presence of dodecylamine. Experiments carried out on cassiterite at pH 3.0 using Aeropromoter 845 (A845) as collector showed a similar effect. Figure 8.1 indicated that the presence of a slow stirring stage of 10 min duration increased cassiterite recovery from 60% to about 85%. If the duration of the slow stirring stage was increased over 10 min a slight decrease (75%) in flotation recovery was observed. These tests were carried out using a constant 35 rpm stirring rate during microbubble injection.

The incorporation of a third stirring stage occurred during the dissolved air flotation studies on cassiterite as preliminary DAF tests showed that maximum recoveries were of the order of 60% if only two stirring stages were used. Tests were therefore carried out to determine the effect of the rate of stirring during microbubble injection on cassiterite recovery. The results (Figure 8.2) showed that stirring during microbubble injection improved cassiterite recovery to about 80% for rates between 30 - 75 rpm, above which cassiterite recovery dropped again.

It is also worthwhile recalling that a high rate of stirring (150 rpm) during the third stirring stage improved the selectivity of mineral separations by DAF with no detrimental effect on cassiterite recovery (section 7.3.2).

These results showed that dissolved air flotation can proceed

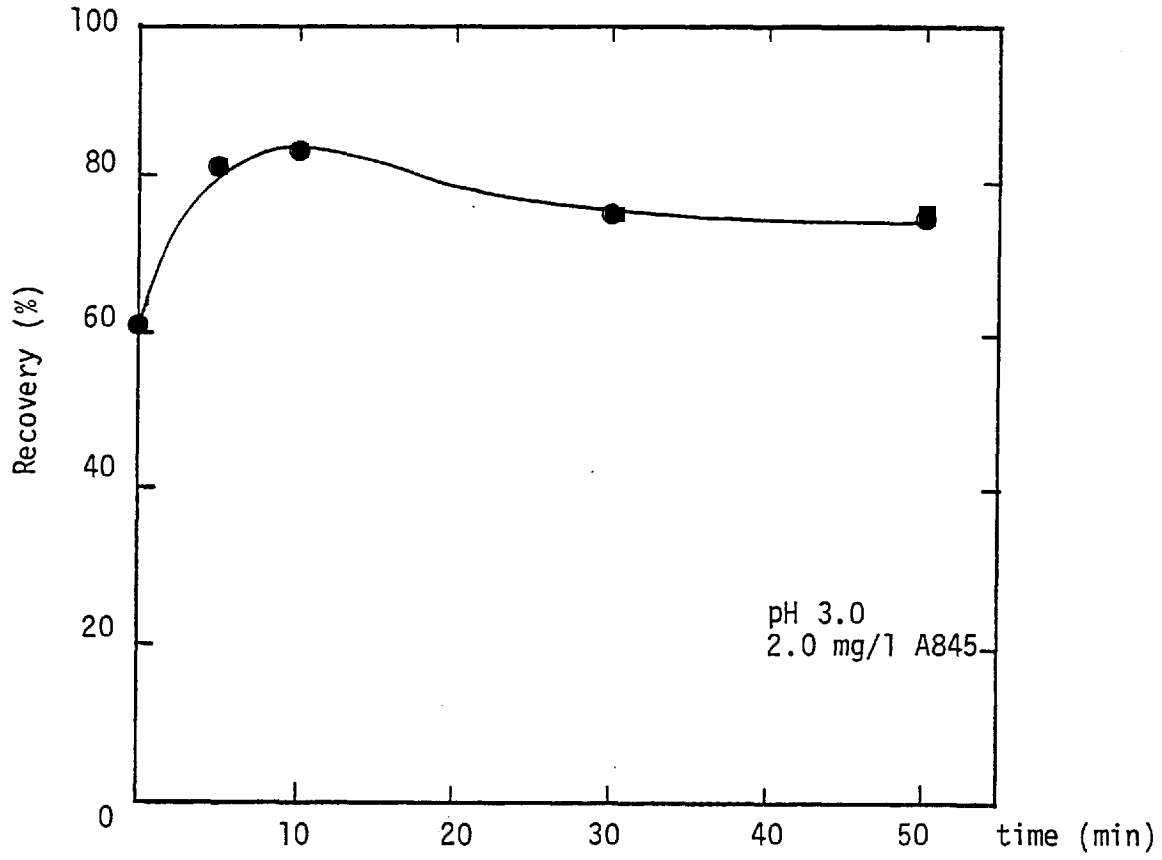

Figure 8.1. Effect of duration of slow stirring stage on the recovery of cassiterite by DAF

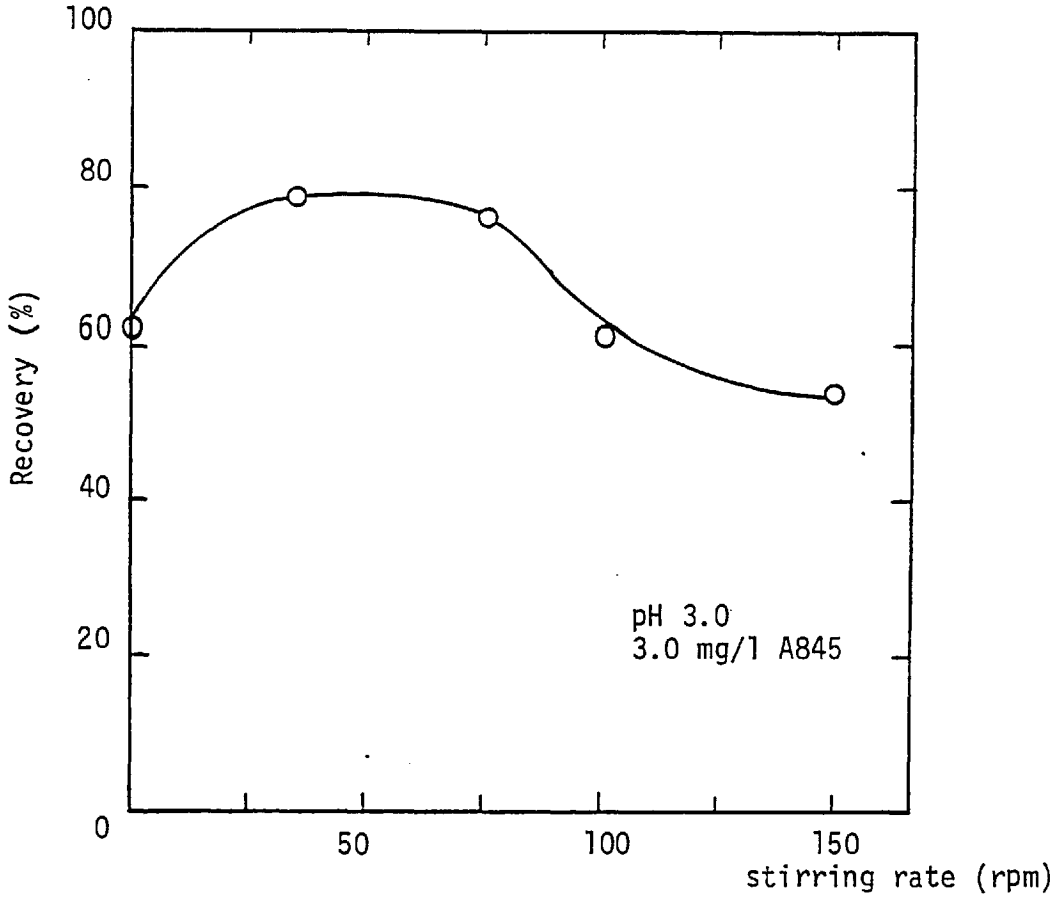

Figure 8.2. Effect of rate of stirring during microbubble injection on the recovery of cassiterite by DAF

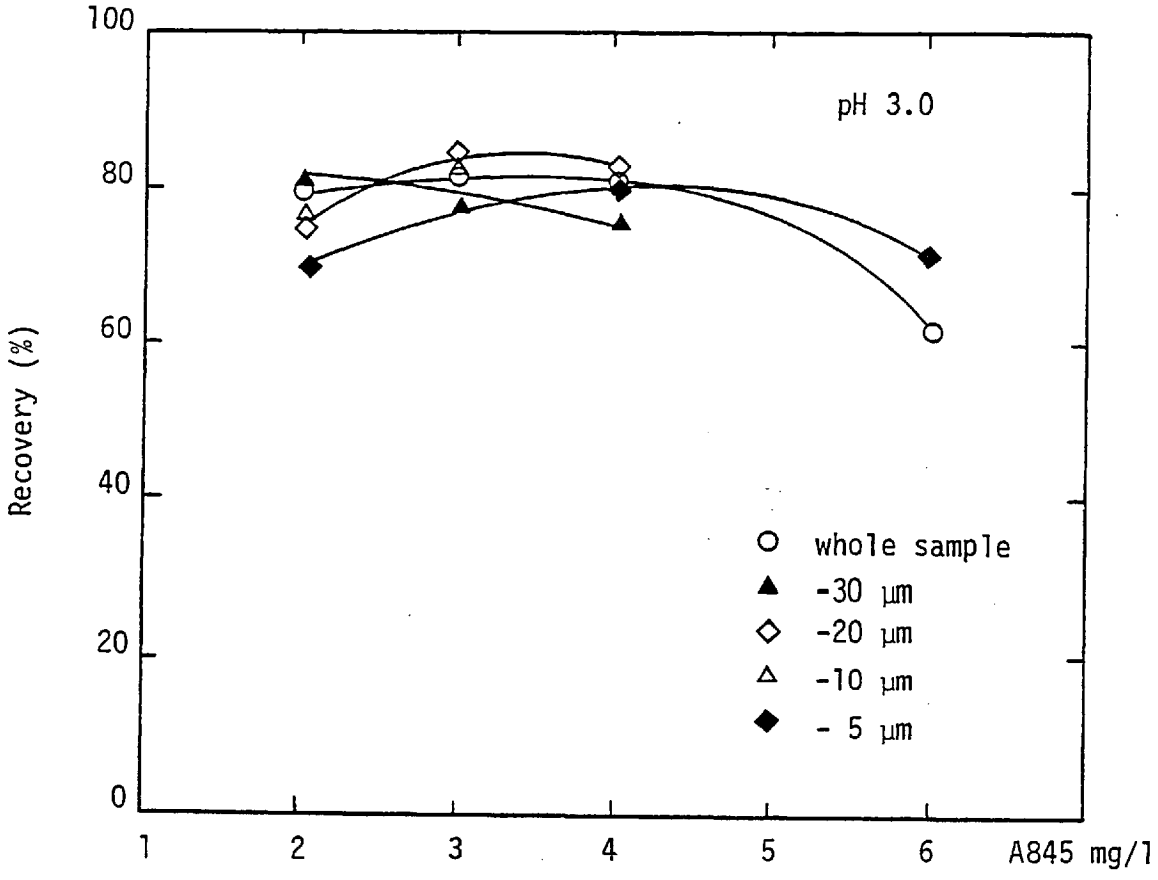

Figure 8.3. Effect of particle size on the DAF of cassiterite as a function of A845 concentration

effectively under much higher shear rates on the particle-bubble aggregates than it is customary to assume in the literature (87).

8.2.3. The effect of particle size

The DAF tests reported for cassiterite in the presence of Aeropromoter 845 (section 6.4.3) showed that maximum recoveries were only of the order of 80 - 85%. As the mineral sample contained only 93.5% SnO_2, there was a fraction of around 10% of the cassiterite particles which were not being recovered. This upper recovery limit shown by the cassiterite/A845 system at pH 3.0 also emerged in the DAF separation tests where maximum recoveries were only of the order of 75% cassiterite

However, it was apparent from the stability and DAF studies that

the fraction of non-floating cassiterite may have corresponded to that portion of the solids that settled out during the stirring stage. To test this theory various cassiterite size distributions were obtained from the sample by successive decantation of cassiterite suspensions. The results of dissolved air flotation tests on these samples are shown in Figure 8.3 as a function of collector concentration (A845).

The experimental results indicated that while the concentration of collector yielding optimum cassiterite recovery was a function of particle size, the same maximum recovery values of about 80% were achieved for all particle size distributions.

These results showed therefore that particle size was not responsible for the unfloated cassiterite at pH 3.0. Since the recovery values at pH 2.0 were of the order of 90%, it is then probable that the effect arises from a lower level of hydrophobicity of cassiterite at pH 3.0.

8.2.4. The effect of solids concentration

A few tests were carried out to study the effect of concentration of solids on the dissolved air flotation of minerals. The quartz/dodecylamine system at pH 9.5 was chosen for these experiments and the concentration of solids was varied between 0.5 and 25 g/l. The results are shown in Table 8.2.

It can be seen from the table that the recovery of quartz particles was greatly hindered as the concentration of solids in suspension was increased. This is in agreement with the results of Shimoiizaka et al (117) who found that the recovery of various solids by dissolved air flotation decreased for concentrations of solids over 0.5% (5 g/l).

The decrease in flotation recovery does not appear to be due to

Table 8.2. Effect of the concentration of solids on the recovery of quartz by dissolved air flotation

Solids Concn. g/l	Dodecylamine Concn. (M)	Saturator Pressure (psig)	Volume Injected (ml)	Float (g)	Recovery (%)
0.5	$5x10^{-5}$	40	100	0.39	78.0
5	"	"	"	2.31	46.2
10	"	"	200	5.43	54.3
25	$1.1x10^{-4}$	80	"	8.50	34.0

insufficient air being available since at 25 mg/l the weight of solid floated exceeded the total weight of solid at 5 mg/l. Since higher solids concentration resulted in the production of much larger flocs than for dilute suspensions it is probably the effect of these larger quartz/dodecylamine flocs that caused the decrease in flotation recovery, as large flocs have been observed to float poorly with microbubbles.

8.2.5. The effect of saturation and injection pressures

The influence of the saturation and injection pressures on the recovery of mineral particles by dissolved air flotation was determined by performing DAF tests on the cassiterite/A845 system at pH 3.0. The distinction between saturation and injection pressures is that while the first is the pressure at which air is dissolved in water and therefore determines the amount of air available for the formation of the microbubbles, the latter is the pressure at which the supersaturated water is forced through the pressure reduction device. Thus, the injection pressure has a direct influence on microbubble formation through controlling the pressure reduction at the orifice. In these DAF tests saturation and injection pressure have always coincided (40 psig, 377 kPa).

and it was decided that by considering them as two separate components more information on the DAF system could be obtained. The tests with varying injection pressures were carried out as described in section 4.6.3.

Figure 8.4 presents the results obtained on the recovery of cassiterite particles as a function of saturation pressure for constant surface chemical conditions of the suspended phase. The figure shows results obtained at constant injection pressure (40 psig) and for the cases where injection and saturation pressure were identical. The curves show that cassiterite recovery was substantially influenced by the pressure of saturation but not by the injection pressure. Thus, cassiterite recovery increased to about 80% at 40 psig saturation pressure above which it increased slightly to 85% at 80 psig for constant injection pressure. When the pressurized water was injected at the saturation pressure, the recoveries were approximately equal to those obtained at 40 psig injection pressure over the range of saturation pressures 20 - 80 psig.

Further experiments on the influence of the pressure of water injection on recovery were carried out at a constant saturation pressure of 40 psig under diverse surface chemical conditions of the dispersed phase. The results shown in Figure 8.5 confirm that the injection pressure had little influence on recovery at the saturation pressure tested.

While the beneficial effect of increasing saturation pressure on mineral recovery may arise from the fact that more air is being introduced into the suspension, the effect of injection pressure would appear to be related to the formation of microbubbles upon water supersaturation. Thus, measurements of the rise-time of microbubbles as a

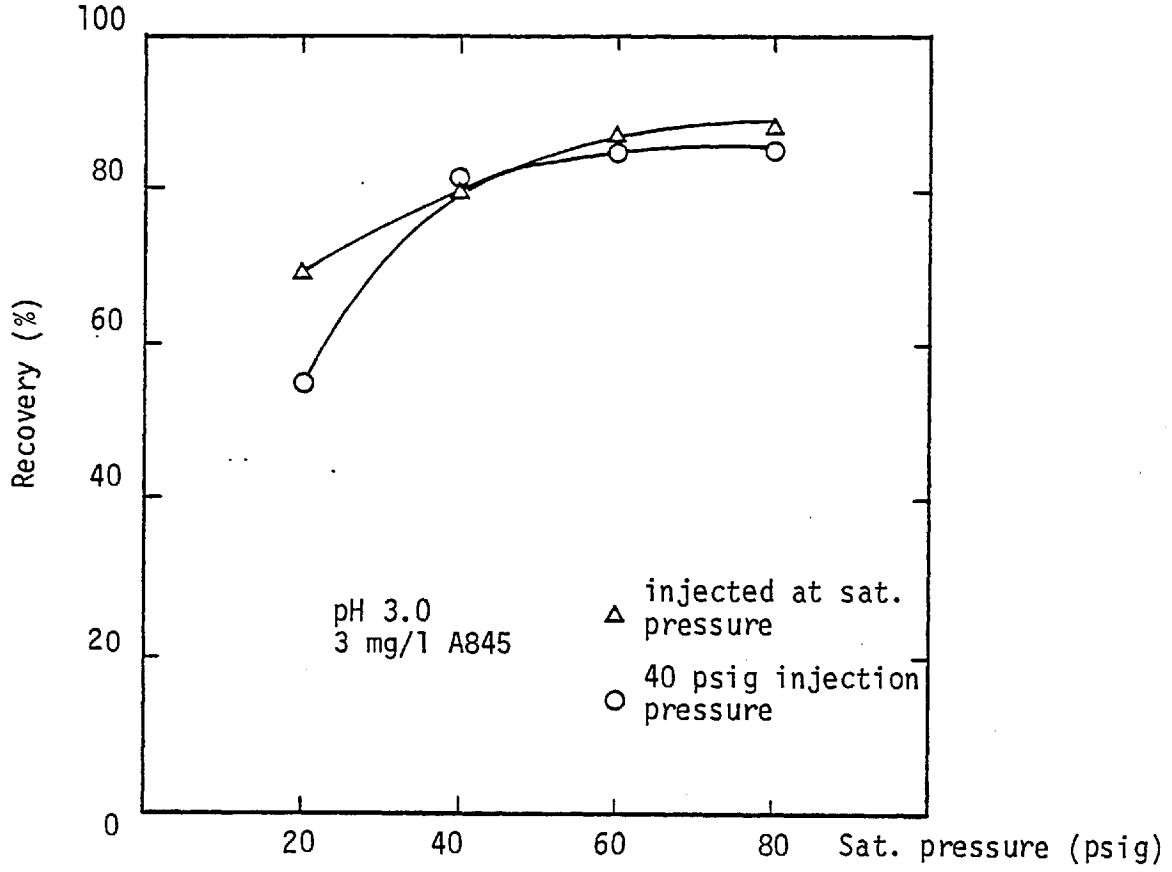

Figure 8.4. Effect of saturation pressure on the recovery of cassiterite by DAF at various injection pressures

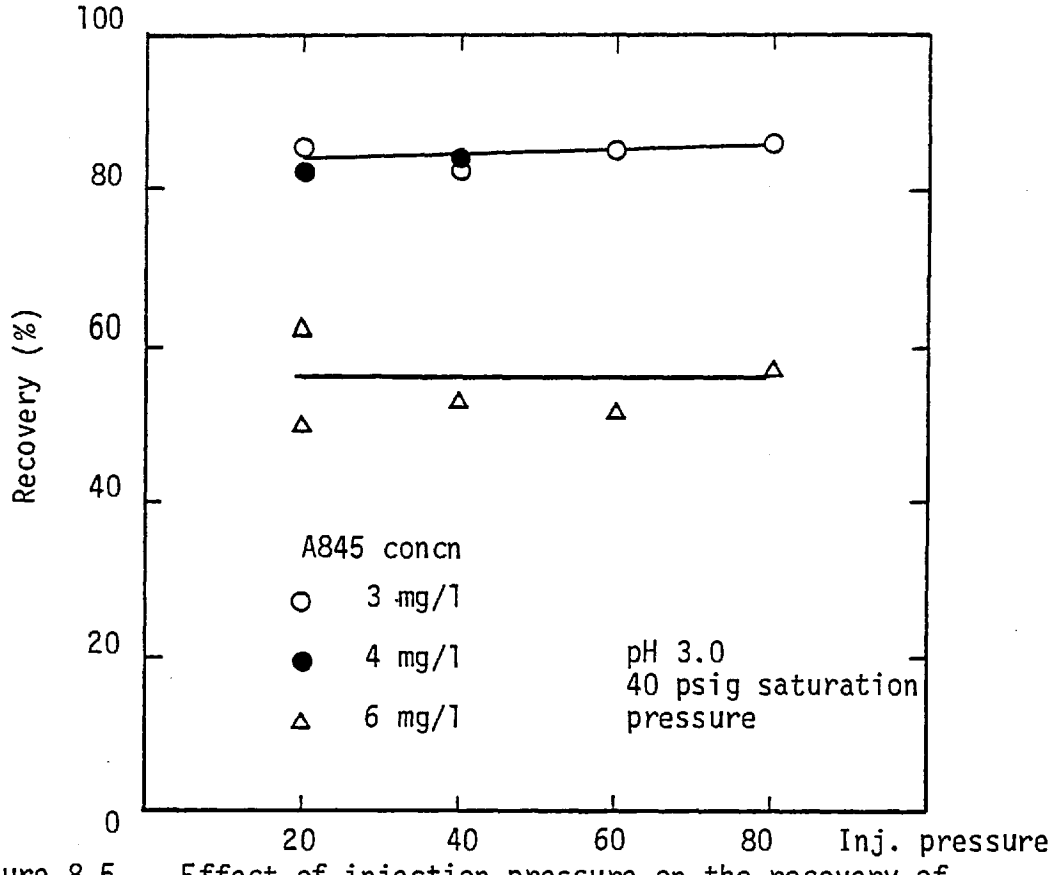

Figure 8.5. Effect of injection pressure on the recovery of cassiterite by DAF at various A845 concentrations

function of the injection pressure (Table 8.3) indicated that this had a deleterious effect on microbubble formation only below 20 psig, therefore explaining the independence of DAF recovery on injection pressures in the range 20 - 80 psig. Furthermore, DAF tests conducted on flocculated quartz particles as a function of the injection pressure (see section 8.3.3.2) confirmed that DAF recovery drops substantially for injection pressures below 20 psig due to the formation of fewer and larger bubbles (Figure 8.8).

Table 8.3. Rise-time of microbubbles as a function of injection pressure at a constant saturation pressure of 40 psig

Injection Pressure (psig)	Rise-time (sec)	Microbubble formation
5	65	little
10	100	"
20	215	significant
30	227	high
40	245	"
60	238	"

8.3. Flotation of minerals by bubbles forming from supersaturated solution

8.3.1. Introduction

As already discussed in sections 1.5 and 2.4, one of the mechanisms believed to be operating in bubble-particle attachment in dissolved air flotation is the direct formation of air bubbles on the suspended phase.

However, no experimental evidence has been presented in the literature which could support such a belief. It was therefore decided to carry out an experimental study into the flotation of minerals by bubbles forming from supersaturated solution to elucidate the existence and importance of that bubble-particle attachment mechanism in dissolved air flotation operations.

The fact that flotation of minerals by bubbles nucleating from supersaturated solution is possible has been shown by vacuum flotation studies (section 2.6.1) where supersaturation of a mineral pulp is produced by the application of a vacuum. In this study, however, the reverse occurred and supersaturation was achieved by the depressurization of the high-pressure saturated water. These studies were directed to establishing firstly, (a) the conditions under which bubbles would form from supersaturated solutions, and secondly (b) the conditions under which flotation through this nucleation mechanism would occur.

8.3.2. Experimental

Most of the tests were carried out using the following procedure:

i) Air was dissolved in water at constant pressure in the saturator (usually at 40 psig, 377 kPa, unless otherwise stated).

ii) The air flow was stopped and the saturator was slowly depressurized to atmospheric pressure. The lid of the saturator was then removed and a volume (usually 100 ml) of this supersaturated water was extracted with a clean, hydrophilic beaker. No, or very few, bubbles appeared from solution during this procedure.

iii) The supersaturated water (SSW) was slowly and gently added to the vessel containing the solution or suspension (800 ml volume) in which bubble formation was to be observed.

In some tests carried out in the flotation cell, SSW was added just by opening the valve and allowing it to flow through the nozzle under the action of gravity. No microbubbles were produced but some bubbles did form at various points in the system.

The levels of supersaturation induced by this experimental procedure were low and of an order of magnitude comparable to those attainable in vacuum flotation. Thus, 100 ml of SSW pressurized at 377 kPa would result in 30% supersaturation when mixed with 800 ml water at atmospheric pressure. If the SSW had been pressurized at 653 kPa (80 psig) the level of supersaturation would have been about 60%, this would have been equivalent to applying a vacuum of about 546 mm Hg. The percent of supersaturation is referred to the initial air solubility of the suspensions (at atmospheric pressure).

The solids used as suspended phase were generally the same as those used in the previous DAF studies. They were conditioned following the procedure described previously. Some tests were carried out on quartz flocculated by a non-ionic polyacrylamide (N100 supplied by BTI) in the presence of copper sulphate. In these tests, copper sulphate was added at fast stirring followed by the flocculant and then the flocs were built up at slow stirring for 10 minutes.

8.3.3. Results

8.3.3.1. Experiments on the formation of bubbles from supersaturated solution - The effect of hydrophobicity

Experiments were carried out to determine the influence of the suspended phase on the formation of bubbles from supersaturated solution. Thus, 100 ml of supersaturated water was added to beakers containing various diverse systems:

(a) double distilled water only

(b) a quartz suspension in double distilled water

(c) a solution of dodecylamine (2.7×10^{-5} M(

(d) quartz/1.25×10^{-4} M ferric sulphate (pH 7.0)

(e) quartz/2.7×10^{-5} M dodecylamine (pH 9.5)

Upon addition of supersaturated water to the beaker containing only double distilled water, no bubbles were observed to form either in the bulk solution or on the walls of the beaker for a period of 24 hours. The same situation was noted for beaker (b). In the case of the dodecylamine solution (c) bubbles were observed to appear on the walls of the beaker almost immediately after the addition of the SSW; after 24 hours the number of these bubbles seemed unchanged but their size had increased. In the quartz/ferric sulphate system, bubbles tended to form on the sedimented bed of quartz/ferric hydroxide flocs and after some time individual bubbles rose up with flocs attached to them. When the vessel was disturbed many bubbles rose up, the majority without attached particles. After 24 hours a layer of floated material was observed on top of the suspension but it represented only a small fraction of the total solids.

When SSW was added to the suspension of coagulated and hydrophobic quartz particles (e) no free bubbles were observed to form in the bulk solution. However, after 1 - 2 minutes a significant portion of the solids was observed to rise up massively and accumulate at the top of the suspension. Bubbles were also observed to grow on the walls of the beaker in larger amount than the other systems. Bubbles continued to grow on the solids and flotation of individual bubble-floc aggregates was noticed to occur continuously. The amount of solids floated was estimated visually to correspond to about 30% of the total. Little

detachment from the froth occurred and after 24 hours there seemed to have been no change in the amount floated.

The results obtained on bubble formation on the quartz/dodecylamine flocs clearly suggested that the hydrophobicity of the suspended phase played an important role in bubble nucleation from supersaturated solutions. The fact that no bubble formation took place in the case of the hydrophilic systems (beakers (a) and (b)) was another strong argument for this conclusion. It was surprising, however, to see that the quartz/ferric hydroxide flocs exhibited a degree of bubble nucleation and flotation as this is a theroetically hydrophilic system. Nevertheless, the kind of attachment observed in the experiments, large bubbles ($\simeq$ 1 mm) lifting small floc structures attached to their rear, suggested the existence of a contact angle between bubble and floc and was therefore a sign of some hydrophobic contamination of the ferric hydroxide flocs.

To elucidate the role of hydrophobicity, similar tests were carried out on hydrophilic flocs which were subsequently rendered hydrophobic. Thus, the addition of SSW to the precipitated silica/cationic polyacrylamide flocculant (C150/23) system under similar conditions to those reported in section 5 did not result in the formation of bubbles on the surface of these hydrophilic flocs. Only a few bubbles were seen rising up (without solids) when the bed of flocculated material was disturbed. Neither were bubbles attached to the walls of the beaker. However, when the supersaturated water was added to these flocs in the presence of dodecylamine (1.35×10^{-4} M at pH 7.5) bubbles appeared immediately on the surface of the flocs and flotation of individual aggregates occurred. A low recovery of these silica flocs was observed and the ease with which they lost their attached

bubbles when disturbed (similar to the behaviour of ferric hydroxide flocs) suggested that they were not strongly hydrophobic.

Another hydrophilic system which showed no bubble nucleation in the presence of a supersaturated solutuion was the quartz/copper sulphate/non-ionic flocculant (N100) system at pH 7.5. These flocs were very large and when sedimented they tended to aggregate further so that if the suspension was stirred large flocs (2 - 4 cm) could be seen in suspension. When dodecylamine was added to these flocs (5.4×10^{-5} M) bubbles formed instantly all over their surfaces and massive, clear-cut floc flotation occurred. The amount of solids recovered was larger than for any other system, visual estimates fluctuating between 50 - 80% of total solids. A photographic study of the flotation of these flocs by bubbles forming from supersaturated solution is presented in Appendix III.

The results of the tests on hydrophilic flocculated systems demonstrated that the hydrophobicity of the suspended phase is essential for bubble formation and subsequent flotation to occur. They also confirmed that the nucleation of bubbles onto ferric hydroxide flocs was probably due to the effect of some kind of surface contamination. However, further tests carried out on the silica gel/dodecylamine system showed that hydrophobicity was not the only prerequisite for bubble nucleation to happen.

8.3.3.2. Experiments on the formation of bubbles from supersaturated solution - The effect of gas nuclei

Addition of SSW to a suspension of silica gel particles similar to that described in section 5.2.4 resulted in the formation of some bubbles in the bulk solution but no attachment on the silica particles was

observed. When the addition of SSW was made to silica gel particles in the presence of 6.7×10^{-5} M dodecylamine at pH 8.0, no bubbles formed on the surface of the particles either. Increases in the concentration of dodecylamine, pH and amount of supersaturated water were attempted but they brought no change.

When the suspension was gently stirred a number of bubbles appeared which rose up carrying no particles. The same suspension was then transferred to the flotation cell and subjected to an injection of microbubbles. It showed excellent floatability and after some time bubbles were observed to grow on the particles which had not been floated by the microbubbles.

The fact that hydrophobic silica gel particles could not induce the formation of bubbles from supersaturated solution suggested the existence of another factor in the nucleation phenomenon. According to the principles outlined in section 2 regarding bubble formation from supersaturated solutions, the factor most likely to influence the nucleation mechanism is the presence of small masses of undissolved gas in the system (Harvey nuclei). Experimental evidence indicates that when these Harvey nuclei are removed from the system bubble nucleation does not occur unless much higher degrees of supersaturation are applied.

It is therefore probable that the factor that prevented bubble formation on the hydrophobic silica gel particles was the absence of readily available Harvey nuclei on their surfaces.

The observation that bubble growth was noted only after an injection of microbubbles had been made, i.e. after microbubbles had attached on the surface via a collision tends to confirm this theory. The fact that silica gel is very hydrophilic and was prepared completely in

aqueous medium may have made it unlikely that they entrapped and retained air pockets which may have constituted sites for bubble formation. This was shown by nucleation tests carried out on silica gel samples which had been left to dry for about 2 weeks at the laboratory atmosphere. When water was added to these samples the formation of a large number of bubbles which rose quickly out of solution was observed. The addition of SSW to this sample in the presence of dodecylamine resulted in only a minor degree of bubble formation on the silica gel flocs.

The role of Harvey nuclei on the formation of bubbles from super-saturated solution was further studied by carrying out experiments on systems in the absence and presence of these nuclei. Thus, bubble nucleation tests were performed on quartz samples which had been boiled for some time to remove any undissolved gas and duplicate tests were conducted on quartz samples prepared following the normal procedures. Boiling has been shown to be effective in removing undissolved gas (247). The systems tested were quartz/dodecylamine (4×10^{-4} M at pH 6.0) and quartz/$CuSO_4$ (1.25×10^{-3} M)/N100 (1.25 mg/l)/dodecylamine (6.7×10^{-5} M) at pH 7.5.

The 'boiled quartz samples were prepared by gently boiling 0.5% quartz suspensions for 1 hour. The samples were then left to cool down and after 48 hours most of the water was decanted off and replaced with air-saturated water. The reagents were then added and the flocs were prepared by stirring at the slowest stirring rate; no significant differences were noticed between the flocs conditioned this way and those prepared following the normal procedure. During the whole preparation process care was exercised not to expose the solids to air.

When SSW was added to the suspensions, significant differences

were observed regarding bubble formation on boiled and normal quartz samples. Thus in the case of the quartz/dodecylamine system, the normal quartz sample showed good flotation upon addition of the SSW, followed by continuous growth of bubbles and the subsequent flotation of the settled material. The recovery was visually estimated at 40% after 1 h, and a stable froth was formed. Many bubbles had deposited all over the walls of the beaker. With the boiled sample, on the other hand, little bubble nucleation was observed and flotation recovery was nil after 1 h. Also, far less bubbles formed on the walls of the beaker (this had also been boiled). A similar behaviour was recorded for the quartz/$CuSO_4$/N100/dodecylamine system when the normal sample showed 25% flotation after 1 h compared with 1 - 2% exhibited by the boiled quartz. The kind of bubble-floc attachment observed in these tests was significant. The very few bubbles (> 1 mm) which formed on the surface of boiled quartz flocs rose up lifting only tiny floc structures of comparable size (< 1 mm), whereas with the normal samples, the multiple formation of bubbles led to the flotation of large flocs by many attached bubbles (as shown photographically in Appendix III). It was also observed that fewer bubbles attached to the glass surface in the boiled beaker than in the non-boiled.

When dissolved air flotation tests, i.e. injecting free microbubbles, were carried out on boiled and non-boiled quartz samples prepared in the same way as above, no differences were observed in terms of recovery. Thus the measured recoveries were 67 - 73% for the quartz/dodecylamine system and 93% for the flocculated quartz particles for both cases, boiled and non-boiled.

The experiments carried out on bubble nucleation on minerals from supersaturated solution showed that prerequisites for this phenomenon

to occur were both the hydrophobicity of the solids and the presence on them of Harvey nuclei (for the levels of supersaturation used in these experiments).

8.3.3.3. Experiments on the flotation of minerals by bubbles forming from supersaturated solution

While the previous tests demonstrated that bubble formation and subsequent flotation could occur only on hydrophobic surfaces (thus providing a basis for selectivity), they also indicated that flotation by the nucleation mechanism was a slow process and that not all the solids were recovered by this method.

Hence, extensive tests carried out on the quartz/dodecylamine system gave a maximum (measured) recovery of about 50% for 4×10^{-4} M dodecylamine at pH 6.0 during a period of 90 minutes. Similar tests were conducted on cassiterite in the presence of Aeropromoter 845 at pH 3.0 (in the flotation cell). The best measured recovery in this case was 34% at a collector concentration of 4 mg/l.

The reasons for this low recovery were not clear but two further tests showed that the addition of a flocculant considerably improved the flotation of mineral particles by bubbles nucleating from supersaturated solution. Thus, the addition of 1 mg/l of the non-ionic flocculant (N100) to a cassiterite suspension at pH 3.0 (3 mg/l Aeropromoter 845) resulted in an increase in flotation recovery from 33 to 87% (measured after 6 min flotation time). These tests were carried out in the flotation cell by adding 100 ml of water saturated at 80 psig (653 kPa) to 1 l suspensions. When similar tests were conducted on (hydrophobic) methylated quartz particles little flotation occurred. However, when the particles were flocculated by the addition of $CuSO_4$ followed by N100, total recovery was observed upon addition

of the supersaturated water.

In both cases described above, the addition of the flocculant is unlikely to have altered the surface properties of the particles in terms of bestowing floatability through an increase in their hydrophobicity. The beneficial effect of the flocculant upon recovery must therefore have arisen from the changes caused in the physical properties of the suspended phase, i.e. smaller number and larger size of the suspended 'particles'.

Additional experiments were carried out to determine whether the rate of the nucleation and flotation processes could be increased by increasing the supersaturation of the system. Thus, water saturated at pressures between 20 - 80 psig (239 - 653 kPa) was added (100 ml) to beakers containing a suspension of quartz particles flocculated by $CuSO_4$ (1.25×10^{-3} M) and N100 (1.25 mg/l) in the presence of 8.1×10^{-5} M dodecylamine at pH 7.5. The flotation of these flocs was observed over a period of 5 hours as follows:

- During the first two hours the suspensions were left to stand untouched and the recovery was measured or estimated visually at 5 min, 30 min, 1 h and 2 h.
- After the 2 h period the beakers were gently rotated at 15 min intervals. The period of rotations lasted 1 h for the beaker at 40 psig and 2 h for the remaining beaker.
- After the period of rotations had elapsed the floated material was suctioned out and the whole suspension was gently stirred with a glass rod for 1 min and left to stand for another hour after which the recovery was measured. A test was also conducted at 40 psig (marked 40* psig in Figure 8.6) in which a volume of only 50 ml was added to the suspensions.

The results of these tests are presented in Figure 8.6 and show clearly that the rate of flotation by bubbles forming from supersaturated solutions was strongly dependent upon the degree of supersaturation of the suspensions. Thus, while a recovery of over 90% was achieved in 5 min by adding water saturated at 80 psig (a 60% supersaturation), 4 hours were required to attain a similar recovery value with water saturated at 40 psig (30% supersaturation). The amount of solids floated was also a function of saturation pressure, the recoveries diminishing for saturation pressures below 40 psig.

It is also interesting to note that higher recoveries were obtained at 40* than at 20 psig saturation pressure, despite the fact that the combination of saturation pressure and volume of SSW added to the suspensions resulted, theoretically, in an equal degree of supersaturation (15%). A possible source of this discrepancy may be deficient instantaneous mixing of the supersaturated water in the suspension, thus causing zones of higher local supersaturation which could have resulted in higher flotation recoveries in the case of 40* psig saturation pressure.

Figure 8.6 also shows that the rate of the flotation process increased after two hours as the period of gentle agitation of the suspensions started. Thus, these results would indicate that agitation increases the rate of flotation by bubbles forming from supersaturated solution.

The question of whether bubble formation from supersaturated solution on the suspended phase was an operating bubble-particle attachment mechanism was studied by carrying out DAF tests and then observing whether the residual supersaturation of the liquid induced flotation of the remaining solids. The solid phase consisted of quartz particles

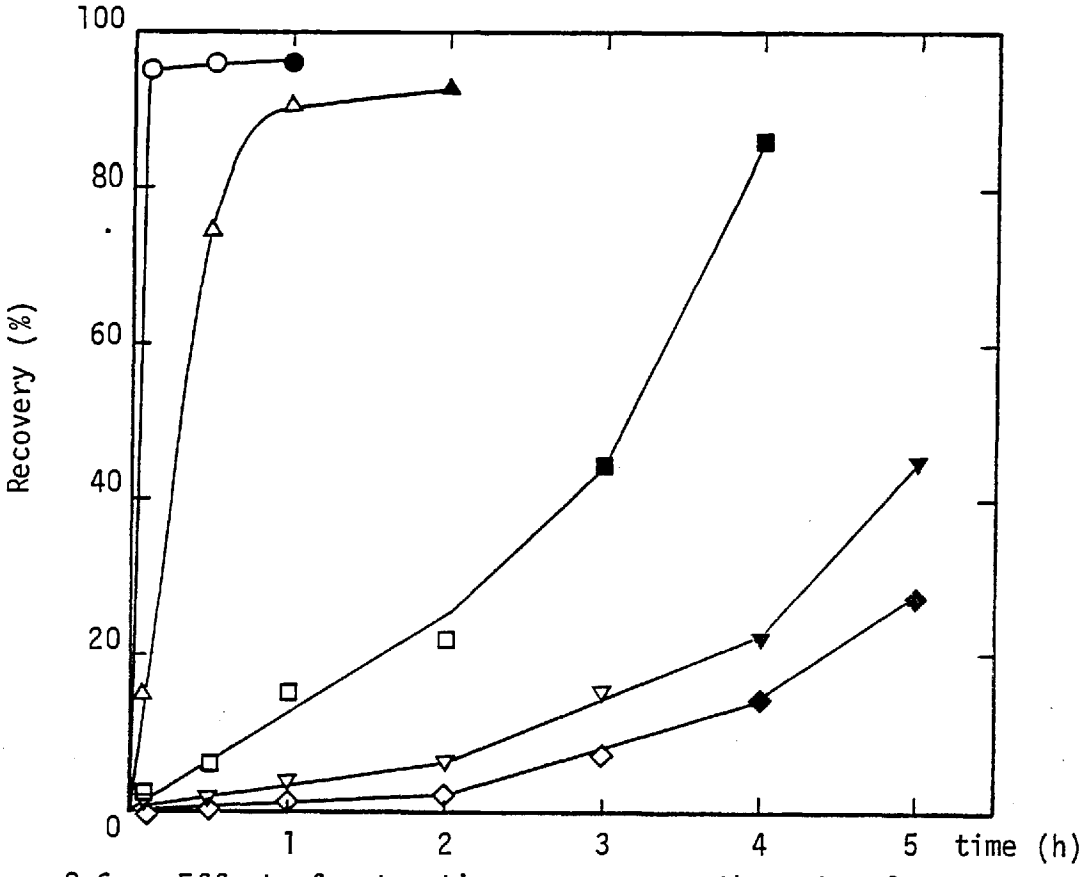

Figure 8.6. Effect of saturation pressure on the rate of recovery of flocculated quartz particles by bubbles forming from supersaturated solution

○ 80 psig saturation pressure
△ 60 " " "
□ 40 " " "
▽ 40* " " " (50 ml added only)
◇ 20 " " "

Open symbols: estimated recoveries
Black symbols: measured recoveries

flocculated by $CuSO_4$, N100 and in the presence of dodecylamine as in the previous test. The experimental procedure was as follows:

- Water was saturated at 40 psig and injected at various injection pressures into the suspension of flocculated particles.
- After the flotation time of the microbubbles had elapsed (4 min) the floated material was recovered. This amount was considered to correspond to the recovery produced only by the action of the microbubbles.
- The beakers were then left to stand for 5 hours being occasionally stirred to increase the rate of flotation. The floated product was then recovered and considered to correspond to the amount floated through bubble formation from supersaturated solution.

The logic behind this procedure was that while a constant amount of dissolved air was being injected into the suspension (determined by the saturation pressure) the variable injection pressure ensured that the water was injected with variable amounts of dissolved air and microbubbles. This was corroborated by measurements of the rise-time of the bubbles formed as a function of injection pressure (Figure 8.8 and Table 8.3).

The results of these experiments have been presented in Figure 8.7 as a function of injection pressure. The blank areas represent recoveries measured for the microbubbles and the hatched areas recoveries obtained by bubbles forming from supersaturated solution. The test shown as 0 injection pressure was carried out by adding only water saturated at 40 psig.

The results shown in Figure 8.7 revealed clearly that the free microbubbles were largely responsible for the recovered material. Flotation through bubbles forming from supersaturated solution was

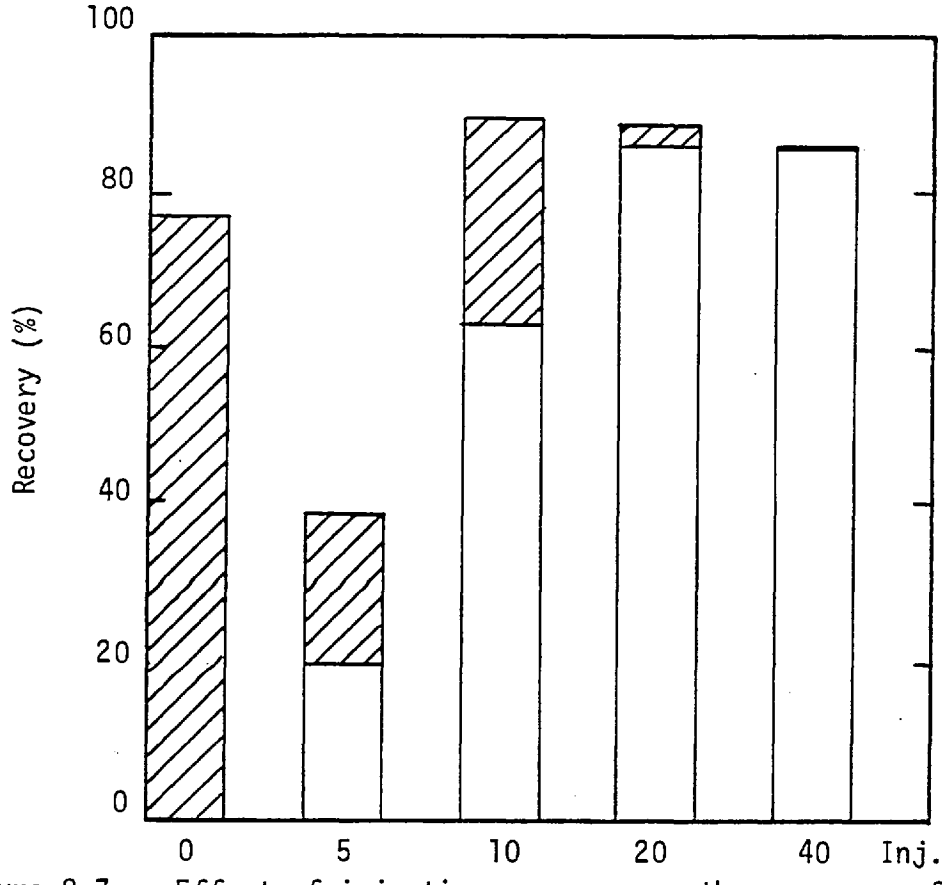

Figure 8.7. Effect of injection pressure on the recovery of flocculated quartz particles (blank area: recovery by microbubbles; hatched area: recovery by bubbles forming from super-saturated solution)

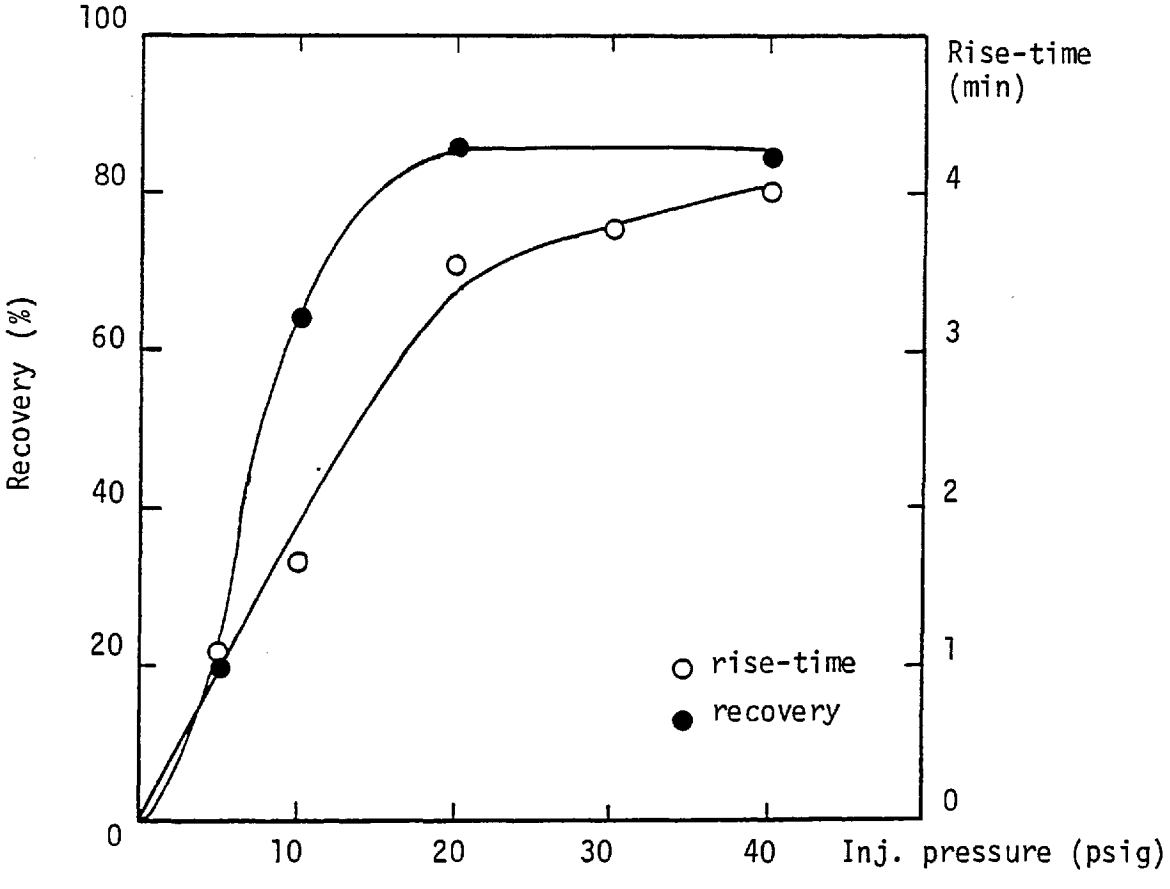

Figure 8.8. Effect of injection pressure on the rise-time of bubbles and the recovery of flocculated quartz particles by DAF

significant only at injection pressures below 20 psig since (as shown by Figure 8.8) below that pressure the formation of microbubbles is much less efficient and therefore the residual supersaturation was greater. Indeed, when the rise-time of the bubbles formed upon the injection of supersaturated water was compared with the flotation recovery obtained for the microbubbles a very close correlation was observed (Figure 8.8). The recovery obtained by the microbubbles was constant for injection pressures in excess of 20 psig, in agreement with the results obtained previously (section 8.2.5). The total recoveries obtained were approximately of the same order of magnitude for all injection pressures which would be consistent with the fact that the total amount of air supplied to the system was constant. The exception to this behaviour was observed at a pressure of injection of 5 psig where the recovery was only about 40%. As the (few) bubbles produced at this injection pressure were quite large, this may explain the low recovery obtained.

These tests showed that the mechanism of bubble-particle attachment via the formation of bubbles from supersaturated solution onto the mineral particles is not likely to have been occurring in the dissolved air flotation tests carried out throughout this thesis as these were usually performed at equal saturation and injection pressures of 40 psig. In this sense, the conclusion reached in Chapter 5 that the mechanism of bubble-particle attachment in DAF is via the adhesion of air bubbles to hydrophobic solids upon bubble-particle collisions received further support from these tests.

8.3.4. Discussion

The studies reported in this section have investigated the basic

factors determining the formation of bubbles from supersaturated solution and the subsequent flotation of minerals by these bubbles. The results also provided experimental evidence to elucidate the role of this flotation mechanism in the dissolved air flotation process.

As described in Chapter 2, there are two mechanisms by which bubbles may form from supersaturated solutions, namely, (a) from the growth of microscopic masses of undissolved air existing in the system (Harvey nuclei), and (b) in the absence of undissolved air, from homogeneous or heterogeneous molecular nucleation ('de novo' nucleation). Theoretical calculations of the degree of supersaturation required to induce homogeneous bubble nucleation in liquids through only the random thermal motion of molecules, show that considerable degrees of supersaturation are required for bubbles to form through this path (74)(76)(80). Harvey et al (73) postulated the existence of mechanism (a) to explain the ease of bubble formation in supersaturated liquids. The main evidence for the occurrence of mechanism (a) is that when measures are taken to remove undissolved gas in a system, subsequent nucleation of bubbles requires higher degrees of supersaturation. This has been shown to occur for cavitation in Ventury-type constrictions (84), for the limit of superheat in various liquids (248)(249)(75), for the supersaturation of water with various dissolved gases (250)(78) and for the onset of ultrasonic cavitation (251).

The experiments carried out on bubble formation from supersaturated solution in this work showed basically that:

- bubbles formed only on hydrophobic solids which probably contained adsorbed undissolved gas (Harvey nuclei)
- hydrophobic solids which did not have Harvey nuclei did not promote the formation of bubbles

- bubbles do not form on clean hydrophilic solids

These conclusions are in agreement with work carried out by Smith et al (252) on bubble formation from supersaturated solution on glass slides with various coatings. These authors further found that there was no bubble formation on oil drops or thick films of oil.

Thus the evidence would indicate that bubble formation in these tests is most likely to have occurred through the growth of Harvey nuclei rather than via 'de novo' nucleation. A further argument for this conclusion is the low level of supersaturation with which bubble formation developed compared with results reported for highly pure systems. Thus, Hemmingsen (253) was able to depressurize pure water saturated with oxygen at 135 atmospheres to 1 atmosphere without bubble formation occurring. By comparison, bubble formation occurred in the present tests for levels of air supersaturation of the water of less than 1 atmosphere.

The masses of undissolved gas referred to as Harvey nuclei are considered to be masses of gas stabilized in hydrophobic cavities, cracks, fractures and crevices of various shapes which are normally present in the solid, the walls of the container or in suspended particles. It can be shown that these nuclei cannot exist as small 'free' bubbles in the liquid as they would either dissolve or rise out of solution in a relatively short time. The behaviour of these stabilized gas nuclei has been studied in some detail by various authors (73) (252)(254)(80) and has been found to depend on crevice size and shape, the values of the advancing and receding contact angles (θ_A and θ_R), the surface tension (γ), the dissolved gas content of the liquid, and the degree of supersaturation to which the system is exposed. Only a brief outline of the behaviour of these nuclei upon supersaturation will

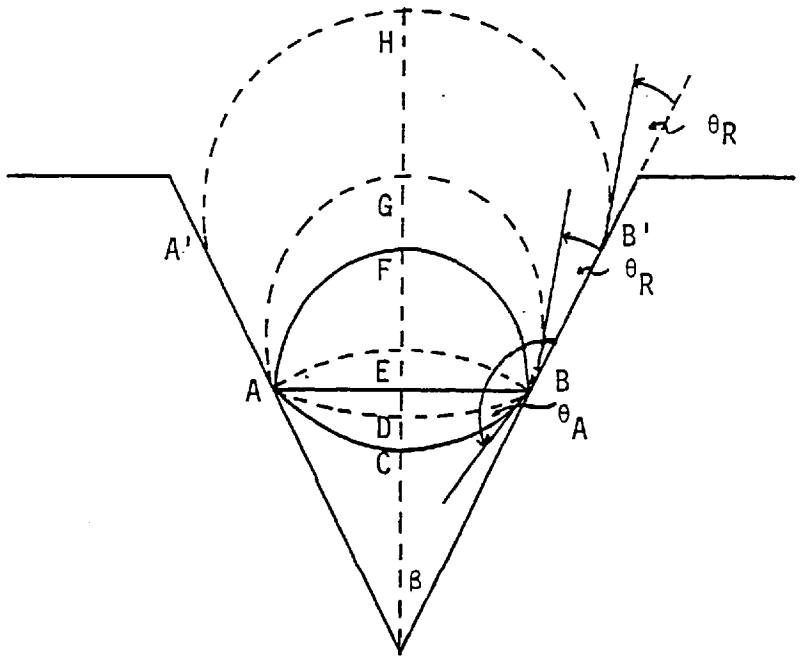

Figure 8.9. Growth from supersaturated solution of an air cavity stabilized in a hydrophobic conical crevice

be given here.

Let us consider a stabilized air cavity (ACB) in a conical crevice of apical angle 2β as shown in Figure 8.9. The equilibrium between the meniscus and the liquid is described at equilibrium by the Laplace equation:

$$P_l - P_g = \frac{2\gamma}{r} \qquad (8.1)$$

where P_l = pressure in the liquid

P_g = pressure in the gas meniscus (constituted by the sum of the vapour pressure of the liquid and the partial pressure of the gases)

γ = surface tension of the liquid

r = radius of curvature of the gas/liquid interface

Equation 8.1 expresses the fact that for the system depicted in Figure

8.9 the pressure at the concave side of the interface (the liquid) is greater than at the convex side. However, if the pressure in the liquid is reduced, air diffuses into the cavity and the interface becomes less concave (ADB) due to the decrease in the pressure difference across the interface. When the pressure in the liquid is reduced enough so that it equals the pressure in the air cavity, the interface becomes flat (AB) and any further decrease in pressure would cause the gas/liquid interface to flex and become concave towards the apex (AEB). The same situation could have been arrived at by heating the liquid or increasing the concentration of dissolved air at constant pressure in the liquid. When the interface is such that it has reached a hemispherical position (AFB, $\theta_R = \beta$), a further decrease in the pressure in the liquid would induce the unstable growth of the meniscus since now the radius of curvature is increasing and therefore the surface forces opposing interfacial movement are decreasing. The meniscus would then grow until the contact angle attains a value of θ_R (AGB) and any further growth would be accompanied by the movement of the line of triple contact over the solid surface at constant θ_R (A'HB').

In the case of the tests carried out in this work, the water was saturated with air at ≈ 1 atmosphere and the pressure in the liquid was atmospheric. Therefore, any Harvey nuclei present in the system would have exhibited a flat interface (AB) and the subsequent increase in the concentration of dissolved air produced by the addition of supersaturated water would have caused it to become concave towards the apex (AEB) and to grow by the diffusion of air from solution into the cavity. If the solution contains sufficient dissolved air, the cavity will grow and its buoyancy will increase, resulting in the eventual flotation of the bubble-particle aggregate provided that the force of adhesion between

them is sufficiently great.

From the analysis of the growth of Harvey nuclei outlined above it follows that the condition for their growth is the existence of a contact angle (θ_A, θ_R) between air meniscus and solid surface. This condition explains why no bubble formation was observed in hydrophilic minerals since it is likely that upon immersion in water all crevices and cracks liable to contain gas nuclei are easily wetted by the liquid. It is probable though, that if some localized hydrophobic contamination is present in those crevices, the mineral may retain adsorbed air which would be available for bubble formation upon supersaturation. Nevertheless, the growth of these air cavities to a size capable of floating mineral particles would only be possible if the hydrophilic mineral has been conditioned with a collector so that a receding contact angle (θ_R) can be established. This behaviour was clearly exemplified by the localized bubble formation observed for ferric hydroxide/quartz flocs which readily lost their attached air, and by tests in various other systems in which flotation only occurred in the presence of dodecylamine.

Regarding the source of Harvey nuclei in these experiments, it would seem unlikely that they would have been only due to air entrapped in cavities in the quartz (or cassiterite) surface, as these are basically hydrophilic solids. Another complementary source of gas nuclei could have been air which was 'picked up' by the hydrophobic mineral particles during the conditioning period. This could have been possible due to the high rate of stirring applied which resulted in some air being entrained into the suspension and because the particles reaching the surface of the suspension would be briefly exposed to air. In this connection it is of interest to recall that flocculation of the hydro-

phobic particles resulted in higher recovery rates through air supersaturation than when the particles were smaller. A probable reason could be that big flocs provided a larger interfacial area to pick up air than single unflocculated particles (methylated silica) or much smaller flocs (cassiterite/Aeropromoter 845). Also, the results obtained with hydrophobic silica gel particles showed bubble growth to occur on their surfaces only after an injection of microbubbles had been made, i.e. after the particle had picked up air externally.

In connection with the source of Harvey nuclei, the fact that the experimental procedure of most vacuum flotation tests reported in the literature involve the mixing or stirring of the pulp with a high degree of turbulence, is also of interest. The flotation of minerals by bubbles produced by the application of a vacuum (vacuum flotation) is most likely to proceed through the growth of Harvey nuclei but their role has not been usually recognized in the literature. Urban (80) considered that gas inclusions in the minerals could also be a source of Harvey nuclei if the conditions prevailing in the wet-grinding stage were favourable. He also proposed that tribonucleation ('de novo' nucleation caused by the rubbing or separation of two solid surfaces in the presence of supersaturated liquids) could result in the formation of bubbles in agitated mineral suspensions.

The results obtained for the influence of the degree of supersaturation on the flotation of quartz flocs from supersaturated solutions are consistent with the hypothesis of bubble formation through the growth of Harvey nuclei. Hence, flotation was faster for higher degrees of supersaturation which is consistent with the fact that the rate of growth of a curved gas/liquid interface by gas diffusion is proportional to the degree of gas supersaturation (73).

The influence of bubble formation from supersaturated solutions via the growth of Harvey nuclei on the mechanism of bubble-particle attachment in dissolved air flotation was found to depend on the level of residual supersaturation of the liquid. The results of studies carried out by Urban (80) showed that at 40 psig the amount of gas evolved was very close to the theoretical amount predicted by Henry's law. Thus all these dissolved air flotation studies were performed under conditions in which bubble-particle attachment occurred as the result of only hydrodynamic bubble-particle collisions.

The importance of bubble formation from Harvey nuclei in the mechanism of bubble-particle attachment in a dissolved air flotation process would depend on the kind of pressurization system used. In the recycle effluent system (Figure 1.1 (c)) where the microbubbles are generated at the pressure reduction device (80), the occurrence of this mechanism will be primarily determined by the supersaturation of the water after the formation of the microbubbles and by the flotation time. The residual supersaturation of the liquid will be a function of (a) the degree of saturation of the influent, (b) the efficiency of the saturator, (c) the efficiency of the pressure reduction device in releasing all dissolved air as microbubbles, and (d) the volume ratio between the recycled effluent and the influent. Calculations carried out on the basis of the results obtained in Figure 8.7 showed that residual supersaturations of the same order of magnitude as those which led to significant flotation in this work can easily be obtained in practice. Also, Roberts et al (96) tested five DAF plants in operation in the USA and found that none of them was supplying more than 60% of the theoretical amount of air as bubbles at the operating saturation pressure (whether the other 40% was present as dissolved air is not known). However,

given that the saturation pressures used in practice never exceed 60 psig, the factor flotation time appears as the controlling variable in determining flotation through this mechanism as the rate of growth of bubbles from supersaturated solution is slow for saturation pressures below 60 psig (Figure 8.6).

In systems where part of or the whole influent is pressurized (Figure 1.1 (a) and (b)) there would appear to be greater chances for the occurrence of bubble growth from supersaturated solution as the degree of supersaturation experienced by the solids is considerably greater than those obtained with the recycle pressurization system. However, there is very little information on these kinds of systems in the literature and therefore it is difficult to assess the importance of this bubble-particle attachment mechanism in those DAF systems.

It should be stressed, nonetheless, that the primary factor in determining the possible contribution of bubbles forming from supersaturated solution to the bubble-particle attachment mechanism in both pressurization systems would be the existence of Harvey nuclei and the hydrophobicity of the solid surfaces. These tests have shown that a high degree of hydrophobicity is required for flotation through the growth of Harvey nuclei, and that systems which would be easily floated by the DAF microbubbles (quartz/ferric hydroxide flocs) would not exhibit floatability by bubbles forming from supersaturated solution. Thus it would appear that the main limitations for the occurrence of this bubble-particle attachment mechanism in current dissolved air flotation operations would arise from the surface characteristics of the suspended phases treated by the process.

Chapter 9. SUMMARY AND CONCLUSIONS

9. SUMMARY AND CONCLUSIONS

An investigation was made into the possibility of employing the dissolved air flotation process for the selective recovery of fine mineral particles. The system studied involved the separation of finely-divided cassiterite from a suspension of quartz particles in a batch dissolved air flotation system. The mechanism of bubble-particle attachment in dissolved air flotation was studied and a basis for selectivity was established by correlating the floatability of these oxide minerals with their interfacial properties in the presence of cationic and anionic collectors. Electrokinetic, adsorption density, stability and dissolved air flotation measurements were made to study the mechanism of adsorption of sodium dodecyl sulphate and sodium sulphosuccinamate (as a commercial solution, Aeropromoter 845) on cassiterite and stannic oxide; similar measurements were carried out on quartz in the presence of dodecylamine. Dissolved air flotation separation tests were performed on cassiterite/quartz suspensions and the influence of various parameters and surface chemical conditions on the recovery and selectivity of the separations was determined.

From the results of these studies the following conclusions have been made:

1. Regarding the mechanism of bubble-particle attachment in dissolved air flotation the studies showed that:

   a) Hydrophilic solids, whether dispersed or aggregated did not float by the dissolved air flotation process.

   b) The suspended phase responded to dissolved air flotation when it exhibited a degree of hydrophobicity. The degree of

hydrophobicity required for floatability appeared to be influenced by the physical characteristics of the aggregates forming the dispersed phase. Hydrophilic destabilized systems composed of flocs with large interfacial area and loose structures (quartz/ ferric sulphate, precipitated silica/polyacrylamide flocculant) showed floatability with minor degrees of hydrophobic contamination.

c) The role of hydrophobicity in dissolved air flotation indicated that the mechanism of bubble-particle attachment relies on the adhesion of the microbubbles to the particles, i.e. the establishment of a contact angle between the gas and solid phases.

d) The adhesion of a microbubble to a particle in these dissolved air flotation experiments occurred as the result of a collision between microbubble and particle.

e) Adhesion produced by the formation of air bubbles from super-saturated solution on to the solid phase was found not to be significant in these studies. The formation of bubbles from super-saturated solution occurred when the solid was hydrophobic and contained undissolved gas on its surface to act as nuclei for bubble growth (Harvey nuclei). Flotation of minerals through this mechanism of bubble-particle attachment was found to depend on the degree of hydrophobicity, the presence of Harvey nuclei on the suspended phase and on the degree of supersaturation at which the system was subjected.

f) No evidence was found for the existence of 'trapping' or 'absorption' of microbubbles into flocs in so far as these postulated mechanisms of bubble-particle attachment do not require the adhesion of an air bubble to the suspended phase.

2. The studies carried out on the dissolved air flotation of fine quartz and cassiterite particles indicated that:

a) Dissolved air flotation of quartz and cassiterite occurred only in the presence of a collector which adsorbed at the oxide mineral/aqueous solution interface. The recovery of these oxide minerals by dissolved air flotation was dependant upon the concentration of collector and the pH value. At a given pH value, both minerals could be floated by dissolved air flotation only within a range of collector concentrations, any overdosage leading to the suppression of flotation. Quartz was floatable with dodecylamine in the range of pH values tested (6.0 - 9.5). Cassiterite floated significantly in the presence of the anionic collectors used (sodium dodecyl sulphate and Aeropromoter 845) only at pH values below the isoelectric point of the oxide (pH 4.2).

b) The recovery of quartz by dissolved air flotation was a maximum for adsorption densities of dodecylamine between about 10 and 100% of a statistical close-packed vertically orientated monolayer depending on the pH value. Dissolved air flotation of cassiterite in the presence of sodium dodecyl sulphate was maximum at adsorption densities of the surfactant corresponding to between 2 - 10% (pH 3.0) and 7 - 50% (pH 2.0) of a close-packed vertically orientated monolayer of alkyl sulphate ions.

c) Dissolved air flotation of the quartz/dodecylamine system was maximum at pH 6.0 at the concentration of dodecylamine which brought the electrophoretic mobility to zero whereas at pH 9.5 maximum flotation occurred for electrophoretic mobility values between - 3.2 and 0 $\mu m\ sec^{-1}/volt\ cm^{-1}$. In the case of the cassiterite/sodium dodecyl sulphate and cassiterite/Aeropromoter 845

systems, maximum recovery always occurred for negative values of the electrophoretic mobility of the mineral particles, i.e. when surfactant adsorption was superequivalent. The mobility values were usually between - 2 and -4 $\mu m\ sec^{-1}/volt\ cm^{-1}$ which corresponded to zeta-potential values between about -26 and -51 mV.

d) As a rule, dissolved air floation was maximum when the suspension exhibited a maximum degree of destabilization. Exceptions to this rule were obtained when the aggregates were hydrophilic and when the particles were dispersed but still hydrophobic. Particle aggregation was determined to be a prerequisite for dissolved air flotation due to its influence on the mechanism of bubble-particle attachment and on the kinetics of the flotation process, and because it allows a more efficient utilization of the dissolved air.

e) Various parameters of the dissolved air flotation system were found to affect the recovery of minerals by dissolved air flotation. The more important variables were: (i) stirring, because of its effects on the formation of flocs and on providing good microbubble-floc mixing, (ii) solids concentration; high values leading to a decrease in mineral recovery probably because of the formation of large aggregates, (iii) saturation pressure, which determines the amount of dissolved air available for flotation. Under these experimental conditions it was found to be critical only below 40 psig (377 kPa), and (iv) injection pressure, which determines the amount of dissolved air which will come out of solution as microbubbles. This was most significant below 20 psig (239 kPa) for water saturated at 40 psig. The stability of the floated product is unlikely to be a problem in flotation of hydrophobic mineral particles.

3. The isoelectric points of quartz and cassiterite occurred at about pH 2.4 and 4.2 respectively. The isoelectric point of a synthetic stannic oxide sample was found to occur at pH 4.0. From the adsorption and electrokinetic measurements on cassiterite and stannic oxide it was estimated that about 1 - 0.1% of the surface hydroxyl groups were charged at pH 2.0 - 3.0.

4. Dilute suspensions of quartz and cassiterite were destabilized by the addition of cationic and anionic surface active agents respectively. Suspension destabilization depended on surfactant concentration and pH value and was associated with a decrease in the electrophoretic mobility of the particles to values near neutrality. Similarly, the restabilization of the suspension corresponded with values of the electrophoretic mobility of between - 2 and -4 $\mu m\ sec^{-1}$/ volt cm^{-1} for cassiterite and for quartz at 2.75 and 1.0 $\mu m\ sec^{-1}$/ volt cm^{-1} for pH 6.0 and 9.5 respectively. Maximum destabilization occurred at the point of zeta-potential reversal for quartz but for cassiterite it occurred at negative values of the electrophoretic mobility. The destabilizing action of dodecylamine on quartz and of sodium dodecyl sulphate and Aeropromoter 845 on cassiterite is in qualitative agreement with the principles of the DLVO theory for the stability of lyophobic colloids; suspension destabilization occurring when the specific adsorption of the surfactant reduces the electrostatic double layer repulsive forces so that the van der Waals attractive forces between the particles can prevail.

5. With regard to the mechanism of adsorption of these surface-active agents on quartz and cassiterite the following points were

established:

a) The mechanism of adsorption of dodecylamine on quartz and of sodium dodecyl sulphate on cassiterite is primarily the coulombic attraction of the surfactant ions for the opposedly charged surface followed by chain-chain interactions at high adsorption densities.

b) The adsorption of dodecylamine on quartz at pH 6.0 was found to proceed in two steps. At low surfactant concentrations it is postulated that the ions adsorbed through ionic exchange in the diffuse layer until at a critical concentration (the critical hemimicelle concentration) they became specifically adsorbed in the Stern layer through hydrophobic chain-chain associations (hemimicelles). The onset of hemimicellization showed up as an abrupt change in both electrophoretic mobility and adsorption density.

c) The adsorption of sodium dodecyl sulphate on cassiterite and stannic oxide was found to depend on the pH value, higher adsorption densities being obtained at the more acid pH values for a given equilibrium concentration. Surfactant adsorption was also found to proceed in two steps as in the quartz/dodecylamine system but the onset of hydrophobic bonding, as extrapolated from the electrokinetic studies, did not coincide with that obtained from the adsorption measurements. The free energy of hemimicellization per mole of CH_2 groups was calculated at the pzr to be -0.70 RT for cassiterite at pH 2.0 and 3.0, and -0.61 and -0.55 RT for stannic oxide. Maximum adsorption was a function of the pH value for both samples and varied between 70 and 105% (at pH 1.4) of a close-packed, vertically orientated monolayer of alkyl sulphate

ions. The adsorption isotherms tended to level off as the critical micelle concentration of the surfactant was reached in the bulk solution. The formation of a reversely orientated bilayer of surfactant ions at saturation is consistent with the results.

d) Electrokinetic, stability and dissolved air flotation measurements on the cassiterite/Aeropromoter 845 system gave a set of results similar to those obtained for cassiterite/sodium dodecyl sulphate and it was therefore concluded that both surfactants adsorbed on cassiterite through the same mechanism.

e) From electrokinetic and adsorption measurements it was shown that surfactant adsorption occurred at and above the isoelectric points of cassiterite and stannic oxide. The reasons for this behaviour are not clear but it is considered that it is unlikely to be the effect of surfactant chemisorption on the mineral surface.

6. The tests carried out on the separation of cassiterite from quartz by dissolved air flotation showed that:

a) The recovery of cassiterite from quartz by dissolved air flotation with Aeropromoter 845 as collector was dependent upon pH and collector concentration in the same way as had been found for the cassiterite/Aeropromoter 845 system. The best compromise between recovery and grade of concentrate occurred at pH 3.0 for a collector addition of 5 mg/l A845 (60% recovery, grade 17% Sn; feed grade 7.38% Sn). The addition of a kerosene/Aeropromoter 845 emulsion at various concentration ratios resulted in much higher recoveries and grades (75% recovery, grade 37% Sn). This was attributed to the effect of the oil in increasing the hydrophobicity and degree of aggregation of the cassiterite flocs.

b) The main factors contributing to a low selectivity in the separations were heterocoagulation of cassiterite and quartz particles, collector adsorption on quartz particles, entrainment of quartz particles in the froth and the recovery of the floated product. The selectivity of the separations was found to increase in the presence of a modifier for quartz and when higher rates of stirring were applied during the flotation stage. Higher levels of selectivity could be obtained if a second dissolved air flotation stage was incorporated in to the process (70% recovery, grade 60% Sn). Separations of cassiterite from quartz at high solids concentration led to a decrease in recovery but the selectivity remained high.

7. The application of dissolved air flotation to the selective separation of fine mineral particles was shown to be possible for the case of a binary cassiterite/quartz suspension. The effectiveness of the separations was found to depend on an adequate control of the surface chemistry of the system in order to render the valuable particles hydrophobic and ensure that they exhibit a degree of aggregation. The separation of cassiterite from quartz by dissolved air flotation gave values of recovery and selectivity comparable to those obtained by selective flocculation and by oil flotation. Further testing on the recovery of cassiterite from a finely-divided tin ore by dissolved air flotation is therefore recommended.

APPENDICES

Appendix I. Experiments on the formation of microbubbles in dissolved air flotation

Although this research was primarily concerned with the recovery of fine particles by the dissolved air flotation process, various experiments were carried out throughout this work related to the formation of microbubbles in DAF systems.

1. It has been mentioned previously (Chapter 8) that water could be saturated with air at high pressures (40 - 80 psig) and decompressed to atmospheric pressure without signs of bubble formation. This high pressure air-saturated water could be injected through the nozzle at low injection pressures and only a few large bubbles would form in solution. Only when the injection pressure was increased above a critical value (the cavitation inception pressure; about 20 psig for water saturated at 40 psig) did massive microbubble formation occur. Calculations of the pressure drop at the orifice of the pressure reduction nozzle using the Bernouilli equation (at the injection pressure corresponding to the cavitation inception pressure) indicated that microbubble formation was associated with an absolute pressure at the orifice close to zero or above it when the water contained dissolved air. This has also been shown by similar calculations carried out by other workers (80)(81). Thus, the experiments demonstrated that a sharp pressure drop at the orifice was a prerequisite for the dissolved air to come out of solution as microbubbles.

2. The need for a sharp pressure drop at the orifice was also shown

by tests on microbubble formation carried out using capillary tubes as pressure reduction devices. A capillary tube of 2 mm bore was used to inject water saturated at 40 psig into a beaker where microbubble formation was observed. The results of various injections indicated that the formation of microbubbles was dependent upon the length of the capillary. Thus no microbubbles were detected for tubes whose length was 40, 16 and 12.5 cm whereas at 3.5 cm a good cloud of microbubbles was observed.

This phenomenon may be interpreted in terms of the dependence of the pressure reduction characteristics on capillary length. As the capillary length increased, the water flow-rate diminished (at constant injection pressure) making the pressure drop per unit capillary length ($\Delta p/L$) smaller for the longer capillary tubes. This pressure drop is given by:

$$\frac{\Delta p}{L} = \frac{2 f \rho v^2}{D} \qquad (I.1)$$

where f = friction factor

ρ = fluid density

v = mean fluid velocity (calculated from flow-rate measurements)

D = internal capillary diameter

Calculations of $\Delta p/L$ for the experiments at capillary lengths of 40 and 3.5 cm gave values of about 0.08 and 0.8 atm/cm. Hence, the failure of the long capillary tubes in producing microbubbles may be attributed to the more gradual pressure reduction at which the air-saturated water is exposed compared with the sharper pressure decrease occurring in the short capillary.

3. Other tests showed that a sharp pressure reduction was not the only prerequisite for microbubbles to form. Hence, experiments carried out on water saturated at 40 psig and injected at the saturation pressure would give no microbubbles if the nozzle was removed. Similar findings have been reported by other authors (80)(81). The latter authors showed that injection of saturated water through Venturi tubes gave good microbubble formation but if the Venturi was cut at the neck no microbubbles would form independently of the injection pressure.
Urban (80) has interpreted this phenonenon in terms of the critical size required for a gas cavity to grow to microbubble size in solution. He showed that in the presence of the nozzle any incipient cavity formed at the orifice would grow at the mouth of the nozzle to a size of the order of magnitude of the theoretical critical size required for survival upon dilution in the flotation cell (d_s in section 2.3.3). On the other hand, in the absence of the nozzle the gas cavities would be below the critical size upon injection in the cell and would then dissolve. Thus the function of the nozzle would be to provide time for the bubbles to grow in supersaturated solution to a size which would enable them to grow when diluted in the cell.

4. As the previous experiments showed that conditions downstream from the orifice would influence the formation of microbubbles, nozzle geometry would therefore be expected to play a role in determining microbubble characteristics. This was shown to be true by Gochin and Kitchener (81) for a range of Venturi tubes of diverse shapes. Also, the present author measured the rise-time

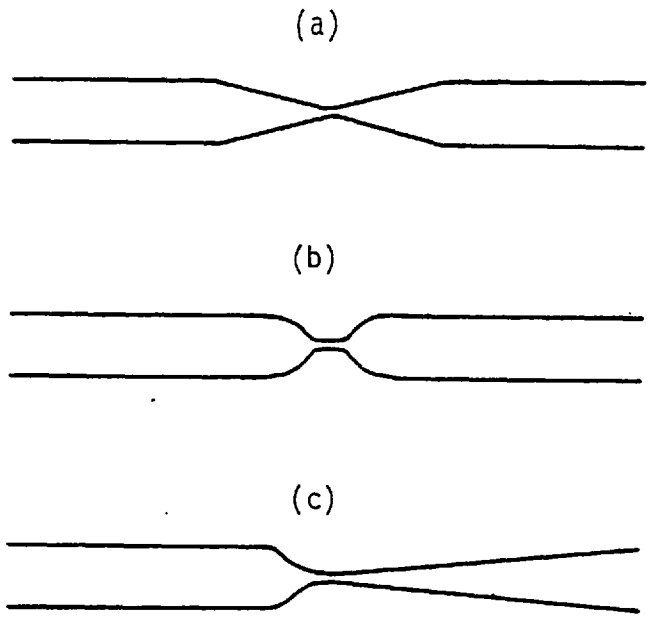

Figure I.1. Venturi tubes used for studies on microbubble formation in DAF

of microbubbles produced in the Venturi tubes shown in Figure I.1 and found that Venturi (a) gave consistently higher rise-times than (b), 240 and 170 seconds respectively. Lower rise-time values are usually associated with a larger microbubble size distribution and with a smaller bubble-number density (section 2.3.4.3). The larger microbubble size distribution obtained for the second Venturi was attributed to the possible formation of eddies just downstream from the constriction. Nascient cavities would then circulate in these eddies and having a longer time in contact with the supersaturated water would grow to a larger size. As these larger bubbles consume more dissolved air the overall result would also be a lesser number of microbubbles. Big bubbles can be seen emerging from all pressure reduction devices used in practice (91), even in the case of a Venturi tube like (a).

5. Given the deleterious influence of big bubbles in DAF systems, an experimental study was carried out in their formation in the

Venturi tube (c) of Figure I.1 as a function of saturation and injection pressures. The tests were conducted by injecting saturated water through the Venturi vertically downwards into a large vessel filled with tap water. Tests were carried out at various saturation pressures and at constant saturation pressure varying the pressure of injection. From these tests the following effects were noticed:

a) Bib bubbles did not form in the throat of the Venturi tube but originated in the bulk water. They were seen to form in the ejecting flow of supersaturated water and to rise quickly out of water, unlike the microbubbles which tended to disperse uniformly throughout the vessel.

b) Big bubbles were observed to form at a distance from the mouth of the Venturi which depended on saturation and injection pressures. The higher the value of both pressures, the shorter the distance at which large bubbles appeared in solution. Low values of saturation and injection pressure resulted in less big bubbles emerging from the jet of supersaturated water but also caused a decrease in the formation of microbubbles.

c) At constant saturation pressure the amount of big bubbles increased with increasing injection pressure whereas their size was largest for low or high injection pressures. Thus for a given amount of dissolved air there was an optimum injection pressure in terms of fewer and smaller big bubbles.

These experiments showed that formation of undesirable big bubbles is a feature of all pressure reduction devices, even those exhibiting optimum hydrodynamic characteristics downstream of the point of pressure reduction. The formation of big bubbles in

these devices may be attributed to the fact that the jet of supersaturated water is not instantaneously diluted in the vessel and therefore some microbubbles remain in contact with supersaturated water for longer time than others. Thus, a way of preventing big bubble formation in these pressure reduction devices would be to dilute the jet of supersaturated water as soon as the microbubbles have reached the critical size for survival in the vessel upon dilution.

7. This set of results is in general agreement with the principles outlined in Chapter 2 for microbubble formation in dissolved air flotation systems. Hence, pressure drop at the pressure reduction device, saturation and injection pressures, and nozzle geometry downstream of the constriction appeared to be critical variables in determining the characteristics of the microbubble cloud. The design of a pressure reduction device in a DAF system should contemplate the means to dilute effectively the ejecting flow of supersaturated water and to avoid creating zones (vortices, eddies) where big bubbles may form. From the results of Chapter 8 (section 3), it would also appear that such a pressure reduction device should be aimed at releasing all dissolved air out of solution as a low residual water supersaturation would be unlikely to contribute to the flotation process.

Appendix II. Calculation of the surface charge of cassiterite and stannic oxide

From the principle of electroneutrality in the double layer it follows that:

$$\sigma_o + \sigma_\delta + \sigma_d = 0 \qquad \text{(II.1)}$$

where σ_o = surface charge density

σ_δ = charge density in the Stern layer

σ_d = charge density in the diffuse layer

in the absence of specific adsorption $\sigma_\delta = 0$ and

$$\sigma_o = -\sigma_d \qquad \text{(II.2)}$$

and thus the surface charge can be calculated from the charge density in the diffuse layer which for a flat diffuse layer in a symmetrical z-z electrolyte is given by (125):

$$\sigma_d = (8\,\varepsilon\,n\,k\,T)^{\frac{1}{2}} \sinh\left(\frac{ze\psi\delta}{2kT}\right) \qquad \text{(II.3)}$$

Values of σ_d can be computed assuming that ψ_δ is equal to the zeta-potential measured during the electrokinetic studies as a function of pH (Figures 6.1 and 6.11). The constants in equation II.3 are:

n = molarity $\times 10^3 \times 6.02 \times 10^{23}$ (ions/m^3); the molarities used were 10^{-2} and 10^{-3} for pH 2.0 and 3.0 respectively

ε = $80 \times 8.85 \times 10^{-12}$ ($J^{-1}C^{-2}m^{-1}$)

kT = 0.4×10^{-20} (J)

kT/ze = 25 ; and the zeta-potential (ζ) may be calculated from

ζ = 12.83 x (electrophoretic mobility)(mV)

so that at pH 2.0 $\sigma_d = 1.17 \times 10^{-2} \sinh (0.02 \ \zeta) \ Cm^{-2}$ (II.4)

and at pH 3.0 $\sigma_d = 3.69 \times 10^{-3} \sinh (0.02 \ \zeta) \ Cm^{-2}$ (II.5)

On the other hand, at the concentration of surfactant that brings the zeta-potential to zero there is no charge in the diffuse layer and therefore,

$$\sigma_o = -\sigma_\delta \qquad \text{(II.6)}$$

and assuming that all charge in the Stern layer corresponds to specifically adsorbed surfactant ions, σ_δ can be calculated from:

$$\sigma_\delta = z \ F \ \Gamma_o \ (C/cm^2) \qquad \text{(II.7)}$$

where Γ_o = adsorption density of surfactant ions at the point of zeta-potential reversal (moles/cm^2)

F = Faraday constant ≡ 96500 C/mol

The results of the calculations have been tabulated below:

	pH	zeta-potential (mV)	σ_d ($\mu C/cm^2$)	Γ_o (moles/cm^2)	σ_δ ($\mu C/cm^2$)
Cassiterite	2.0	47.47	1.28	8.7×10^{-12}	0.84
"	3.0	30.79	0.24	4.4×10^{-12}	0.42
Stannic oxide	2.0	43.62	1.16	1.2×10^{-11}	1.16
" "	3.0	33.36	0.26	1.7×10^{-12}	0.16

Appendix III. Photographic study of flotation by bubble forming from supersaturated solution

The study was conducted on preformed flocs in a spectrophotometer cell by adding water saturated with air at 40 psig (377 kPa). The flocs were quartz flocculated with $CuSO_4$/N100 and rendered hydrophobic by the addition of dodecylamine (section 8.3). The flocs were placed in the cell (No. 1 in the photographic sequence) and then about 1.5 ml of supersaturated water was added (No. 2). This constituted a supersaturation of about 80% in the dissolved air content of the water. The width of the cell was 1.7 cm (5 ml total volume). The photographic sequence was taken with a camera equiped with bellows attachment at time intervals of 10 - 15 s.

From the sequence, the following points may be established:

a) Bubbles formed immediately after the addition of the supersaturated water (No. 2).

b) Floc flotation was a rapid process, the first floating floc being observed at 20 s (No. 3). Bubble size was estimated to be about 100 μm.

c) Flotation of large floc structures began at a bubble size of about 200 - 250 μm (60 s) as estimated from the size of the bubbles attached to the wall of the cell. Note the accumulation of floated material at the top of the cell (No. 7), and the bubbles lifting the floc in photograph No. 8.

d) Total flotation was obtained in 230 s and the bubble size at that time was estimated to be of the order of 500 μm (No. 12).

e) Bubbles only formed at solid surfaces, no bubbles were observed to appear in the bulk solution and almost all bubbles appearing in the

sequence can be traced back to the beginning of the test (No. 2).

f) The large majority of bubbles that formed on the walls of the cell did it in the upper part, that is, in that part of the cell which had been exposed to air prior to the addition of the supersaturated water.

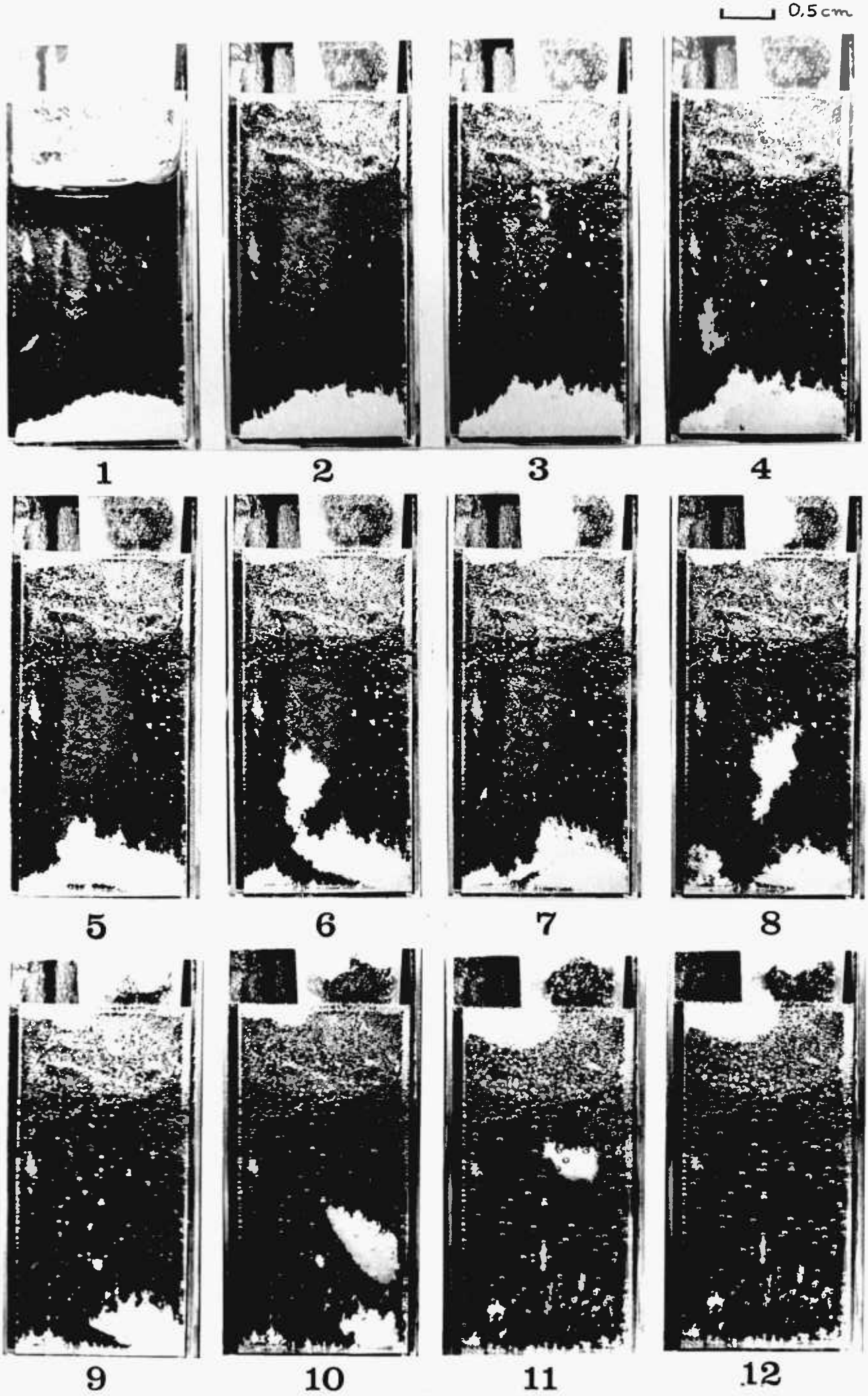
0.5 cm
1
2
3
4
5
6
7
8
9
10
11
12

REFERENCES

REFERENCES

1. GAUDIN, A.M., 'Flotation', 2nd ed., McGraw-Hill, New York, 1957.

2. KLASSEN, V.I., and MOKROUSOV, V.A., 'An Introduction to the Theory of Flotation', Butterworths, London, 1963.

3. REHBINDER, P.A., General Course in Colloidal Chemistry, Moscow University, 1949.

4. FUERSTENAU, D.W., and RAGHAVAN, S., Some aspects of the thermodynamics of flotation, in 'Flotation. A.M. Gaudin Memorial Volume', ed. Fuerstenau, M.C., I, 1976, 21-65.

5. MELLGREN, O., GOCHIN, R.J., SHERGOLD, H.L., and KITCHENER, J.A., Thermochemical measurements in flotation research, Proc. 10th I.M.P.C., London, 1973, 451-472.

6. DE BRUYN, P.L., OVERBEEK, J.Th.G., and SCHUHMANN, R., Flotation and the Gibbs adsorption equation, Min. Eng., 6, 1954, 519-523.

7. DE BRUYN, P.L., and AGAR, G.E., Surface chemistry of flotation, in 'Froth Flotation - 50th Anniversary Volume', ed. Fuerstenau, D.W., A.I.M.E., New York, 1962, 91-138.

8. DERJAGUIN, B.V., and DUKHIN, S.S., Theory of flotation of small and medium sized particles, Trans. I.M.M., 70, 1961, 221-226.

9. SAMYGIN, V.D., DERJAGUIN, B.V., and DUKHIN, S.S., Investigation of the Dorn effect on oil bubbles, Colloid J. USSR, 26, 1964, 424-431.

10. BLAKE, T.D., Current problems in the theory of froth flotation, Symposium on Bubbles and Foams, Nürnberg, Germany, Sept. 1971, V.D.I. Beriche, 182, 1972, 117-121.

11. LASKOWSKI, J., Particle-bubble attachment in flotation, Min. Sci. Eng., 6 (4), 1974, 223-235.

12. SVEN-NILSSON, I., Effect of contact time between mineral and air bubbles on flotation, Kolloid Z., 69, 1934, 230-232.

13. EVANS, L.F., Bubble-mineral attachment in flotation, Ind. Eng. Chem., 416, 1954, 2420-2424.

14. EIGELES, M.A., and VOLOVA, M.L., Kinetic investigation of effect of contact time, temperature and surface condition on the adhesion of bubbles to mineral surfaces, Proc. 5th I.M.P.C., London, 1960. I.M.M., London, 271-284.

15. FRUMKIN, A.N., Phenomena of wetting and the adhesion of bubbles. I., Zh. Fiz. Khim., 12, 1938, 337-345.

16. FRUMKIN, A.N., and GORODETSKAJA, A., Phenomena of wetting and the adhesion of bubbles. II., Acta Physicochim U.R.S.S., 9, 1938, 327-340.

17. SHCHERBAKOV, L.M., Thermodynamics of thin liquid layers, Kolloidn. Zh., 22, 1960, 111-116.

18. KITCHENER, J.A., Surface forces in thin liquid films, Endeavour, 22, 1963, 118-122.

19. DERJAGUIN, B.V., and KUSAKOV, M.M., Experimental investigation of solvation of surface and its application to the development of a mathematical theory of lyophilic colloids, Bull. Acad. Sci. U.R.S.S. Ser. Chem., 5, 1937, 1119-1150.

20. TOMLINSON, H.S., and FLEMING, M.G., Flotation rate studies, Proc. 6th I.M.P.C., Cannes, 1963, Pergamon Press, Oxford, 1965, 563-573.

21. LASKOWSKI, J., and ISKRA, J., Role of capillary effects in bubble-particle collision in flotation, Trans. I.M.M., 79, 1970, C6-C10.

22. WARK, I., The physical chemistry of flotation. I. The significance of contact angle in flotation, J. Phys. Chem., 37, 1933, 623-630.

23. KABANOV, B., and FRUMKIN, A.N., Über die Grösse elektrolytisch entwickelten Gasblasen, Z. Phys. Chem., Abt. A., 165a, 1933, 433-452.

24. 'Froth Flotation - 50th Anniversary Volume', ed. Fuerstenau, D.W., A.J.M.E., New York, 1962.

25. OTTLEY, D.J., Technical, economic and other factors in the gravity concentration of tin, tungsten, columbium and tantalum ores, Min. Sci. Eng., 11, 1979, 99-121.

26. MARABINI, A.M., Study of adsorption of salicylaldehyde on cassiterite, Trans. I.M.M., 87, C76-78.

27. BUSTAMANTE, H.A., The flotation of zinc oxide minerals with chelating agents, Ph.D. Thesis, University of London, 1979.

28. DOREN GATTAS, A., VAN LIERDE, A., and DE CUYPER, I., Influence d'un tensio-actif non ionique sur la flottation de la cassiterite', Proc. XII I.M.P.C., I, Warsaw, 1979.

29. BOGDANOV, O.S., YEROPKIN, Y.I., KOLTUNOVA, T.E., KHOBOTOVA, N.P., and SCHTCHUKINA, N.E., Hydroxamic acids as collectors in the flotation of wolframite, cassiterite and pyrochlore, Proc. 10th I.M.P.C., London, 1973, 553-564.

30. FUERSTENAU, M.C., HARPER, R.W., and MILLER, J.D., Hydroxamate vs. fatty acid flotation of iron oxide, Trans. A.I.M.E., 247, 1970, 69-73.

31. TRAHAR, W.J., and WARREN, L.J., The floatability of very fine particles, Int. J. Min. Proc., 3, 1976, 103-131.

32. COLLINS, D.N., and READ, A.D., The treatment of slimes, Min. Sci. Eng., 3, 1971, 19-31.

33. JAMESON, G.J., NAM, S., and MOO YOUNG, M., Physical factors affecting recovery rates in flotation, Min Sci. Eng., 9, 1977, 103-118.

34. MONCRIEFF, A.G., and LEWIS, P.J., Treatment of tin ores, Trans. I.M.M., 86, 1977, A56-60.

35. STRATTON-CRAWLEY, R., Displacement of water from a titanium dioxide surface by an organic liquid, Ph.D. Thesis, University of London, 1977.

36. GAUDIN, A.M., SCHUHMANN, R., and SCHLECHTEN, A.W., Flotation kinetics. II. The effect of size on the behaviour of galena particles, J. Phys. Chem., 46, 1942, 902-918.

37. MORRIS, T.M., Measurement and evaluation of the rate of flotation as a function of particle size, Trans. A.I.M.E., 193, 1952, 794-798.

38. BUSHELL, C.H.G., Kinetics of flotation, Trans. A.I.M.E., 223, 1962, 266-278.

39. DE BRUYN, P.L., and MODI, H.J., Particle size and flotation rate of quartz, Trans. A.I.M.E., 205, 1956, 415-419.

40. FLINT, L.R., and HOWARTH, W.J., The collision efficiency of small particles with spherical air bubbles, Chem. Engng. Sci., 26, 1971, 1155-1168.

41. REAY, D., and RATCLIFF, G.A., Removal of fine particles from water by dispersed air flotation: effects of bubble size and particle size on collection efficiency, Can. J. Chem. Engng., 51, 1973, 178-185.

42. REAY, D., and RATCLIFF, G.A., Experimental testing of the hydrodynamic collision model of fine particle flotation, Can. J. Chem. Engng., 53, 1975, 481-486.

43. COLLINS, G.L., and JAMESON, G.J., Experiments on the flotation of fine particles - the influence of particle size and charge, Chem. Engng. Sci., 31, 1976, 985-991.

44. COLLINS, G.L., and JAMESON, G.J., Double-layer effects in the flotation of fine particles, Chem. Engng. Sci., 32, 1977, 239-246.

45. ANFRUNS, J.P., and KITCHENER, J.A., The rate of capture of small particles in flotation, Trans. I.M.M., 86, 1977, C9-15.

46. SUTHERLAND, K.L., Physical chemistry of flotation. XI. Kinetics of the flotation process, J. Phys. Chem., 52, 1948, 394-425.

47. COLLINS, G.L., Dispersed air flotation of fine particles, Ph.D. Thesis, University of London, 1975.

48. DUKHIN, S.S., and RULEV, N.N., Hydrodynamic interaction between a solid spherical particle and a bubble in the elementary act of flotation, Coll. J. U.S.S.R., 39, 1977, 231-236.

49. RULEV, N.N., DERJAGUIN, B.V., and DUKHIN, S.S., Kinetics of the flotation of fine particles by a group of bubbles, Coll. J. U.S.S.R., 39, 1977, 267-274.

50. DERJAGUIN, B.V., DUKHIN, S.S., and RULEV, N.N., Importance of hydrodynamic interaction in the flotation of fine particles, Coll. J. U.S.S.R., 38, 1976, 227-232.

51. DERJAGUIN, B.V., DUKHIN, S.S., and RULEV, N.N., Thin-film capillary hydrodynamic methods in the theory of flotation, Coll. J. U.S.S.R., 39, 1977, 926-933.

52. DERJAGUIN, B.V., RULEV, N.N., and DUKHIN, S.S., Effect of the particle size on heterocoagulation in an elementary flotation act, Coll. J. U.S.S.R., 39, 1977, 598

53. DERJAGUIN, B.V., DUKHIN, S.S., RULEV, N.N., and SEMENOV, P.V., Influence of bubble surface blocking on the hydrodynamic interaction with particles in the elementary act of flotation, Coll. J. U.S.S.R., 38, 1976, 233-238.

54. SAMYGIN, V.D., CHERTILIN, B.S., and NEBERA, V.P., Effect of bubble size on the floatability of inertial particles, Coll. J. U.S.S.R., 39, 1977, 965-970.

55. BLAKE, T.D., and KITCHENER, J.A., Stability of aqueous films on hydrophobic methylated silica, J. Chem. Soc., Faraday Trans. J., 68, 1972, 1435-42.

56. RULEV, N.N., OSOSKOV, V.K., and SKRYLEV, L.D., Capture efficiency of small emulsion droplets by air bubbles during flotation, Coll. J. U.S.S.R., 39, 1977, 522

57. KLASSEN, V.I., and MOKROUSOV, V.A., 'An Introduction to the Theory of Flotation', Butterworths, London, 1963, p 141.

58. RULEV, N.N., Efficiency of particle capture in non-inertial flotation, Coll. J. U.S.S.R., 40, 1978, 747-756.

59. KLASSEN, V.I., and MOKROUSOV, V.A., 'An Introduction to the Theory of Flotation', Butterworths, London 1963, p 142.

60. KLASSEN, V.I., Theoretical basis of flotation by gas precipitation? 5th I.M.P.C., London, 1960, 309-322.

61. HEMMING, M.L., COTTRELL, W.R.T., and OLDFELT, S., Experiences in the treatment of domestic sewage by the microflotation process, 'Flotation for water and waste treatment, A Water Research Centre Conference, Felixstowe, Paper 2, 1960.

62. KUHN, A.T., and HOGAN, P., Electroflotation studies based on cassiterite ores, Trans I.M.M., 88, 1979, C83-87.

63. REES, A.J., RODMAN, D.J., and ZABEL, T.F., Water clarification by flotation - 5, Technical Report TR114, Water Research Centre, Medmenham, Marlow, Bucks., 1979.

64. KOMLINE, T.R., Sludge thickening by dissolved air flotation in the USA, 'Flotation for water and waste treatment', A Water Research Centre Conference, Felixstowe, Paper 7, 1976.

65. BIESINGER, M.G., VINING, T.S., and SHELL, G.L., Industrial experience with dissolved air flotation, Proc. 29th Ind. Waste Conf., Engng. Bull. Purdie University, Ext. Ser. No. 145, I, 1974.

66. MOORE, W.J., 'Physical Chemistry', 4th edition, Longmans, London, 1968.

67. VRABLIK, E.R., Fundamental principles of dissolved air flotation of industrial wastes, Proc. 14th Ind. Waste Conf., Engng. Bull. Purdue University, Ext. Ser. No. 104, 1959, 743-779.

68. 'Lange's Handbook of Chemistry', 12th edition, ed. Dean, J.A., McGraw-Hill, New York, 1979, p 10-3.

69. BRATBY, J., and MARAIS, G.v.R., Saturation performance in dissolved-air (pressure) flotation, Water Research, 9, 1975, 929-936.

70. BRATBY, J., and MARAIS, G.v.R., Flotation, in 'Solid/Liquid Separation Scale-Up', ed. Purchas, D.B., Upland Press, London, 1977.

71. GEHR, R., and HENRY, J.G., Measuring and predicting flotation performance, J. Water Poll. Control Fed., 50, 1978, 203-215.

72. ZABEL, T.F., and HYDE, R.A., Factors influencing dissolved air flotation as applied to water clarification, 'Flotation for water and waste treatment', A Water Research Centre Conference, Felixstowe, Paper 3, 1976.

73. HARVEY, E.N., BARNES, D.K., McELROY, W.D., WHITELEY, A.H., PEASE, D.C., and COOPER, K.W., Bubble formation in animals, I. Physical factors, J. Cell. Comp. Physiology, 24, 1944, 1-22.

74. McDONALD, J.E., Homogeneous nucleation of vapor condensation.
I. Thermodynamic aspects, Am. J. of Physics, 30, 1962, 870-877.
II. Kinetic aspects, Am. J. of Physics, 31, 1963, 31-41.

75. APFEL, R.E., Water superheated to 279.5^{o}C at atmospheric pressure, Nature, 238, 63-64.

76. EBERHART, J.G., The thermodynamic and the kinetic limits of superheat of a liquid, J. Colloid Interf. Sci., 56, 1976, 262-269.

77. HEMMINGSEN, E.A., Supersaturation of gases in water: absence of cavitation on decompression from high pressures, Science, 167, 1493-1494.

78. HEMMINGSEN, E.A., Spontaneous formation of bubbles in gas-supersaturated water, Nature, 267, 141-142.

79. MADDOCK, J.E.L., Research experience in the thickening of activated sludge by dissolved air flotation, 'Flotation for water and waste treatment', A Water Research Centre Conference Felixstowe, Paper 5, 1976.

80. URBAN, M.R., Aspects of bubble formation in dissolved air flotation, Ph.D. Thesis, University of London, 1978

81. GOCHIN, R.J., and KITCHENER, J.A., Mechanism of dissolved air flotation in water treatment, Private communication, 1978.

82. KNAPP, R.T., DAILY, J.W., and HAMMITT, F.G., 'Cavitation', McGraw-Hill, New York, 1970.

83. HUNSAKER, J.C., Cavitation Research, Mech. Engng., 57, 211-216.

84. KNAPP, R.T., Cavitation and nuclei, Trans A.S.M.E., 80, 1958, 1315-1324.

85. VOLLMÜLLER, H., and WALBURG, R., Blasengröße bei der Begasung mit Venturidusen, VDI-Berichte, 182, 1972, 23-29.

86. TAKAHASHI, T., MIYAHARA, T., and MOCHIZUKI, H., Fundamental study of bubble formation in dissolved air pressure flotation, J. Chem. Engng. Japan, 12, 1979, 275-280.

87. DEFAY, R., and PRIROGINE, I., 'Surface Tension and Adsorption', Longmans, London, 1966.

88. WARD, C.A., BALAKRISHNAN, A., and HOOPER, F.G., On the thermodynamics of nucleation in weak gas-liquid solutions, Trans. A.S.M.E., J. Basic Engng., 92, 1970, 695-704.

89. WOOD, R.F., and DICK, R.I., Factors influencing batch flotation tests, J. Water Poll. Control Fed., 45, 1973, 304-315.

90. GULAS, V., LINDSEY, R., BENEFIELD, L., and RANDALL, C., Factors affecting the design of dissolved air flotation systems, J. Water Poll Control Fed., 50, 1978, 1835-1840.

91. PACKHAM, R.F., and RICHARDS, W.N., Water clarification by flotation - 1, Report TP87, Water Research Centre, Medmenham, Marlow, Bucks., 1972.

92. LUTHY, R.G., SELLECK, R.E., and GALLOWAY, T.R., Removal of emulsified oil with organic coagulants and dissolved air flotation, J. Water Poll. Control Fed., 50, 1978, 331-346.

93. BRATBY, J., and MARAIS, G.v.R., Dissolved air flotation, Filtration and Separation, 11, 1974, 614-624.

94. PEARSON, D., and SHIRLEY, J.M., Precipitate flotation in the treatment of metal-bearing effluents, J. Appl. Chem. Biotechnol., 23, 1973, 101-109.

95. KALINSKE, A.I., Flotation in waste treatment, in 'Biological treatment of sewage and industrial wastes', 2, ed. McCable, J., Eckenfelder, W.W., Jr., Reinhold, New York, 1958, 222-231.

96. ROBERTS, K.L., WEETER, D.W., and BALL, R.O., Dissolved air flotation performance, Proc. 33rd. Ind. Waste Conf., Purdue Univ., Ann Arbor Sci., Michigan, 1978, 194-199.

97. LUNDGREN, H., Theory and practice of dissolved air flotation, Filtration and Separation, 13, 1976, 24-28.

98. REED, S.W., and WOODWARD, F.E., Dissolved air flotation of poultry processing waste, J. Water Poll. Control Fed., 48, 1976, 107-119.

99. PACKHAM, R.F., and RICHARDS, W.N., Water clarification by flotation - 3, Report TR2, Water Research Centre, Medmenham, Marlow, Bucks., 1975.

100. WATER RESEARCH CENTRE, A nozzle for introducing gas into liquid, British Patent 1, 444, 027, 1976.

101. VAN VUUREN, L.R., MEIRING, P.E.J., HENZEN, M.R., and KOLBE, F.F., The flotation of algae in water reclamation, Int. J. Air Wat. Poll., 9, 1965, 823-832.

102. BRATBY, J., and MARAIS, G.v.R., Dissolved-air (pressure) flotation - an evaluation of inter-relationships between process variables and their optimization, Water S.A., 1, 1975, 57-69.

103. BRATBY, J., and MARAIS, G.v.R., A guide for the design of dissolved-air (pressure) flotation systems for activated sludge processes, Water S.A., 2, 1976, 87-100.

104. BRATBY, J., and MARAIS, G.v.R., Thickening of brown water sludges by dissolved-air (pressure) flotation, Water S.A., 3, 1977, 202-212.

105. HYDE, R.A., Water clarification by flotation - 4, Report TR13, Water Research Centre, Medmenham, Marlow, Bucks., 1975.

106. CHURCHILL, R.J., and TACCHI, K.J., A critical analysis of flotation performance, in 'Water - 1977', A.I.Ch.E. Symposium Series, No. 178, ed. Bennet, G.F., 74, 1978, 290-299.

107. RANCE BARE, W.F., JONES, N.B., and MIDDLEBROOKS, E.J., Algae removal using dissolved air flotation, J. Water Poll. Control Fed., 47, 1975, 153-169.

108. MERRIL, D.T., and JORDEN, R.M., The high rate treatment of raw domestic sewage by lime precipitation-dissolved air flotation, Progress in Water Technology, 7, 1975, 379-389.

109. ELMORE, F.E., Improvements in apparatus for use in separating certain constituents of finely divided materials or ores by causing them to rise or float in a liquid, British Patents 17, 816 and 29, 282, 1904.

110. SCHUHMAN, R., and PRAKASH, B., Effect of $BaCl_2$ and other activators on soap flotation of quartz, Min. Engng., 187, 1950, 591-600.

111. JOY, A.S., WATSON, D., AZIM, Y.Y.A., and MANSER, R.M., Flotation of silicates, Trans. I.M.M., 75, 1966, C75-80.

112. LIN, I.J., Measurement of contact angles with bubbles generated by vacuum, Trans, I.M.M., 76, 1967, C288-290.

113. LIN, I.J., and METZER, A., Kinetics of batch vacuum flotation, Israel J. Technol., 7, 1969, 371-4.

114. HUBER PANU, I., PANDELESCU, C., and PROTOPESCU, A., Contributions à l'étude de la flottation des minerals très fins, à air dégagé de la solution, Rev. Roumaine Sci. Tech., Ser. Met., 9, 1964, 325-351.

115. HUBER PANU, I., andPANDELESCU, C., Recherches concernant la flottation des mineraux sulfureux très finement broyées, Paper D-2, 8th I.M.P.C., Lenningrad, 1968.

116. SHALIH, M.S.M., Flotation of mineral slimes by dissolved air flotation techniques, M.Phil. Thesis, University of Leeds, 1975.

117. SHIMOIIZAKA, J., et al., Pressure flotation of kaolinite, Proc. Annual Meeting Mining and Metallurgical Soc. of Japan, April 1978, 189-190.

118. HAIR, M., Infrared Spectroscopy in Surface Chemistry, Dekker, New York, 1967.

119. PARKS, G.A., and DE BRUYN, P.L., The zero point of charge of oxides, J. Phys. Chem., 66 (6), 1962, 967-972.

120. PARKS, G.A., Aqueous surface chemistry of oxides and complex oxide minerals, Advances in Chem. Ser., 67, A.C.S., Washington 1967, 121-160.

121. GOUY, G., Constitution of the electric charge at the surface of an electrolyte, J. Physique., 4, (9), 1910, 457-467.

122. CHAPMAN, D.L., A contribution to the theory of electrocapillarity, Phil. Mag., 25, (6), 1913, 475-481.

123. STERN, O., Zur theorie der electrolytischen doppelschicht, Z. Elektrochem., 30, 1924, 508-516.

124. GRAHAME, D.C., The electrical double layer and the theory of electrocapillarity, Chem. Rev., 41, 1947, 441-501.

125. LYKLEMA, J., Surface chemistry of colloids in connection with stability, in 'The Scientific Basis of Flocculation', ed. Ives, K.J., Sijthoff and Noordhoff, Alphen aan den Rijn, The Netherlands, 1978, 3-36.

126. PARKS, G.A., 'Adsorption in the Marine Environment' in 'Chemical Oceanography', ed. Riley, J.P., and Skirrow, G., 2nd edition, Academic Press, New York, 1975, 241-308.

127. LEVINE, S., MINGINS, J., and BELL, G.M., The discrete-ion effect in ionic double-layer theory, J. Electroanalyt. Chem., 13, 1967, 280-329.

128. SMITH, A.L., Electrical phenomena associated with the solid-liquid interface, in 'Dispersion of Powders in Liquids', ed. Parfitt, G.D., 2nd edition, Applied Science Pub., London, 1973.

129. FUERSTENAU, D.W., Interfacial processes in mineral/water systems, Pure Appl. Chem., 24, 1970, 135-164.

130. JAYCOCK, M.J., and OTTEWILL, R.H., Adsorption of ionic surface active agents by charged solids, Trans. I.M.M., 72, 1963, 497-506.

131. FUERSTENAU, D.W., and HEALY, T.W., Principles of mineral flotation in 'Adsorptive Bubble Separation Techniques', ed. Lemlich, R., Wiley, New York, 1972, 91-131.

132. FUERSTENAU, D.W., The adsorption of surfactants at solid-water interfaces, in 'Chemistry of Biosurfaces', ed. Hair, M.L., Dekker, New York, 1, 1971, 143-176.

133. SHAW, D.J., Introduction to Colloid and Surface Chemistry, 2nd edition, Butterworths, London, 1970.

134. GAUDIN, A.M., and FUERSTENAU, D.W., Streaming flotation studies - quartz flotation with cationic collectors, Trans. A.I.M.E., 202, 1955, 958-962.

135. FUERSTENAU, D.W., Correlation of contact angles, adsorption density, zeta-potentials and flotation rate, Trans. A.I.M.E., 208, 1957, 1365-1367.

136. FUERSTENAU, D.W., and MODI, H.J., Streaming potentials of corundum in aqueous organic electrolyte, J. Electrochem. Soc., 106, 1959, 336-341.

137. SOMASUNDARAN, P., and FUERSTANAU, D.W., Mechanism of alkyl sulphonate adsorption at the alumina-water interface, J. Phys. Chem., 70 (1), 1966, 90-96.

138. ROY, P., and FUERSTENAU, D.W., The heat of immersion of alumina into aqueous sodium dodecyl sulphonate solutions, J. Colloid Interface Sci., 26, 1968, 102-109.

139. RINELLI, G., MARABINI, A.M., and ALESSE, V., Flotation of cassiterite with salycylaldehyde as collector, in 'Flotation. A.M. Gaudin Memorial Volume', ed. Fuerstenau, M.C., 1, 1976, 549-560.

140. PECK, A.S., RABY, L.H., and WADSWORTH, M.E., An infrared study of the flotation of hematite with oleic acid and sodium oleate, Trans A.I.M.E., 238, 301-307.

141. HAN, K.N., HEALY, T.W., and FUERSTENAU, D.W., The mechanism of adsorption of fatty acids and other surfactants at the oxide-water interface, J. Colloid Interface Sci., 44 (3), 1973, 407-414.

142. LAI, R.W.M., and FUERSTANAU, D.W., Model for the surface charge of oxides and flotation response, Trans. A.I.M.E., 260, 1976, 104-107.

143. CASES, J.M., On the normal interaction between adsorbed species and absorbing surface, Trans. A.I.M.E., 247, 1970, 123-127.

144. PREDALI, J.J., and CASES, J.M., Thermodynamics of the adsorption of collectors, Proc. 10th I.M.P.C., London, 1973, 473-493.

145. CASES, J.M., GOUJON, G., and SMANI, S., Adsorption of n-alkylamine chlorides on heterogeneous surfaces, A.I.Ch.E. Symp. Ser., 71 (150), 1975, 100-109.

146. DERJAGUIN, B.V., and LANDAU, L., Theory of stability of strongly charged lyophobic sols and of the adhesion of strongly charged particles in solutions of electrolytes, Acta Physicochim. U.R.S.S., 14, 1941, 633-162.

147. VERWEY, E.J.W., and OVERBEEK, J.Th.G., 'Theory of the Stability of Lyophobic Colloids', Elsevier, Amsterdam, 1948.

148. OTTEWILL, R.H., RASTOGI, M.C., and WATANABE, A., The stability of hydrophobic sols in the presence of surface-active agents. Part I. Theoretical treatment, Trans. Far. Soc., 56, 1960, 854-865.

149. STUMM, W., and O'MELIA, C.R., Chemical aspects of coagulation. II. Stoichiometry of coagulation, J. Am. Water Wks. Assm., 60, 1968, 514-539.

150. LA MER, V.K., and HEALY, T.W., Adsorption-flocculation reactions of macromolecules at the solid-liquid interface, Rev. Pure and Applied Chem., 13, 1963, 112-133.

151. LA MER, V.K., Coagulation Symposium, Introduction, J. Colloid Sci., 19, 1964, 291-3.

152. KITCHENER, J.A., Principles of action of polymeric flocculants, Br. Polym. J., 4, 1972, 217-229.

153. GREGORY, J., Effects of polymers on colloid stability in 'The Scientific Basis of Flocculation, ed. Ives, K.J., Sijthoff and Noordhoff, Alphen aan den Rijn, The Netherlands, 1978, 101-130.

154. FRIEND, J.P., and KITCHENER, J.A., Some physico-chemical aspects of the separation of finely-divided minerals by selective flocculation, Chem. Engng. Sci., 28, 1973, 1071-1080.

155. KITCHENER, J.A., Flocculation in mineral processing, in 'The Scientific Basis of Flocculation', ed. Ives, K.J., Sijthoff and Noordhoff, Alphen aan den Rijn, The Netherlands, 1978, 283-328.

156. IVES, K.J., Rate theories, in 'The Scientific Basis of Flocculation', ed. Ives, K.J., Sijthoff and Noordhoff, Alphen aan den Rijn, The Netherlands, 1978, 37-61.

157. PUGH, R.J., and KITCHENER, J.A., Theory of selective coagulation of mixed colloidal suspensions, J. Coll. Interface Sci., 35, 1971, 656-664.

158. YARAR, B., and KITCHENER, J.A., Selective flocculation of minerals. 1. Basic principles. 2. Experimental investigation of quartz, calcite and galena, Trans. I.M.M., 79, 1970, C23-33.

159. RUBIO, J., and KITCHENER, J.A., New basis for selective flocculation of slimes, Trans. I.M.M., 86, 1977, C97-100.

160. READ, A.D., and HOLLICK, C.T., Selective flocculation techniques for recovery of fine particles, Min. Sci. Engng., 8, 1976, 202-213.

161. OTTEWILL, R.H., and RASTOGI, M.C., The stability of hydrophobic sols the presence of surface-active agents. Part 2 - The stability of silver iodide sols in the presence of cationic surface-active agents, Trans. Far. Soc., 56, 1960, 866-879. Part 3 - An examination by microelectrophoresis of the behaviour of silver iodide sols in the presence of cationic surface-active agents, Trans. Far. Soc., 56, 1960, 880-892.

162. OTTEWILL, R.H., and WATANABE, A., Studies on the mechanism of coagulation. Part 1. The stability of positive silver iodide sols in the presence of anionic surface-active agents, Kolloid-Z, 170, 1960, 38-48. Part 2. The electrophoretic behaviour of positive silver iodide sols in the presence of anionic surface-active agents, Kolloid-Z, 170, 1960, 132-139.

163. SOMASUNDARAN, P., HEALY, T.W., and FUERSTENAU, D.W., The aggregation of colloidal alumina dispersions by adsorbed surfactant ions, J. Coll. Interface Sci., 22, 1966, 599-605.

164. FUERSTENAU, D.W., Fine particle flotation, Proc. Fine Particle Processing Symposium, Las Vegas, 1980, 669-705.

165. WARREN, L.J., Shear-flocculation of ultrafine scheelite in sodium oleate solutions, J. Coll. Interface Sci., 50, 1975, 307-318.

166. THORNTON, E.W., and HARRISON, P.G., Tin oxide surfaces. Part 1. Surface hydroxyl groups and the chemisorption of carbon dioxide and carbon monoxide on tin(IV) oxide, J.C.S. Faraday I, 71, 1975, 461-472.

167. KITTAKA, S., and KANEMOTO, S., Interaction of water molecules with the surface of tin(IV) oxide, J.C.S. Faraday I, 74, 1978, 676-685.

168. EDWARDS, G.R., and EWERS, W.E., The adsorption of sodium cetyl sulphate on cassiterite, Aust. J. Sci. Res., 4, 1951, 627-643.

169. JAYCOCK, M.J., OTTEWILL, R.H., and TAR, I., Adsorption of sodium dodecyl sulphate on activated and non-activated stannic oxide, Trans. I.M.M., 51, 163-64, 255-266.

170. JOHANSEN, P.G., and BUCHANAN, A.S., An application of the micro-electrophoresis method to the study of the surface properties of insoluble oxides, Aust. J. Chem., 10, 1957, 398-403.

171. JOHANSEN, P.G., and BUCHANAN, A.S., An electrokinetic study by the streaming potential method of ion exchange at oxide mineral surfaces, Aust. J. Chem., 10, 1957, 392-397.

172. O'CONNOR, D.J., and BUCHANAN, A.S., Electrokinetic properties of cassiterite, Aust. J. Chem., 6, 1953, 278-293.

173. DE CUYPER, J., and GUTIERREZ, C., Proprietes electrocinetiques de la cassiterite et de la siderite en relation avec leur flottabilite, Paper S6, Proc. 8th I.M.P.C., Leningrad, 1968.

174. AHMED, S.M., and MAKSIMOV, D., Studies of the double layer on cassiterite and rutile, J. Coll. Interface Sci., 29, 1969, 97-104.

175. ZAMBRANA, G., ROMERO, R., and GUTIERREZ, G., Selective flotation of cassiterite from quartz by activation with lead salts in alkaline media, 9th I.M.P.C., Prague, 1970; Rudy, 3-4, 1970, 152-157.

176. TRAHAR, W.J., The present status of cassiterite flotation, Proc. 8th Commonwealth Min. and Met. Congress, ed. Woodcock, J.T., Madigan, R.T., and Thomas, R.C., Australia and New Zealand, 6, 1965, 1125-1132.

177. HERGT, H.F.A., ROGERS, J., and SUTHERLAND, K.L., Flotation of cassiterite and associated minerals, Trans. A.I.M.E., 169, 1946, 448-465.

178. GAUDIN, A.M., SCHUHMAN, R., Jr., and BROWN, E.G., Making tin flotation work. I. Canutillos ore, Engng. Min. J., 147, 1946, 54-59.

179. GAUDIN, A.M., and SCHUHMAN, R., Jr., Making tin flotation work. III. Colquiri ore (Part I), Engng. Min. J., 147, 1946, 68-72.

180. SCHUHMAN, R., Jr., and PRAKASH, B., Effects of activators and alizarin dyes on soap flotation of cassiterite and fluorite, Trans. A.I.M.E., 187, 1950, 601-608.

181. GAUDIN, A.M., and ERGUNALP, F., Making tin flotation work. II. Oplaca ore, Engng. Min. J., 147,, 1946, 72-74.

182. GOOLD, L.A., Preliminary investigations into the flotation of tin dioxide, cassiterite and some related gangue minerals, Report No. 1589, National Institute for Metallurgy, South Africa, 1973.

183. POL'KIN, S.I., LAPTEV, S.F., MATSUEV, L.P., ADAMOV, E.V., KRASNUKHINA, A.V., and PURVINSKII, O.F., Theory and practice in the flotation of cassiterite fines, Proc. 10th I.M.P.C., London, 1973, 593-614.

184. WOTTGEN, E., Adsorption of phosphonic acids on cassiterite, Trans. I.M.M., 78, 1969, C91-97.

185. WOTTGEN, E., Physikalisch-chemische Eigenschaften der Phosphonsäuren im Zusammentang mit der Flotation, Tenside, 2, 1965, 405-408.

186. ZAMBRANA, G., DE GROOT, W., NAVAJAS, J.C., and SUAREZ, A., The flotation response of cassiterite using new anionic collectors, 4th World Conf. on Tin, Kuala Lumpur, 3, 1974, 59-74.

187. COLLINS, D.N., Investigation of collector systems for the flotation of cassiterite, Trans. I.M.M., 76, 1967, C77-93.

188. COLLINS, D.N., Discussion of ref. 183, Proc. 10th I.M.P.C., London, 1973, 617-618.

189. CLAUS, C.R.A., APPLETON, E.A., and VINK, J.J., Selective flocculation of cassiterite in mixtures with quartz using a modified polyacrylamide flocculant, Int. J. Miner. Process., 3, 1976, 27-34.

190. MUKERJEE, P., and MYSELS, K.J., Critical micelle concentrations of aqueous surfactant systems, National Bureau of Standards, NSRDS, Washington D.C., NBS 36, 1971.

191. OVERBEEK, J.Th.G., Electrokinetic phenomena, in 'Colloid Science', ed. Kruyt, H.R., Elsevier, 1, 1952, 194-244.

192. HAYDON, D.A., The electrical double layer and electrokinetic phenomena, Recent Progress in Surface Sci., ed. Danielli, J.F., Pankhurst, K.G.A., and Riddiford, A.C., Academic Press, New York, 1, 1964, 94-158.

193. DUKHIN, S.S., and DERJAGUIN, B.V., Electrokinetic phenomena, in Surface and Colloid Science, ed. Matijovic, E., Wiley, New York, 7, 1974.

194. MACKENZIE, J.M.W., Zeta-potential studies in mineral processing: Measurement, techniques and applications, Min. Sci. Engng., 3 (3), 1971, 25-43.

195. HENRY, D.C., The cataphoresis of suspended particles. Part I. The equation of cataphoresis, Proc. Roy. Soc., A133, 1931, 106-129.

196. HENRY, D.C., The electrophoresis of suspended particles. IV. The surface conductivity effect, Trans. Far. Soc., 44 (2), 1948, 1021-1026.

197. OVERBEEK, J.Th.G., Theory of electrophoresis - the relaxation effect, Kolloid Beih, 54, 1943, 287-364.

198. BOOTH, F., The cataphoresis of spherical, non-conducting particles in a symmetrical electrolyte, Proc. Roy. Soc., A203, 1950, 514-533.

199. LYKLEMA, J., and OVERBEEK, J.Th.G., On the interpretation of electrokinetic potentials, J. Colloid Sci., 16, 1961, 501-512.

200. HUNTER, R.J., The interpretation of electrokinetic potentials J. Coll. Interface Sci., 22, 1966, 231-239.

201. WIERSEMA, P.H., LOEB, A.L., and OVERBEEK, J.Th.G., Calculation of the electrophoretic mobility of a spherical colloid particle, J. Coll. Interface. Sci., 22, 1966, 78-99.

202. PEARCE, A.S., and STREATFIELD, E.L., Determination of amines in water, Ger. pat. 1,190,229, 1961, (Analyt. Abs. 12, 1965, 6766).

203. GREGORY, G.R.E.C., The determination of residual anionic surface-active reagents in mineral flotation liquors, Analyst, 91, 1966, 251-257.

204. BOWMAN, J.A., The determination of tin in tin ores and concentrates by atomic absorption spectrophotometry in the nitrous oxide-acetylene flame, Anal. Chim. Acta, 42, 1968, 285-291.

205. NIXON, P.J., New chemical methods for the processing of low grade cassiterite concentrates, Ph.D. Thesis, University of London, 1970.

206. MANTELL, C.L., 'Tin: Its Mining, Production, Technology and Applications', Hafner Pub. Co., New York, 1970.

207. SLATER, R.W., and KITCHENER, J.A., Characteristics of flocculation of mineral suspensions by polymers, Disc. Faraday Soc., 42 1966, 267-275.

208. IVES, K.J., Experimental methods (2) Dilute suspensions, in 'The Scientific Basis of Flocculation', ed. Ives, K.J., Sijthoff and Noordhoff, Alphen aan den Rijn, The Netherlands, 1978, 165-191.

209. METSCHL, J., The supersaturation of gases in water and certain organic liquids, J. Phys. Chem., 28, 1924, 417-437.

210. SHERGOLD, H.L., and MELLGREN, O., Concentration of minerals at the oil-water interface, Trans. A.I.M.E., 247, 1970, 149-159.

211. LI, H.C., and DE BRUYN, P.L., Electrokinetics and adsorption studies on quartz, Surface Sci., 5, 1966, 203-220.

212. OVERBEEK, J.Th.G., Stability of hydrophobic colloids and emulsions, in 'Colloid Science', ed. Kruyt, H.R., Elsevier, London, 1, 1952,

213. SHERGOLD, H.L., The flotation of ultra-fine particles, h.D. Thesis, Univ. London, 1968.

214. BALL, B., and FUERSTENAU, D.W., Thermodynamics and adsorption behaviour in the quartz/aqueous surfactant system, Disc. Faraday Soc., 52, 1971, 361-371.

215. SMITH, R.W., Co-Adsorption of dodecylamine ion and molecule on quartz, Trans. A.I.M.E., 226, 1963, 427-433.

216. WATSON, D., and MANSER, R.M., Some factors affecting the limiting conditions in cationic flotation of silicates, Trans. I.M.M., 77, 1968, C57-60.

217. SOMASUNDARAN, P., Interfacial chemistry of particulate flotation, A.I.Ch.E. Symposium Series, 71, No. 150, 1975, 1-15.

218. DE BRUYN, P.L., Flotation of quartz by cationic collectors, Trans. A.I.M.E., 202, 1955, 291-296.

219. TAMAMUSHI, B., The action of surface active large ions on the stability of hydrophobic colloids, Kolloid-Z., 150, 1957, 44-49.

220. SMITH, R.W., and AKHTAR, S., Cationic flotation of oxides and silicates in 'Flotation. A.M. Gaudin Memorial Volume', ed. Fuerstanau, M.C., 1, 1976, 87-116.

221. O'MELIA, C.R., and STUMM, W., Aggregation of silica dispersions by iron(III), J. Coll. Interface Sci., 23, 1967, 437-447.

222. ALLEN, L.H., and MATIJEVIC, E., Stability of colloidal silica III. Effect of hydrolyzable cations, J. Coll. Interface Sci., 35, 1971, 66-75.

223 RUBIN, A.J., and HABERKOST, D.C., Coagulation and flotation of colloidal titanium dioxide, Separation Sci., 8, 1973, 363-373.

224. RUBIN, A.J., and LACKEY, S.C., Effects of coagulation on the microflotation of bacillus ceveus, J. A. Wat. Wks. Ass., 60, 1971, 1156-1166.

225. INOUE, T., OKAMURA, K., YOSHIHARA, K., and TEZUKA, A., Pressure flotation of the suspended solids in a low concentration range, Annual Report Eng. Res. Inst., Fac. of Engng., Tokyo Univ., 36, 1977.

226. MANGRAVITE, F.J., CASSELL, E.A., and MATIJEVIC, E., The microflotation of silica, J. Coll. Interface Sci., 39, 1972, 357-366.

227. DE VIVO, D.G., and KARGER, B.L., Studies in the flotation of colloidal particulates: effects of aggregation in the flotation process, Separation Sci., 5, 1970, 145-167.

228. CASSELL, E.A., KAUFMAN, K.M., and MATIJEVIC, E., The effects of bubble size on microflotation, Water Res., 9, 1975, 1025-1036.

229. DIXON, J.K., LA MER, V.K., LI, C., MESSINGER, S., and LINFORD, H.B., Effect of the structure of cationic polymers on the flocculation and the electrophoretic mobility of crystalline silica, J. Coll. Interface Sci., 23, 1967, 465-473.

230. LINDQUIST, G.M., and STRATTON, R.A., The role of polyelectrolyte charge density and molecular weight on the adsorption and flocculation of colloidal silica with polyethyleneimine, J. Coll. Interface Sci., 55, 1976, 45-59.

231. RUBIO, J., Flocculation by poly (ethylene oxide): mechanism and applications, Ph.D. Thesis, Univ. of London, 1977.

232. ONODA, G.V., and FUERSTENAU, D.W., Amine flotation in the presence of inorganic electrolytes, Proc. 7th I.M.P.C., New York, 1, 1967, 301-306.

233. GILES, C.H., MACEWAN, T.H., NAKHURA, S.N., and SMITH, D., Studies in adsorption. Part XI. A system of classification of solution isotherms, and its use in diagnosis of adsorption mechanisms and in measurement of specific surface areas of solids, J. Chem. Soc., 3, 1960, 3973-3993.

234. WAKAMATSU, T., and FUERSTENAU, D.W., The effect of hydrocarbon chain length on adsorption of sulphonates at the solid/water interface, Adv. Chem. Ser., 79, A.C.S., Washington, 1968, 161-172.

235. SOMASUNDARAN, P., HEALY, T.W., and FUERSTENAU, D.W., Surfactant adsorption at the solid-liquid interface - dependence of mechanism on chain length, J. Phys. Chem., 68 (12), 1964, 3562-3566.

236. CORNELL, R.M., POSNER, A.M., and QUIRK, J.P., A titrimetric and electrophoretic investigation of the p.z.c. and the i.e.p. of pigment rutile, J. Colloid Interface Sci., 53 (1), 1975, 6-13

237. DAY, A., American Cyanamid Co., Private Communication, 1979.

238. JAYCOCK, M.J., Physical chemistry of flotation processes, Ph.D. Thesis, Univ. of Cambridge, 1963.

239. WATSON, D., Discussion of ref. 169, Trans. I.M.M., 51, 1963-64, 536.

240. LIN, I.J., and SOMASUNDARAN, P., Free-energy changes on transfer of surface-active agents between various colloidal and interfacial states, J. Coll. Interface Sci., 37, 1971, 731-743.

241. BIJSTERBOSCH, B.H., Characterization of silica surfaces by adsorption from solution. Investigations into the mechanism of adsorption of cationic surfactants, J. Coll. Interface Sci., 47, 1974, 186-198.

242. KITCHENER, J.A., Discussion of ref. 169, Trans. I.M.M., 51, 1963-64, 535.

243. MACKENZIE, J.M.W., Interactions between oil drops and mineral surfaces, Trans. A.I.M.E., 247, 1970, 202-208.

244. WARREN, L.J., and KITCHENER, J.A., Role of fluoride in the flotation of feldspar: adsorption on quartz, corundum and potassium feldspar, Trans. I.M.M., 81, 1972, C137-147.

245. ZAMBRANA, G.Z., MEDINA, R.T., GUTIÉRREZ, G.B., and VARGAS, R.R., Recovery of minus 10 μm cassiterite by liquid-liquid extraction, Int. J. Min. Proc., 1, 1974, 335-345.

246. PARFITT, G.D., Fundamental aspects of dispersion, in 'Dispersion of powders in liquids', ed. Parfitt, G.D., 2nd edition, Applied Science Pub., London, 1973, 1-43.

247. DEAN, R.B., The formation of bubbles, J. Applied Phys., 15, 1944, 446-451.

248. EBERHART, J.G., and SCHNYDERS, H.C., Application of the mechanical stability condition to the prediction of the limit of superheat for normal alkanes, ether and water, J. Phys. Chem., 77, 1973, 2730-2736.

249. SKRIPOV, V.P., 'Metastable liquids', Israel program for scientific translations, Halstead Press, 1974.

250. KENRICK, F.B., WISEMEN, K.L., and WYATT, K.S., Supersaturation of gases in liquids, J. Phys. Chem., 28, 1924, 1308-1315.

251. STRASBERG, M., Onset of ultrasonic cavitation in tap water, J. Acoust. Soc. Amer., 31, 1959, 163-176.

252. SMITH, H.G., ABBOTT, J., and FRANGISKOS, A., Particle-bubble attachment in coal flotation, 2nd Symposium on Coal Preparation, Univ. of Leeds, 1957, 329-345.

253. HEMMINGSEN, E.A., Cavitation in gas-supersaturated solutions, J. Applied Phys., 46, 1975, 213-218.

254. APFEL, R.E., The role of impurities in cavitation-threshold determination, J. Acoust. Soc. Amer., 48, 1970, 1179-1186.